NACA TN 2831

9166

NACA TN 2831

TECH LIBRARY KAFB, NM

0065820

NATIONAL ADVISORY COMMITTEE FOR AERONAUTICS

TECHNICAL NOTE 2831

SPAN LOAD DISTRIBUTIONS RESULTING FROM CONSTANT ANGLE OF ATTACK, STEADY ROLLING VELOCITY, STEADY PITCHING VELOCITY, AND CONSTANT VERTICAL ACCELERATION FOR TAPERED SWEPTBACK WINGS WITH STREAMWISE TIPS

SUBSONIC LEADING EDGES AND SUPERSONIC TRAILING EDGES

By Margery E. Hannah and Kenneth Margolis

Langley Aeronautical Laboratory
Langley Field, Va.

Washington
December 1952

AFMDC
TECHNICAL LIBRARY
AFL 2811

TECH LIBRARY KAFB, NM

0065820

1p

NATIONAL ADVISORY COMMITTEE FOR AERONAUTICS

TECHNICAL NOTE 2831

SPAN LOAD DISTRIBUTIONS RESULTING FROM CONSTANT ANGLE OF ATTACK, STEADY ROLLING VELOCITY, STEADY PITCHING VELOCITY, AND CONSTANT VERTICAL ACCELERATION FOR TAPERED SWEPTBACK WINGS WITH STREAMWISE TIPS

SUBSONIC LEADING EDGES AND SUPERSONIC TRAILING EDGES

By Margery E. Hannah and Kenneth Margolis

SUMMARY

On the basis of linearized supersonic-flow theory, the theoretical spanwise distributions of circulation (which are proportional to the span load distributions) resulting from constant angle of attack, steady rolling velocity, steady pitching velocity, and constant vertical acceleration were calculated for a series of thin, sweptback, tapered wings with streamwise tips. The analysis is valid at those speeds for which the wing is wholly contained between the Mach cones springing from the wing apex and the trailing edge of the root section, that is, subsonic leading edges and supersonic trailing edges. An added restriction is that the Mach cones emanating from the leading edges of the wing tips must not intersect on the wing.

Formulas for the spanwise distributions of circulation are given in closed form. Numerical results are presented as a series of design charts from which the desired loading may be obtained for given values of aspect ratio, taper ratio, Mach number, and leading-edge sweepback. The axis of pitch is taken at the wing apex although, by use of the calculated results and a simple transformation, span load distributions for steady pitching velocity may be readily obtained for arbitrary location of the pitch axis. Variations of the spanwise distributions of circulation with the various plan-form parameters, Mach number, and axis-of-pitch location are also presented for illustrative purposes.

INTRODUCTION

A knowledge of the spanwise loading or spanwise distribution of circulation (which is proportional to the spanwise loading) is of great value in solving aerodynamic problems and performing aerodynamic calculations. For example, it has been shown that the upwash and sidewash downstream of an airfoil are largely determined by the spanwise circulation except in the region directly behind the trailing edge. In addition to the estimation of flow fields and evaluation of forces and moments on the surface itself, the spanwise distribution of circulation may also be applied to problems in aerodynamic loads and aeroelasticity. In view of these considerations, a series of charts giving the spanwise distributions of circulation for a variety of wing plan forms at various Mach numbers will serve many useful purposes.

The present paper considers the spanwise distributions of circulation resulting from a constant angle of attack, a constant rate of roll, a constant rate of pitch, and constant vertical acceleration for a series of sweptback tapered wings with streamwise tips, subsonic leading edges, and supersonic trailing edges. Reference 1 treats the first three motions mentioned above for the same general class of wings but at Mach numbers for which both the leading and trailing edges are supersonic. It may be noted at this point that within the limits of linearized theory as used herein, the analyses for constant rate of roll and constant rate of pitch are applicable to wings with linear lateral twist and linear camber, respectively.

The results of the analysis are given in the form of equations for the spanwise distributions of circulation. (For the case of steady pitching velocity, the axis of pitch is taken at the wing apex.) A series of design charts permitting the rapid estimation of spanwise circulation for a wing with given aspect ratio, taper ratio, leading-edge sweepback, and Mach number are presented. By use of the calculated results in conjunction with a transformation formula, the spanwise distribution of circulation due to steady pitching velocity with arbitrary axis of pitch may readily be obtained. Some illustrative variations of the spanwise distributions of circulation with the various wing parameters, Mach number, and axis-of-pitch location are also included.

SYMBOLS

x, y Cartesian coordinates (see fig. 1)

c_r root chord

b span

λ taper ratio (ratio of tip chord to root chord)

Λ angle of sweepback of leading edge

ϵ semiapex angle

$\bar{c}$ mean aerodynamic chord, $\dfrac{2c_r\left(\lambda^2 + \lambda + 1\right)}{3(1 + \lambda)}$

c chord at spanwise station y

S wing area

A aspect ratio, $\dfrac{b^2}{S} = \dfrac{2b}{\left(1 + \lambda\right)c_r}$

$m = \cot \Lambda = \tan \epsilon$

μ Mach angle

M Mach number

B cotangent of the Mach angle, $\sqrt{M^2 - 1}$

ϕ disturbance velocity potential on upper surface

χ value of ϕ for unit angle of attack

V free-stream velocity

ρ density

ΔP pressure difference between upper and lower surfaces, positive in sense of lift

ΔC_P pressure-difference coefficient, $\dfrac{\Delta P}{\frac{1}{2}\rho V^2}$

α angle of attack, radian measure

p rate of roll, radian measure

q rate of pitch, radian measure

$\dot{\alpha}$ rate of change of α with time

t time

Γ circulation at any spanwise station y, $\frac{V}{2}\int_{x_{LE}}^{x_{TE}} \Delta C_p \, dx$

Γ_1, Γ_2 components of circulation due to constant vertical acceleration, $\Gamma = \Gamma_1 + \Gamma_2$

c_l section lift coefficient

cc_l spanwise loading parameter

y_i spanwise coordinate of intersection of Mach line emanating from wing tip with wing trailing edge (see fig. 2)

$$K = \frac{x_{TE}}{Bb/2} = \frac{\frac{y}{b/2}\left[AB(1 + \lambda) - 4Bm(1 - \lambda)\right] + 4Bm}{AB(Bm)(1 + \lambda)}$$

$\bar{x}$ distance from apex to center of pressure due to angle of attack, $-\bar{c}\,\frac{\left(C_{m_\alpha}\right)_a}{C_{L_\alpha}}$

d distance from apex to assumed center-of-gravity location

x_{sm} static margin, $\bar{x} - d$

C_{L_α} lift-curve slope, $\left(\frac{\partial}{\partial\alpha}\frac{\text{Lift}}{\frac{1}{2}\rho V^2 S}\right)_{\alpha \to 0}$

$$C_{m_\alpha} = \left(\frac{\partial}{\partial\alpha}\frac{\text{Pitching moment due to angle of attack}}{\frac{1}{2}\rho V^2 S\bar{c}}\right)_{\alpha \to 0}$$

$$k = \sqrt{1 - (Bm)^2}$$

$F'(Bm)$ complete elliptic integral of first kind with modulus k,

$$\int_0^{\pi/2} \frac{dz}{\sqrt{1 - k^2 \sin^2 z}}$$

$E'(Bm)$ complete elliptic integral of second kind with modulus k,

$$\int_0^{\pi/2} \sqrt{1 - k^2 \sin^2 z}\, dz$$

$$E''(Bm) = \frac{1}{E'(Bm)}$$

$$I(Bm) = \frac{2\left(1 - B^2m^2\right)}{\left(2 - B^2m^2\right)E'(Bm) - B^2m^2F'(Bm)}$$

$$G(Bm) = \frac{1 - B^2m^2}{\left(1 - 2B^2m^2\right)E'(Bm) + B^2m^2F'(Bm)}$$

Subscripts:

LE leading edge

TE trailing edge

ML Mach line from leading edge of tip

ex wing region external to Mach cone from leading edge of tip (see fig. 2)

in wing region internal to Mach cone from leading edge of tip (see fig. 2)

q pitching

α angle of attack

a pitching about apex

d pitching about assumed center-of-gravity location

ANALYSIS

Scope

The sweptback wings considered in this paper are sketched in figure 1. The system of coordinates, wing parameters, and associated data used in the analysis are indicated in figures 1 and 2. For the motions analyzed, the results are the same to the first order in α (the angle of attack) in both the axes system used herein and the stability axes system. The analysis is based on linearized supersonic-flow theory and is limited to nonsideslipping streamwise-tip wings of vanishingly small thickness that have zero camber.

The results are valid for a range of supersonic speeds for which the leading edge is subsonic and the trailing edge supersonic (i.e., the wing is wholly contained between the Mach cones springing from the wing apex and the trailing edge of the root section). An added restriction is that the Mach cones emanating from the leading edge of the wing tips may not intersect on the wing. These conditions expressed mathematically as restrictions on the parameter $B \cot \Lambda$ are as follows:

For $BA(1 + \lambda) \geqq 2$

$$\frac{BA(1 + \lambda)}{BA(1 + \lambda) + 4(1 - \lambda)} \leqq B \cot \Lambda \leqq 1$$

and for $BA(1 + \lambda) < 2$

$$\frac{BA(1 + \lambda)}{BA(1 + \lambda) + 4(1 - \lambda)} \leqq B \cot \Lambda \leqq \frac{BA(1 + \lambda)}{4 - BA(1 + \lambda)}$$

Basic Considerations

The evaluation of spanwise loadings generally requires a knowledge of the pressure difference between the upper and lower surfaces of the wing. The distribution of circulation along the span is related to the spanwise loading parameter and pressure-difference coefficient as follows:

$$\Gamma = \frac{V}{2} cc_l = \frac{V}{2} \int_{x_{LE}}^{x_{TE}} \Delta C_p \, dx \tag{1}$$

The spanwise distribution of circulation Γ is used throughout the remainder of this paper instead of the spanwise loading parameter.

Inasmuch as the spanwise distribution of circulation is symmetrical about the root section for angle of attack, pitching, and vertical acceleration and is antisymmetrical for rolling, it is necessary to work with only one half-wing. Accordingly, the right half-wing has been chosen (see fig. 2). The half-wing is divided into two regions: one region external to the Mach cone springing from the leading edge of the tip and the other region internal to this Mach cone. Use of equation (1) yields the following expression for the circulation function Γ (refer to fig. 2 for appropriate regions on the wing and limits of integration):

For $0 \leqq y \leqq y_i$

$$\Gamma = \frac{V}{2}\int_{x_{LE}}^{x_{TE}} \left(\Delta C_P\right)_{ex} dx \tag{2}$$

and for $y_i < y \leqq \frac{b}{2}$

$$\Gamma = \frac{V}{2}\int_{x_{LE}}^{x_{ML}} \left(\Delta C_P\right)_{ex} dx + \frac{V}{2}\int_{x_{ML}}^{x_{TE}} \left(\Delta C_P\right)_{in} dx \tag{3}$$

or

$$\Gamma = \frac{V}{2}\int_{x_{LE}}^{x_{ML}} \left(\Delta C_P\right)_{ex} dx + 2\phi_{in}\Bigg|_{x_{ML}}^{x_{TE}} \tag{4}$$

The functions $\left(\Delta C_P\right)_{ex}$, $\left(\Delta C_P\right)_{in}$, and ϕ_{in} may be obtained from or by use of previously published reports. Reference 2 presents the pressure-difference coefficients for the various wing motions that are valid for the "external" wing region. All expressions for $\left(\Delta C_P\right)_{ex}$ used in the subsequent derivations are obtained from this source. Reference 3 presents approximate expressions for $\left(\Delta C_P\right)_{in}$ and ϕ_{in} for the cases of constant angle of attack and steady rolling velocity;

reference 4 gives these same functions for steady pitching velocity. For the case of constant vertical acceleration, $\left(\Delta C_P\right)_{in}$ is obtained by use of reference 5 in conjunction with the results given in references 3, 4, and 6.

Substituting the appropriate expressions into equations (2) to (4) and performing the indicated operations yields the formulas for Γ. It should be noted that ϕ_{in} and $\left(\Delta C_P\right)_{in}$ as derived in references 3 and 4 are approximate. As discussed in these references, the results obtained by their use are felt to be sufficiently accurate for most practical purposes.

Derivation of Expressions for Spanwise Distributions of Circulation

Constant angle of attack.- For the case of constant angle of attack,

$$\left(\Delta C_P\right)_{ex} = \frac{4m\alpha E''(Bm)}{\sqrt{1 - \left(\frac{y}{mx}\right)^2}} \tag{5}$$

$$\phi_{in} = \frac{2V\alpha}{\pi}\sqrt{\frac{2(y + mx)(b - 2y)}{1 + Bm}} \tag{6}$$

After substitution of these values into equations (2) and (4), integration, and substitution of the limits of integration (see fig. 2), the following formulas are obtained:

For $0 \leqq \frac{y}{b/2} \leqq \frac{y_i}{b/2}$

$$\frac{\Gamma}{V\alpha\frac{b}{2}} = 2E''(Bm)\sqrt{(BmK)^2 - \left(\frac{y}{b/2}\right)^2} \tag{7}$$

and for $\frac{y_i}{b/2} < \frac{y}{b/2} \leqq 1$

$$\frac{\Gamma}{V\alpha\frac{b}{2}} = 2\sqrt{\frac{\left(1 - \frac{y}{b/2}\right)\left[\left(1 + \frac{y}{b/2}\right) + Bm\left(1 - \frac{y}{b/2}\right)\right]}{1 + Bm}}\left[(1 + Bm)E''(Bm) - \frac{4}{\pi}\right] + \frac{8}{\pi}\sqrt{\frac{\left(\frac{y}{b/2} + BmK\right)\left(1 - \frac{y}{b/2}\right)}{1 + Bm}} \tag{8}$$

Steady rolling velocity.- For steady rolling velocity,

$$\left(\Delta C_p\right)_{ex} = \frac{2m^2pI(Bm)}{V}\frac{xy}{\sqrt{m^2x^2 - y^2}} \tag{9}$$

$$\phi_{in} = \frac{p}{3\pi}\frac{2y(2Bm + 1) + b(Bm + 1) - 2mx}{\left(1 + Bm\right)^{3/2}}\sqrt{2(y + mx)(b - 2y)} \tag{10}$$

Substituting these values into equations (2) and (4) and integrating between the proper limits yields:

For $0 \leqq \frac{y}{b/2} \leqq \frac{y_i}{b/2}$

$$\frac{\Gamma}{p\left(\frac{b}{2}\right)^2} = I(Bm)\frac{y}{b/2}\sqrt{\left(BmK\right)^2 - \left(\frac{y}{b/2}\right)^2} \tag{11}$$

and for $\frac{y_i}{b/2} < \frac{y}{b/2} \leqq 1$

$$\frac{\Gamma}{p\left(\frac{b}{2}\right)^2} = \sqrt{\frac{\left(1 - \frac{y}{b/2}\right)\left[1 + \frac{y}{b/2} + Bm\left(1 - \frac{y}{b/2}\right)\right]}{1 + Bm}}\left[I(Bm)\frac{y}{b/2}(1 + Bm) - \frac{8}{3\pi}\frac{\frac{y}{b/2}(3Bm + 1)}{1 + Bm}\right] + \frac{8}{3\pi}\sqrt{\left(\frac{y}{b/2} + BmK\right)\left(1 - \frac{y}{b/2}\right)}\frac{\frac{y}{b/2}(2Bm + 1) + (Bm + 1) - BmK}{(1 + Bm)^{3/2}} \tag{12}$$

<u>Steady pitching velocity</u>.- For steady pitching velocity,

$$\left(\Delta C_P\right)_{ex} = \frac{4qmG(Bm)}{V}\frac{x\left[2 - \left(\frac{y}{mx}\right)^2\right]}{\sqrt{1 - \left(\frac{y}{mx}\right)^2}} \tag{13}$$

$$\phi_{in} = \frac{q}{3\pi(1 + Bm)^{3/2}}\left[2(3 + 2Bm)x + 2B^2my - bB(1 + Bm)\right]\sqrt{2(mx + y)(b - 2y)} \tag{14}$$

Using these values in equations (2) and (4), integrating, and substituting the limits of integration gives the following:

For $0 \leqq \frac{y}{b/2} \leqq \frac{y_i}{b/2}$

$$\frac{\Gamma}{B\left(\frac{b}{2}\right)^2 q} = 2G(Bm)K\sqrt{(BmK)^2 - \left(\frac{y}{b/2}\right)^2} \tag{15}$$

and for $\frac{y_i}{b/2} < \frac{y}{b/2} \leqq 1$

$$\frac{\Gamma}{B\left(\frac{b}{2}\right)^2 q} = 2\sqrt{\frac{\left[\left(1+\frac{y}{b/2}\right)+Bm\left(1-\frac{y}{b/2}\right)\right]\left(1-\frac{y}{b/2}\right)}{1+Bm}}\left(\frac{(1+Bm)\left[1+Bm\left(1-\frac{y}{b/2}\right)\right]G(Bm)}{Bm} - \frac{4}{3\pi(1+Bm)}\left\{\frac{(3+2Bm)\left[1+Bm\left(1-\frac{y}{b/2}\right)\right]}{Bm} + Bm\frac{y}{b/2} - (1+Bm)\right\}\right) + \frac{8}{3\pi(1+Bm)^{3/2}}\left[(3+2Bm)K + Bm\frac{y}{b/2} - (1+Bm)\right]\sqrt{\left(BmK+\frac{y}{b/2}\right)\left(1-\frac{y}{b/2}\right)} \tag{16}$$

Constant vertical acceleration.- For constant vertical acceleration, the expression for ΔC_P for the external region is given by

$$\left(\Delta C_P\right)_{ex} = \frac{4\dot{\alpha}}{VB^2}\left\{M^2 mG(Bm)\frac{x\left[2-\left(\frac{y}{mx}\right)^2\right]}{\sqrt{1-\left(\frac{y}{mx}\right)^2}} - \frac{M^2 mxE''(Bm)}{\sqrt{1-\left(\frac{y}{mx}\right)^2}} - mxE''(Bm)\sqrt{1-\left(\frac{y}{mx}\right)^2}\right\} \tag{17}$$

From the discussion presented on pages 3 and 4 of reference 5, the pressure difference at time $t = 0$ for the angle of attack $\dot{\alpha}t$ is

$$\Delta P = \frac{\dot{\alpha}}{B^2}\left[M^2(\Delta P)_{q=1} - \frac{M^2 x}{V}(\Delta P)_{\alpha=1} - 2\rho X\right] \tag{18}$$

Hence

$$\Delta C_P = \frac{\dot{\alpha}}{B^2}\left[M^2\left(\Delta C_P\right)_{q=1} - \frac{M^2 x}{V}\left(\Delta C_P\right)_{\alpha=1} - \frac{4X}{V^2}\right] \tag{19}$$

where the subscripts $q=1$ and $\alpha=1$ refer to unit pitching velocity and unit angle of attack, respectively (see ref. 5). It is to be noted that $\left(\Delta C_P\right)_{q=1}$ and $\left(\Delta C_P\right)_{\alpha=1}$ for the internal region may be obtained directly by substituting the values $q = 1$ and $\alpha = 1$ into the appropriate expressions for the pressure coefficient given in reference 4 and that the expression for X is given in reference 6. The right-hand side of equation (19) is then readily evaluated as follows:

$$\left(\Delta C_P\right)_{in} = \frac{4\dot{\alpha}}{VB^2}\left\{\frac{M^2\left[6m(3 + 2Bm) + (12 + 8Bm + 2B^2m^2)y - Bmb(1 + Bm)\right]}{3\pi\left(1 + Bm\right)^{3/2}}\sqrt{\frac{\frac{b}{2} - y}{mx + y}} - \right.$$

$$\left. \frac{2M^2mx}{\pi}\sqrt{\frac{\frac{b}{2} - y}{(1 + Bm)(mx + y)}} - \frac{4}{\pi}\sqrt{\frac{(mx + y)\left(\frac{b}{2} - y\right)}{1 + Bm}}\right\} \tag{20}$$

Substituting these expressions for ΔC_P (eqs. (17) and (20)) into equations (2) and (3) and performing the indicated operations results in the following formulas for Γ:

For $0 \leqq \frac{y}{b/2} \leqq \frac{y_i}{b/2}$:

$$\Gamma = \frac{2\dot{\alpha}}{B}\left\{\left(B^2 + 1\right)G(Bm)\left(\frac{b}{2}\right)^2 K\sqrt{(BmK)^2 - \left(\frac{y}{b/2}\right)^2} - \right.$$

$$\left. E''(Bm)\left[\left(1 + \frac{B^2}{2}\right)\left(\frac{b}{2}\right)^2 K\sqrt{(BmK)^2 - \left(\frac{y}{b/2}\right)^2} + \frac{B^2y^2}{2Bm}\cosh^{-1}\left(\frac{BmK}{\frac{y}{b/2}}\right)\right]\right\} \tag{21}$$

and for $\frac{y_i}{b/2} < \frac{y}{b/2} \leqq 1$

$$\Gamma = \frac{2\dot{\alpha}}{B}\left\{\left(\frac{b}{2}\right)^2\left[(B^2 + 1)G(Bm) - \left(\frac{B^2}{2} + 1\right)E''(Bm)\right]\frac{1 + Bm\left(1 - \frac{y}{b/2}\right)}{Bm}\sqrt{\left[1 + \frac{y}{b/2} + Bm\left(1 - \frac{y}{b/2}\right)\right]\left(1 - \frac{y}{b/2}\right)(1 + Bm)} - \right.$$

$$\left.\frac{B^2y^2}{2Bm}E''(Bm)\cosh^{-1}\left[\frac{1 + Bm\left(1 - \frac{y}{b/2}\right)}{\frac{y}{b/2}}\right]\right\} + \frac{8\dot{\alpha}}{3\pi Bm}\left(\frac{b}{2}\right)^2\sqrt{\frac{1 - \frac{y}{b/2}}{(1 + Bm)^3}}\left\{\left[B\left(B^2m^2K + B^2m^2\frac{y}{b/2} + 2BmK + \right.\right.\right.$$

$$\left.2Bm\frac{y}{b/2} + 2\frac{y}{b/2} - Bm - B^2m^2\right) + \frac{1}{B}\left(B^2m^2\frac{y}{b/2} - B^2m^2K - B^2m^2 - Bm\right)\Bigg]\sqrt{BmK + \frac{y}{b/2}} -$$

$$\left.\sqrt{1 + \frac{y}{b/2} + Bm\left(1 - \frac{y}{b/2}\right)}\left[2B\left(1 + Bm + \frac{y}{b/2}\right) + \frac{2}{B}\left(B^2m^2\frac{y}{b/2} - B^2m^2 - Bm\right)\right]\right\} \tag{22}$$

In the foregoing equations, Γ is seen to be a function of B as well as the parameters K, Bm, and $\frac{y}{b/2}$ that appear in the previous formulas. In order to facilitate the calculation and plotting of design charts, equations (21) and (22) have each been divided into two components $\frac{B\Gamma_1}{\dot{\alpha}(b/2)^2}$ and $\frac{\Gamma_2}{B\dot{\alpha}(b/2)^2}$ so as to reduce the number of independent parameters. The circulation Γ is then obtained by adding Γ_1 and Γ_2 $\left(\text{i.e., } \Gamma = \Gamma_1 + \Gamma_2\right)$. The components are given as follows:

For $0 \leqq \frac{y}{b/2} \leqq \frac{y_i}{b/2}$

$$\frac{B\Gamma_1}{\dot{\alpha}(b/2)^2} = K\sqrt{(BmK)^2 - \left(\frac{y}{b/2}\right)^2}\left[2G(Bm) - 2E''(Bm)\right] \tag{23}$$

$$\frac{\Gamma_2}{B\dot{\alpha}(b/2)^2} = K\sqrt{(BmK)^2 - \left(\frac{y}{b/2}\right)^2}\left[2G(Bm) - E''(Bm)\right] - E''(Bm)\frac{\left(\frac{y}{b/2}\right)^2}{Bm}\cosh^{-1}\left(\frac{\frac{BmK}{y}}{b/2}\right) \tag{24}$$

and for $\frac{y_i}{b/2} < \frac{y}{b/2} \leqq 1$

$$\frac{B\Gamma_1}{\dot{\alpha}(b/2)^2} = \sqrt{1 - \frac{y}{b/2}}\left(\frac{8}{3\pi(1 + Bm)^{3/2}}\left\{\sqrt{BmK + \frac{y}{b/2}}\left[-Bm\left(1 - \frac{y}{b/2}\right) - 1 - BmK\right] + 2\sqrt{1 + \frac{y}{b/2} + Bm\left(1 - \frac{y}{b/2}\right)}\left(1 + Bm - Bm\frac{y}{b/2}\right)\right\} + \sqrt{(Bm + 1)\left[1 + \frac{y}{b/2} + Bm\left(1 - \frac{y}{b/2}\right)\right]}\,\frac{1 + Bm\left(1 - \frac{y}{b/2}\right)}{Bm}\left[2G(Bm) - 2E''(Bm)\right]\right) \tag{25}$$

$$\frac{\Gamma_2}{B\dot{\alpha}(b/2)^2} = \frac{8\sqrt{1 - \frac{y}{b/2}}}{Bm(1 + Bm)^{3/2}}\left\{\frac{\sqrt{BmK + \frac{y}{b/2}}}{3\pi}\left[BmK(2 + Bm) - B^2m^2\left(1 - \frac{y}{b/2}\right) + \frac{2y(1 + Bm)}{b/2} - Bm\right] - \sqrt{1 + \frac{y}{b/2} + Bm\left(1 - \frac{y}{b/2}\right)}\left[\frac{2\left(1 + Bm + \frac{y}{b/2}\right)}{3\pi} + (Bm + 1)^2\left(1 + Bm - Bm\frac{y}{b/2}\right)\frac{E''(Bm) - 2G(Bm)}{8}\right]\right\} - \frac{E''(Bm)}{Bm}\left(\frac{y}{b/2}\right)^2\cosh^{-1}\left[\frac{1 + Bm\left(1 - \frac{y}{b/2}\right)}{\frac{y}{b/2}}\right] \tag{26}$$

RESULTS AND DISCUSSION

The foregoing analysis has enabled the evaluation of the spanwise distributions of circulation for sweptback wings of arbitrary aspect ratio and taper ratio at supersonic speeds for which the wing leading edge is subsonic and the wing trailing edge supersonic. The wing tips are parallel to the free-stream direction of flow (herein termed streamwise tips) and the permissible combinations of plan form and Mach number exclude the situation where the Mach cones emanating from the leading edge of the wing tips intersect on the wing itself. The types of wing motions considered and the resulting equations for the spanwise distributions of circulation may be summarized as follows:

	Equations
Constant angle of attack	(7) and (8)
Steady rate of roll	(11) and (12)
Steady rate of pitch	(15) and (16)
Constant vertical acceleration	(23) to (26)

These equations are seen to be functions of the parameters $\frac{y}{b/2}$, Bm, and K. The parameter K is in turn a function of $\frac{y}{b/2}$, AB, Bm, and λ. Thus generalized curves of the spanwise distributions of circulation may be readily computed by considering different combinations of the parameters AB, Bm, and λ. Values of the elliptic functions E"(Bm), G(Bm), and I(Bm) that appear in the equations for the spanwise distributions of circulation have been calculated and are presented in figure 3. The mathematical restrictions governing the permissible combinations of the parameters are given in the section of this paper entitled "Scope."

Calculations have been made for values of AB from 2 to 20, for $\lambda = 0, 0.25, 0.50, 0.75$, and 1.00, and for appropriate values of Bm. Results of the numerical calculations have been prepared in the form of design charts. The curves of spanwise distributions of circulation due to constant angle of attack are shown in figures 4 to 9 and an index to these figures is given in table I. Analogous results for steady rolling velocity, steady pitching velocity, and constant vertical acceleration are shown in figures 10 to 15, 16 to 21, and 22 to 27, respectively. Indexes to these figures are given in tables II, III, and IV, respectively.

It will be noted that in all cases for a finite taper ratio there is a more or less abrupt change in slope at the spanwise station y_i where the tip Mach cone intersects the wing trailing edge. This discontinuity in slope is due to the abrupt change in pressures across the Mach cone boundary (see refs. 3, 4, 6, and 7). The fact that approximate potentials have been used for the tip region is not expected to introduce any appreciable error in calculations involving the use of these circulations. The curves in figures 16 to 21 are for wings pitching about the apex. The spanwise distribution of circulation for a wing pitching about an arbitrary axis located at a distance d from the wing apex is

$$\left(\Gamma q\right)_d = \left(\Gamma q\right)_a - \frac{qd}{\alpha V}\Gamma_\alpha \tag{27}$$

where the subscript q indicates the spanwise distribution of circulation associated with a pitching wing and the subscript α indicates the spanwise distribution of circulation associated with a wing at constant angle of attack. It is frequently desirable to perform calculations for a given static-margin condition, where static-margin is defined as the distance between the center of pressure and the center of gravity

(i.e., $x_{sm} = \bar{x} - d$). It can be shown that the distance d is given as

$$d = -\left[\frac{\left(C_{m_\alpha}\right)_a \bar{c}}{C_{L_\alpha}} + x_{sm}\right] \tag{28}$$

After substitution of equation (28) into equation (27) and some simplification the following expression is obtained:

$$\left[\frac{\Gamma_q}{Bq(b/2)^2}\right]_d = \left[\frac{\Gamma_q}{Bq(b/2)^2}\right]_a + \frac{8\left(1 + \lambda + \lambda^2\right)}{3AB(1 + \lambda)^2} \frac{\Gamma_\alpha}{V\alpha b/2}\left[\frac{\left(C_{m_\alpha}\right)_a}{C_{L_\alpha}} + \frac{x_{sm}}{\bar{c}}\right]. \tag{29}$$

Values of C_{m_α} and C_{L_α} may be obtained from references 2 to 4. Charts for $\left[\frac{\Gamma_q}{Bq(b/2)^2}\right]_a$ are given in figures 16 to 21 $\left(\text{labeled } \frac{\Gamma}{B(b/2)^2 q}\right)$ and charts for $\frac{\Gamma_\alpha}{V\alpha b/2}$ are given in figures 4 to 9 $\left(\text{labeled } \frac{\Gamma}{V\alpha b/2}\right)$. The distribution of circulation along the span for a wing pitching about an arbitrary axis may thus readily be obtained by use of equation (29) in conjunction with the charts presented in this paper.

Some illustrative curves showing the variation of the spanwise distribution of circulation for wings at constant angle of attack with Mach number and with various wing parameters – aspect ratio, taper ratio, leading-edge sweepback – are shown in figure 28. Variations of spanwise distribution of circulation with these same parameters due to steady rolling velocity, steady pitching velocity, and constant vertical acceleration are shown in figures 29, 30, and 31, respectively. In figure 30 the values presented were calculated by using equation (27) for a center of gravity (i.e., pitching axis) located to give a static margin of $0.05\bar{c}$. Variations of the spanwise distribution of circulation with the position of axis of pitch are presented in figure 32. It is to be noted that the spanwise distribution of circulation Γ due to constant vertical acceleration (shown in fig. 31) is the sum, $\Gamma_1 + \Gamma_2$.

CONCLUDING REMARKS

On the basis of linearized supersonic-flow theory, the spanwise distributions of circulation resulting from constant angle of attack, steady rolling velocity, steady pitching velocity, and constant vertical acceleration have been calculated for a series of thin, sweptback, tapered wings with streamwise tips.

Results are applicable for a range of supersonic speeds for which the wing is wholly contained between the Mach cones springing from the wing apex and the trailing edge of the root section, that is, subsonic leading edges and supersonic trailing edges. An added restriction (which, for practical configurations, materially limits the range of Mach numbers for small aspect ratios only) is that the Mach cones emanating from the leading edge of the wing tips may not intersect on the wing.

Generalized design curves are presented which permit rapid estimation of the spanwise distributions of circulation resulting from the various wing motions for given values of aspect ratio, taper ratio, Mach number, and leading-edge sweepback. For illustrative purposes some specific variations of the spanwise distributions of circulation with the aforementioned parameters and axis-of-pitch location are also presented.

Langley Aeronautical Laboratory,
National Advisory Committee for Aeronautics,
Langley Field, Va., September 5, 1952.

REFERENCES

1. Martin, John C., and Jeffreys, Isabella: Span Load Distributions Resulting From Angle of Attack, Rolling, and Pitching for Tapered Sweptback Wings with Streamwise Tips. Supersonic Leading and Trailing Edges. NACA TN 2643, 1952.

2. Malvestuto, Frank S., Jr., and Margolis, Kenneth: Theoretical Stability Derivatives of Thin Sweptback Wings Tapered to a Point With Sweptback or Sweptforward Trailing Edges for a Limited Range of Supersonic Speeds. NACA Rep. 971, 1950. (Supersedes NACA TN 1761.)

3. Malvestuto, Frank S., Jr., Margolis, Kenneth, and Ribner, Herbert S.: Theoretical Lift and Damping in Roll at Supersonic Speeds of Thin Sweptback Tapered Wings With Streamwise Tips, Subsonic Leading Edges, and Supersonic Trailing Edges. NACA Rep. 970, 1950. (Supersedes NACA TN 1860.)

4. Malvestuto, Frank S., Jr., and Hoover, Dorothy M.: Lift and Pitching Derivatives of Thin Sweptback Tapered Wings With Streamwise Tips and Subsonic Leading Edges at Supersonic Speeds. NACA TN 2294, 1951.

5. Ribner, Herbert S., and Malvestuto, Frank S., Jr.: Stability Derivatives of Triangular Wings at Supersonic Speeds. NACA Rep. 908, 1948. (Supersedes NACA TN 1572.)

6. Malvestuto, Frank S., Jr., and Hoover, Dorothy M.: Supersonic Lift and Pitching Moment of Thin Sweptback Tapered Wings Produced by Constant Vertical Acceleration. Subsonic Leading Edges and Supersonic Trailing Edges. NACA TN 2315, 1951.

7. Cohen, Doris: The Theoretical Lift of Flat Swept-Back Wings at Supersonic Speeds. NACA TN 1555, 1948.

TABLE I

INDEX TO CURVES FOR SPANWISE DISTRIBUTION OF CIRCULATION

DUE TO CONSTANT ANGLE OF ATTACK, $\frac{\Gamma}{V\alpha b/2}$

λ	AB	Figure	Page
0 (Delta wing)	2	4	27
	3		
	4		
0	2	5(a)	28
	3	5(b)	29
	4	5(c)	30
	5	5(d)	31
	6	5(e)	32
	8	5(f)	33
	10	5(g)	34
	12	5(h)	35
	15	5(i)	36
	20	5(j)	37
.25	2	6(a)	38
	3	6(b)	39
	4	6(c)	40
	5	6(d)	41
	6	6(e)	42
	8	6(f)	43
	10	6(g)	44
	12	6(h)	45
	15	6(i)	46
	20	6(j)	47

λ	AB	Figure	Page
0.50	2	7(a)	48
	3	7(b)	49
	4	7(c)	50
	5	7(d)	51
	6	7(e)	52
	8	7(f)	53
	10	7(g)	54
	12	7(h)	55
	15	7(i)	56
	20	7(j)	57
.75	2	8(a)	58
	3	8(b)	59
	4	8(c)	60
	5	8(d)	61
	6	8(e)	62
	8	8(f)	63
	10	8(g)	64
	12	8(h)	65
	15	8(i)	66
	20	8(j)	67
1.00	2	9(a)	68
	3		
	4		
	5		
	6		
	8	9(b)	69
	10		
	12		
	15		
	20		

TABLE II

INDEX TO CURVES FOR SPANWISE DISTRIBUTION OF CIRCULATION

DUE TO STEADY ROLLING VELOCITY, $\frac{\Gamma}{p\left(\frac{b}{2}\right)^2}$

λ	AB	Figure	Page
0 (Delta wing)	2	10	70
	3		
	4		
0	2	11(a)	71
	3	11(b)	72
	4	11(c)	73
	5	11(d)	74
	6	11(e)	75
	8	11(f)	76
	10	11(g)	77
	12	11(h)	78
	15	11(i)	79
	20	11(j)	80
.25	2	12(a)	81
	3	12(b)	82
	4	12(c)	83
	5	12(d)	84
	6	12(e)	85
	8	12(f)	86
	10	12(g)	87
	12	12(h)	88
	15	12(i)	89
	20	12(j)	90
0.50	2	13(a)	91
	3	13(b)	92
	4	13(c)	93
	5	13(d)	94
	6	13(e)	95
	8	13(f)	96
	10	13(g)	97
	12	13(h)	98
	15	13(i)	99
	20	13(j)	100
.75	2	14(a)	101
	3	14(b)	102
	4	14(c)	103
	5	14(d)	104
	6	14(e)	105
	8	14(f)	106
	10	14(g)	107
	12	14(h)	108
	15	14(i)	109
	20	14(j)	110
1.00	2	15(a)	111
	3		
	4		
	5		
	6		
	8	15(b)	112
	10		
	12		
	15		
	20		

NACA

TABLE III

INDEX TO CURVES FOR SPANWISE DISTRIBUTION OF CIRCULATION

DUE TO STEADY PITCHING VELOCITY, $\frac{\Gamma}{B\left(\frac{b}{2}\right)^2 q}$

[Wing pitching about apex]

λ	AB	Figure	Page
0 (Delta wing)	2	16	113
	3		
	4		
0	2	17(a)	114
	3	17(b)	115
	4	17(c)	116
	5	17(d)	117
	6	17(e)	118
	8	17(f)	119
	10	17(g)	120
	12	17(h)	121
	15	17(i)	122
	20	17(j)	123
.25	2	18(a)	124
	3	18(b)	125
	4	18(c)	126
	5	18(d)	127
	6	18(e)	128
	8	18(f)	129
	10	18(g)	130
	12	18(h)	131
	15	18(i)	132
	20	18(j)	133

λ	AB	Figure	Page
0.50	2	19(a)	134
	3	19(b)	135
	4	19(c)	136
	5	19(d)	137
	6	19(e)	138
	8	19(f)	139
	10	19(g)	140
	12	19(h)	141
	15	19(i)	142
	20	19(j)	143
.75	2	20(a)	144
	3	20(b)	145
	4	20(c)	146
	5	20(d)	147
	6	20(e)	148
	8	20(f)	149
	10	20(g)	150
	12	20(h)	151
	15	20(i)	152
	20	20(j)	153
1.00	2	21(a)	154
	3		
	4		
	5		
	6		
	8	21(b)	155
	10		
	12		
	15		
	20		

NACA

TABLE IV

INDEX TO CURVES FOR SPANWISE DISTRIBUTION OF CIRCULATION

DUE TO CONSTANT VERTICAL ACCELERATION, $\frac{B\Gamma_1}{\dot{\alpha}\left(\frac{b}{2}\right)^2}$ and $\frac{\Gamma_2}{B\dot{\alpha}\left(\frac{b}{2}\right)^2}$

$\left[\Gamma = \Gamma_1 + \Gamma_2\right]$

λ	AB	Figure	Page
0 (Delta wing)	2	22	156
	3		
	4		
0	2	23(a)	158
	3	23(b)	160
	4	23(c)	162
	5	23(d)	164
	6	23(e)	165
	8	23(f)	166
	10	23(g)	167
	12	23(h)	168
	15	23(i)	169
	20	23(j)	170
.25	2	24(a)	171
	3	24(b)	173
	4	24(c)	175
	5	24(d)	177
	6	24(e)	178
	8	24(f)	179
	10	24(g)	180
	12	24(h)	181
	15	24(i)	182
	20	24(j)	183

λ	AB	Figure	Page
0.50	2	25(a)	184
	3	25(b)	186
	4	25(c)	188
	5	25(d)	189
	6	25(e)	190
	8	25(f)	191
	10	25(g)	192
	12	25(h)	193
	15	25(i)	194
	20	25(j)	195
.75	2	26(a)	196
	3	26(b)	198
	4	26(c)	200
	5	26(d)	201
	6	26(e)	202
	8	26(f)	203
	10	26(g)	204
	12	26(h)	205
	15	26(i)	206
	20	26(j)	207
1.00	2	27(a)	208
	3		
	4		
	5		
	6		
	8	27(b)	210
	10		
	12		
	15		
	20		

NACA

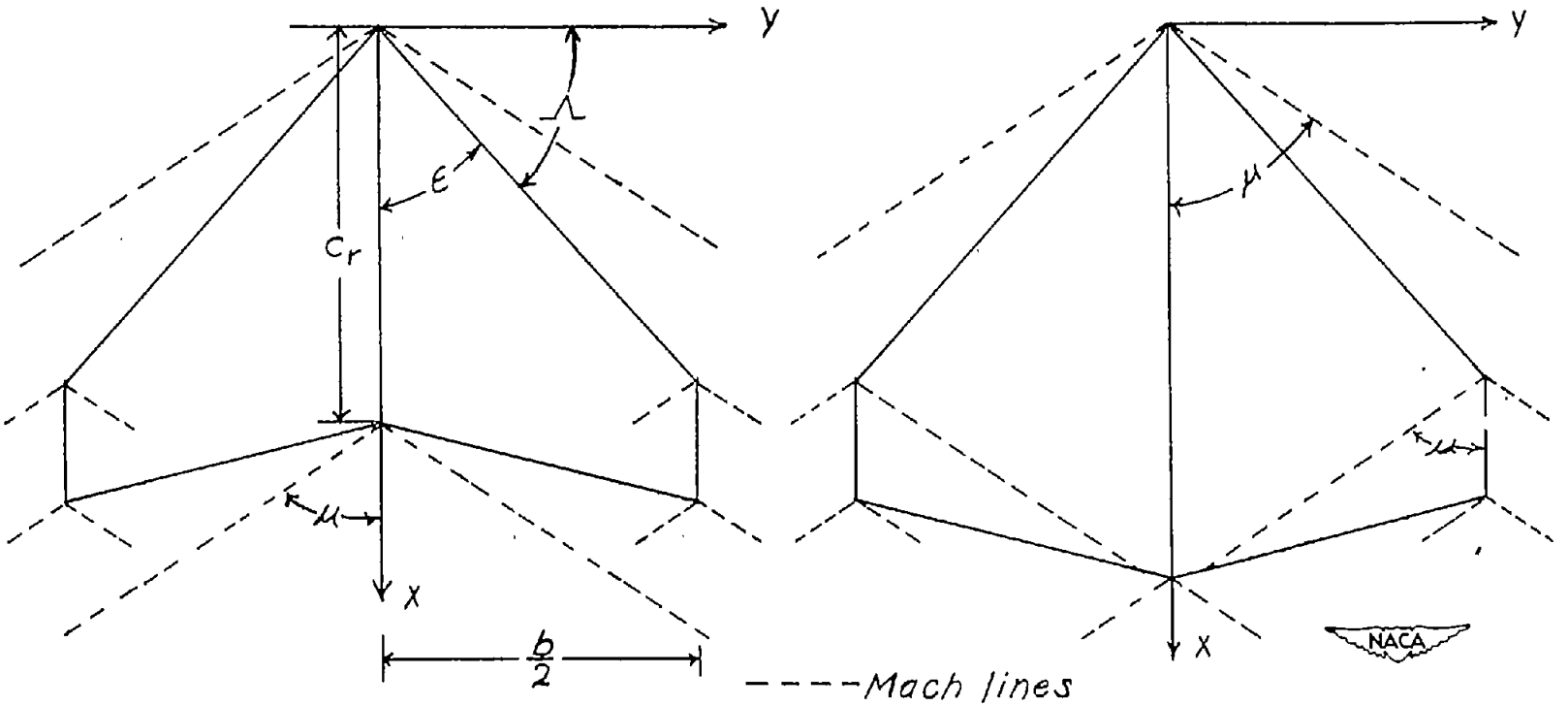

(a) Sweptback trailing edge. (b) Sweptforward trailing edge.

Figure 1.- Sweptback tapered wing with streamwise tips and either sweptback or sweptforward trailing edges. Note that trailing edge is always inclined at an angle greater than the Mach angle and that the Mach cones emanating from the wing tips do not intersect on the wing.

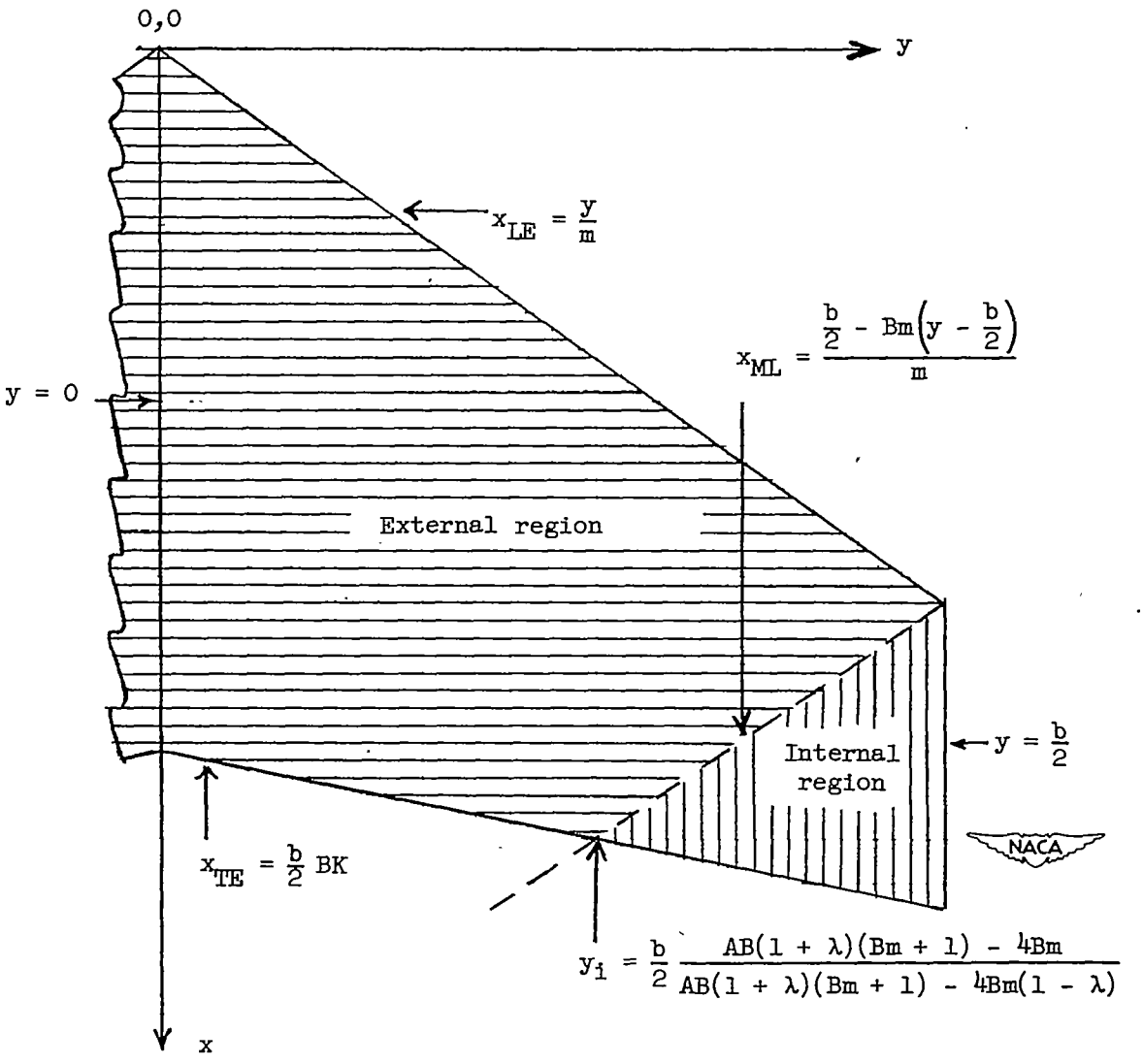

Figure 2.- Sketch of right half-wing showing regions and limits of integration for evaluation of span loads.

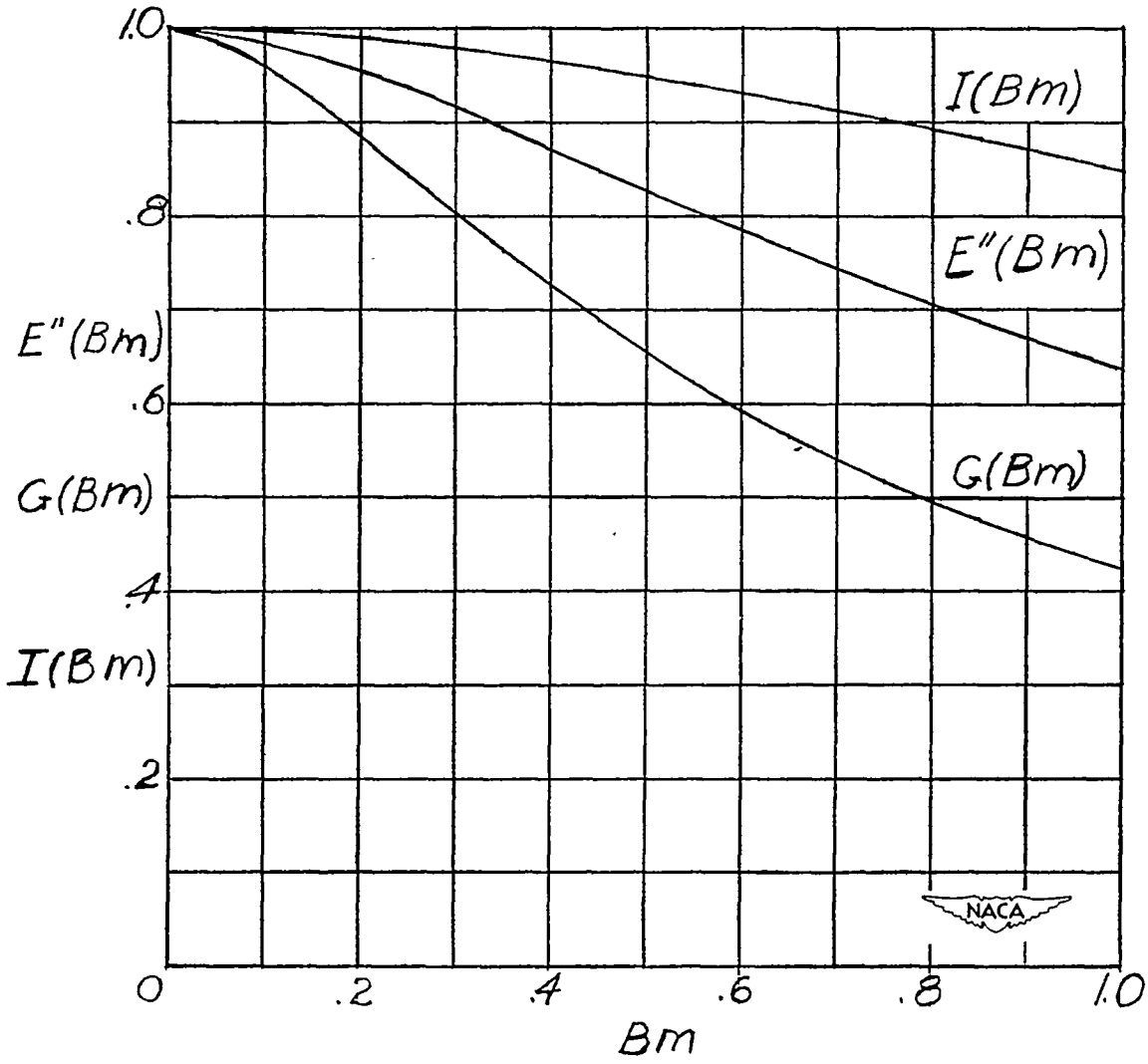

Figure 3.- Variation of elliptic integral functions with $Bm = B \cot \Lambda$.

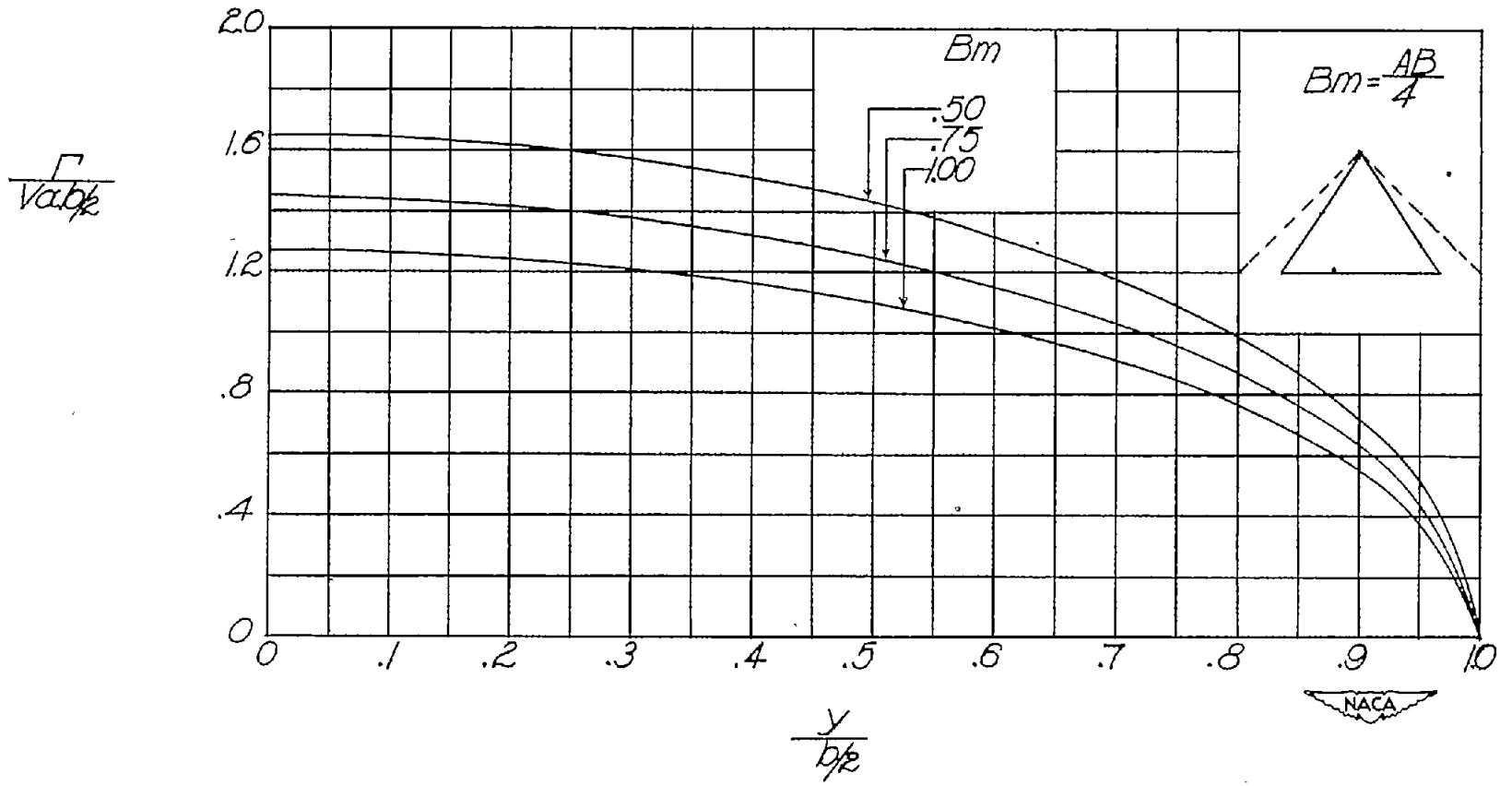

Figure 4.- Distribution of circulation along span for delta wing at constant angle of attack.

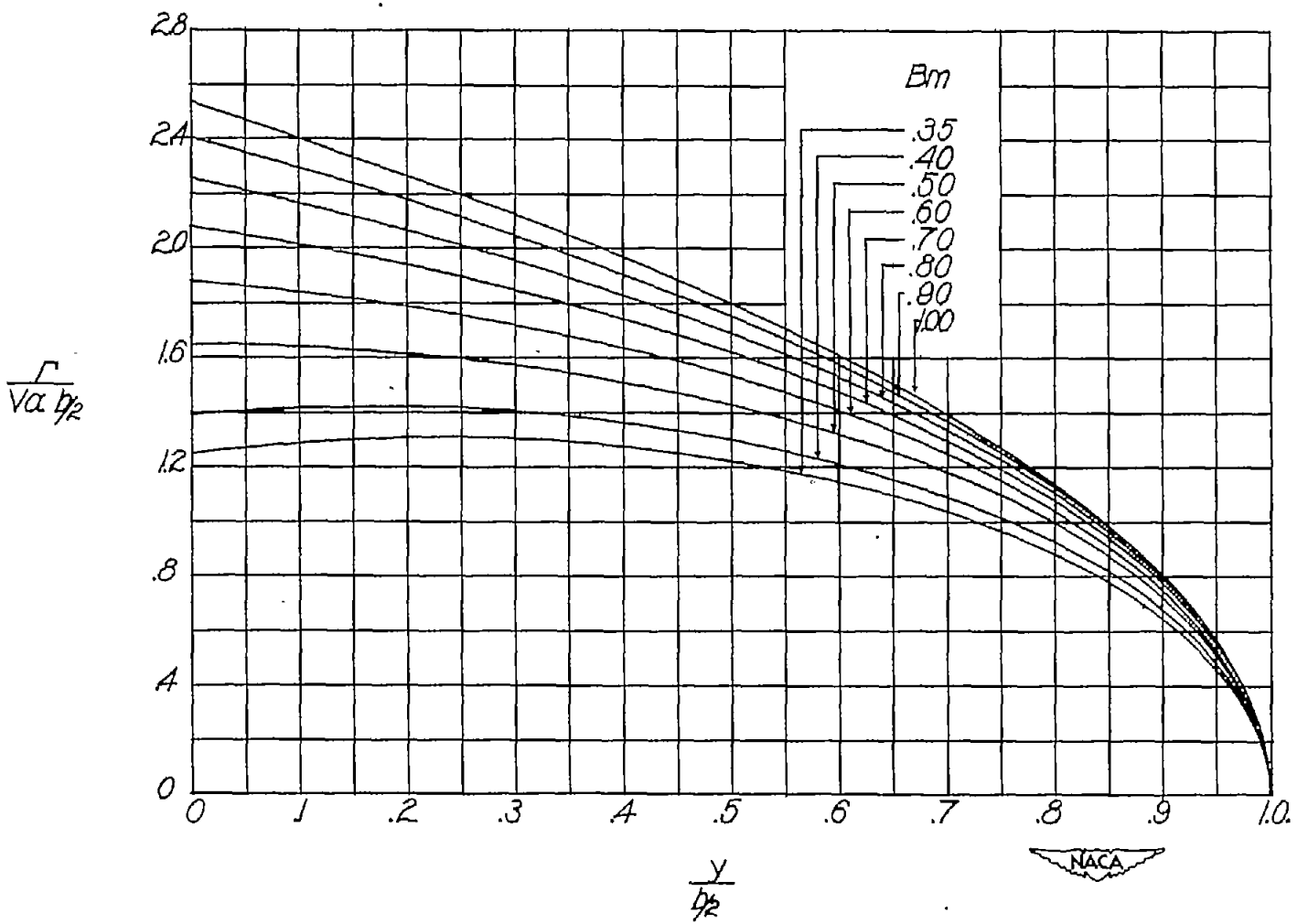

(a) AB = 2.

Figure 5.- Distribution of circulation along span for wings at constant angle of attack with $\lambda = 0$.

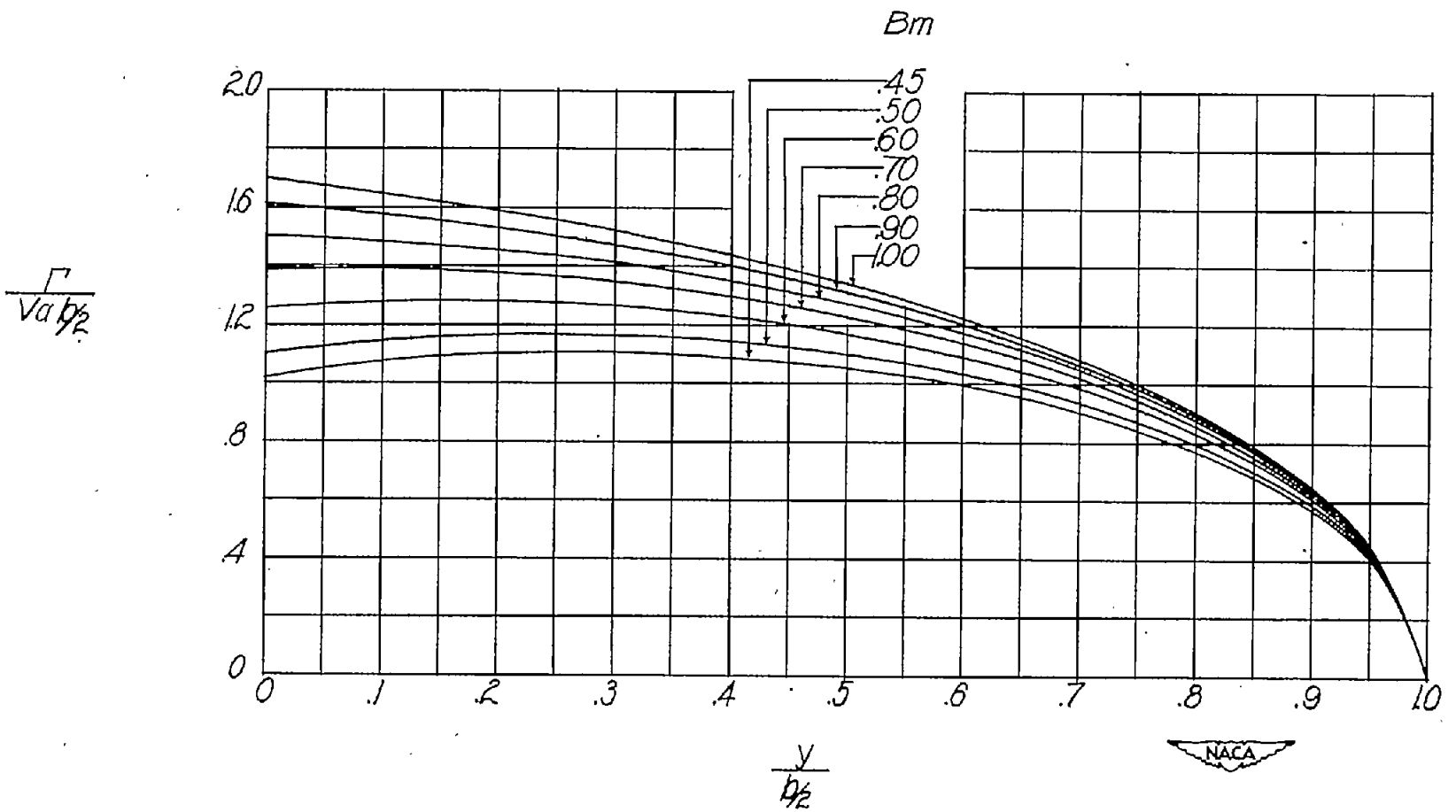

(b) AB = 3.

Figure 5.- Continued.

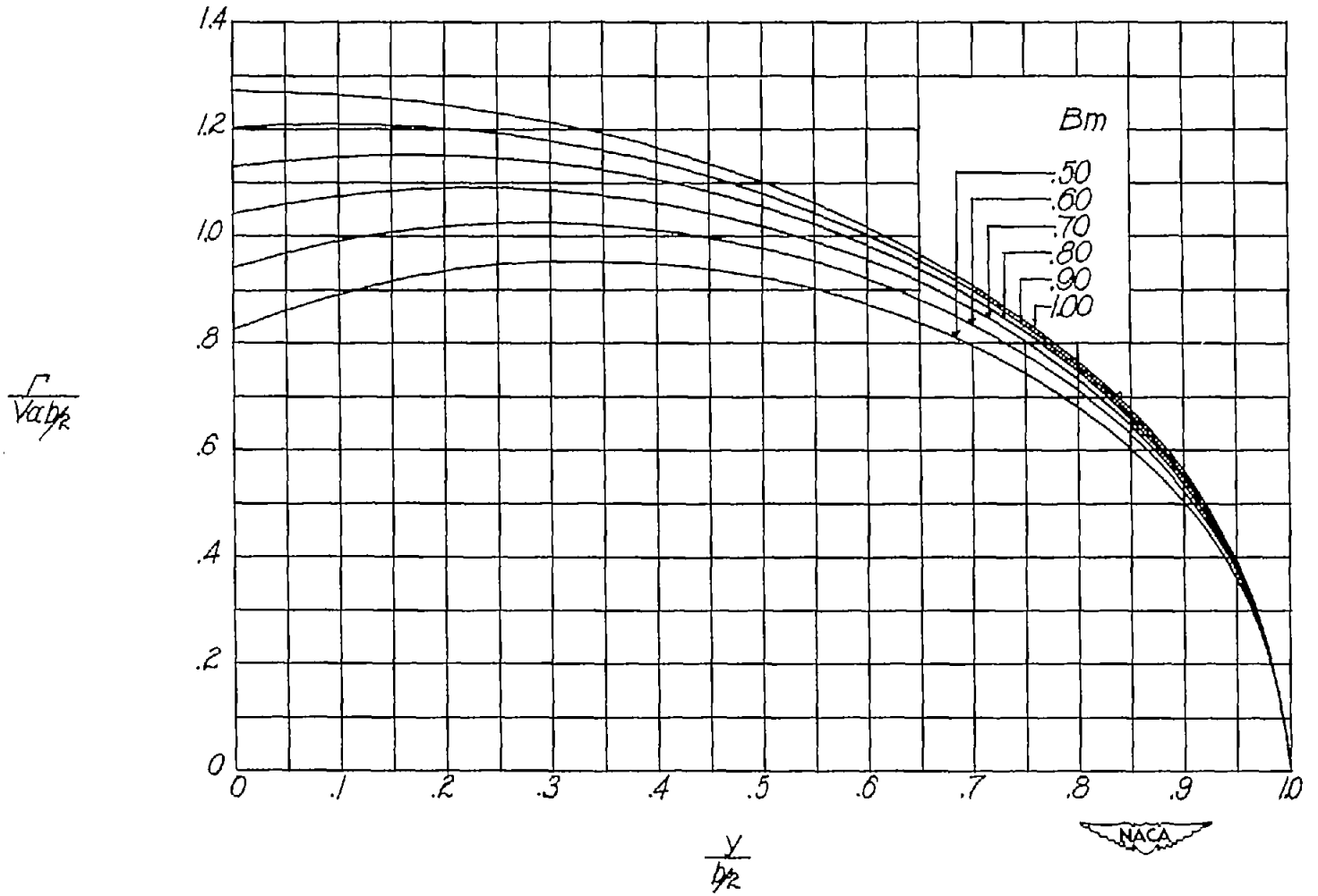

(c) AB = 4.

Figure 5.- Continued.

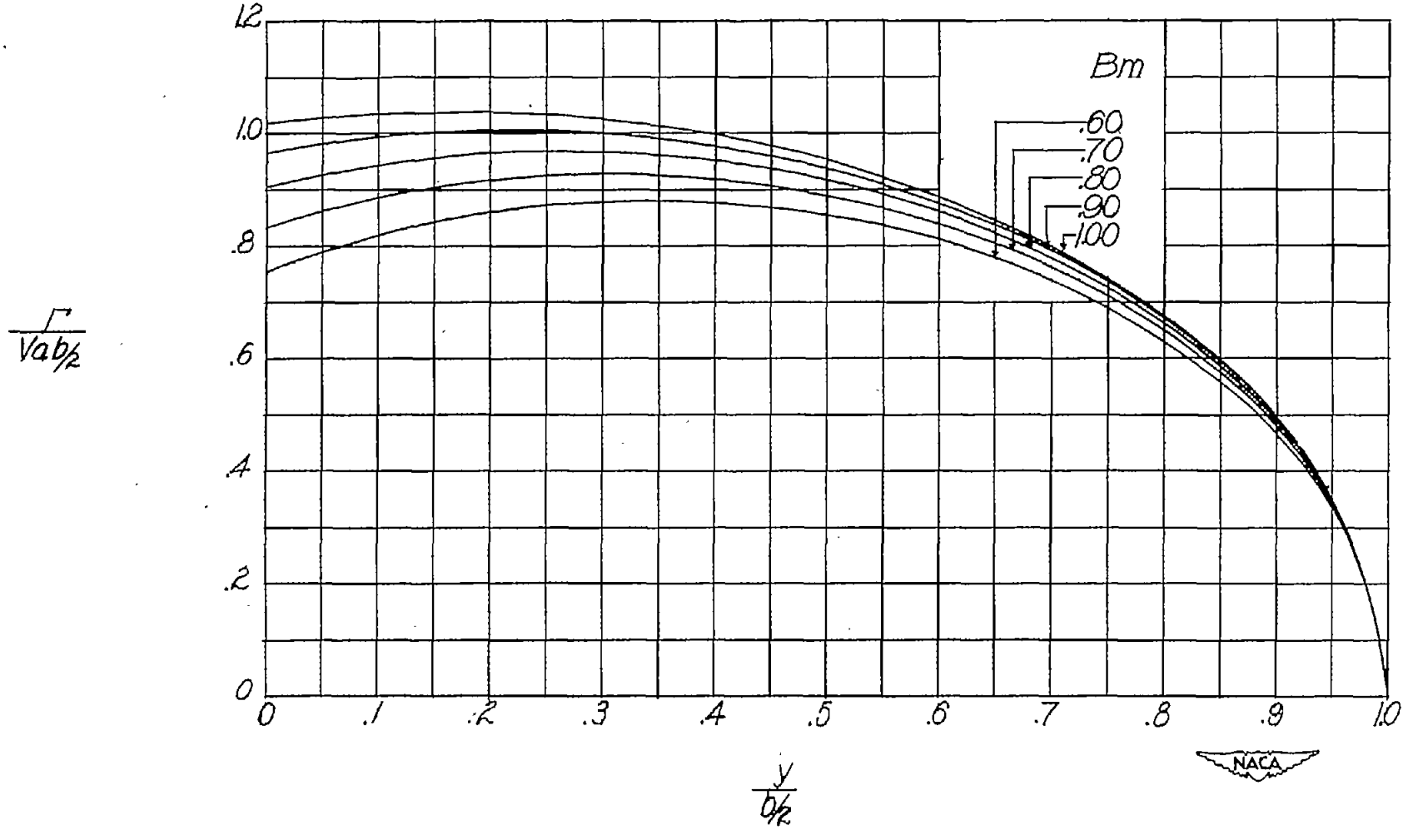

(d) AB = 5.

Figure 5.- Continued.

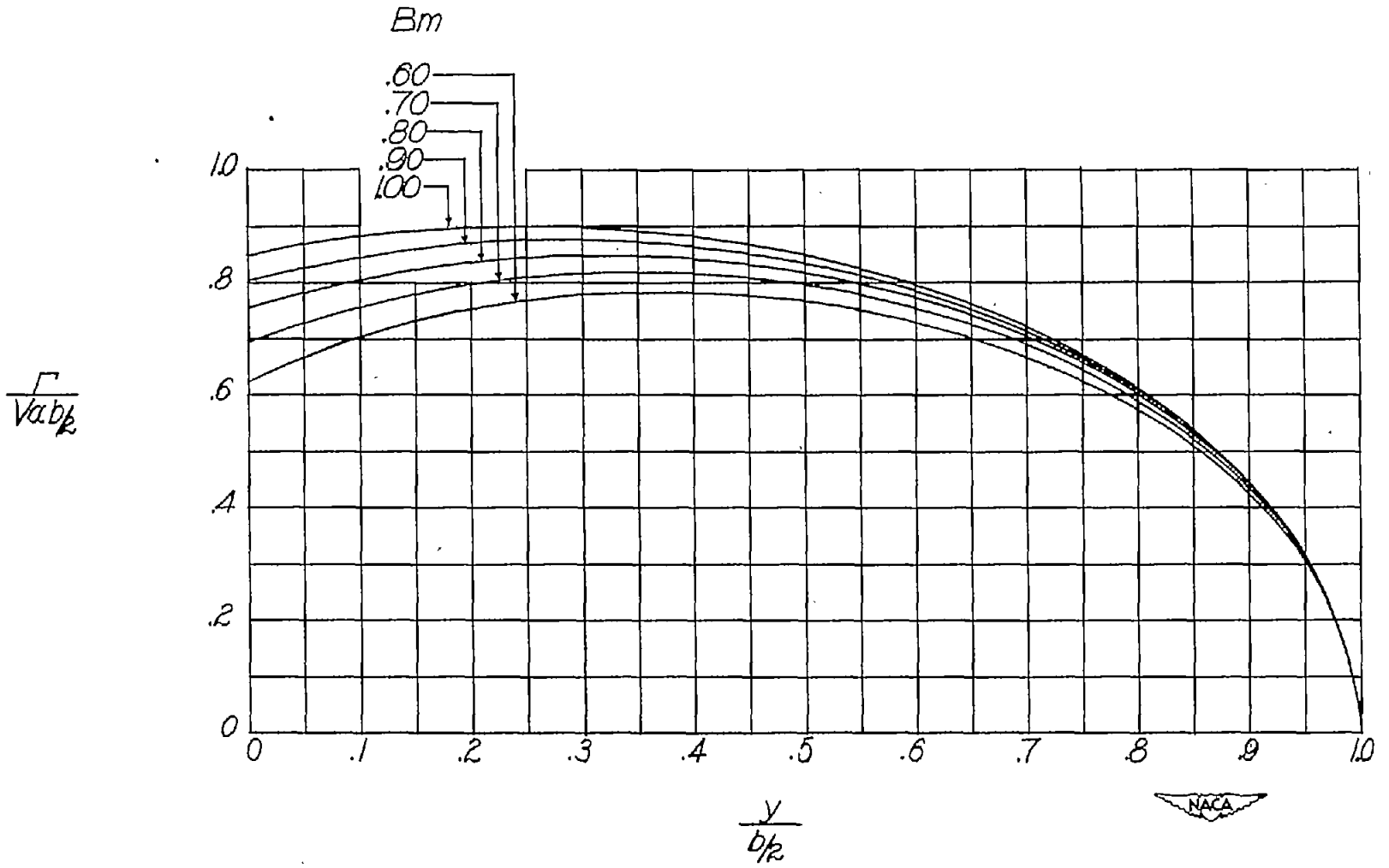

(e) AB = 6.

Figure 5.- Continued.

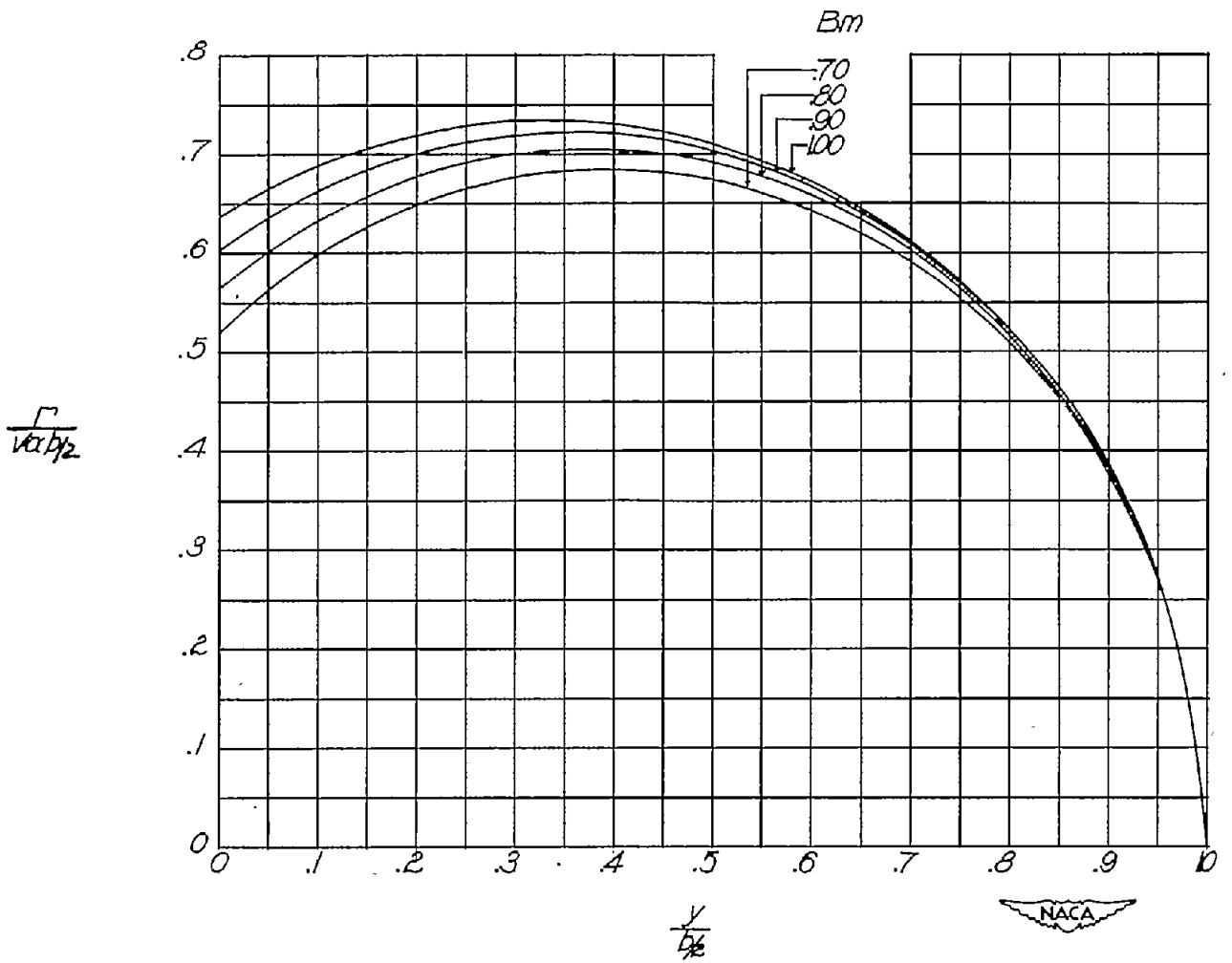

(f) AB = 8.

Figure 5.- Continued.

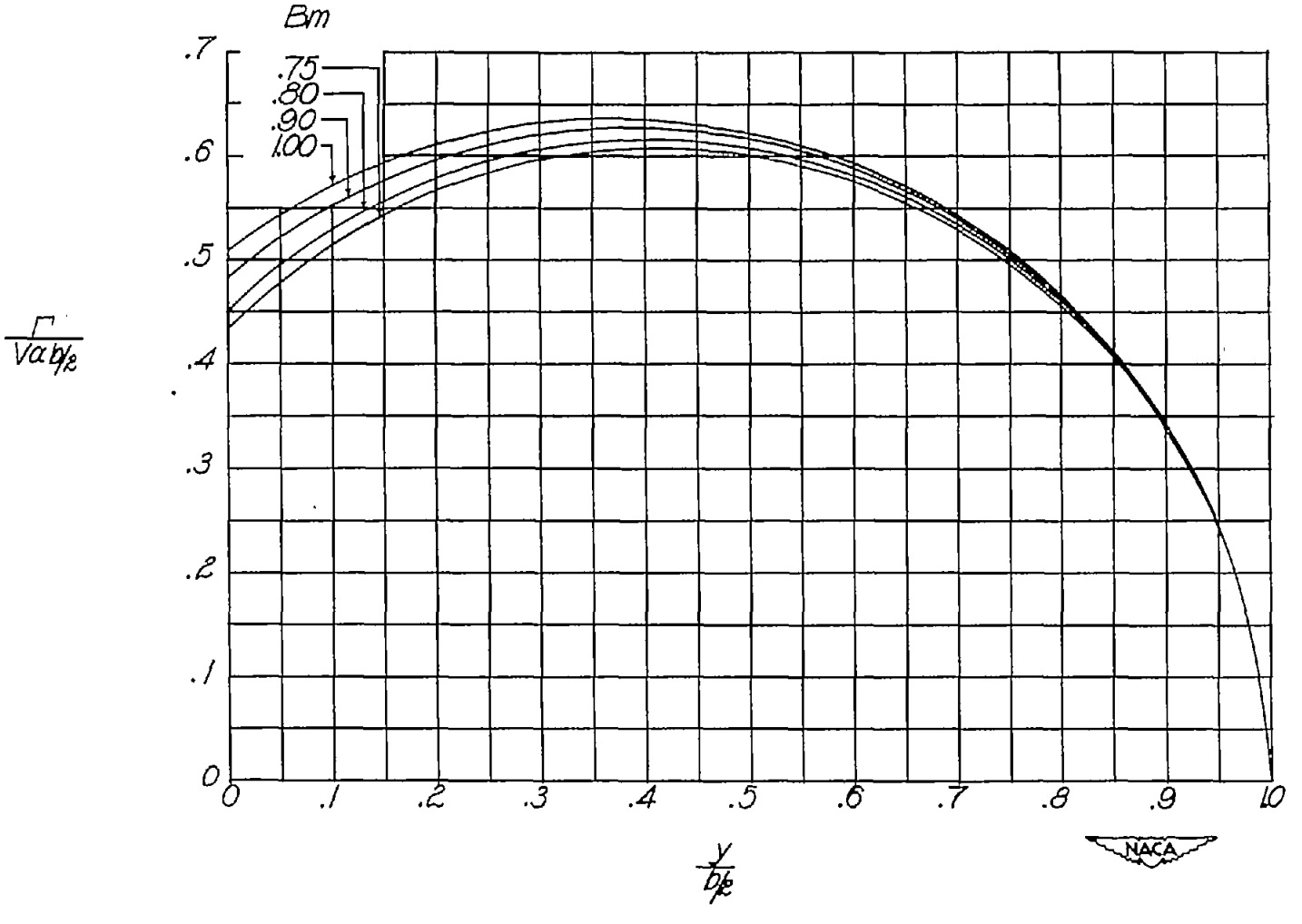

(g) AB = 10.

Figure 5.- Continued.

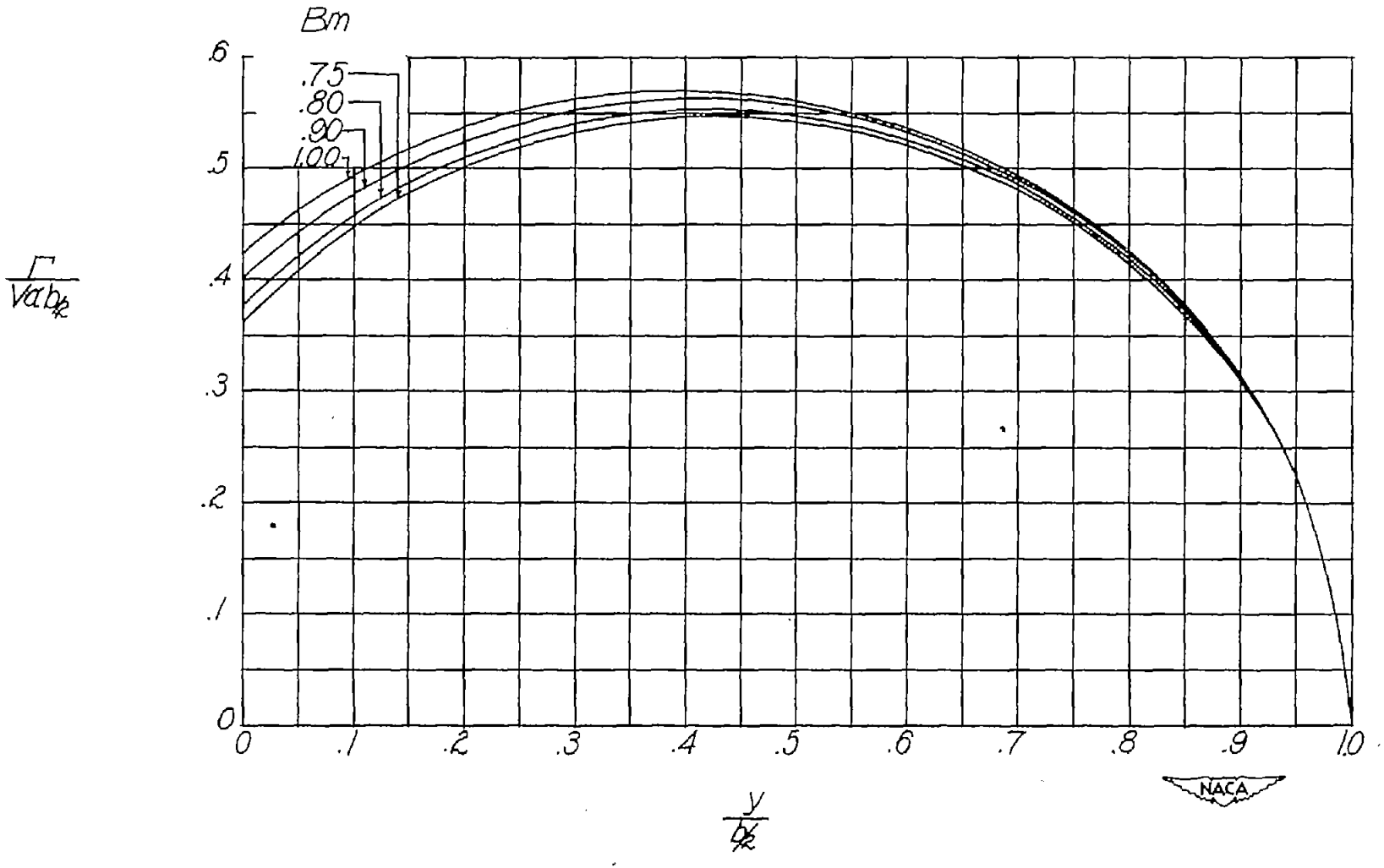

(h) AB = 12.

Figure 5.- Continued.

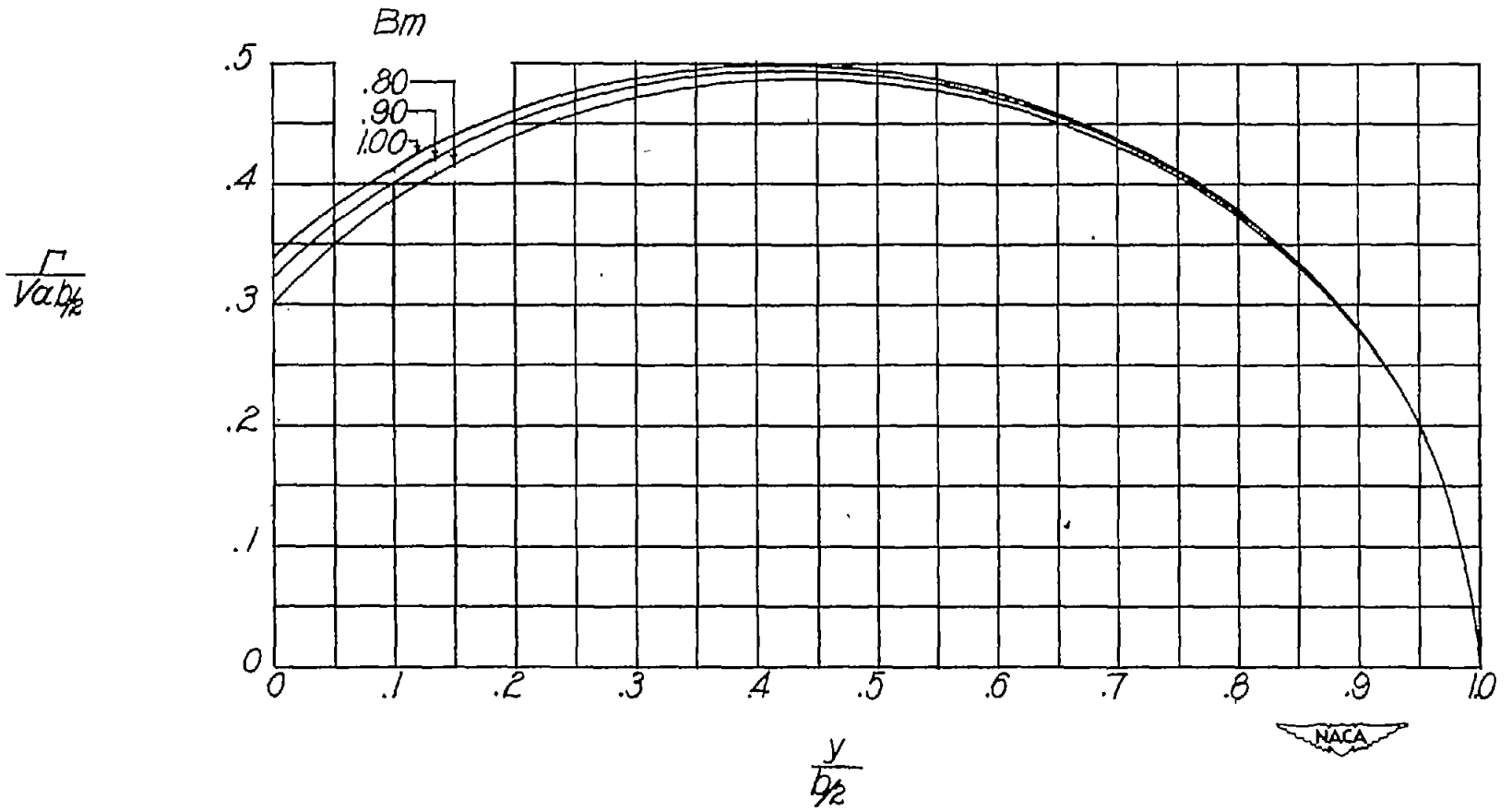

(i) AB = 15.

Figure 5.- Continued.

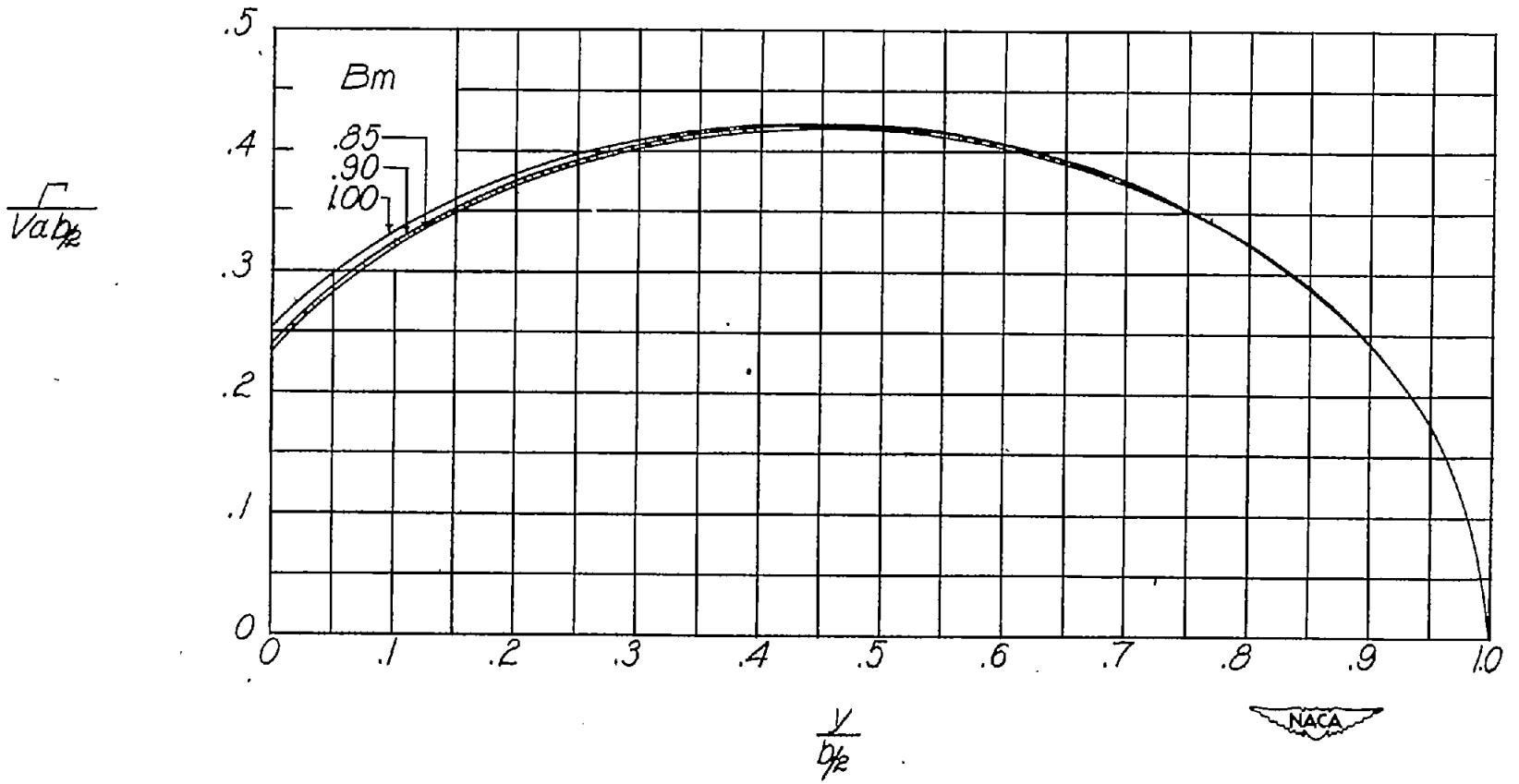

(j) AB = 20.

Figure 5.- Concluded.

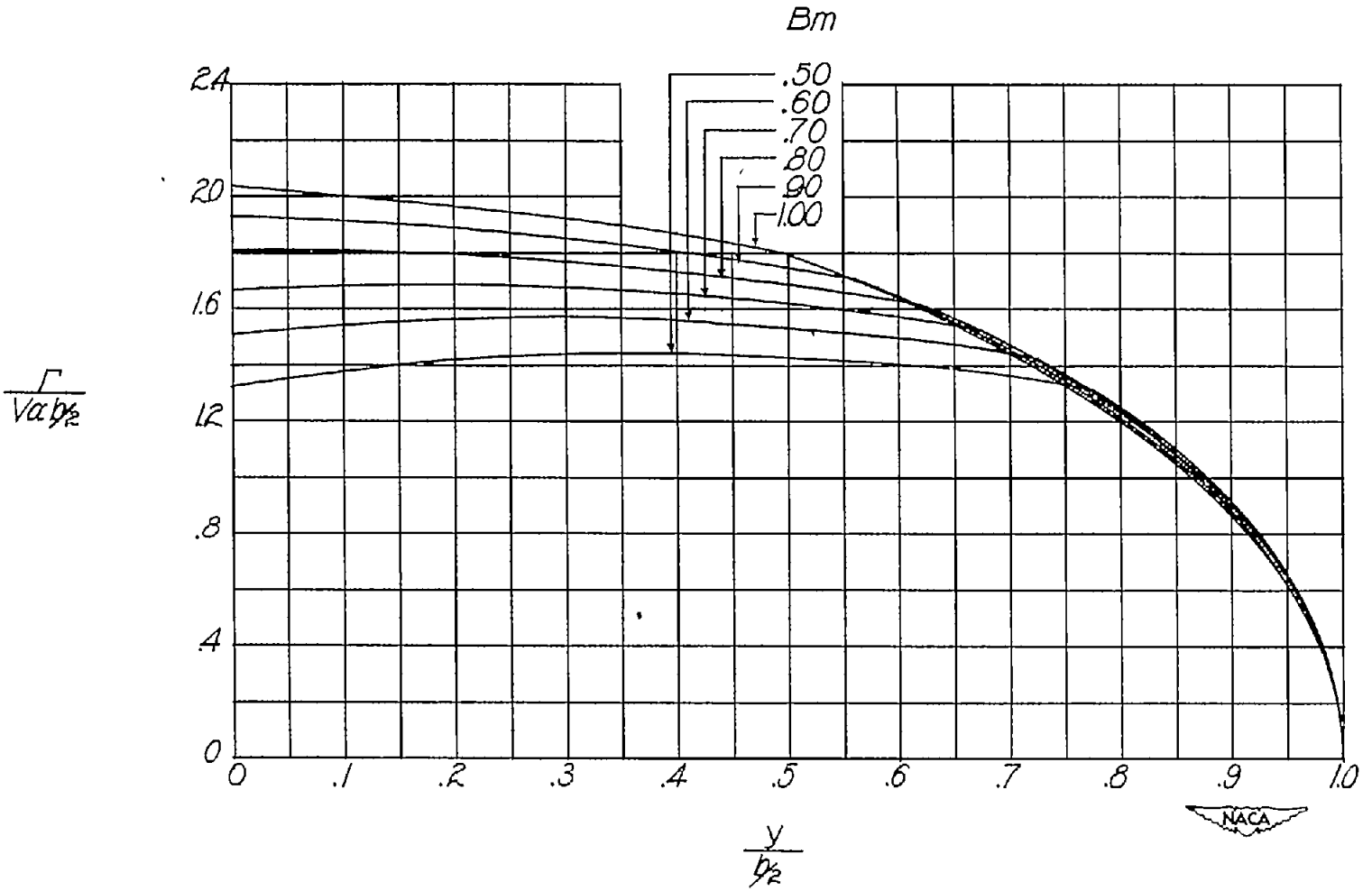

(a) AB = 2.

Figure 6.- Distribution of circulation along span for wings at constant angle of attack with $\lambda = 0.25$.

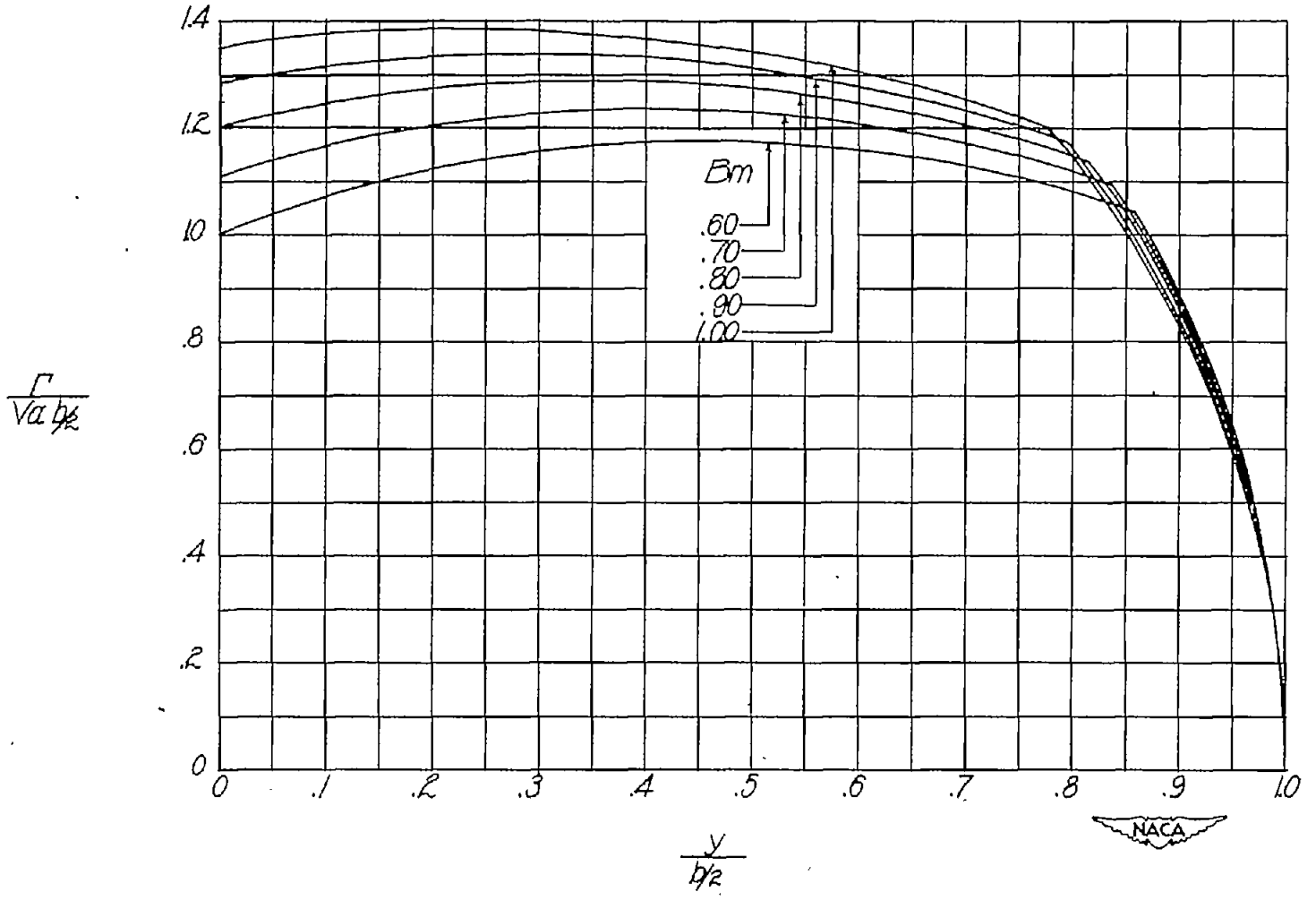

(b) AB = 3.

Figure 6.- Continued.

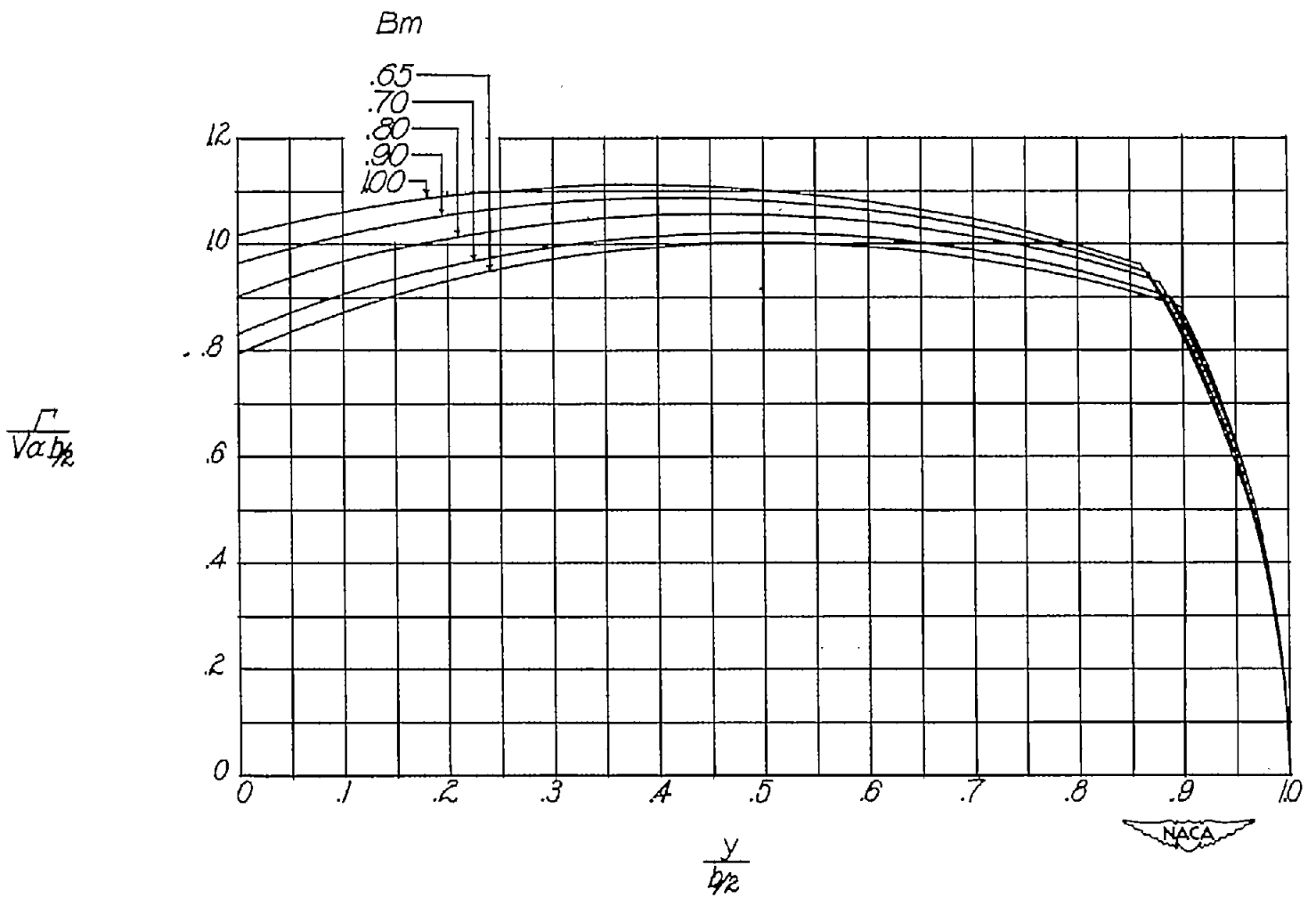

(c) AB = 4.

Figure 6.- Continued.

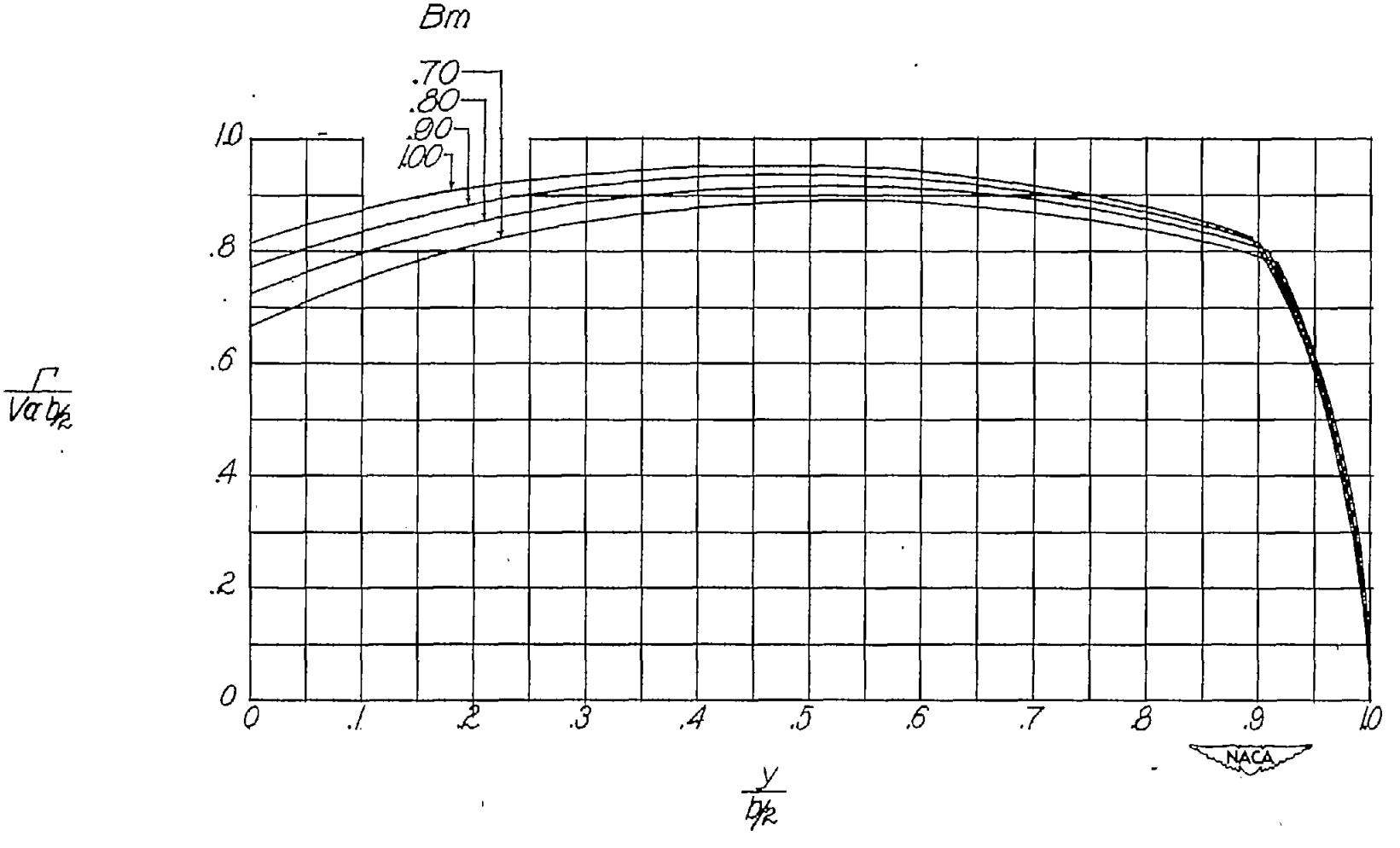

(d) AB = 5.

Figure 6.- Continued.

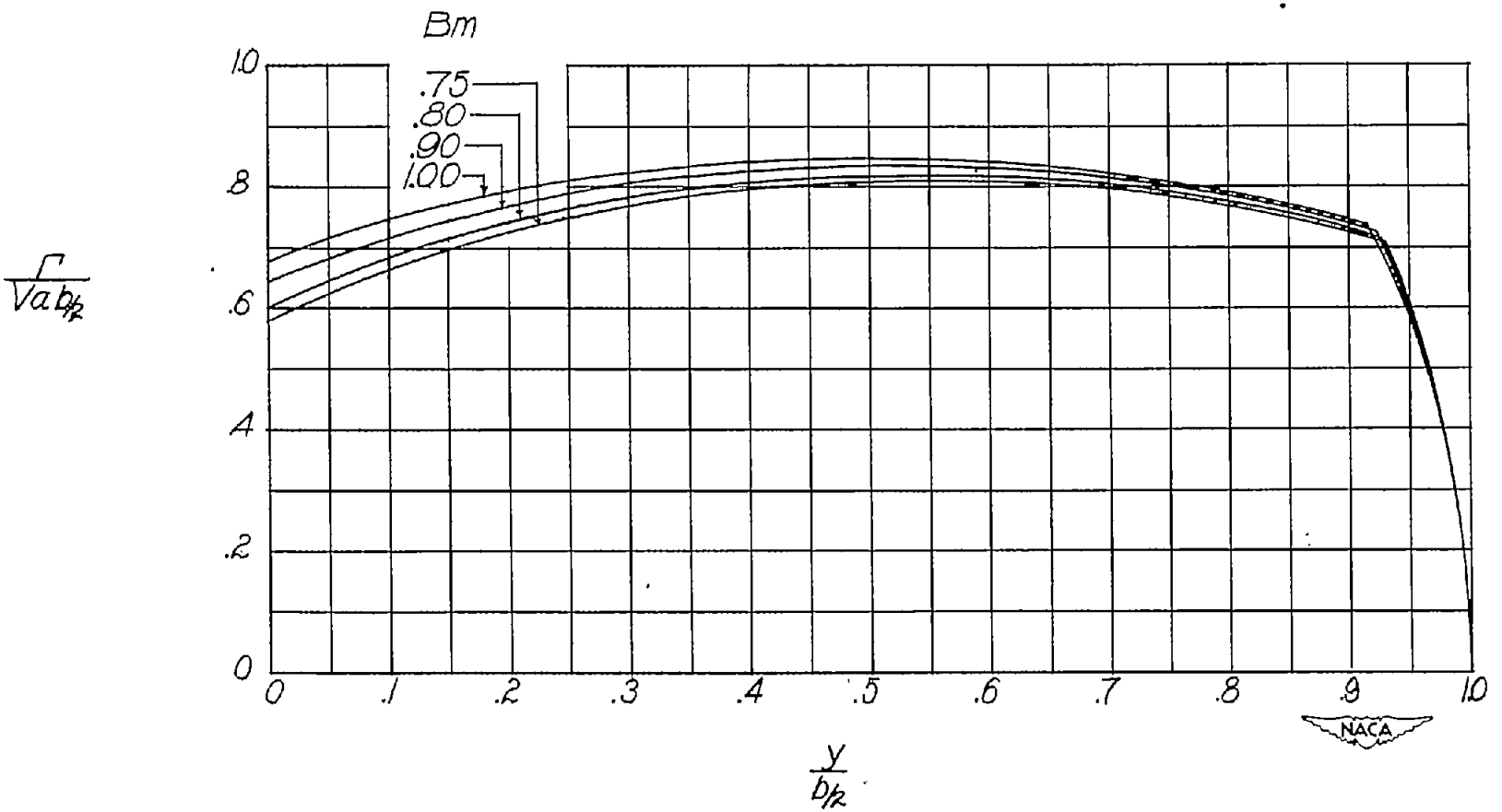

(e) AB = 6.

Figure 6.- Continued.

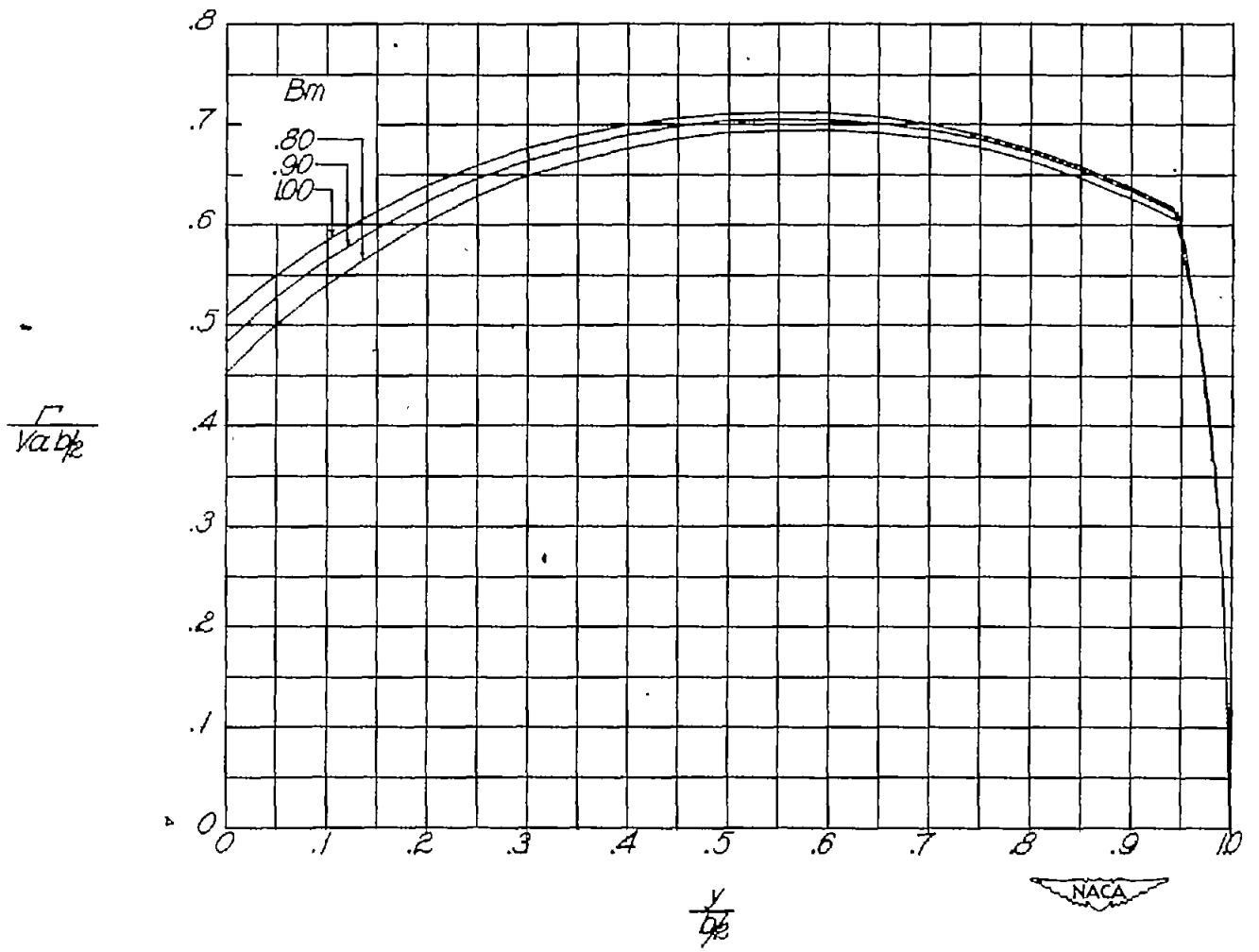

(f) AB = 8.

Figure 6.- Continued.

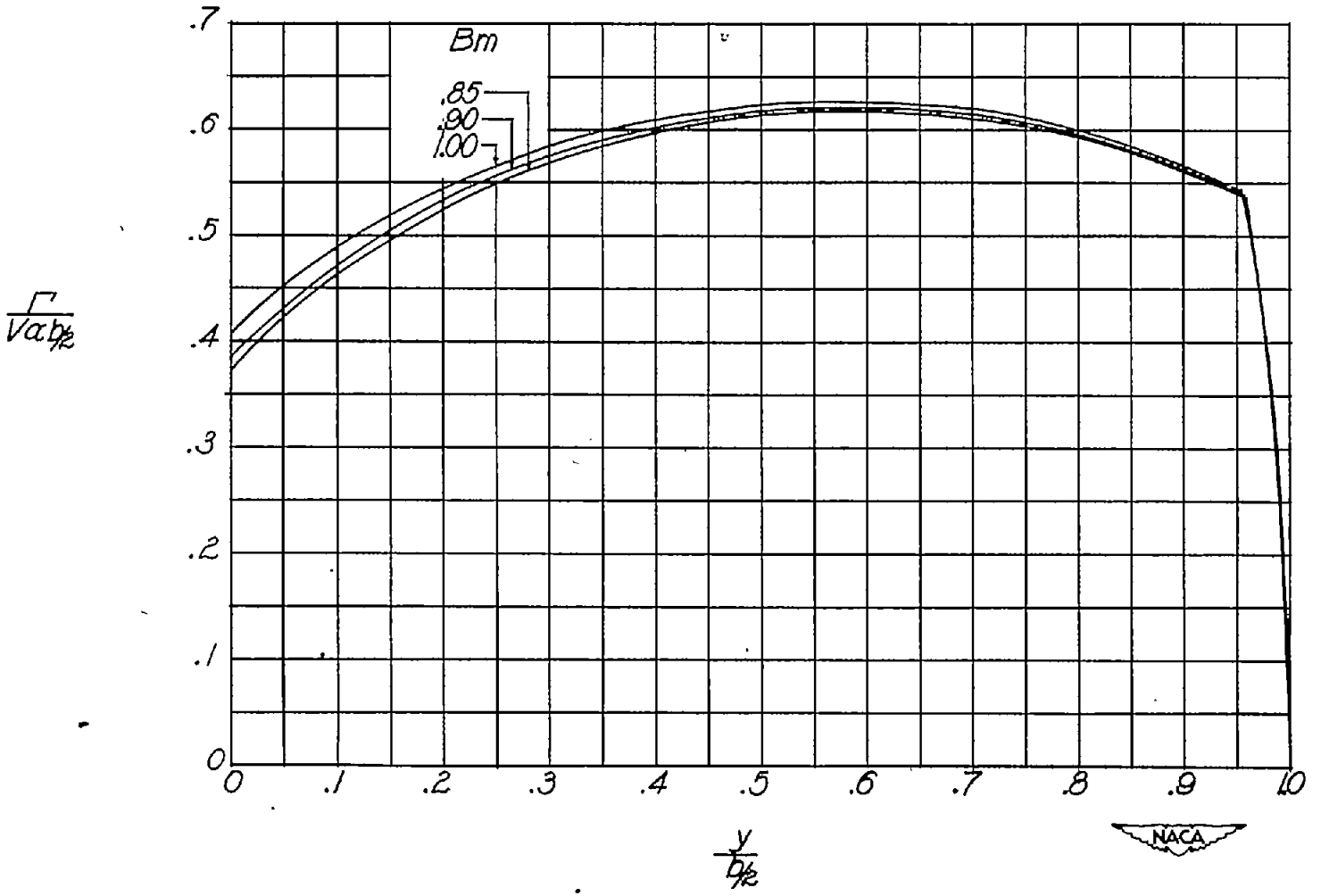

(g) AB = 10.

Figure 6.- Continued.

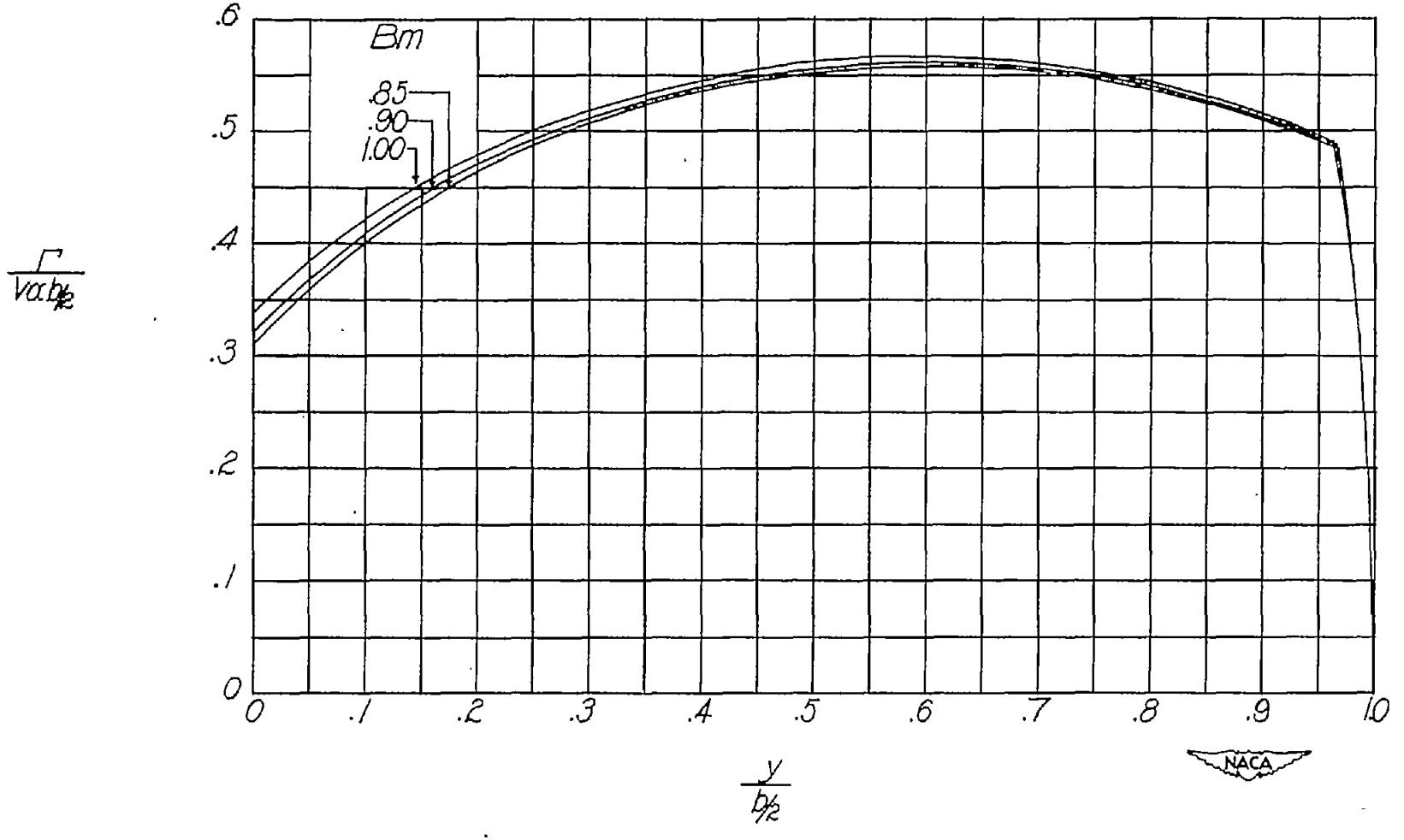

(h) AB = 12.

Figure 6.- Continued.

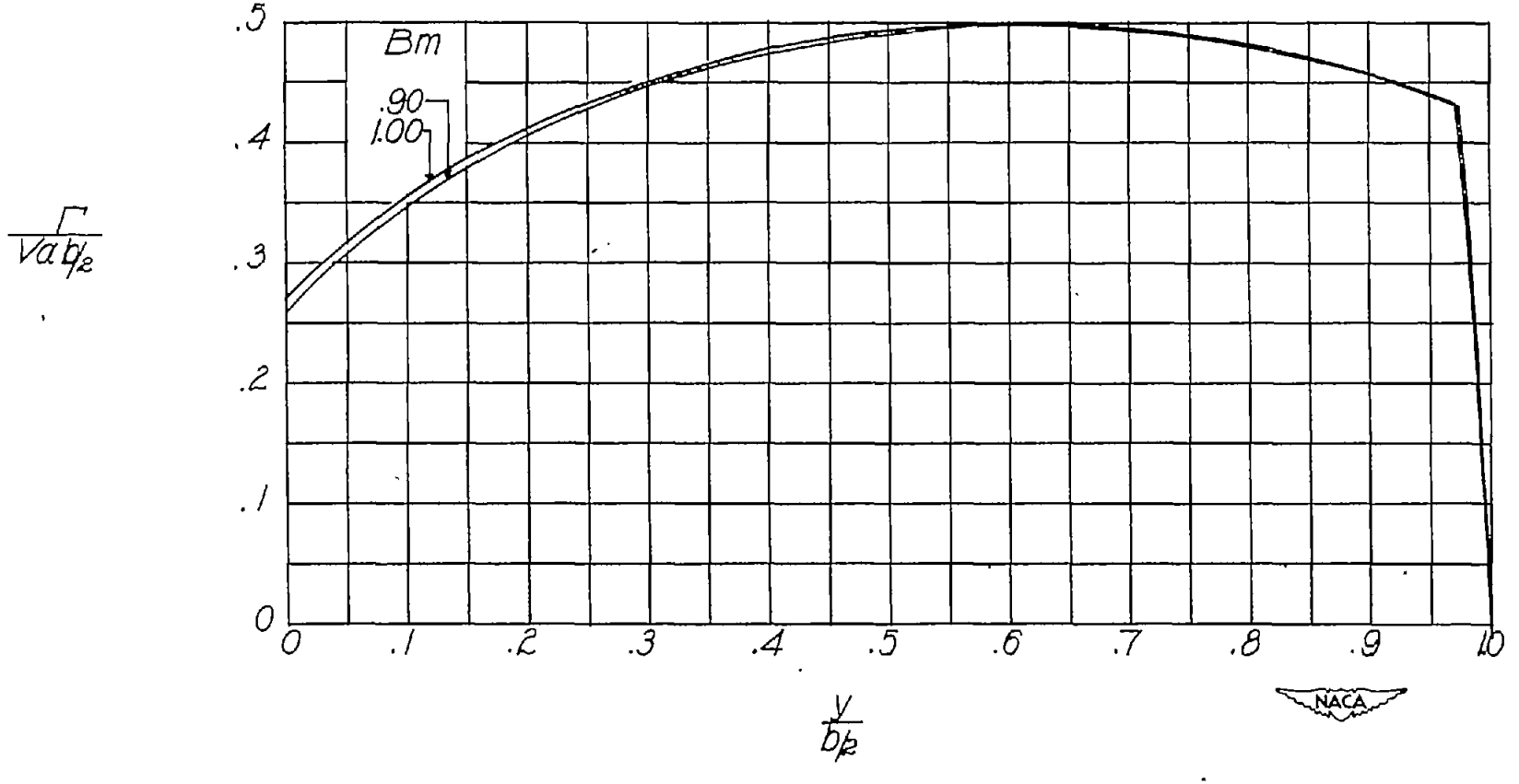

(i) AB = 15.

Figure 6.- Continued.

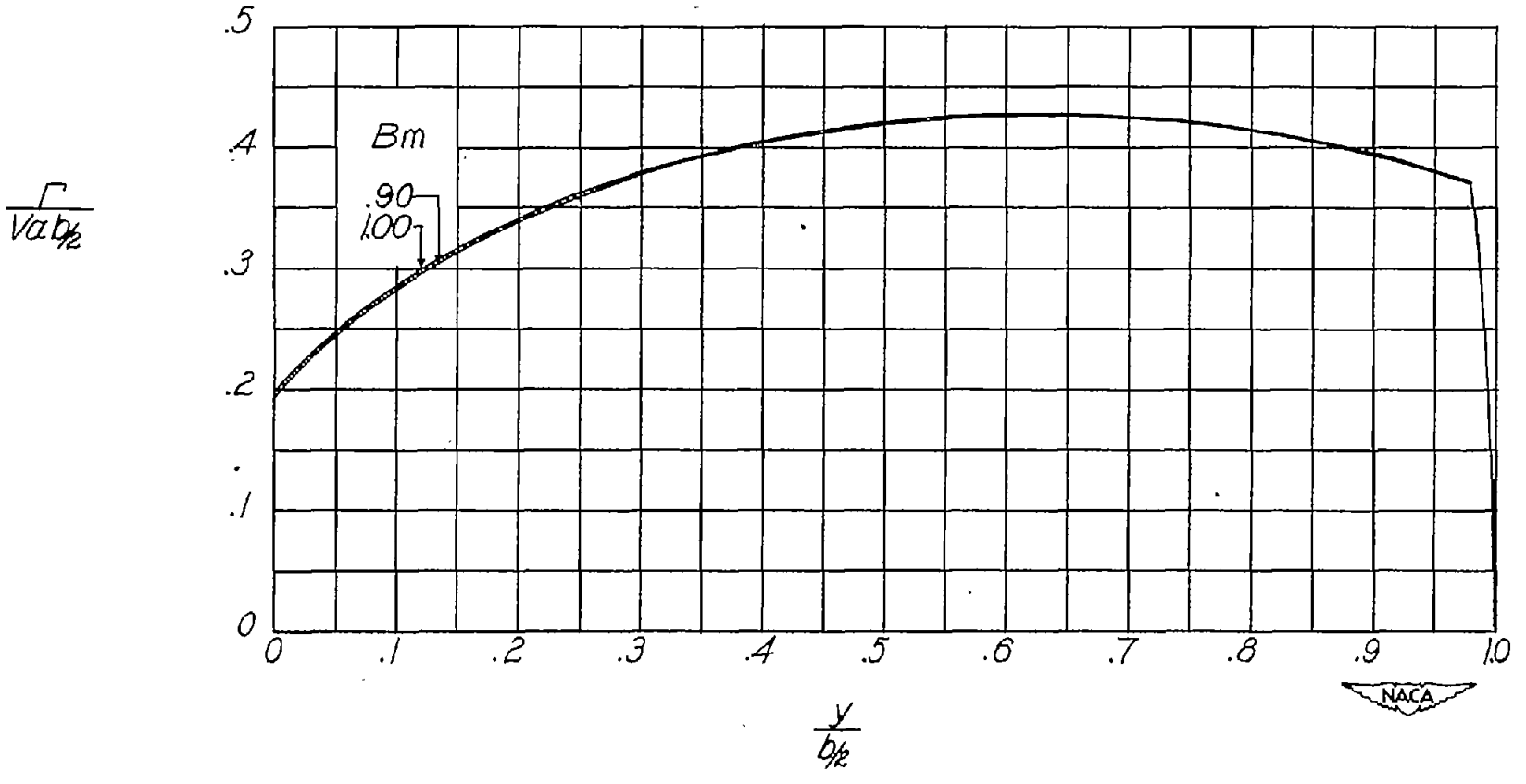

(j) AB = 20.

Figure 6.- Concluded.

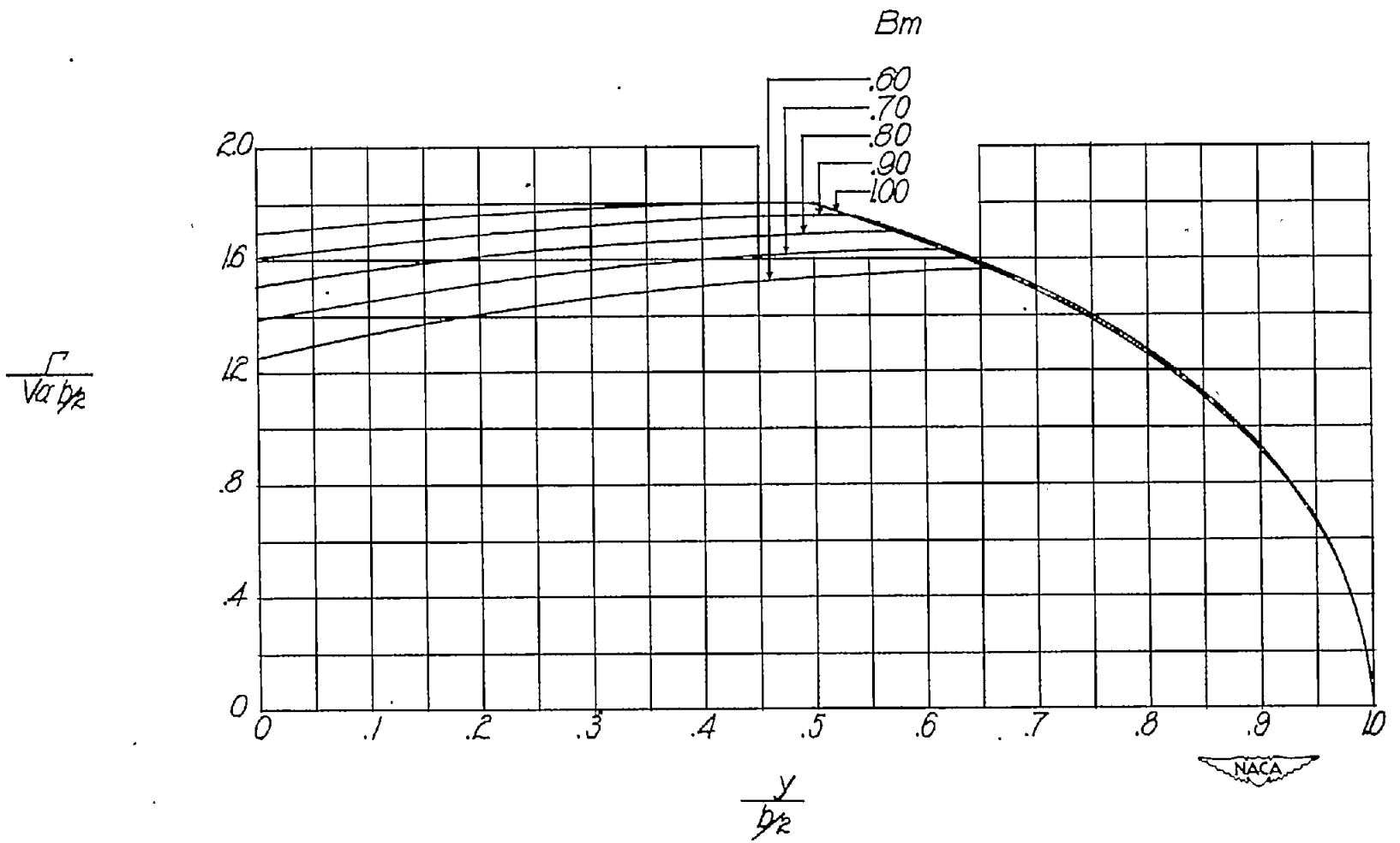

(a) AB = 2.

Figure 7.- Distribution of circulation along span for wings at constant angle of attack with $\lambda = 0.50$.

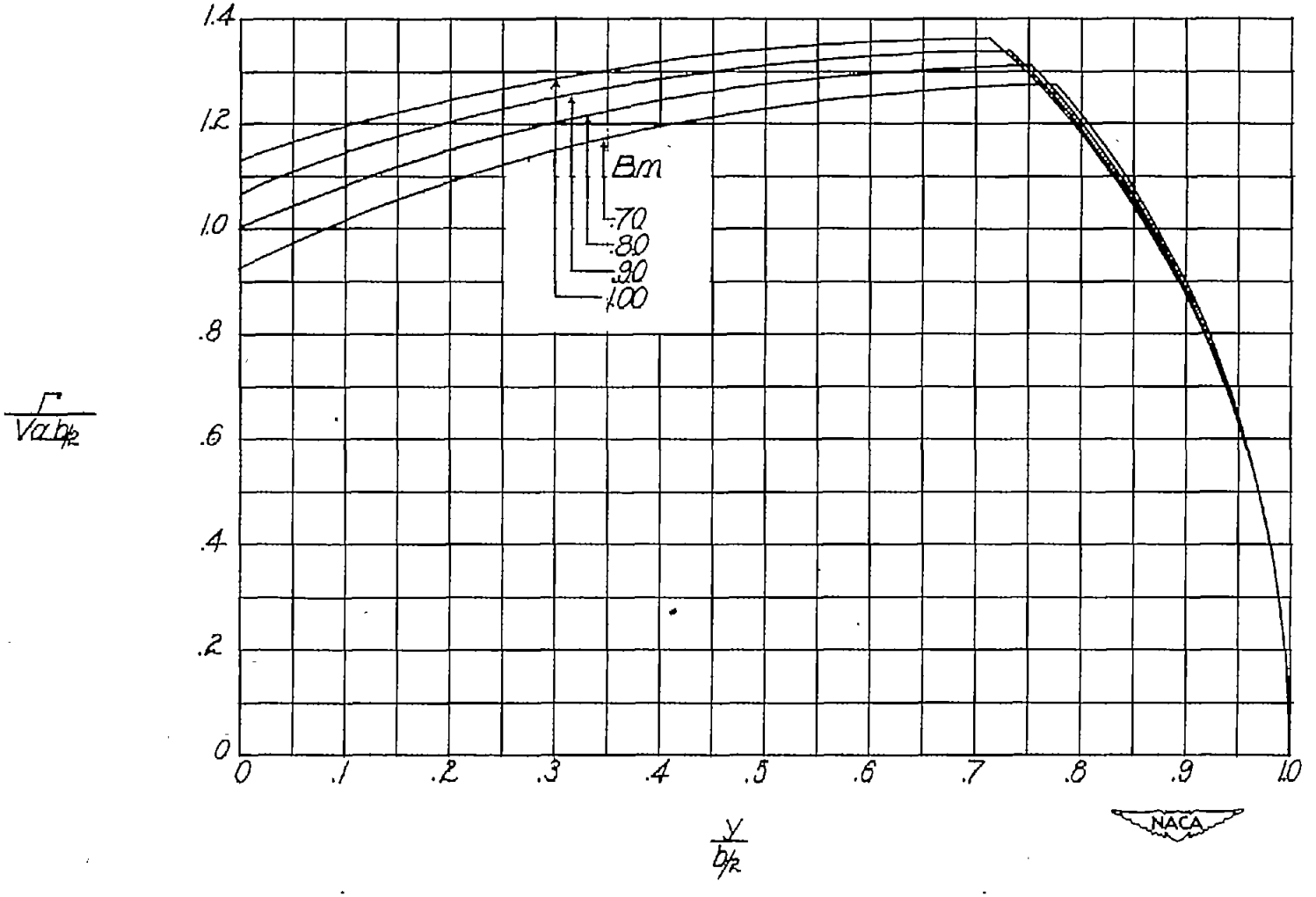

(b) AB = 3.

Figure 7.- Continued.

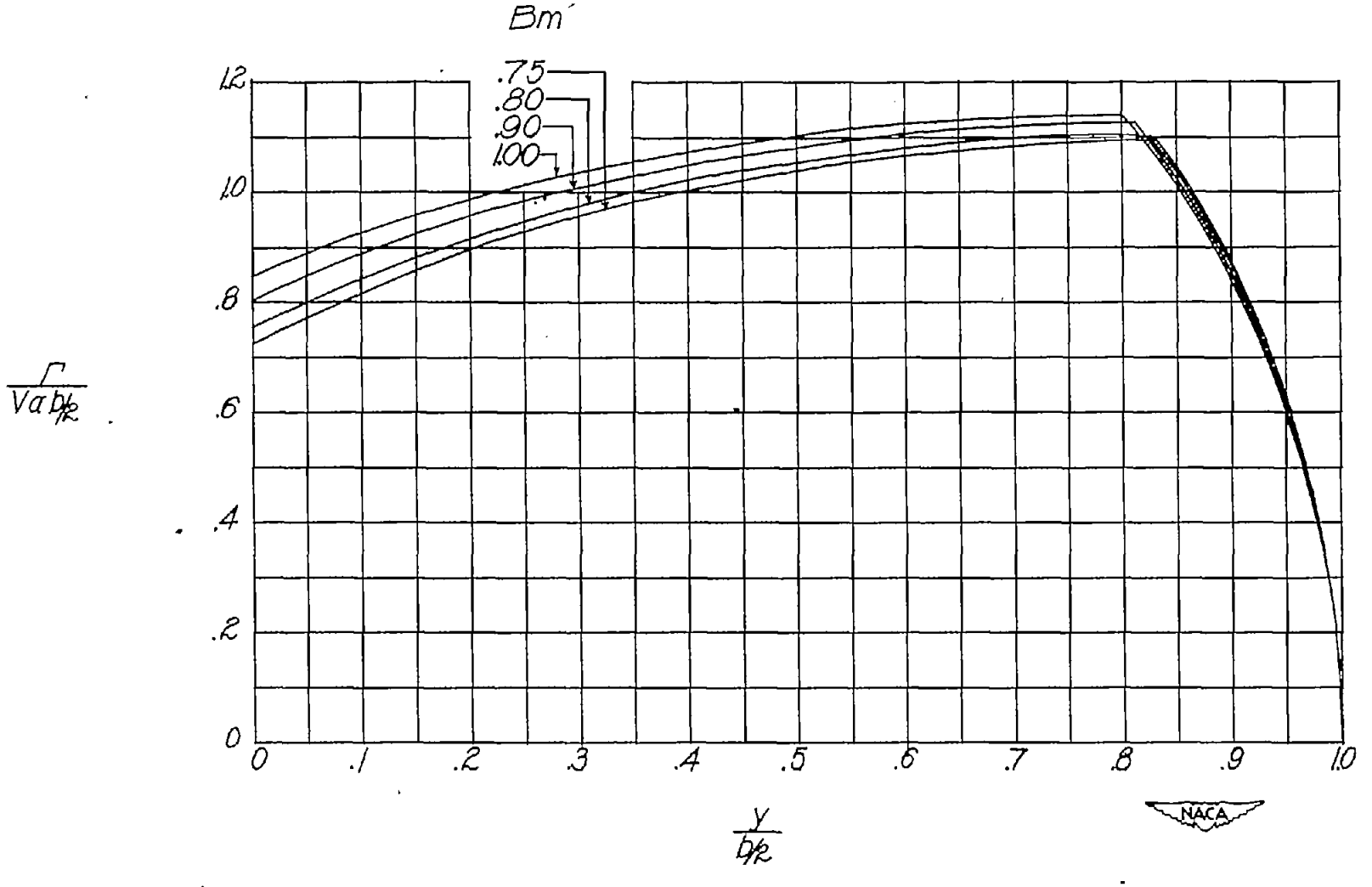

(c) AB = 4.

Figure 7.- Continued.

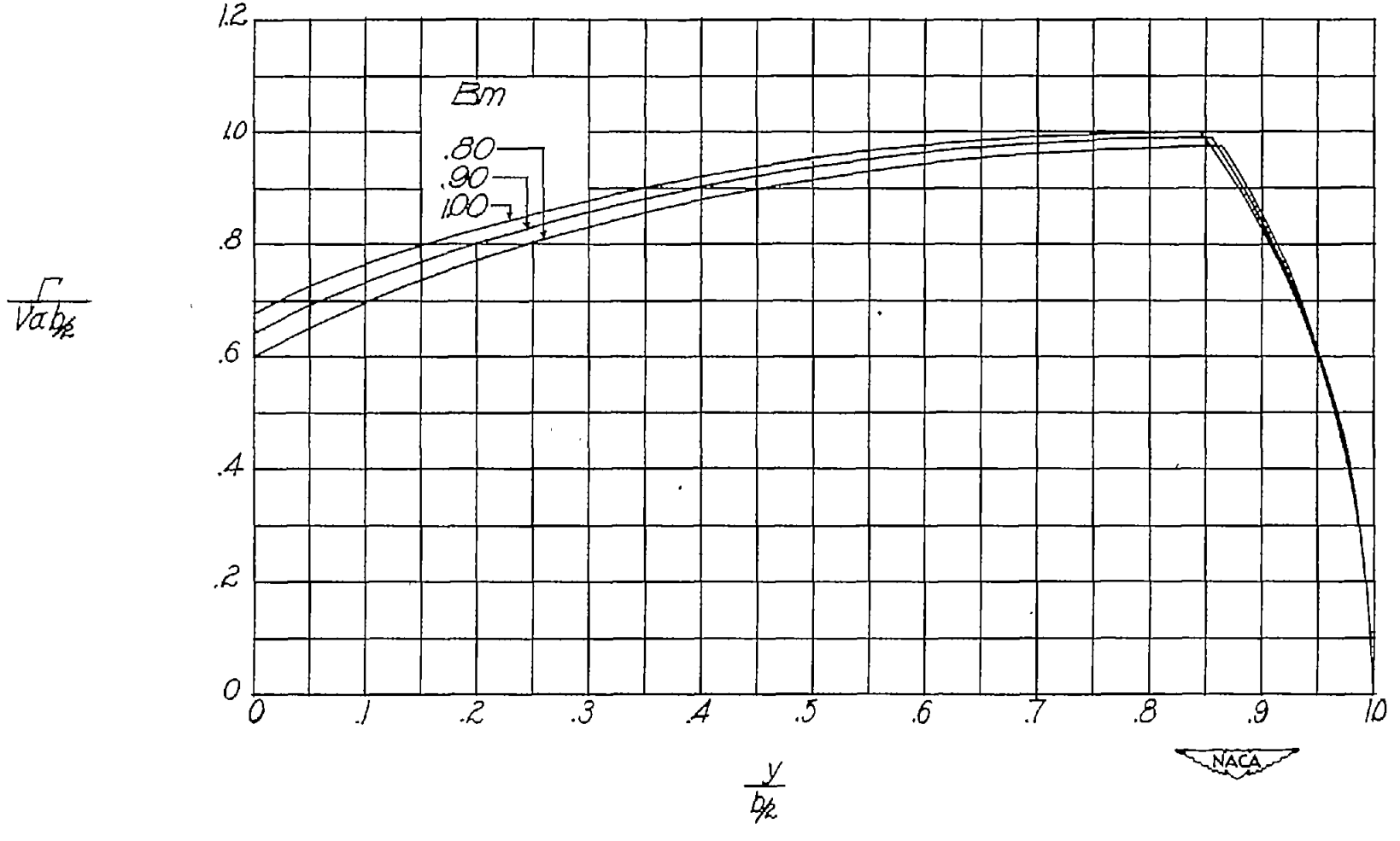

(d) AB = 5.

Figure 7.- Continued.

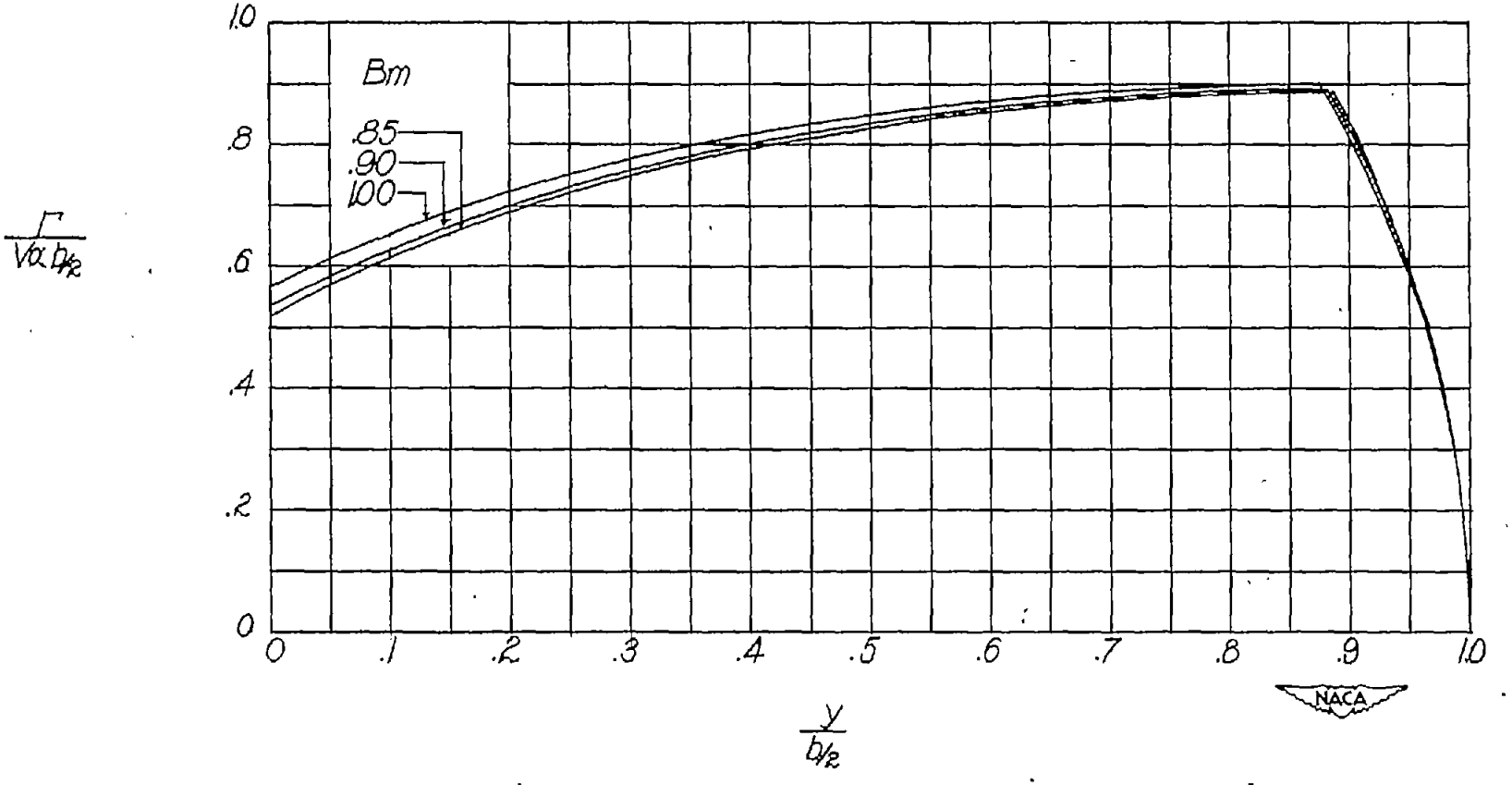

(e) AB = 6.

Figure 7.- Continued.

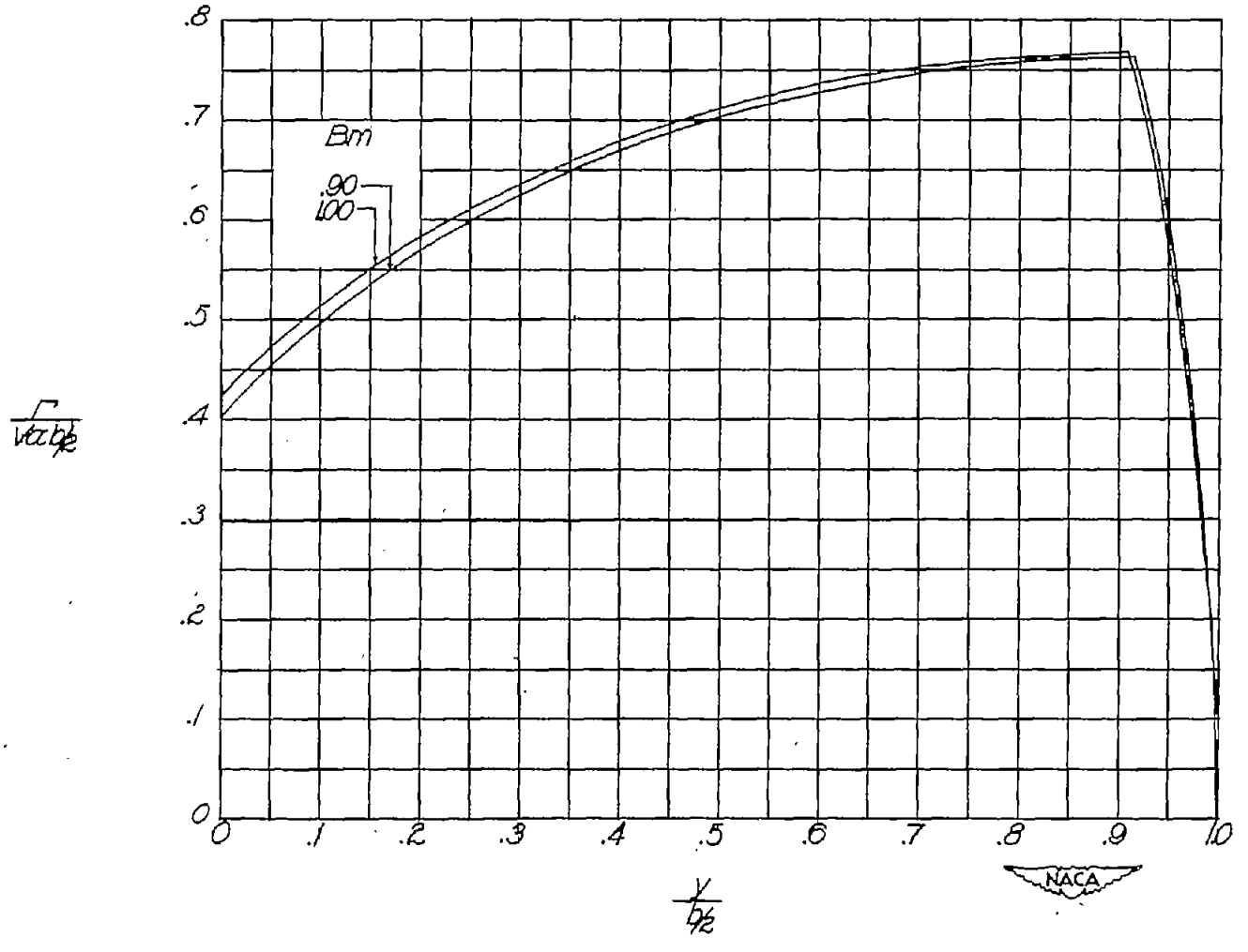

(f) AB = 8.

Figure 7.- Continued.

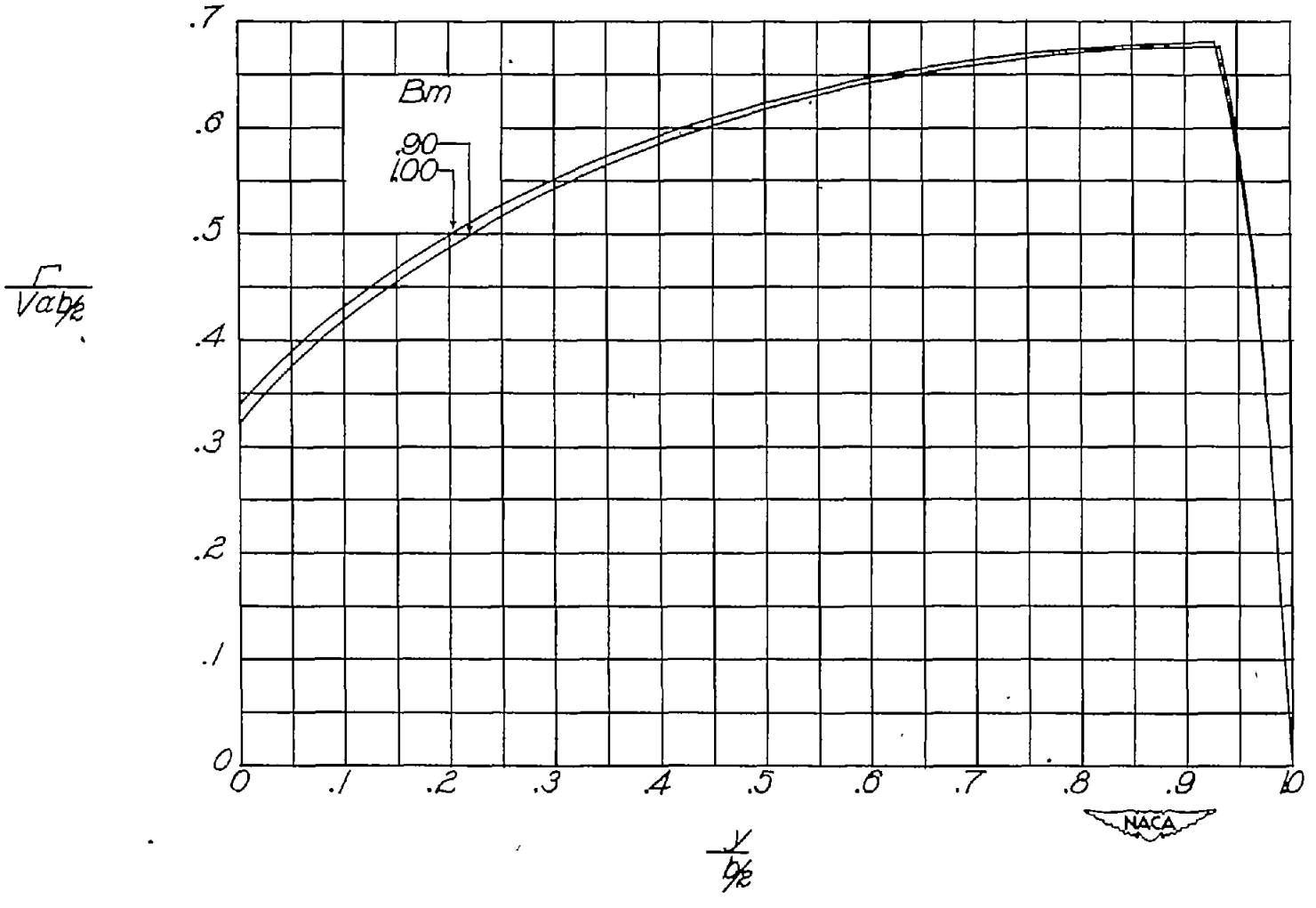

(g) AB = 10.

Figure 7.- Continued.

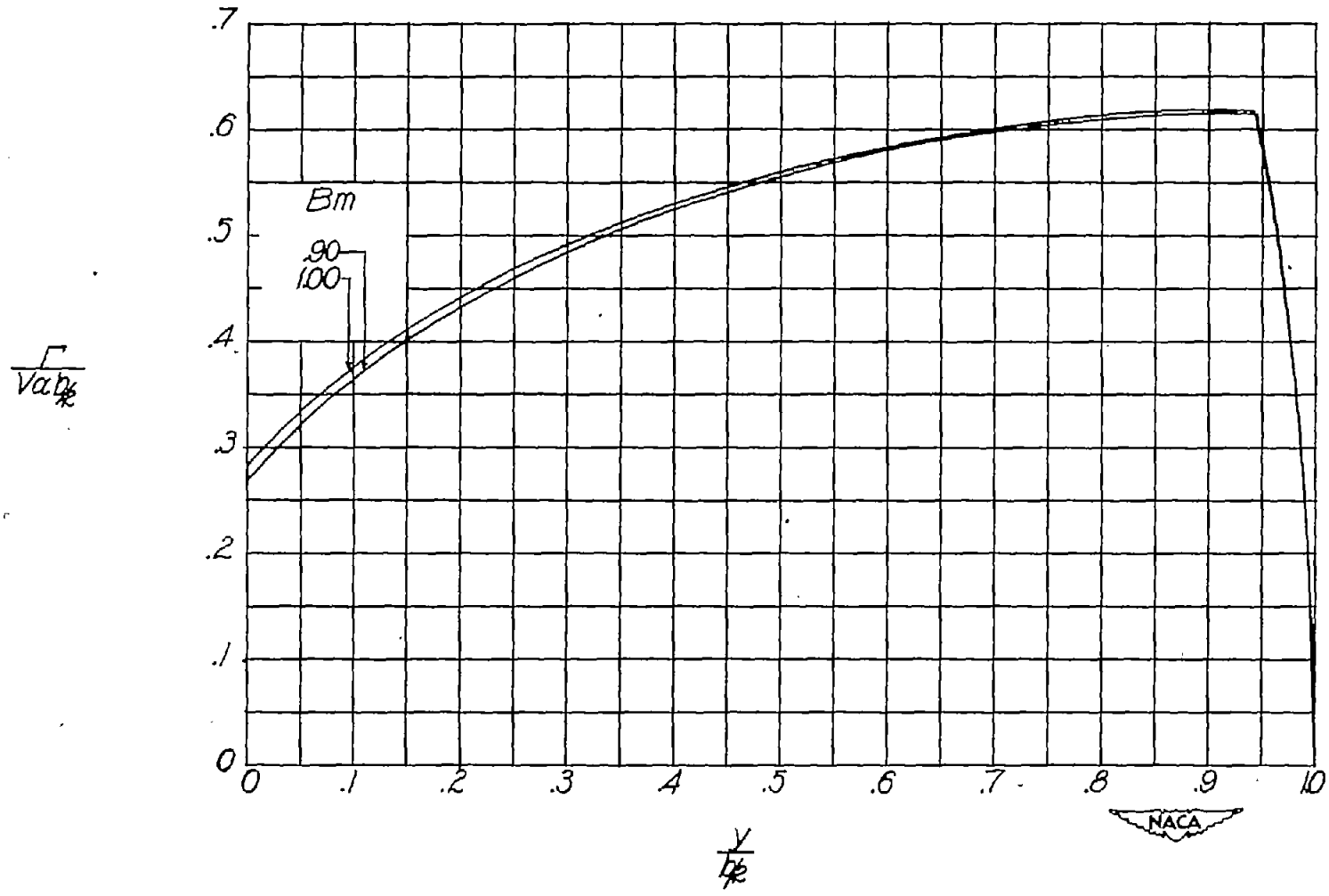

(h) AB = 12.

Figure 7.- Continued.

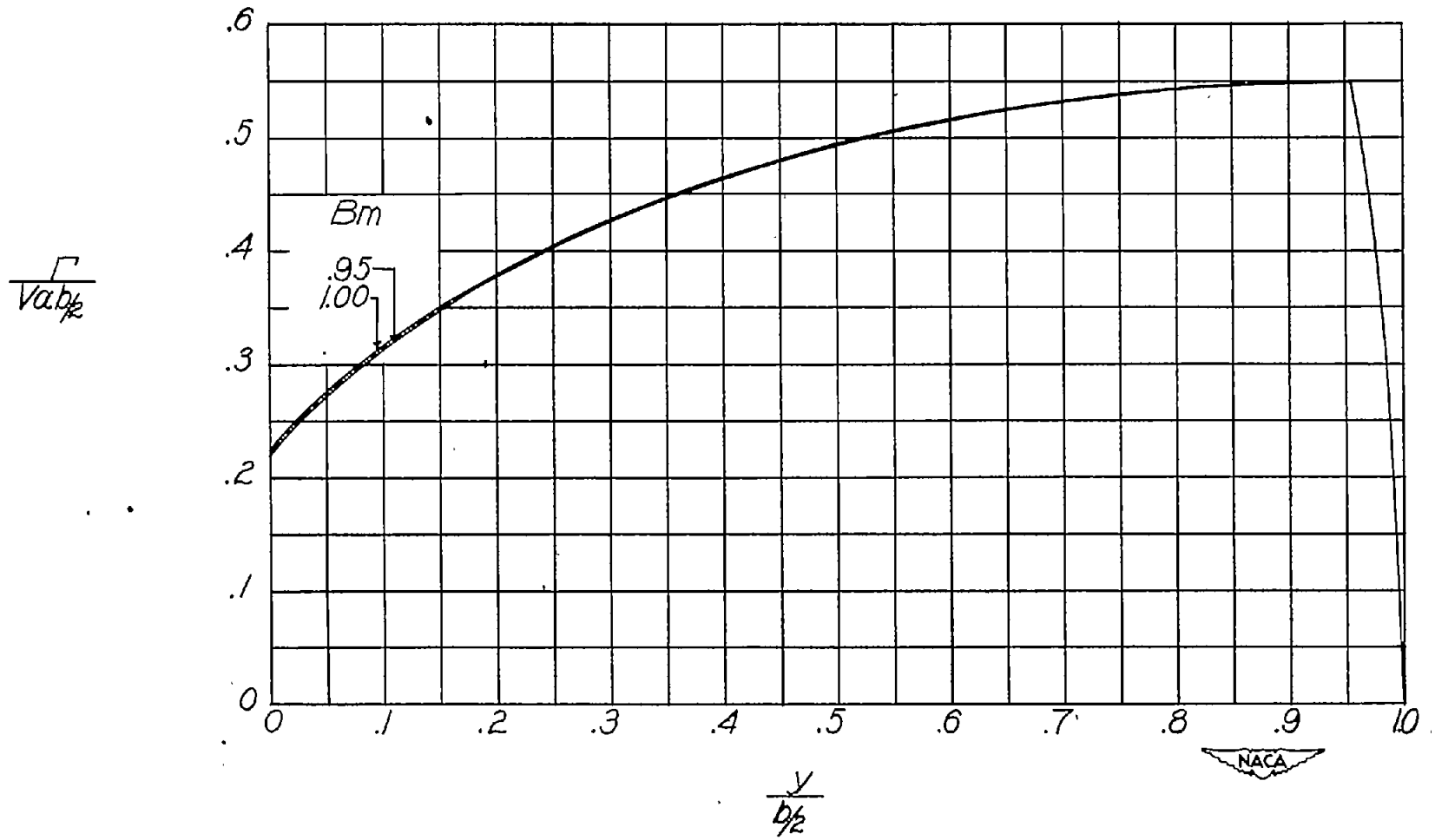

(i) AB = 15.

Figure 7.- Continued.

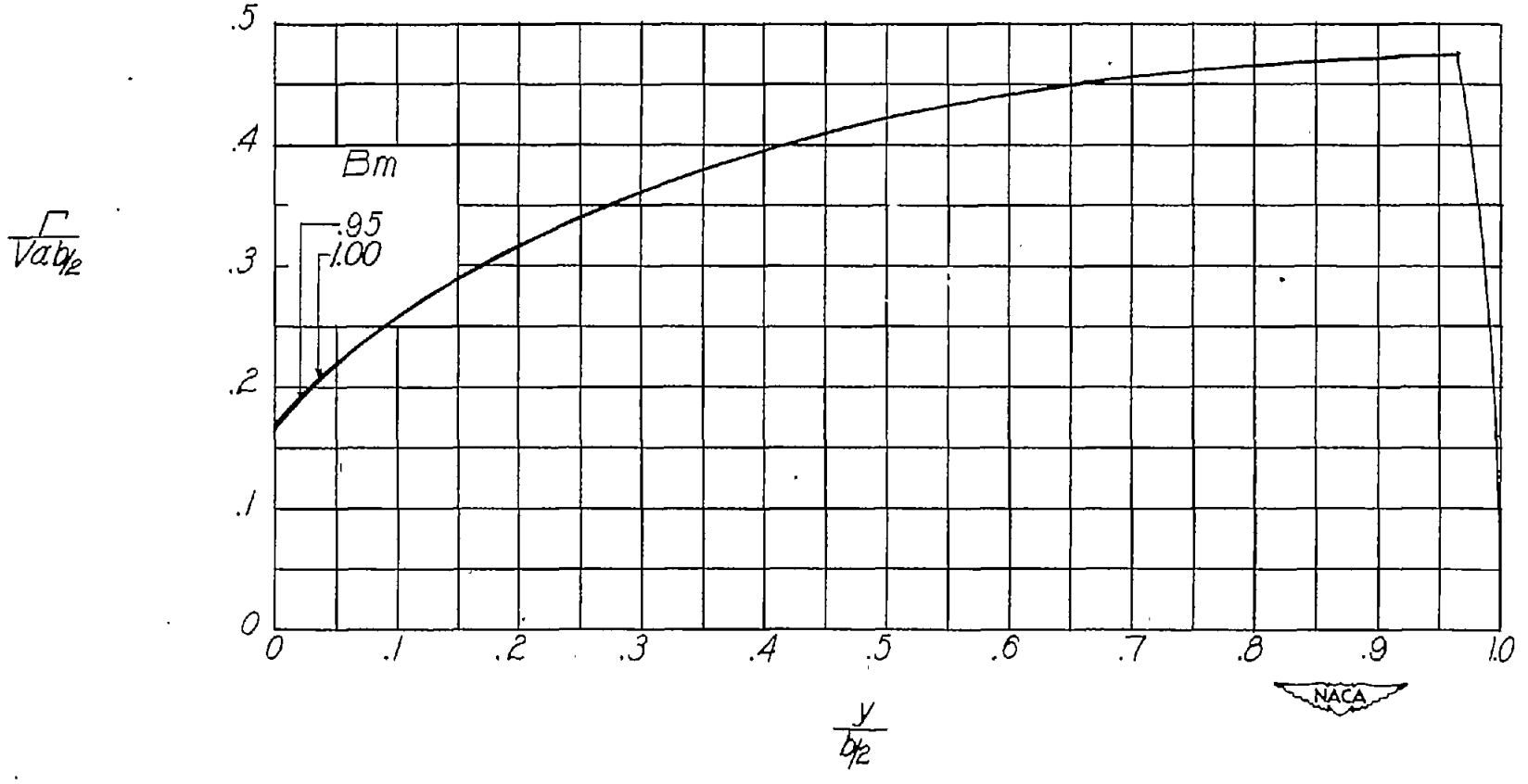

(j) AB = 20.

Figure 7.- Concluded.

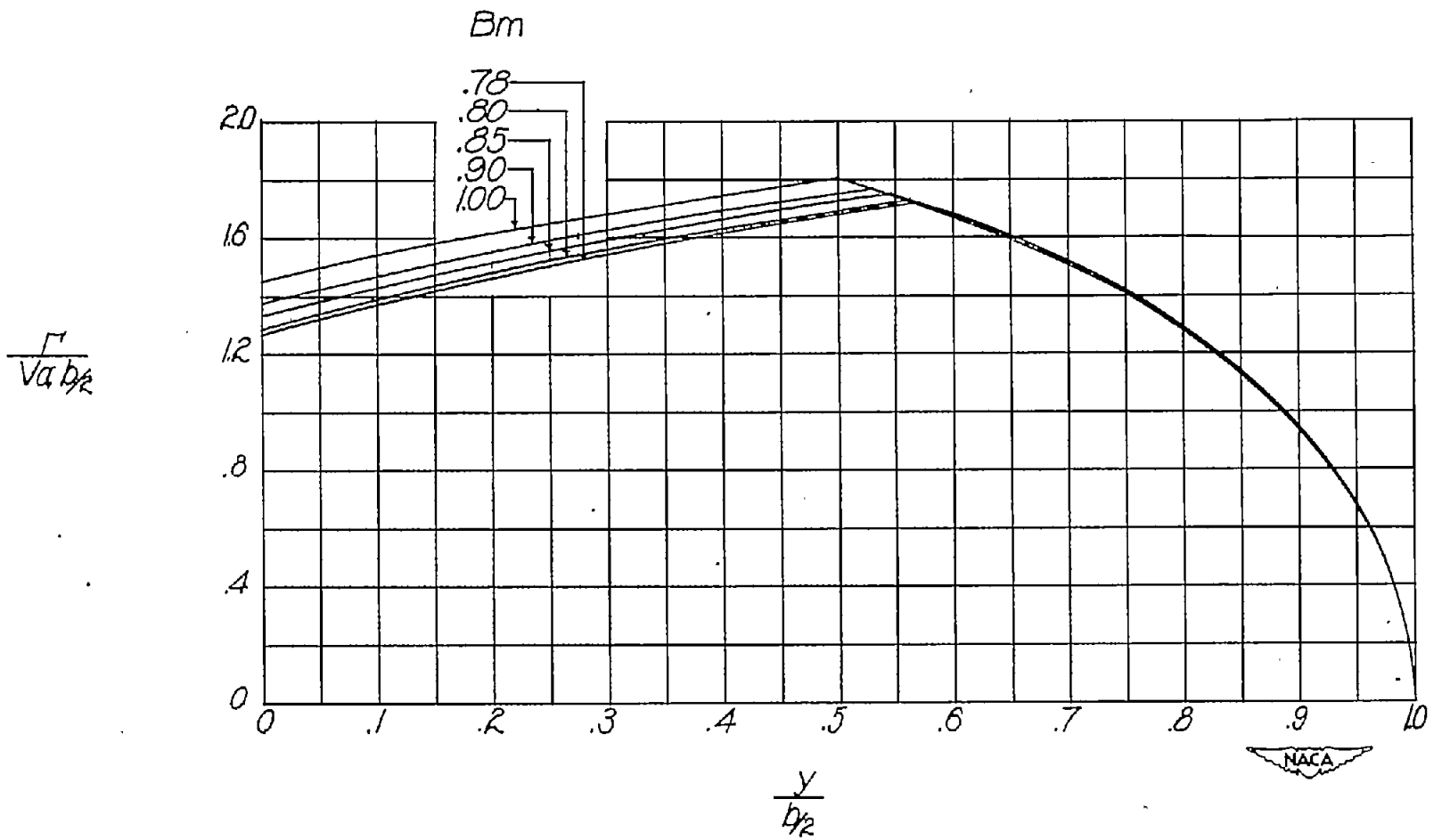

(a) AB = 2.

Figure 8.- Distribution of circulation along span for wings at constant angle of attack with $\lambda = 0.75$.

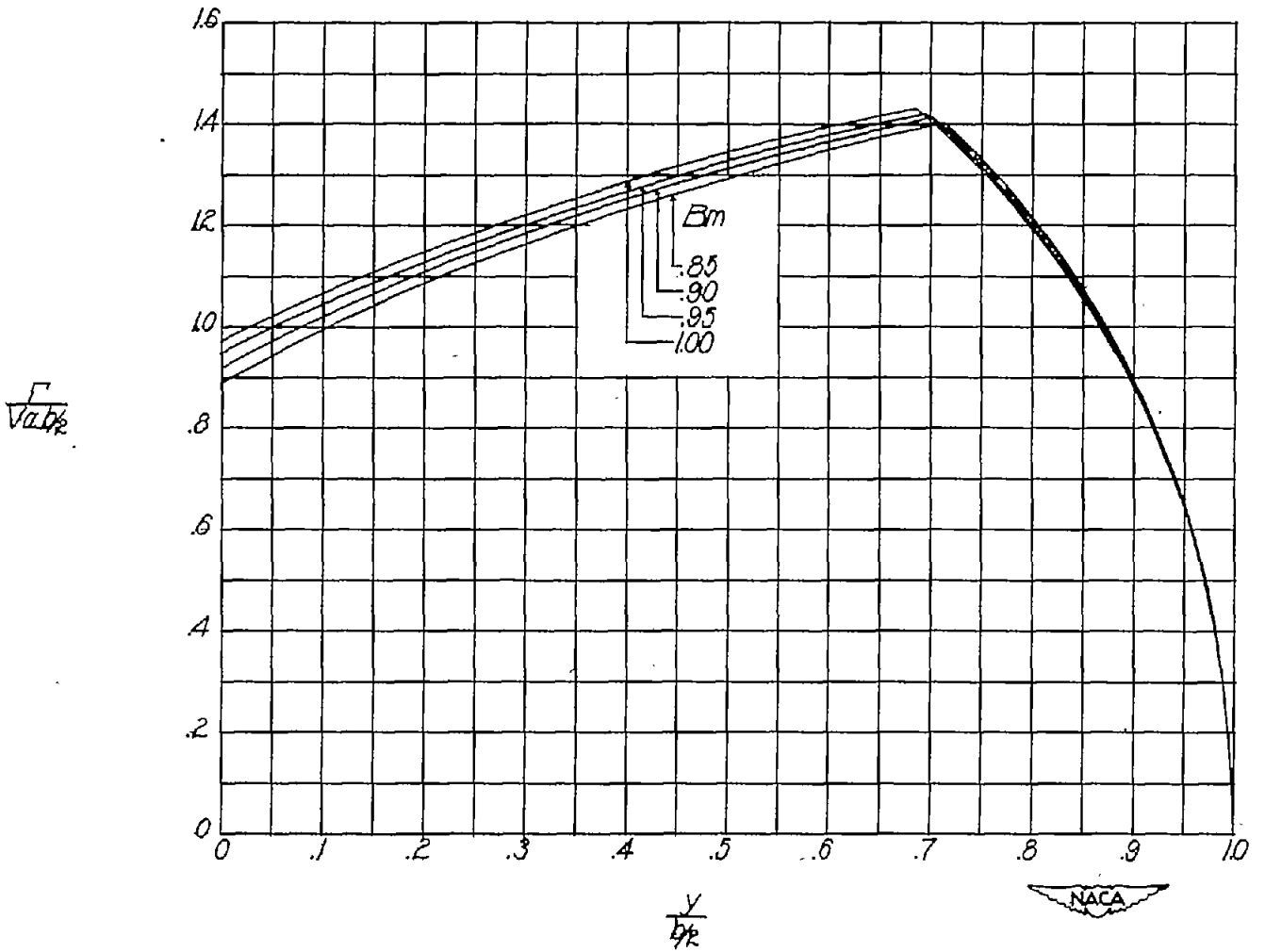

(b) AB = 3.

Figure 8.- Continued.

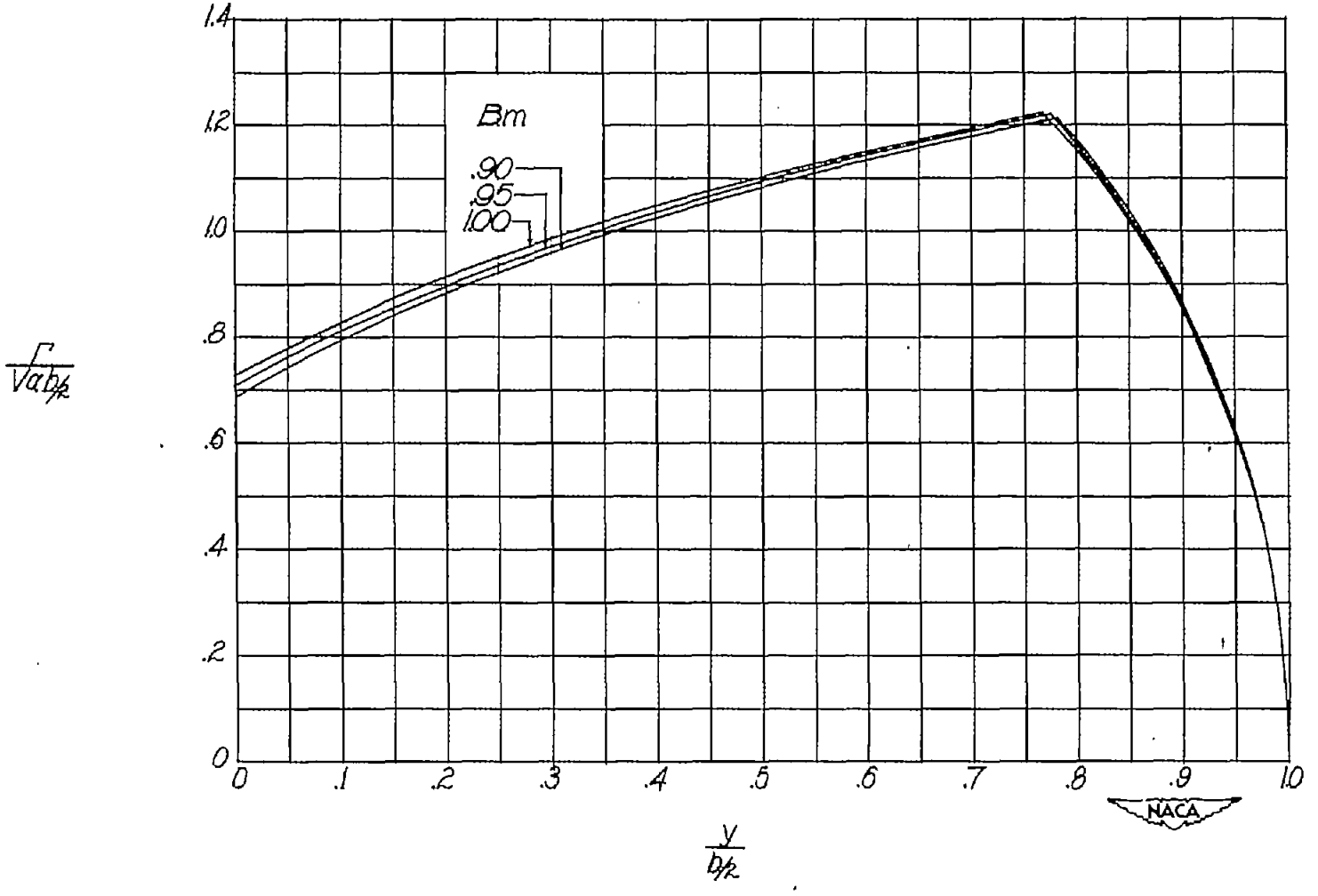

(c) AB = 4.

Figure 8.- Continued.

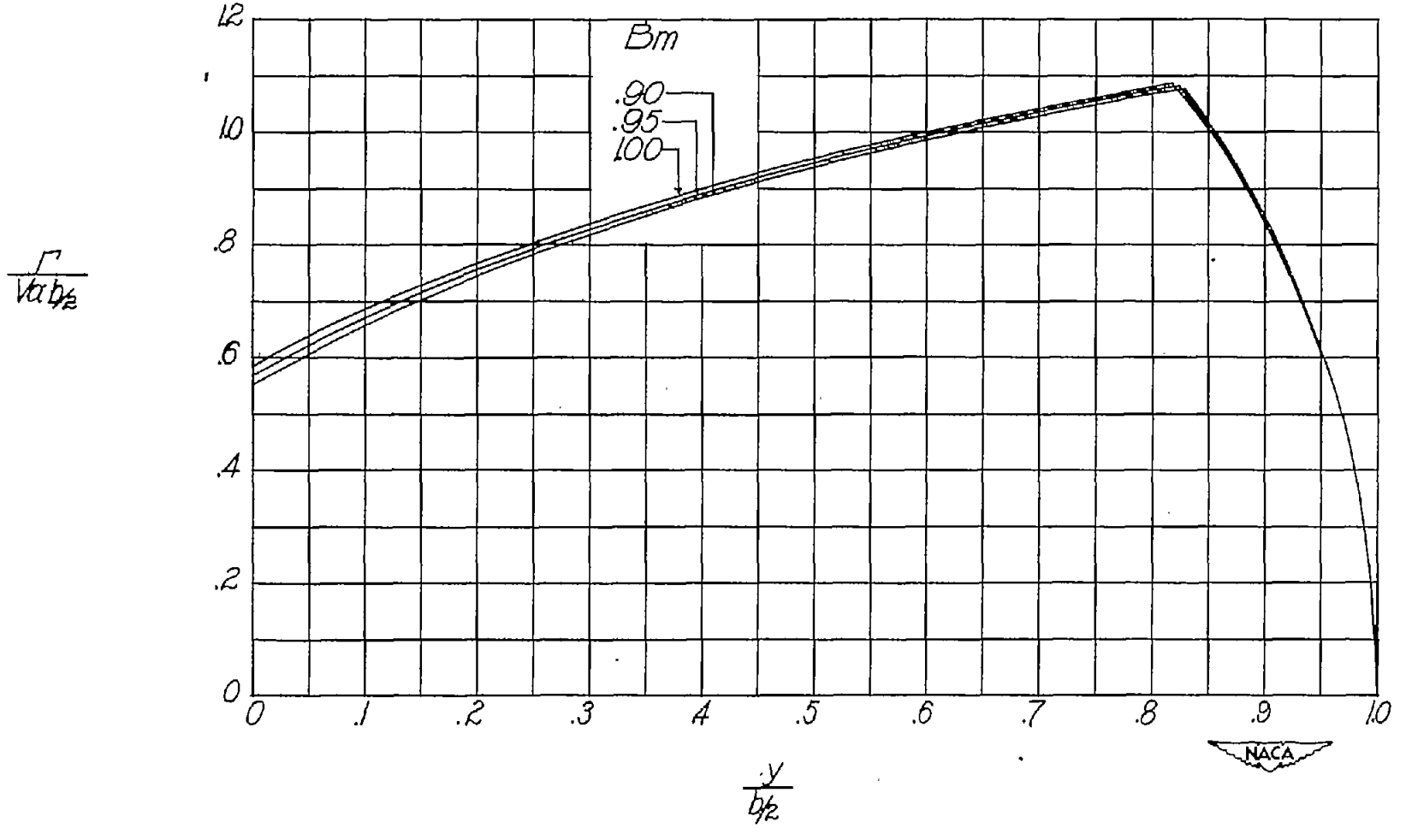

(d) AB = 5.

Figure 8.- Continued.

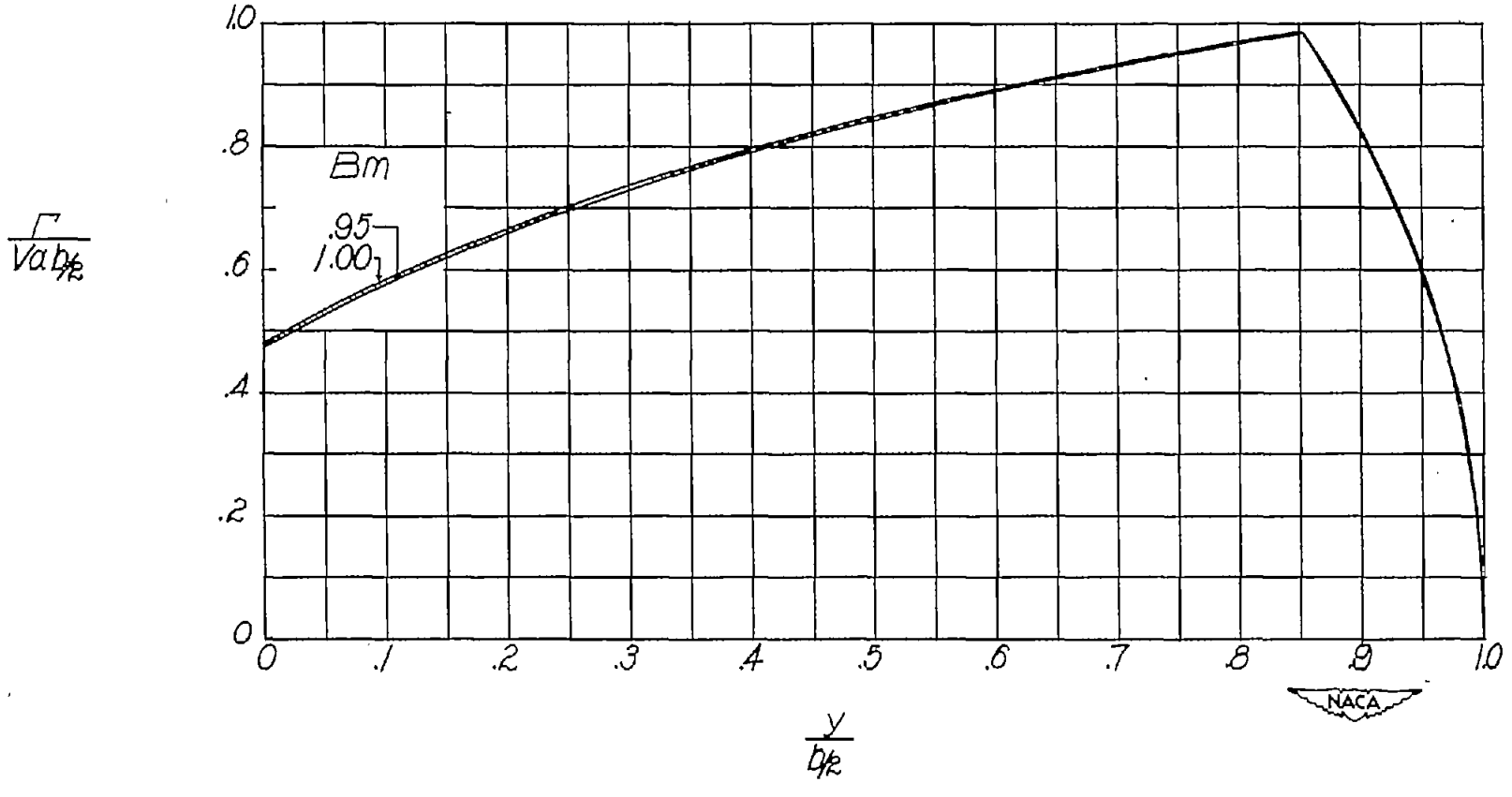

(e) AB = 6.

Figure 8.- Continued.

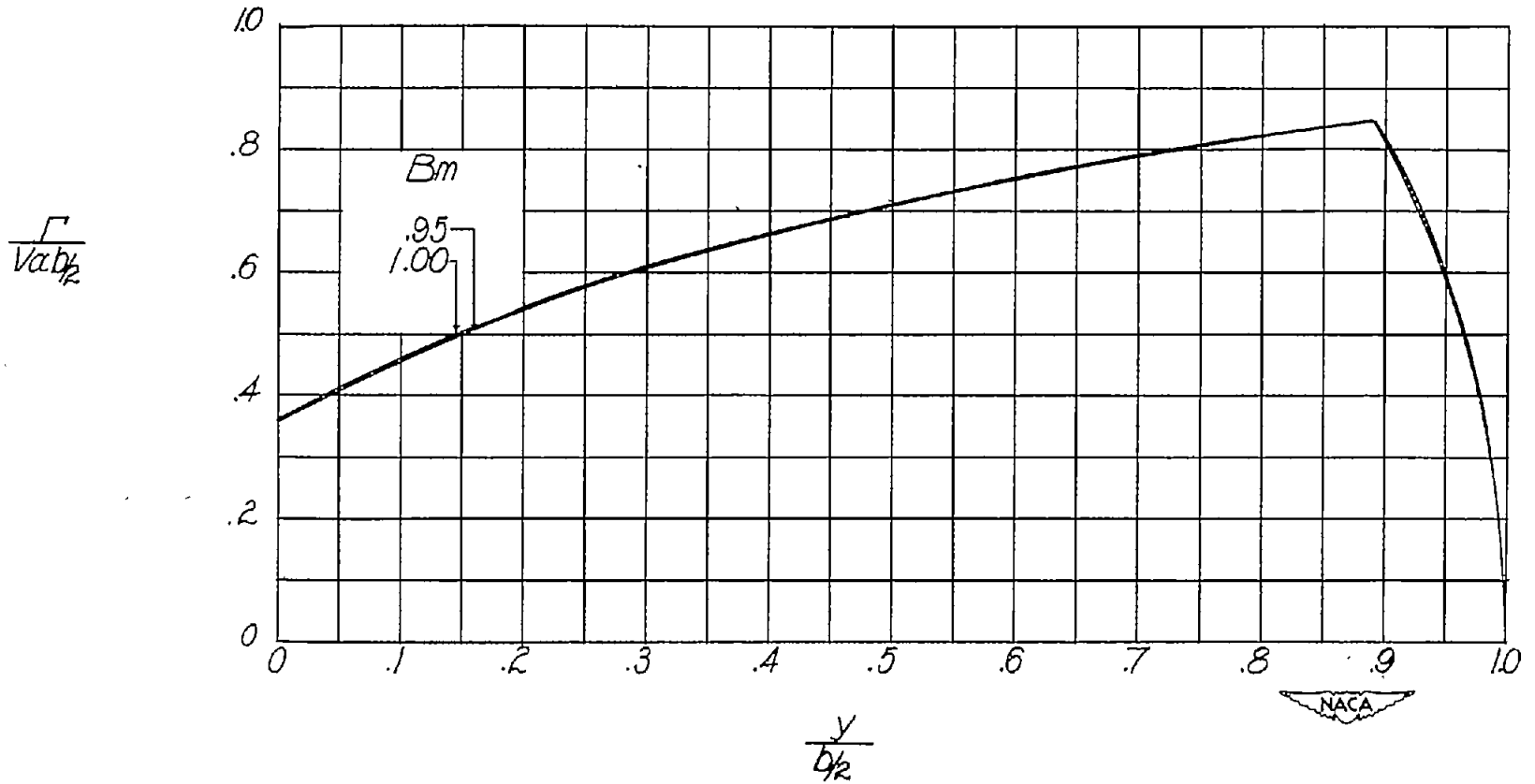

(f) AB = 8.

Figure 8.- Continued.

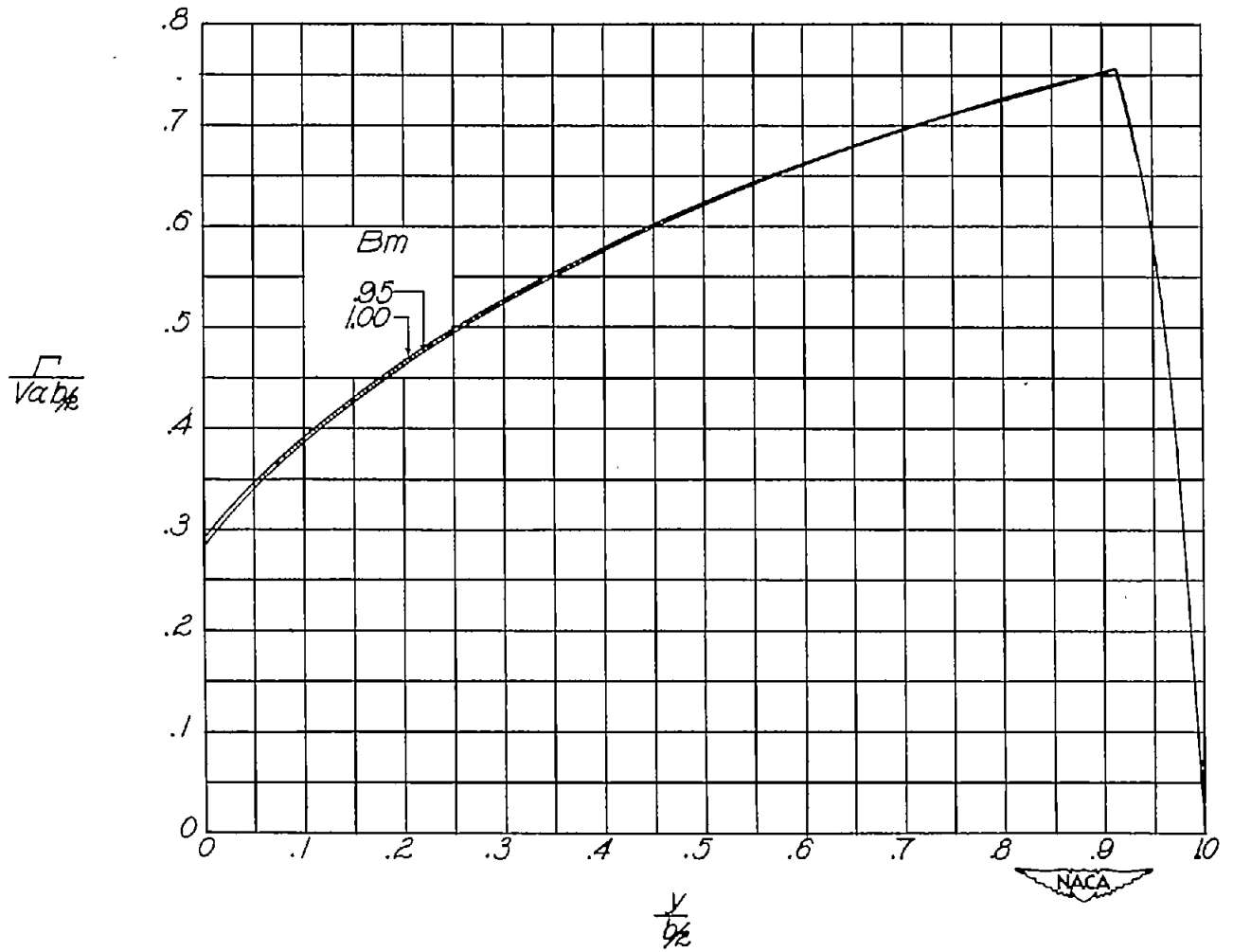

(g) AB = 10.

Figure 8.- Continued.

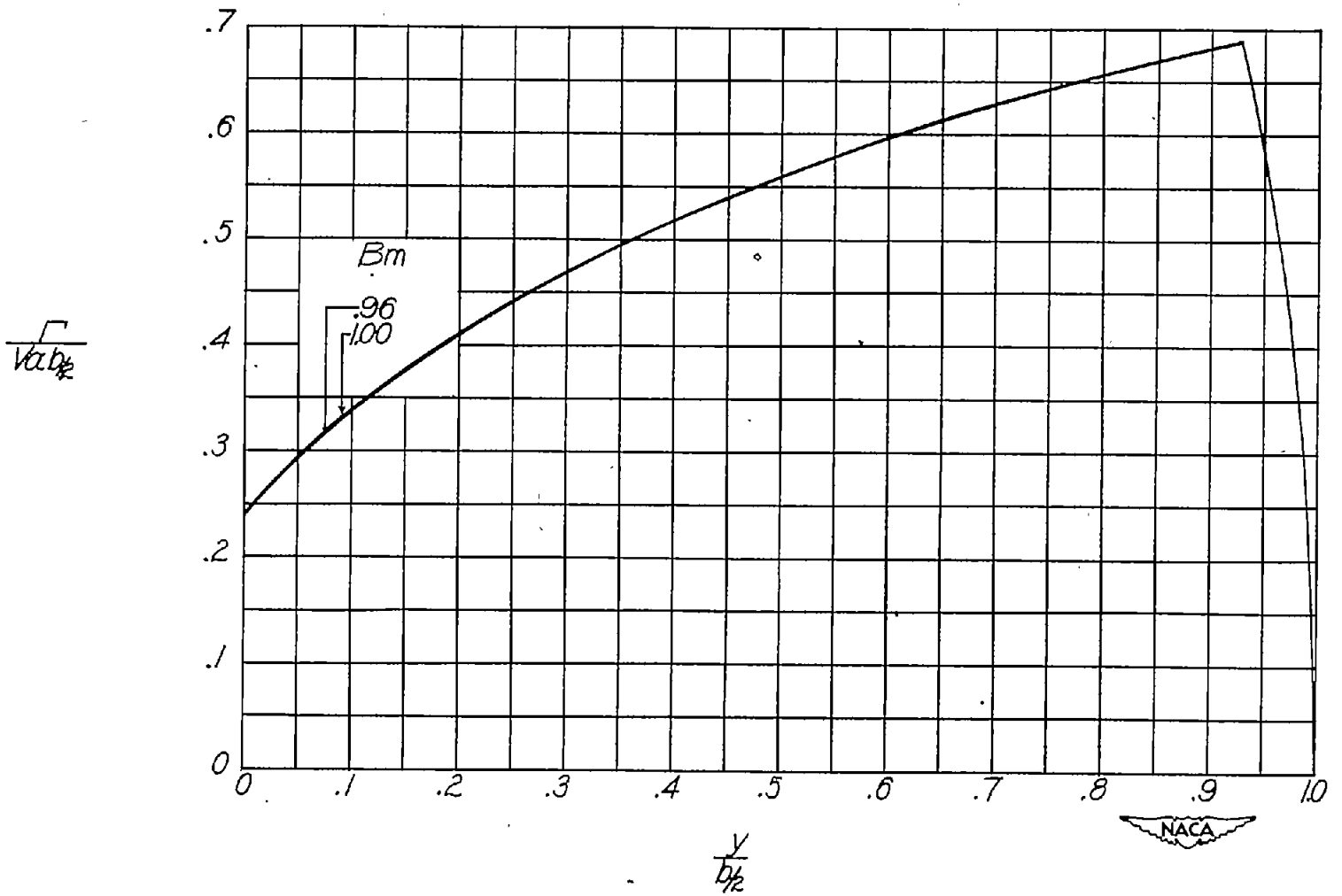

(h) AB = 12.

Figure 8.- Continued.

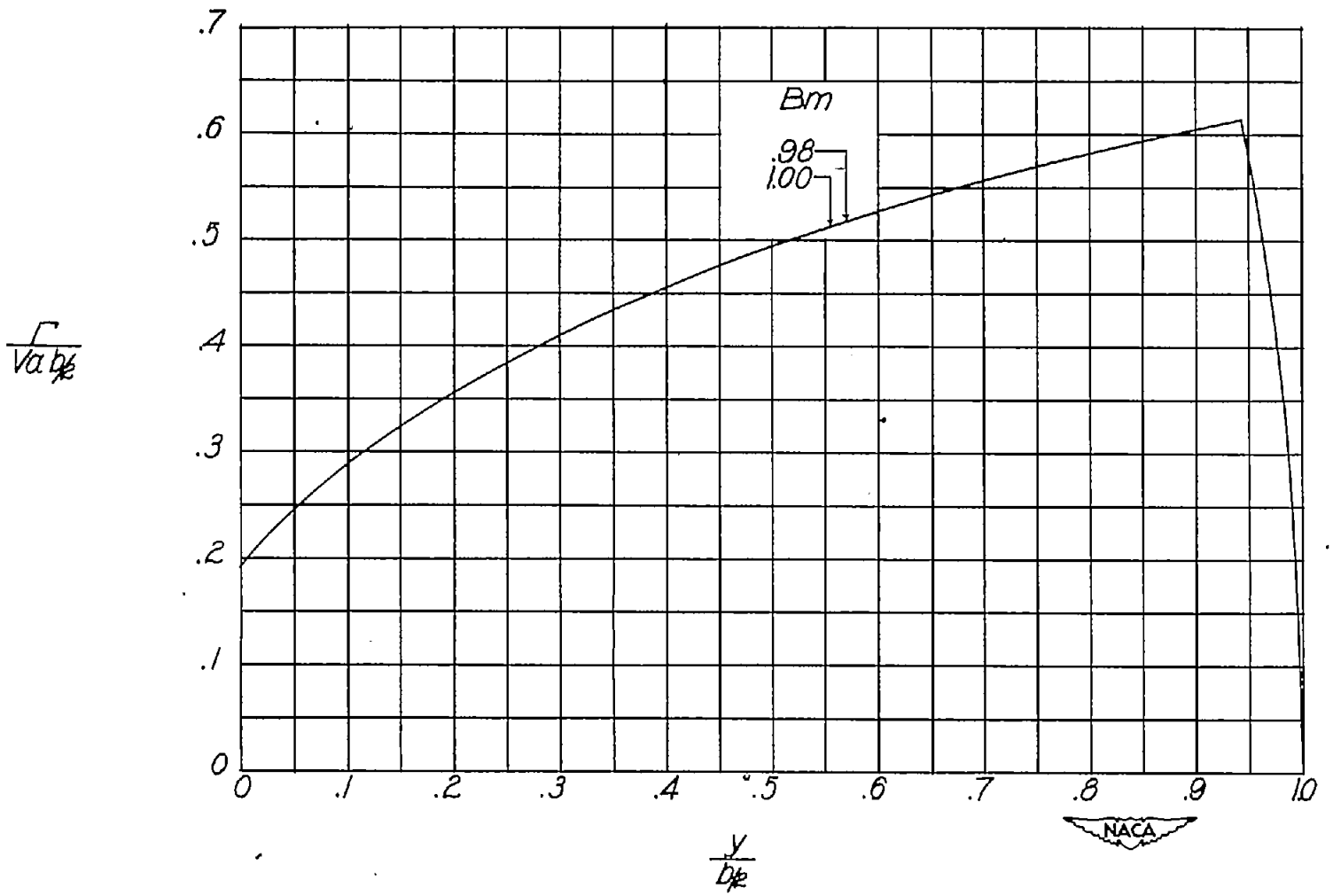

(i) AB = 15.

Figure 8.- Continued.

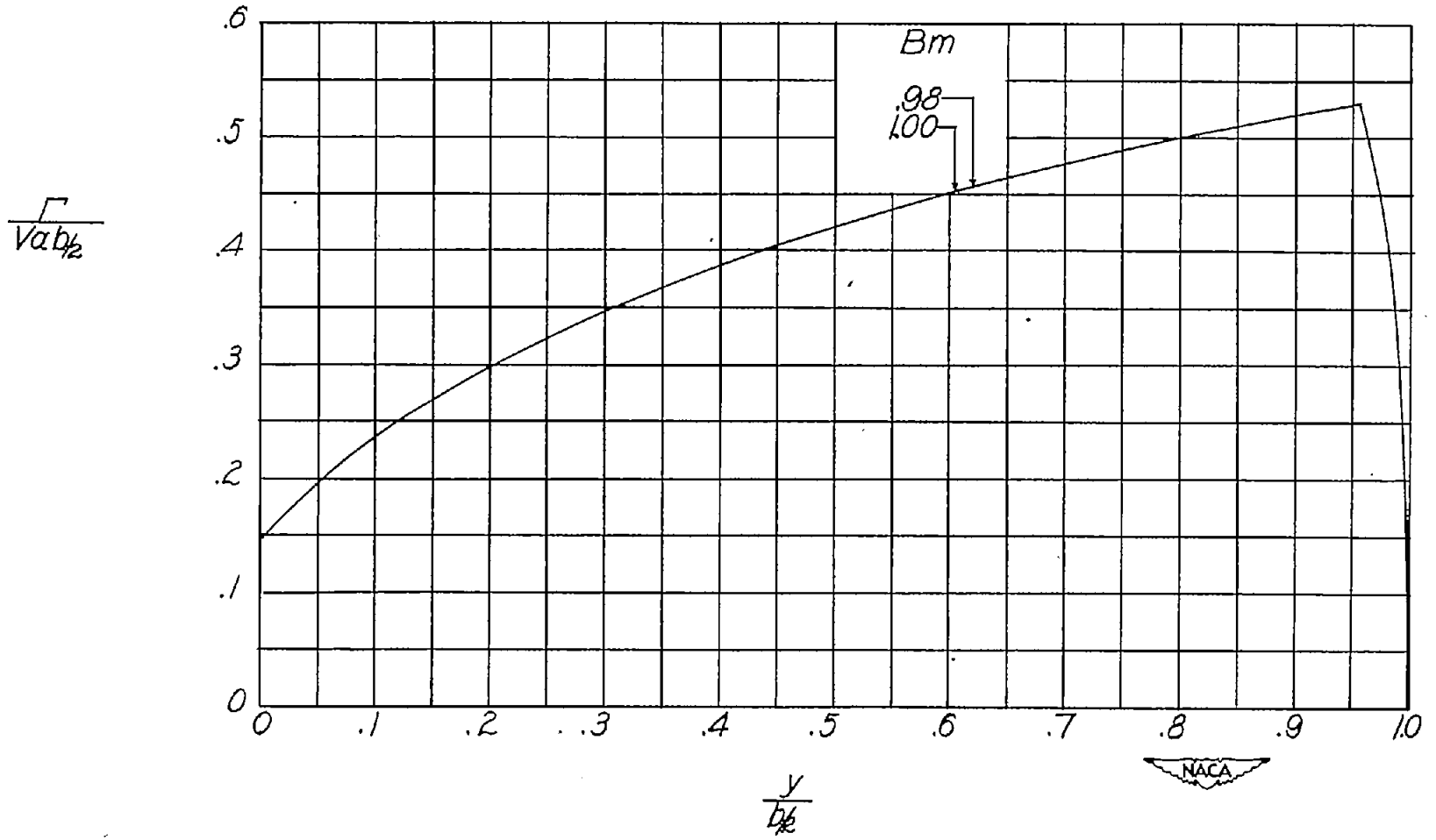

(j) AB = 20.

Figure 8.- Concluded.

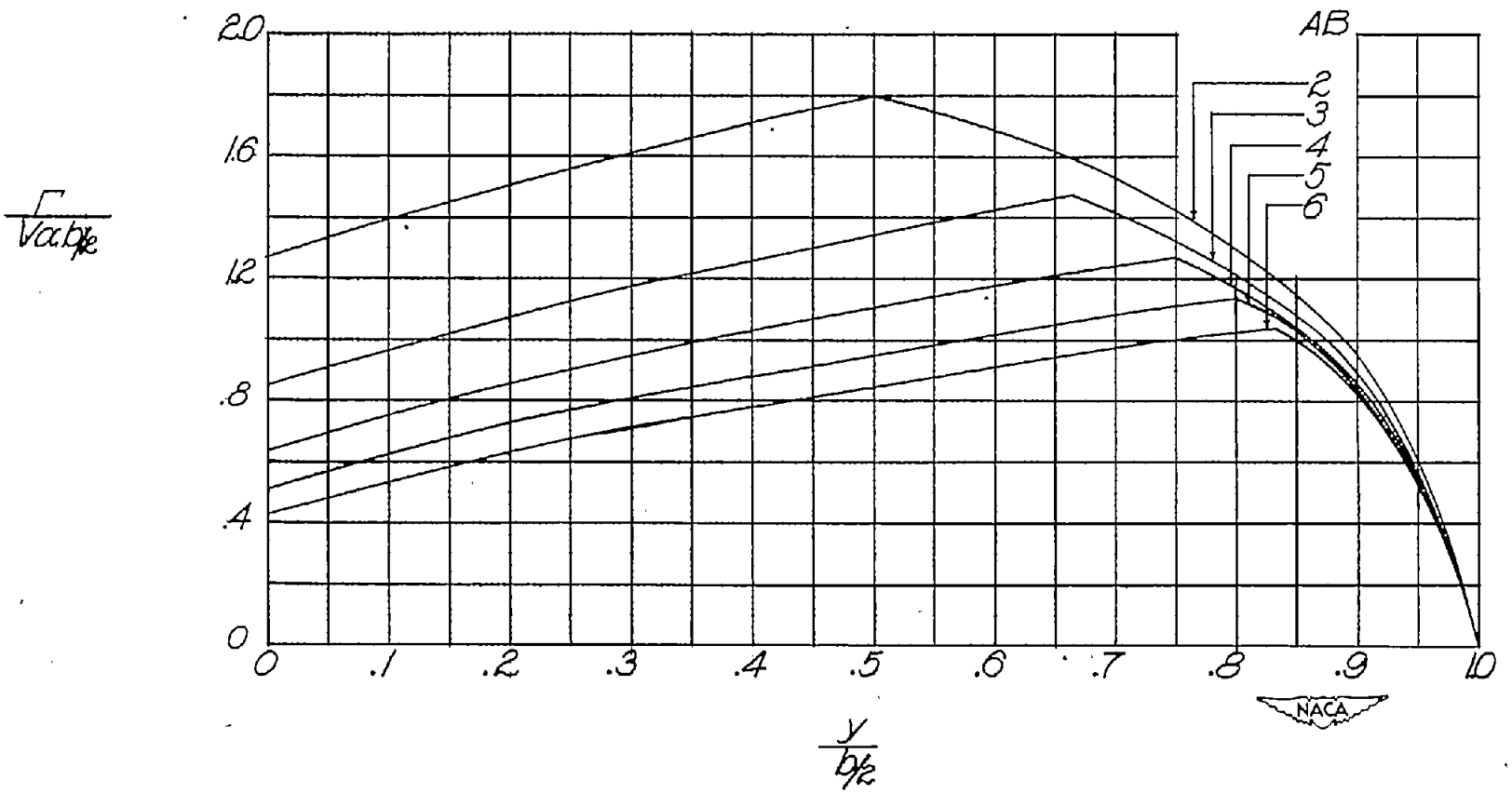

(a) AB = 2 to 6.

Figure 9.- Distribution of circulation along span for wings at constant angle of attack with $\lambda = 1.00$. $B_m = 1.00$.

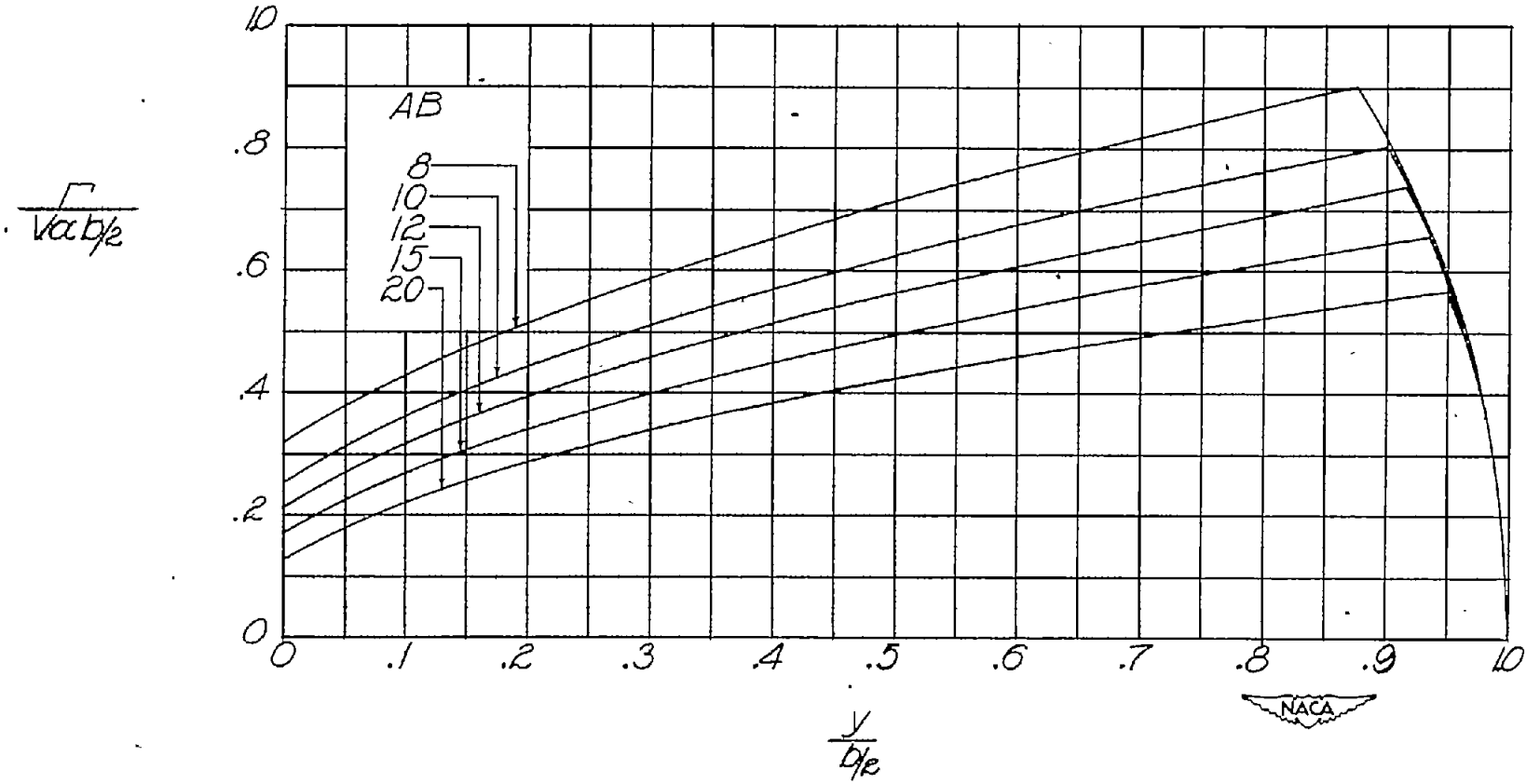

(b) AB = 8 to 20.

Figure 9.- Concluded.

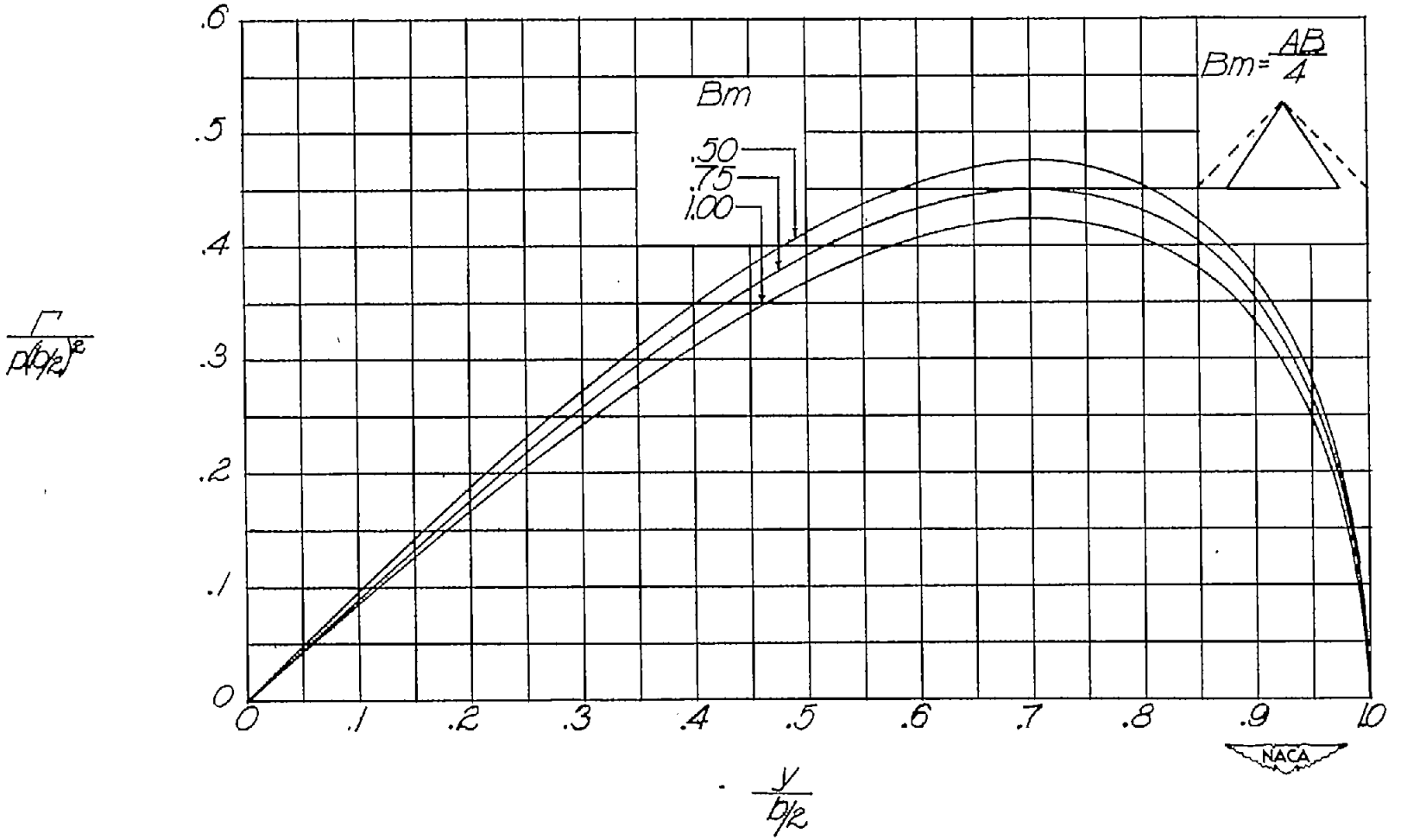

Figure 10.- Distribution of circulation along span for delta wings with steady rolling velocity.

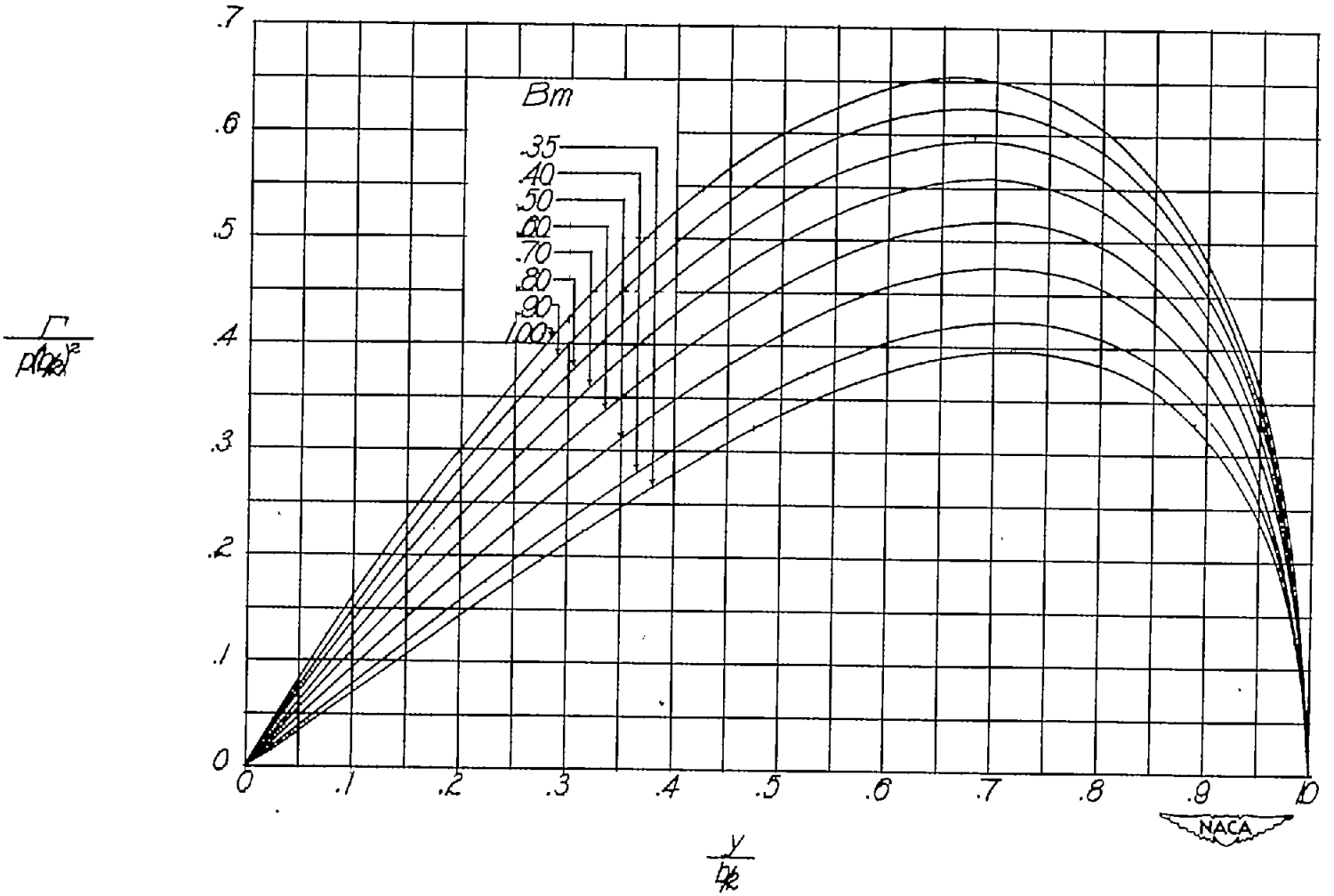

(a) AB = 2.

Figure 11.- Distribution of circulation along span for wings with steady rolling velocity with $\lambda = 0$.

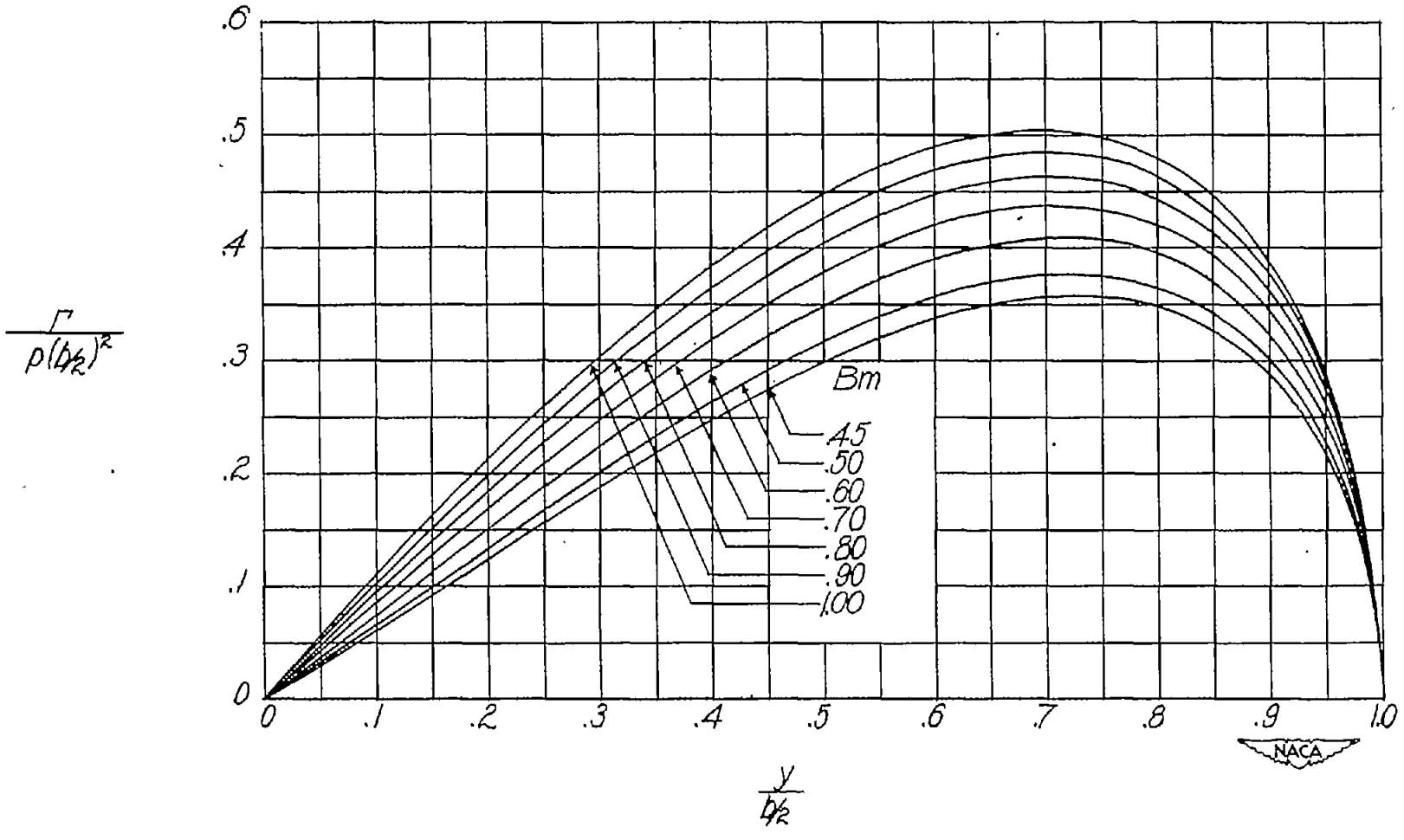

(b) AB = 3.

Figure 11.- Continued.

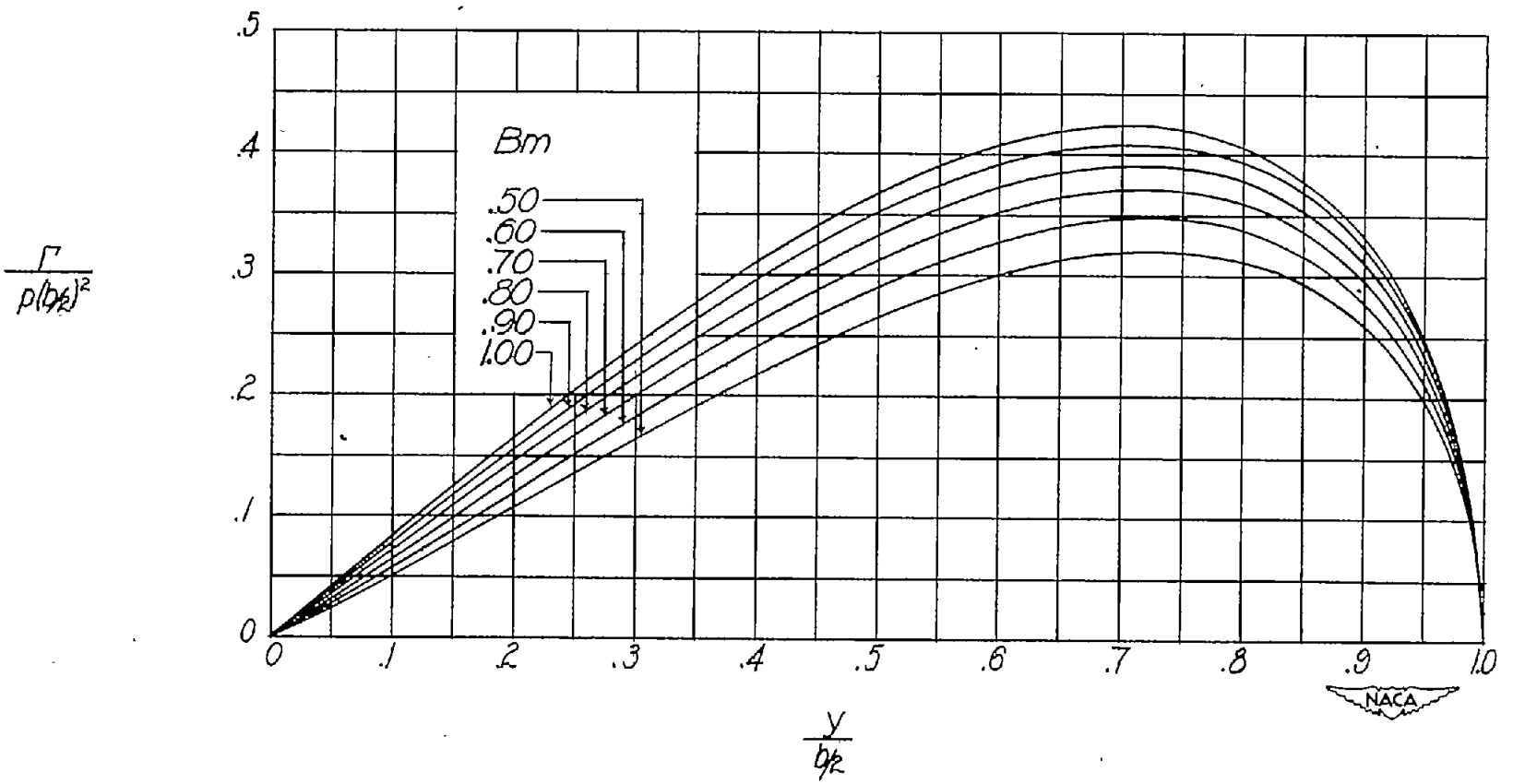

(c) AB = 4.

Figure 11.- Continued.

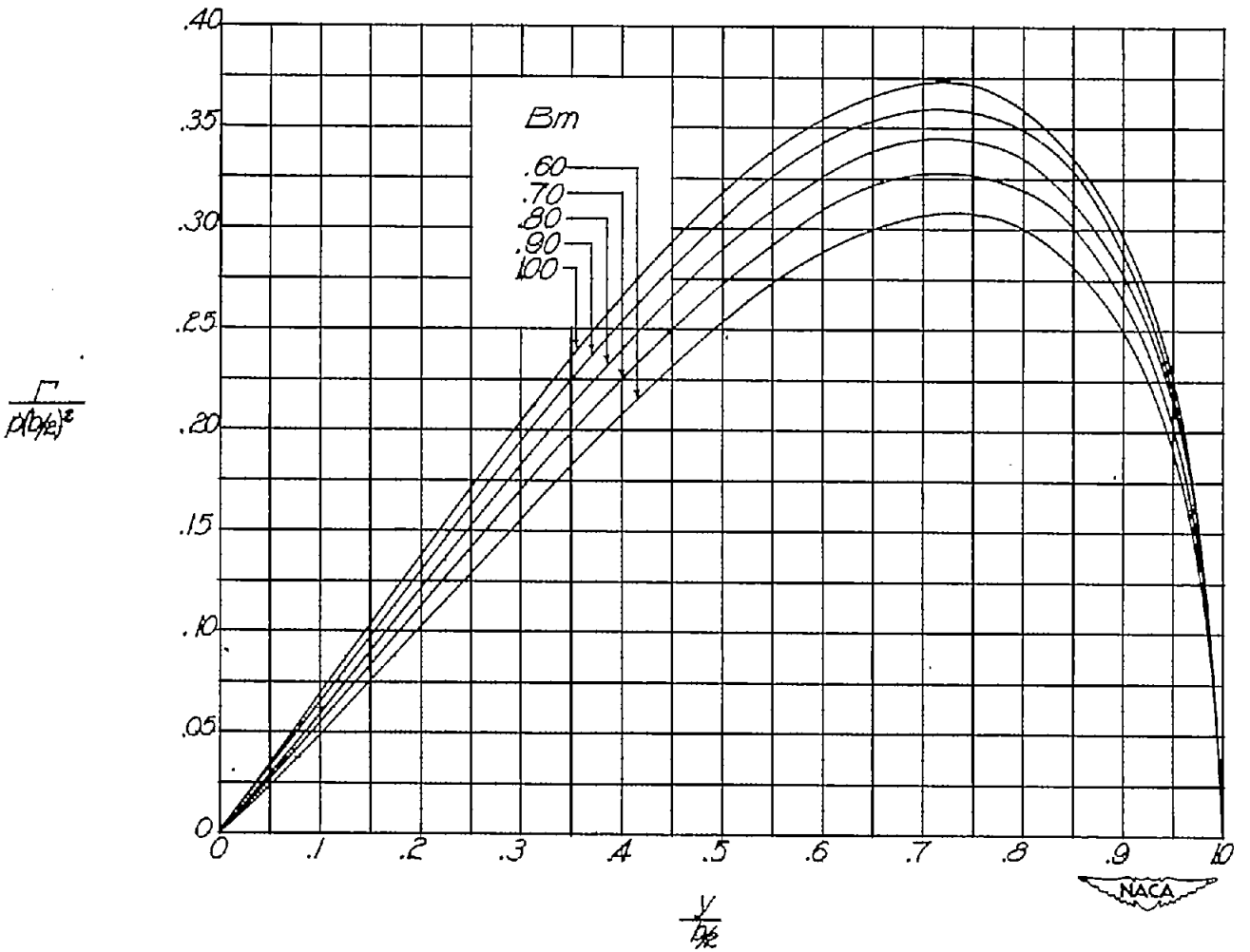

(d) AB = 5.

Figure 11.- Continued.

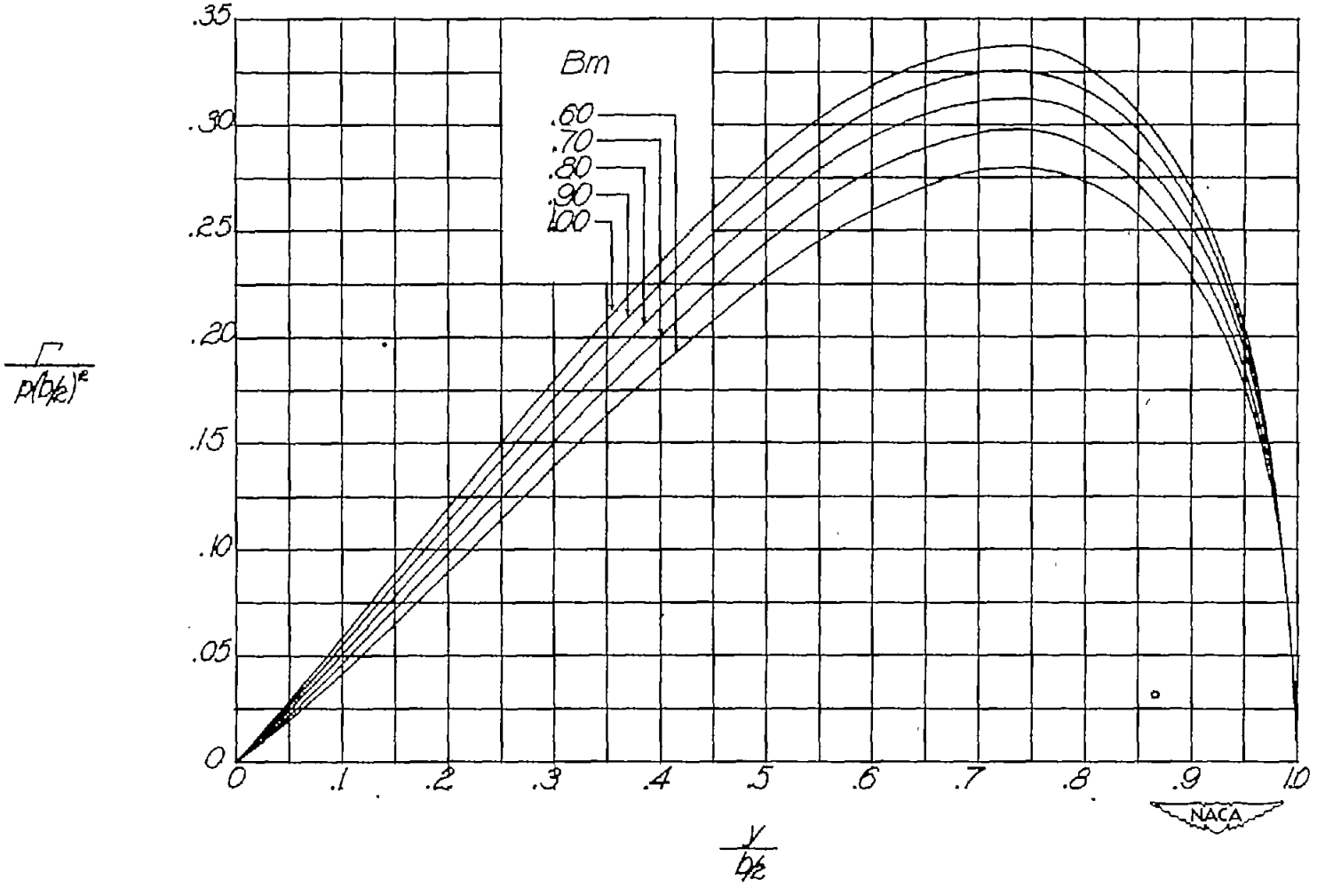

(e) AB = 6.

Figure 11.- Continued.

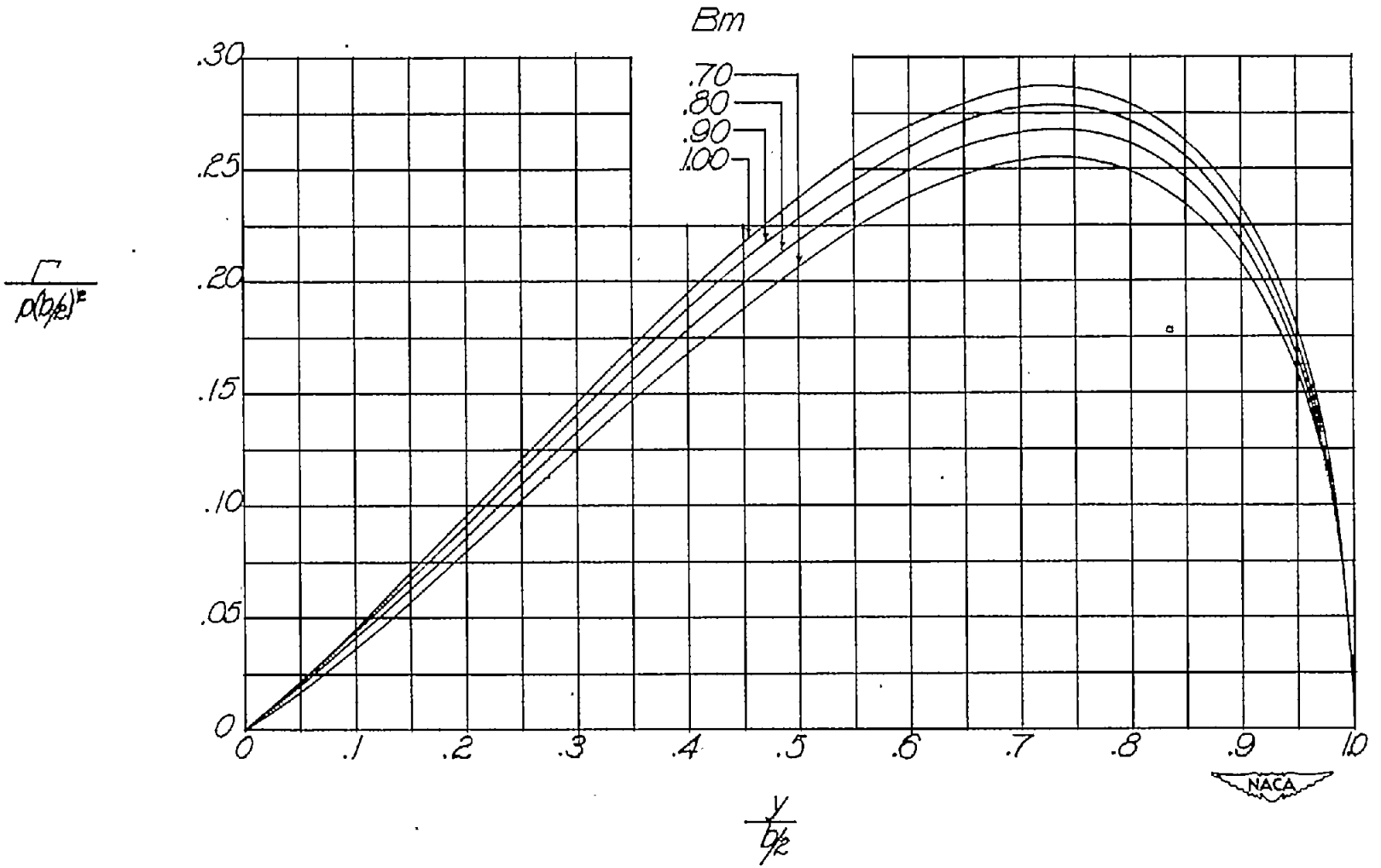

(f) AB = 8.

Figure 11.- Continued.

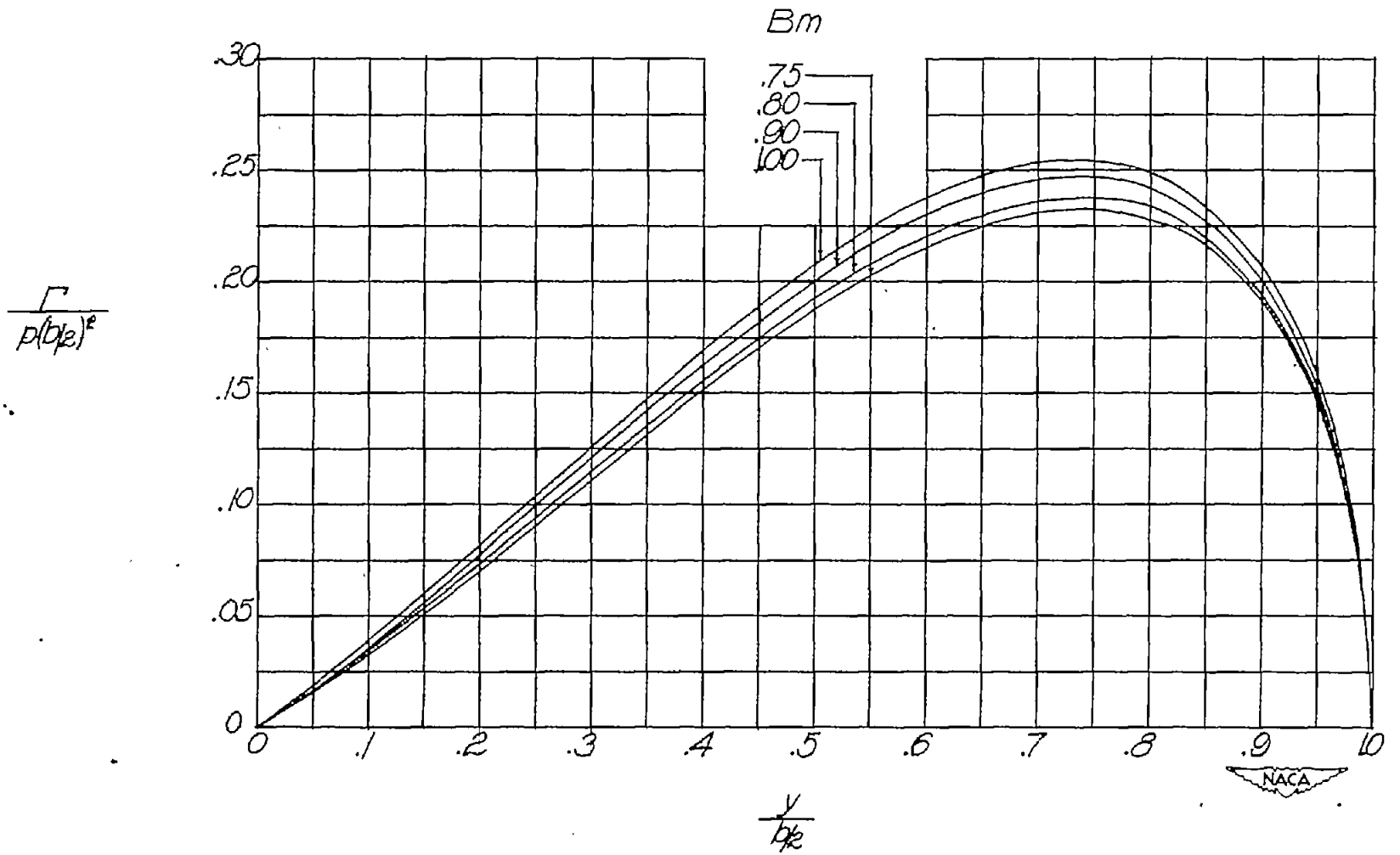

(g) AB = 10.

Figure 11.- Continued.

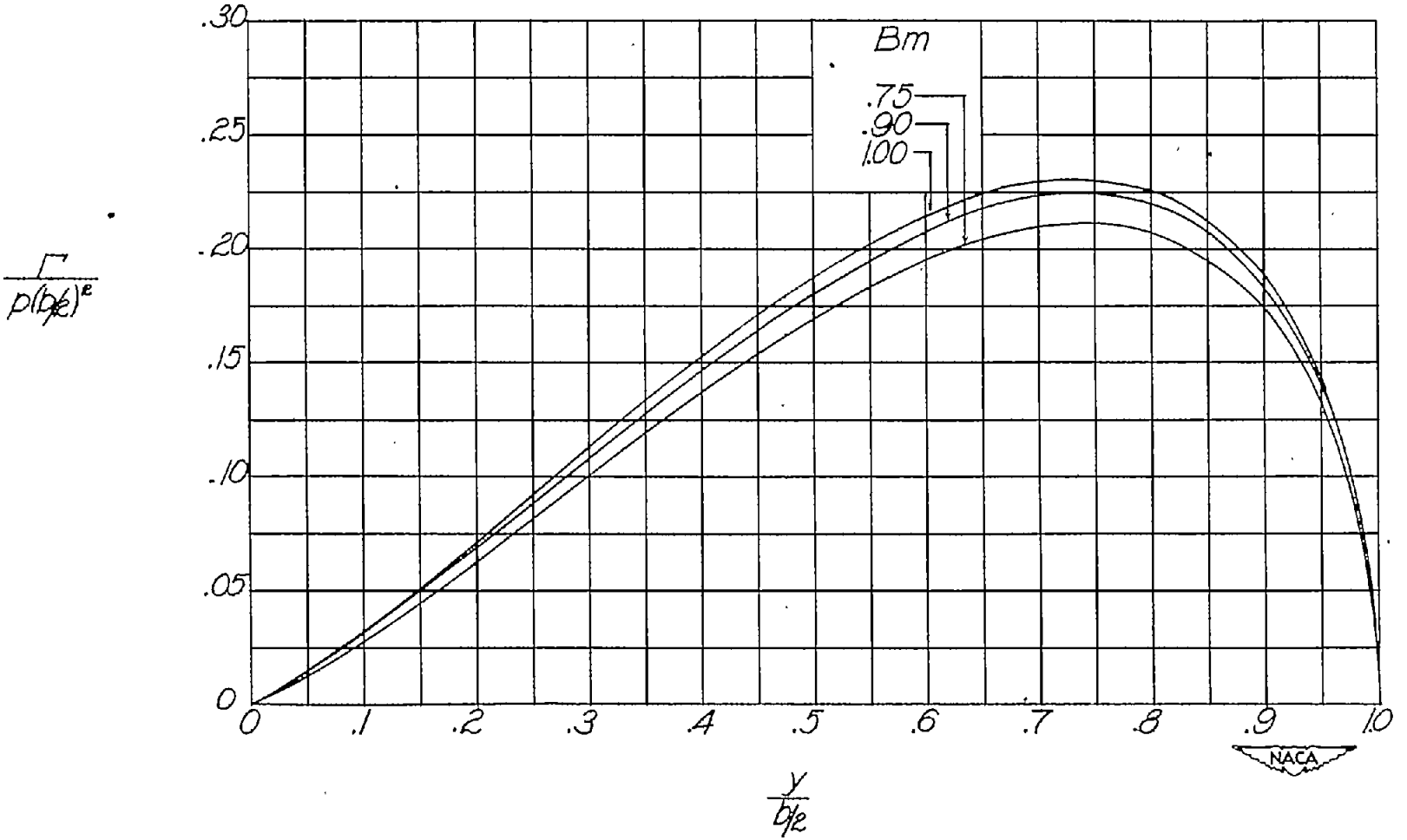

(h) AB = 12.

Figure 11.- Continued.

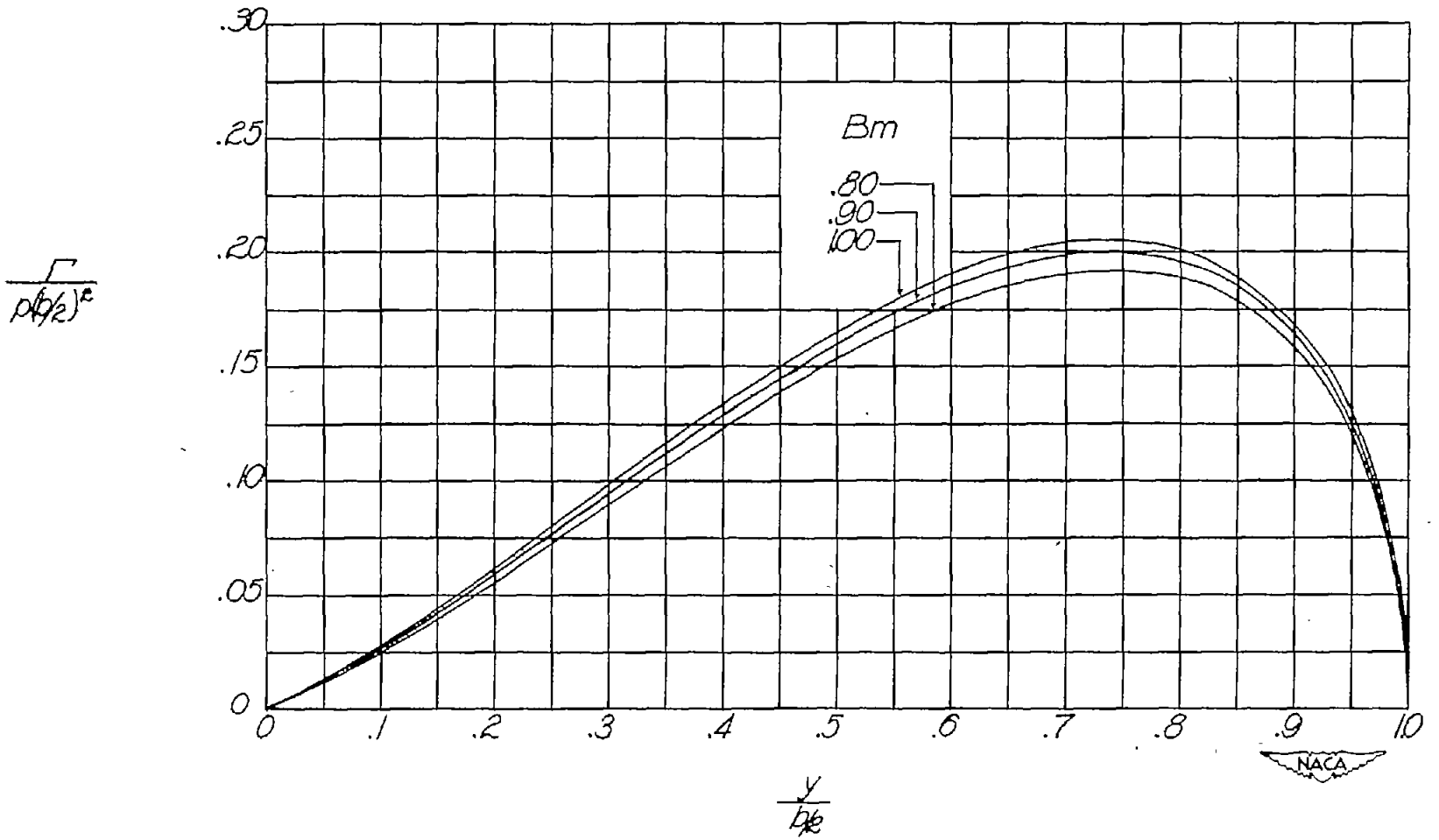

(i) AB = 15.

Figure 11.- Continued.

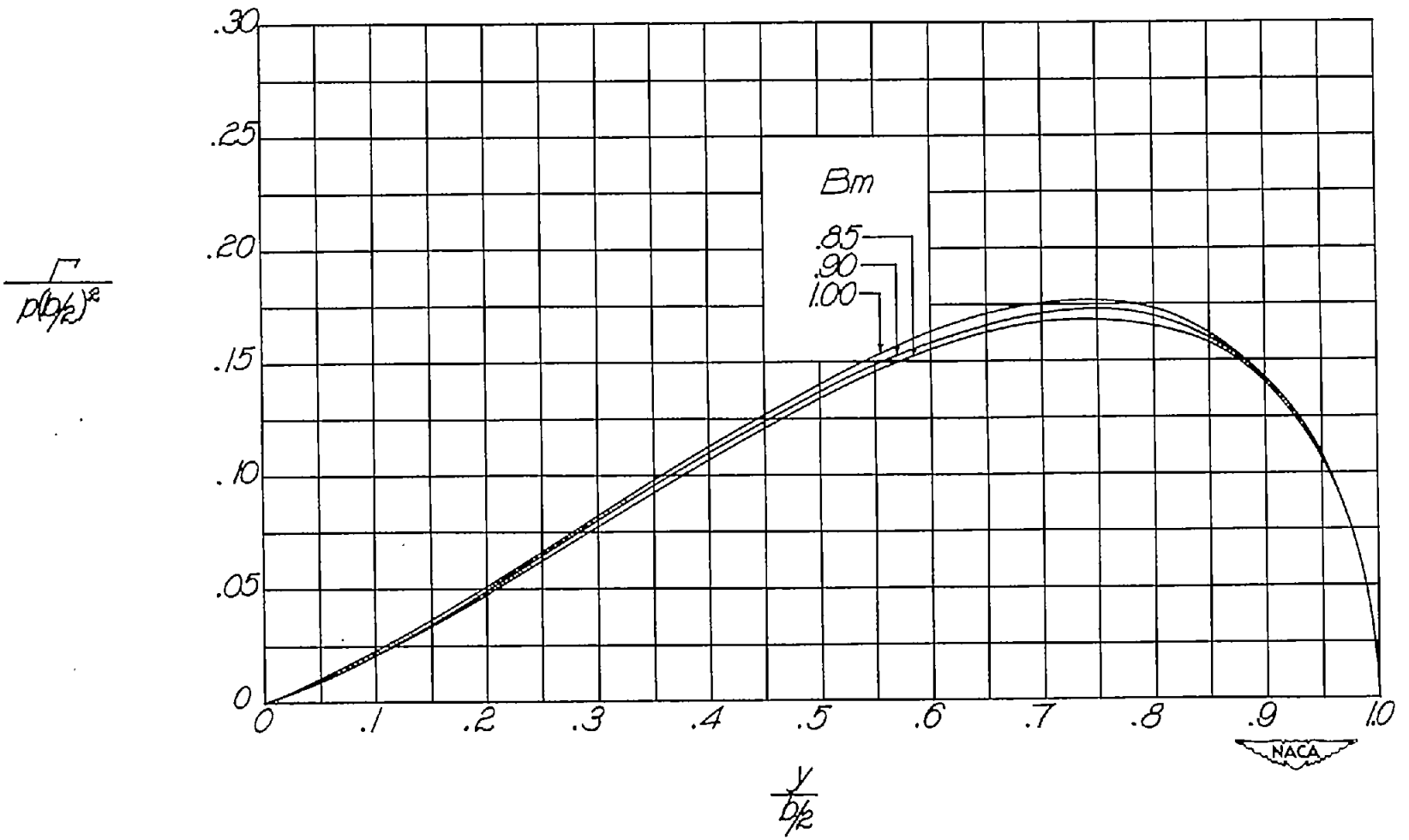

(j) AB = 20.

Figure 11.- Concluded.

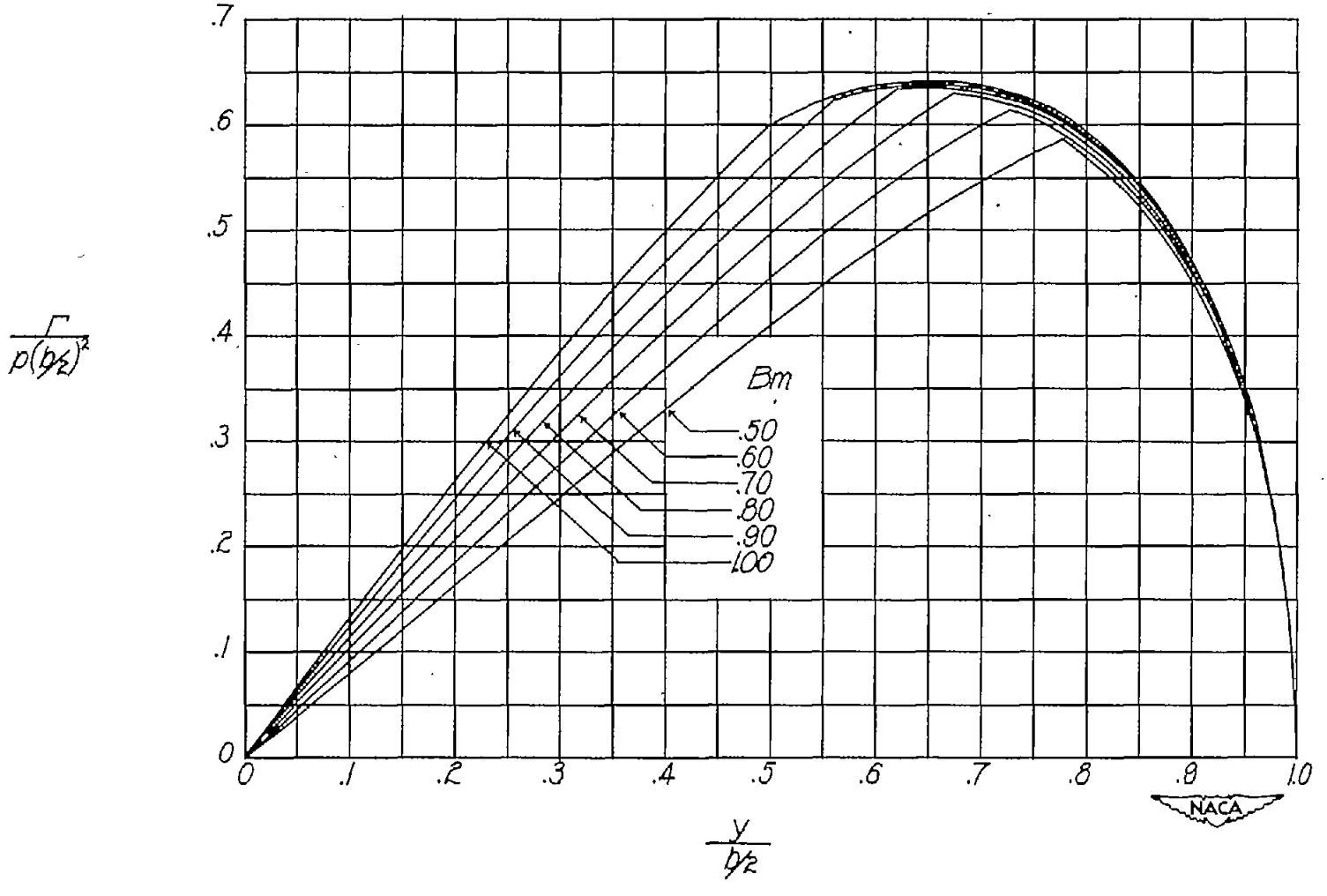

(a) AB = 2.

Figure 12.- Distribution of circulation along span for wings with steady rolling velocity with $\lambda = 0.25$.

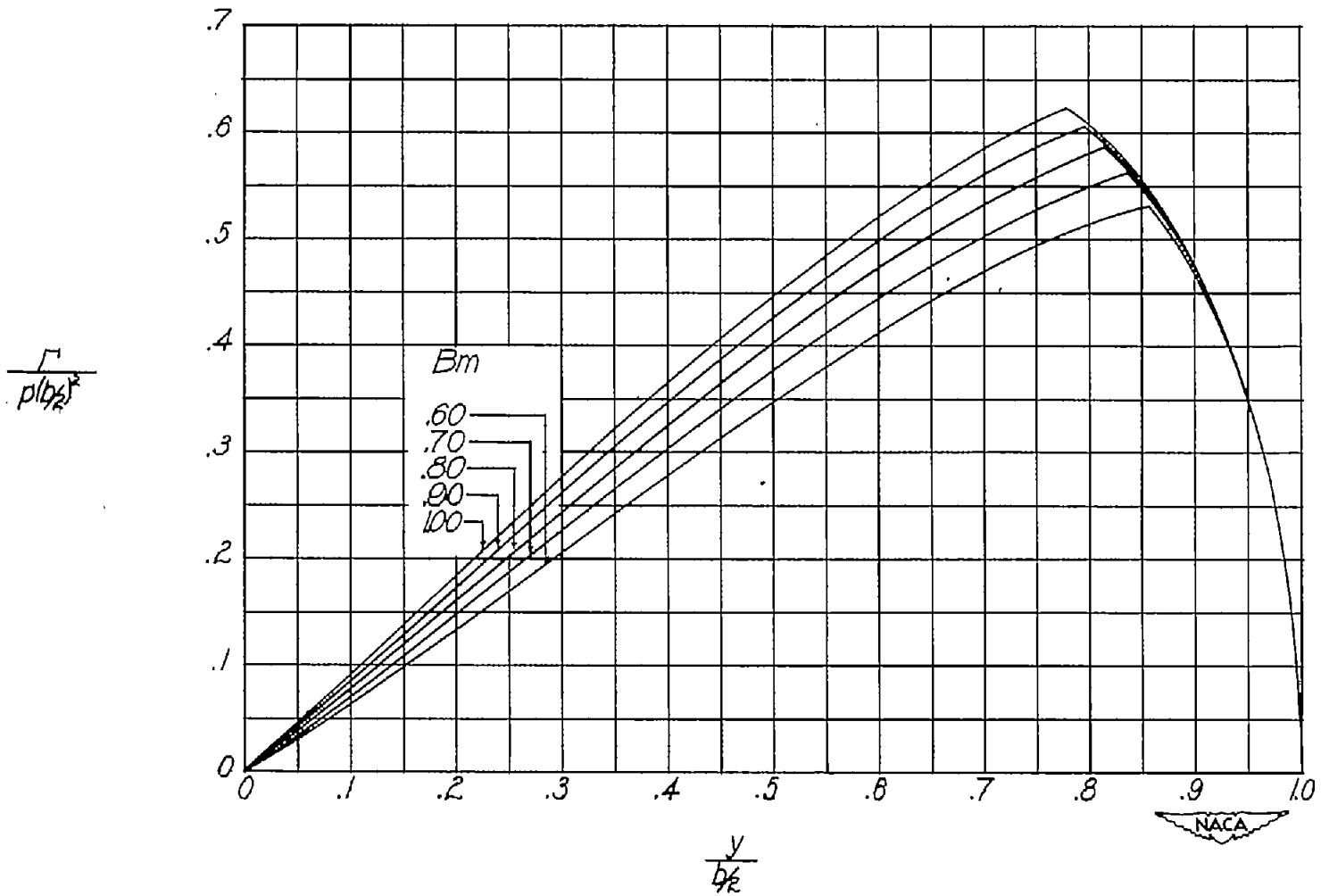

(b) AB = 3.

Figure 12.- Continued.

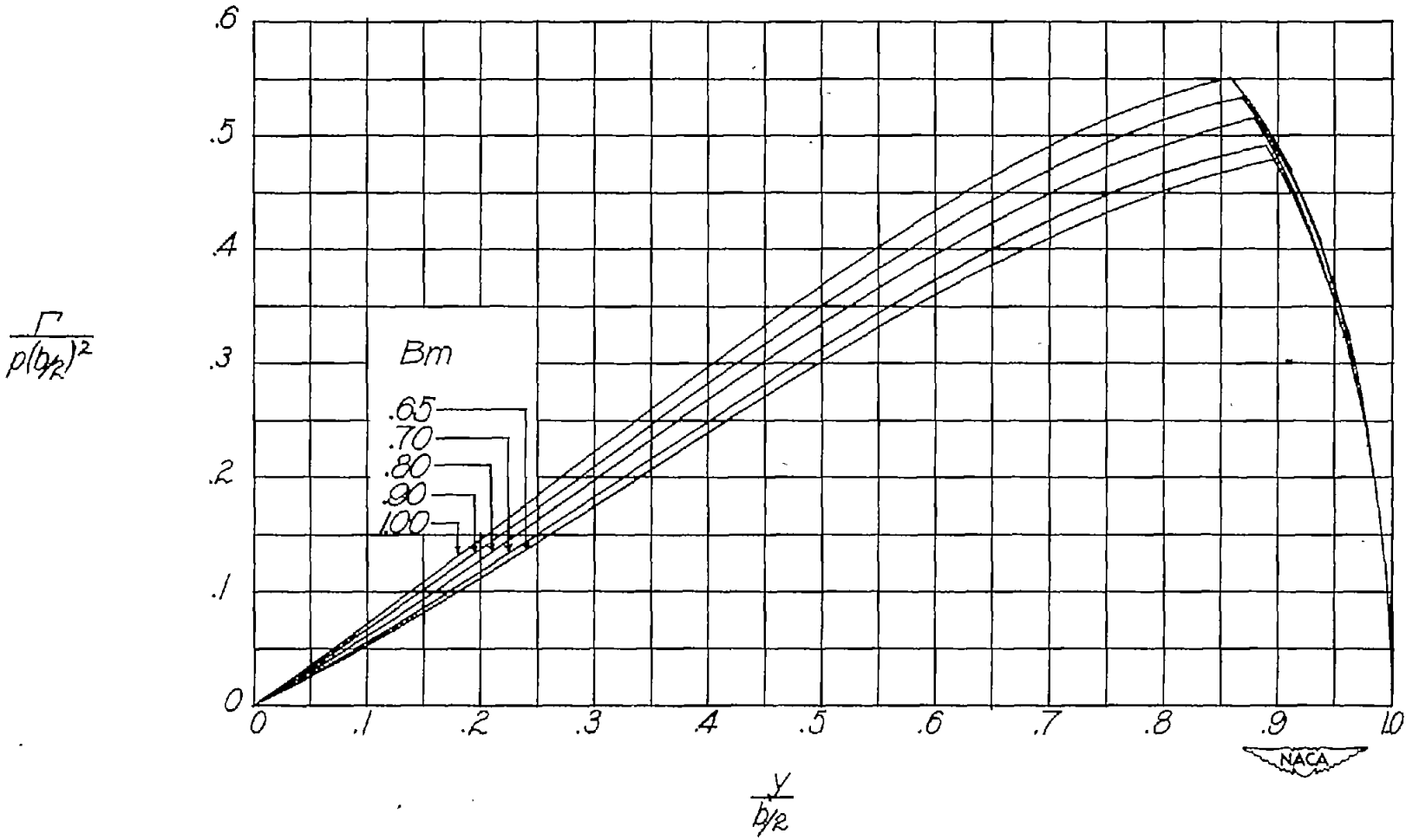

(c) AB = 4.

Figure 12.- Continued.

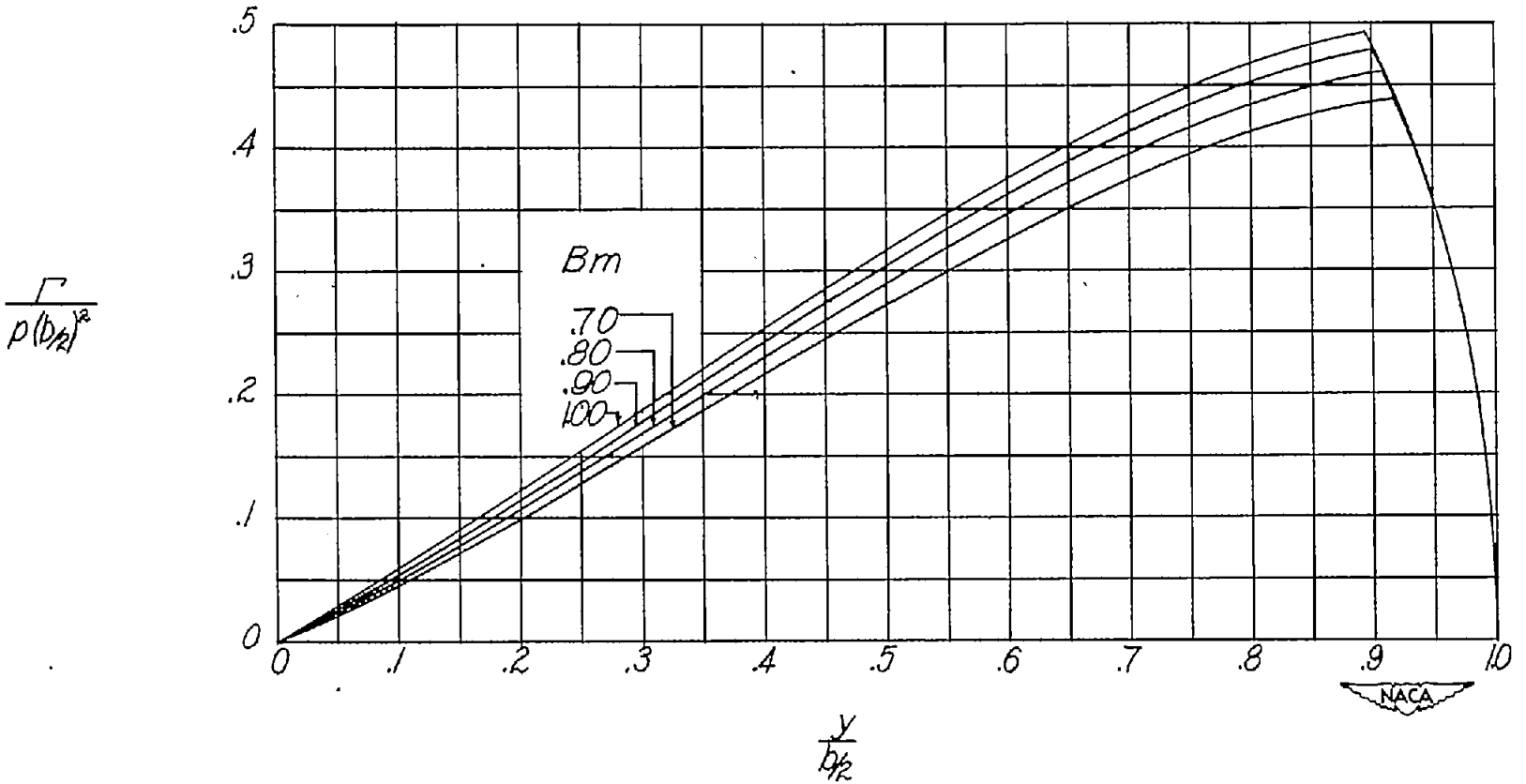

(d) AB = 5.

Figure 12.- Continued.

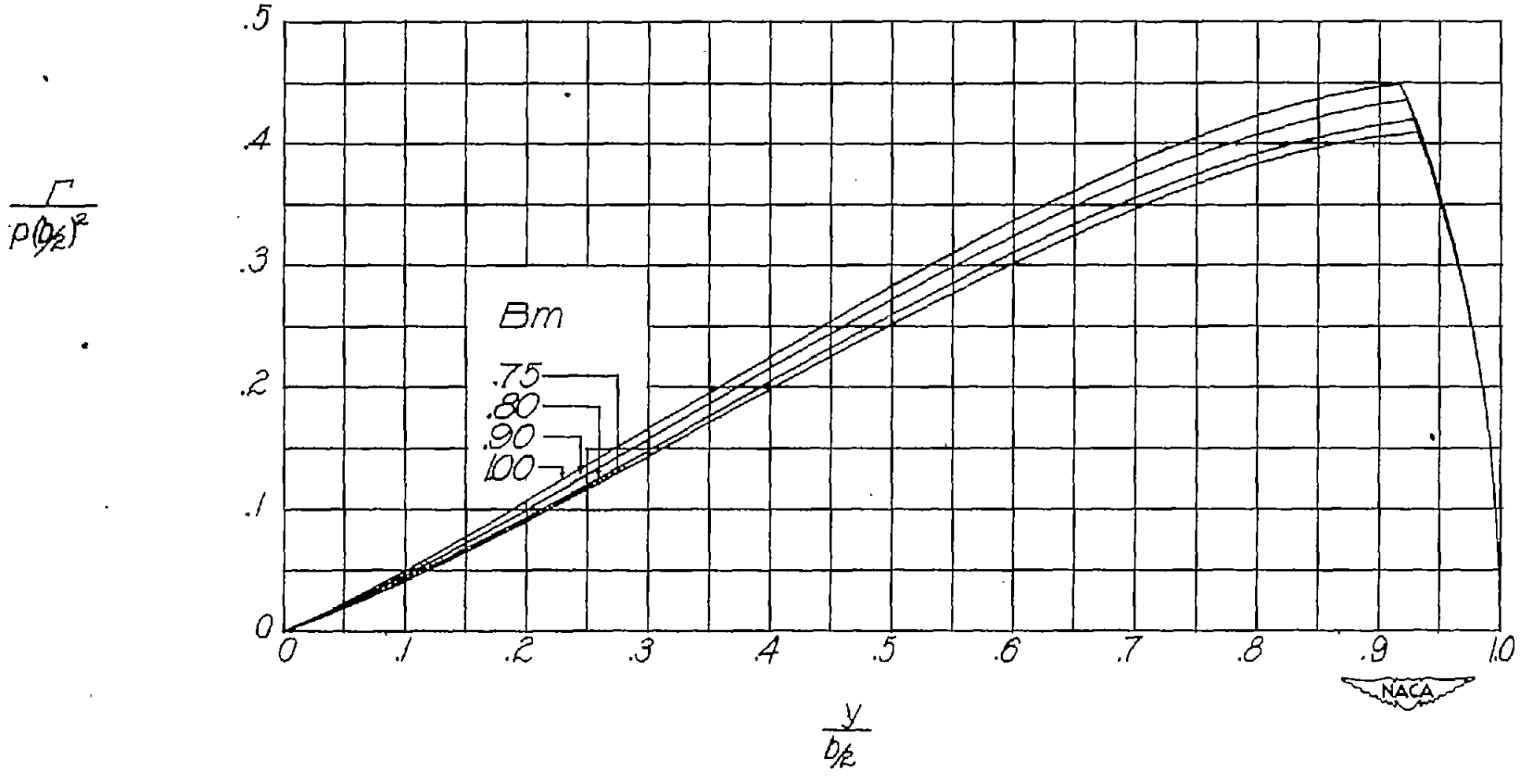

(e) AB = 6.

Figure 12.- Continued.

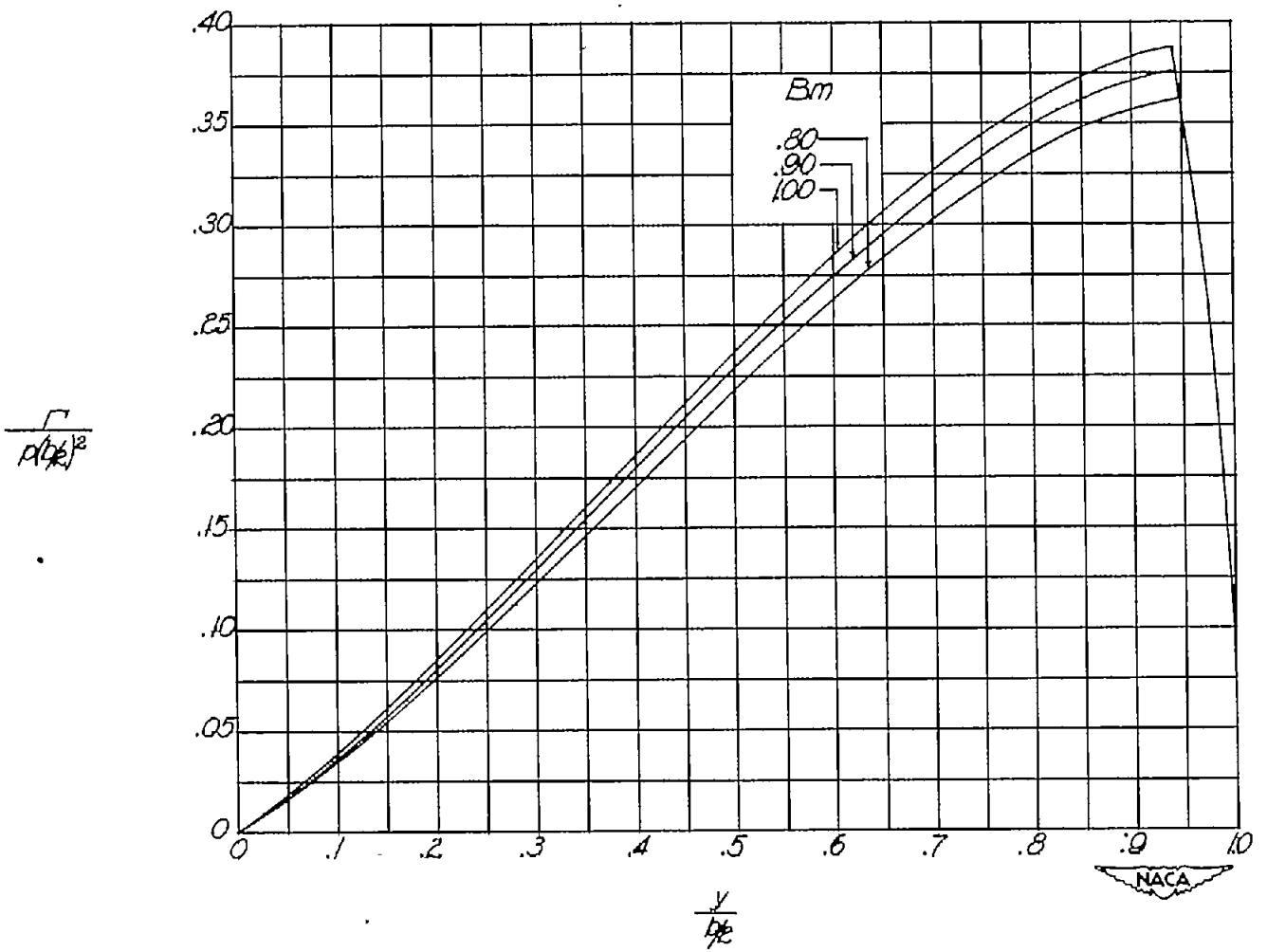

(f) AB = 8.

Figure 12.- Continued.

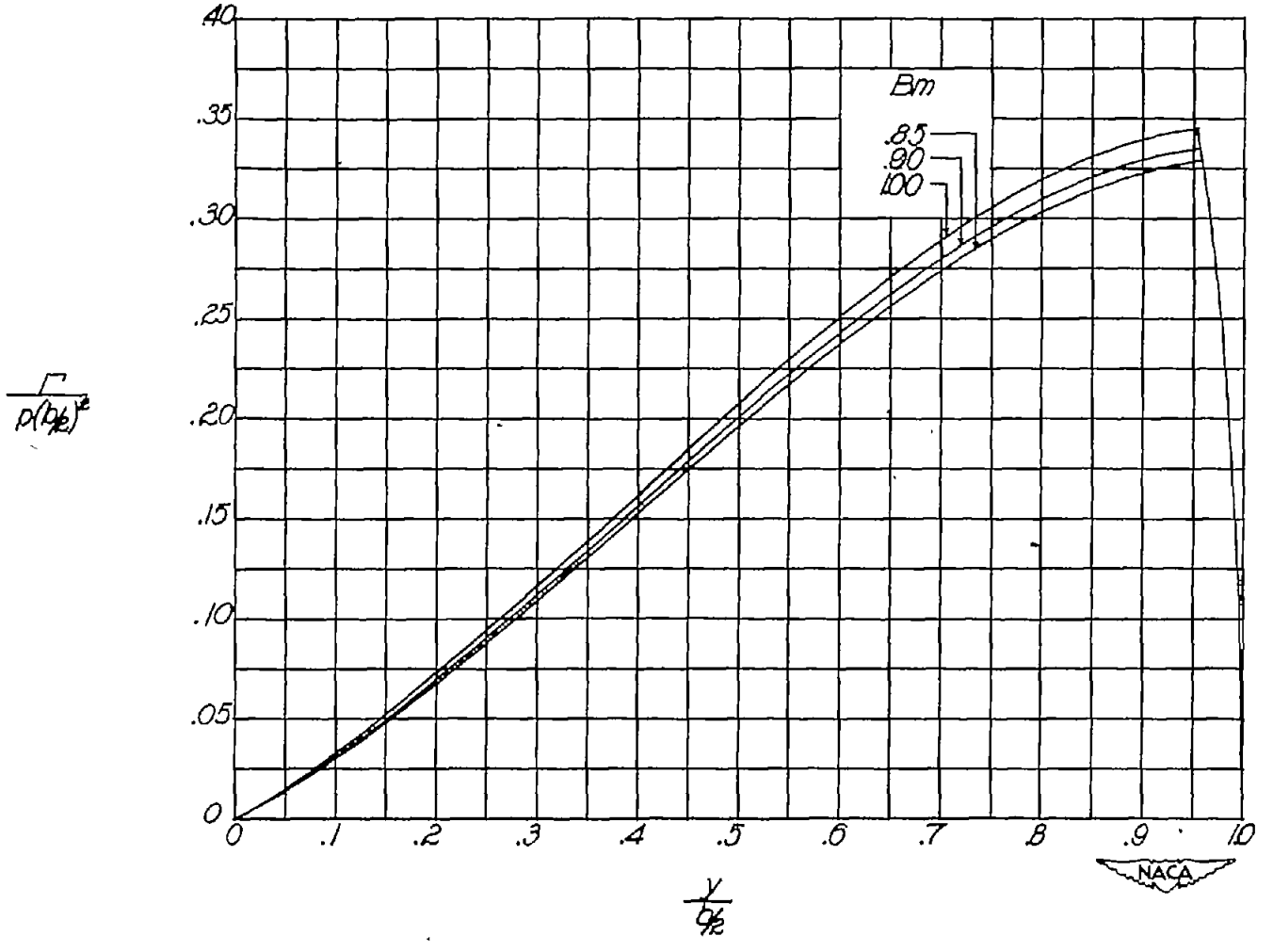

(g) AB = 10.

Figure 12.- Continued.

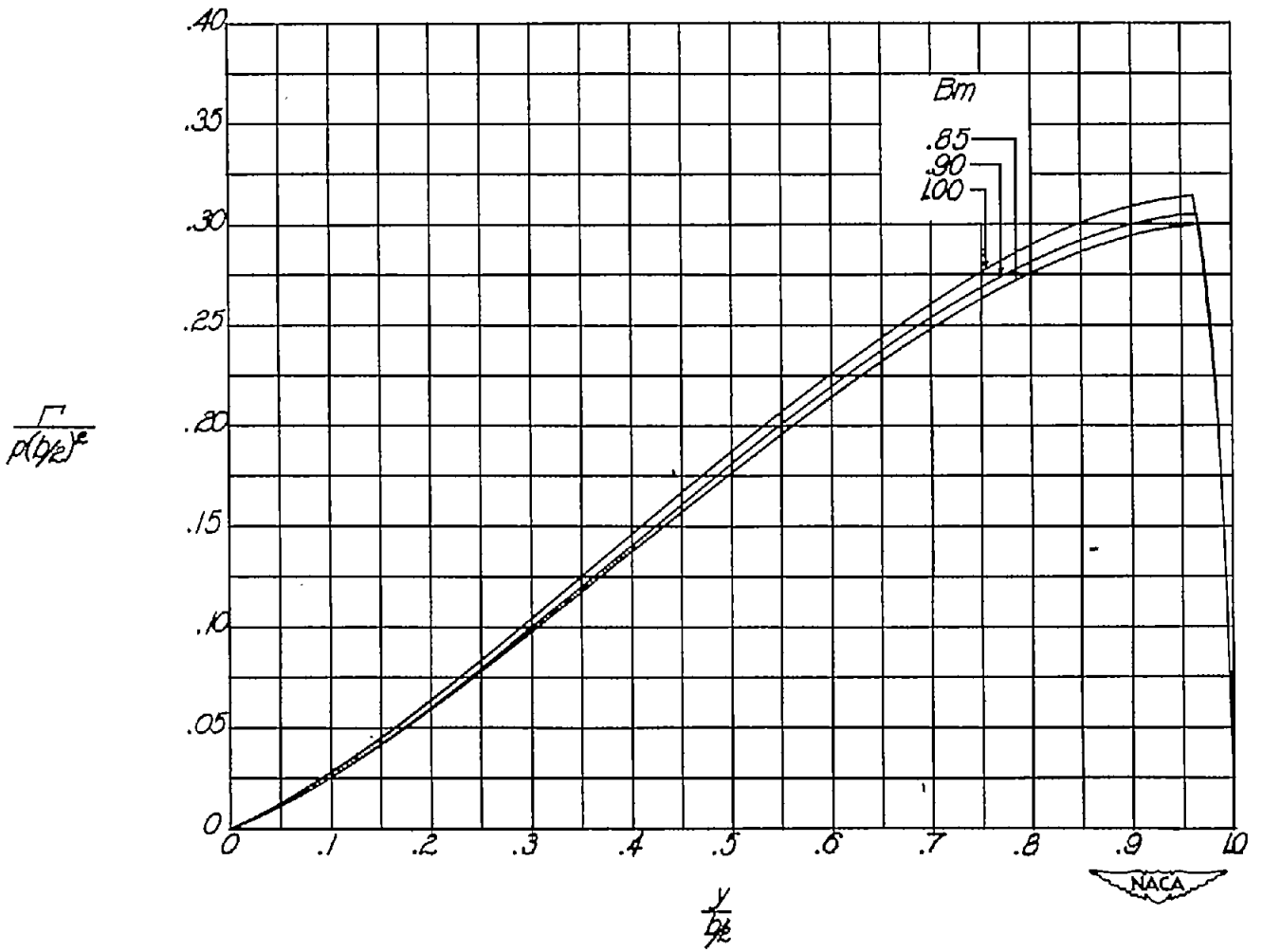

(h) AB = 12.

Figure 12.- Continued.

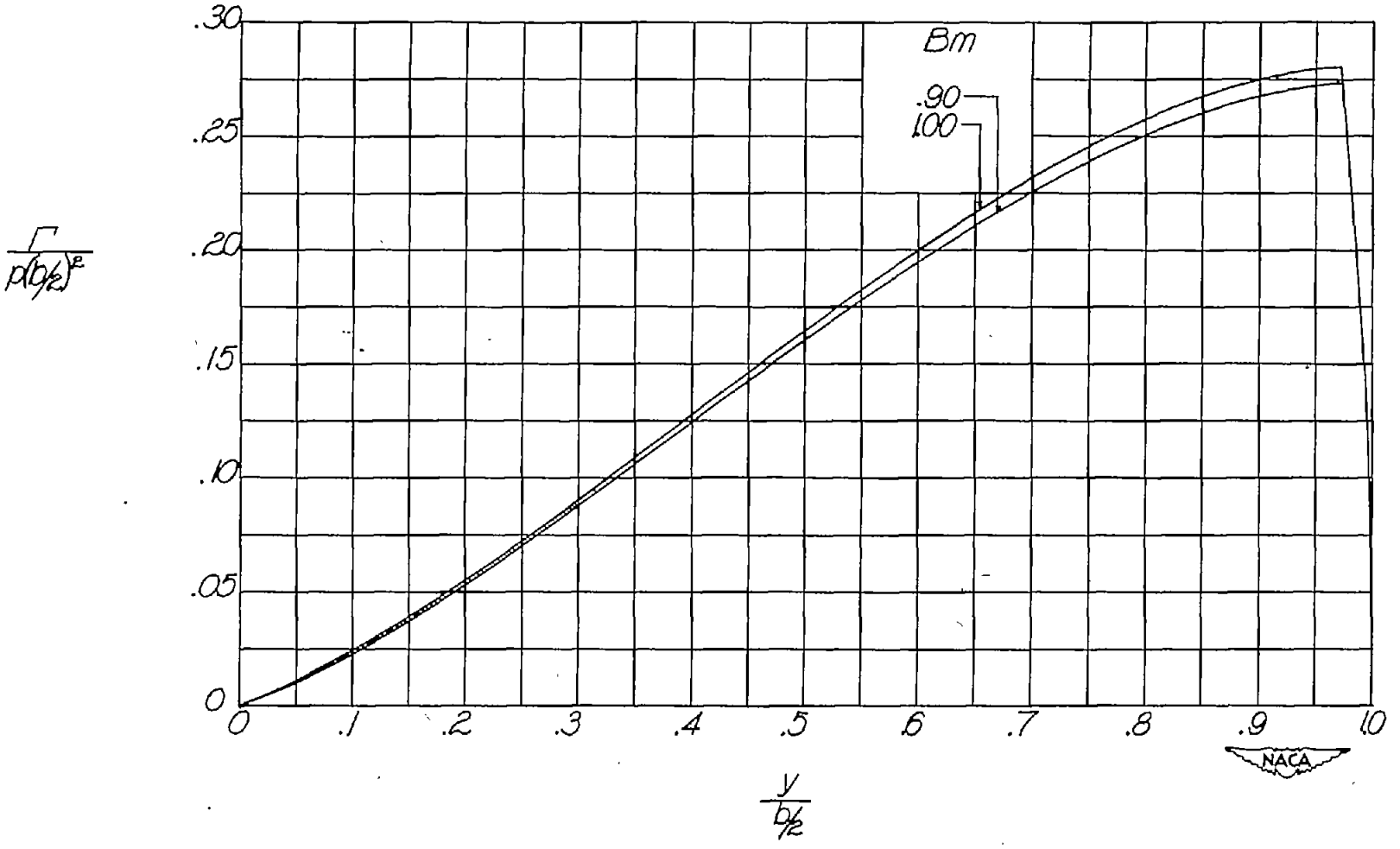

(i) AB = 15.

Figure 12.- Continued.

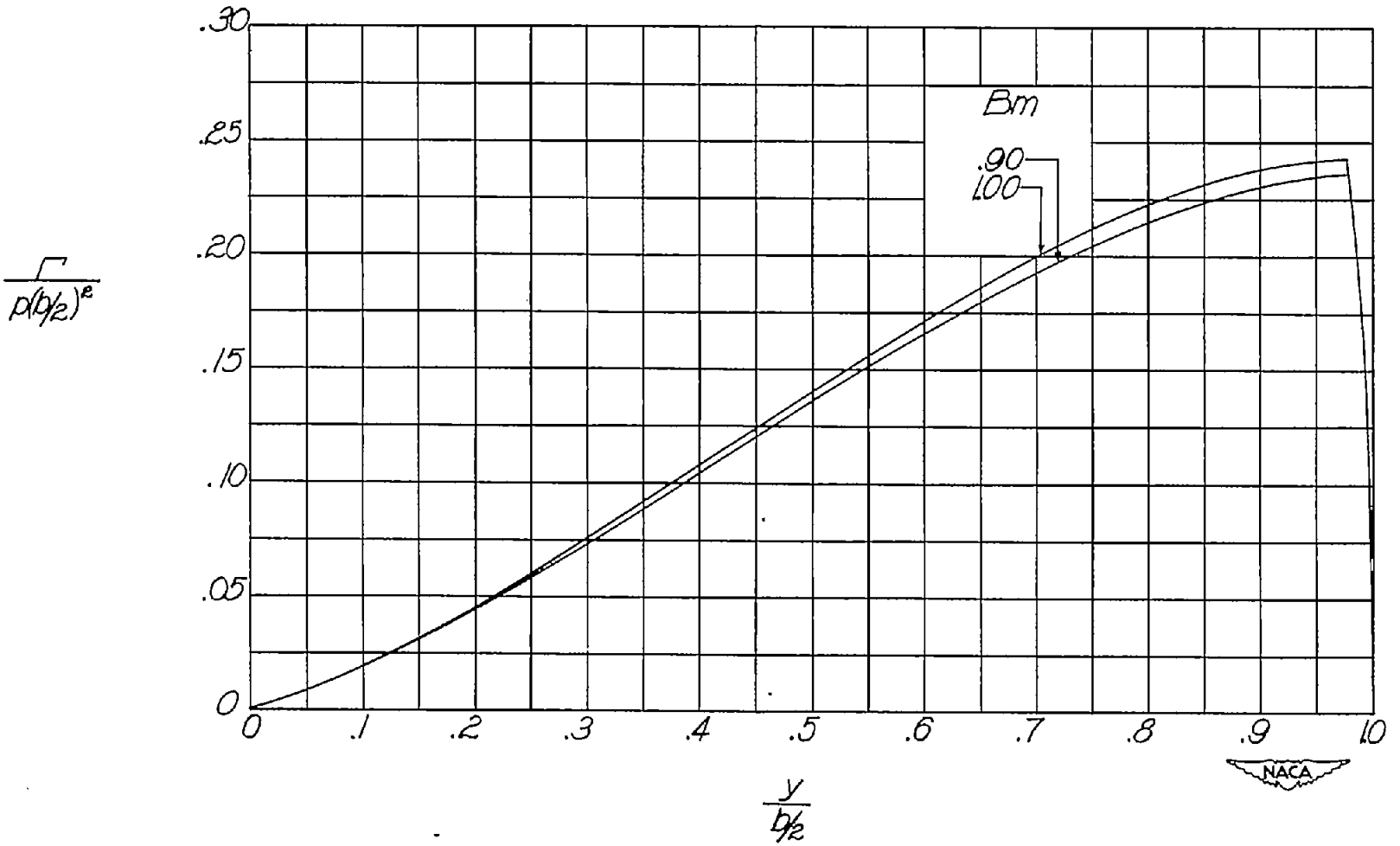

(j) AB = 20.

Figure 12.- Concluded.

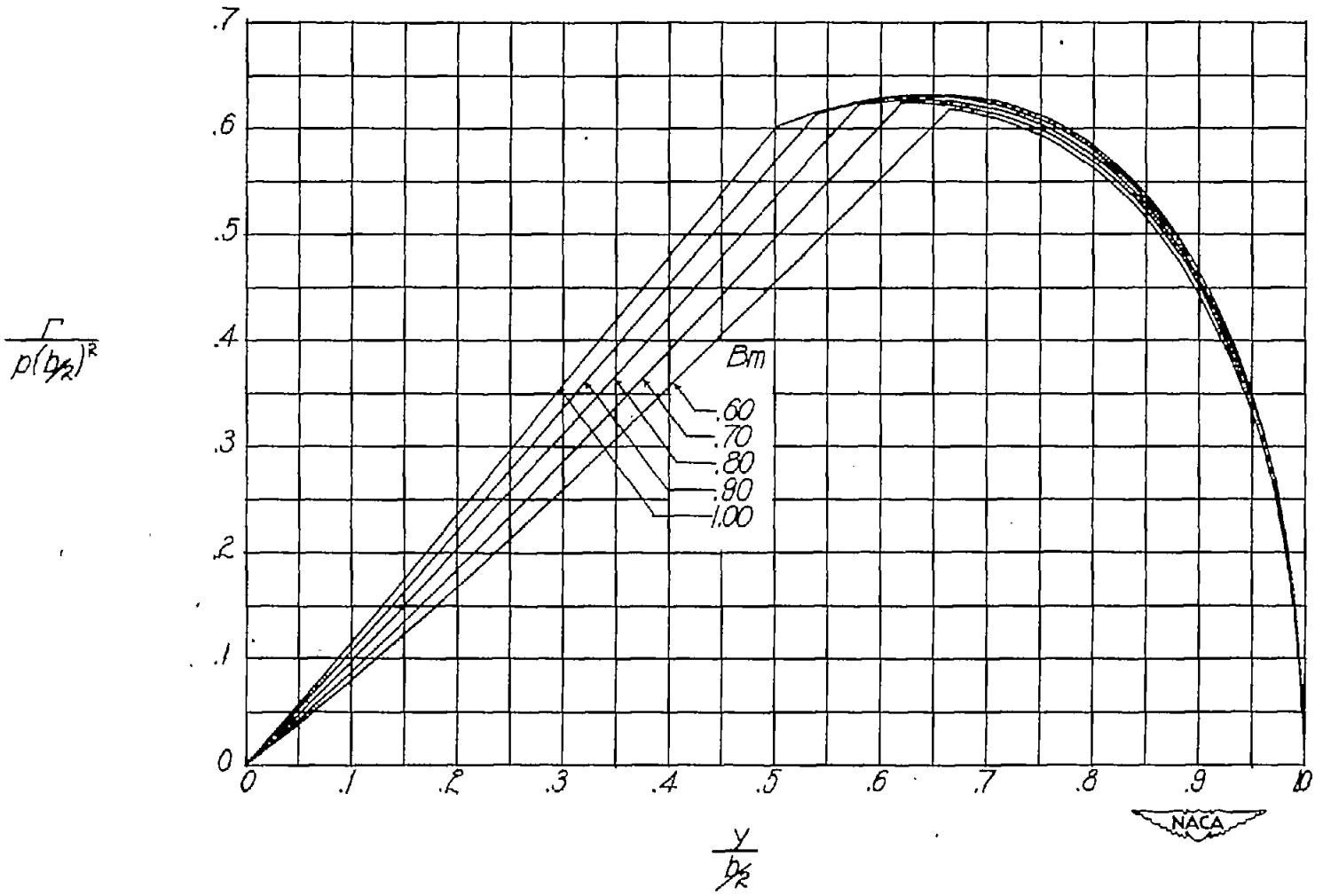

(a) AB = 2.

Figure 13.- Distribution of circulation along span for wings with steady rolling velocity with $\lambda = 0.50$.

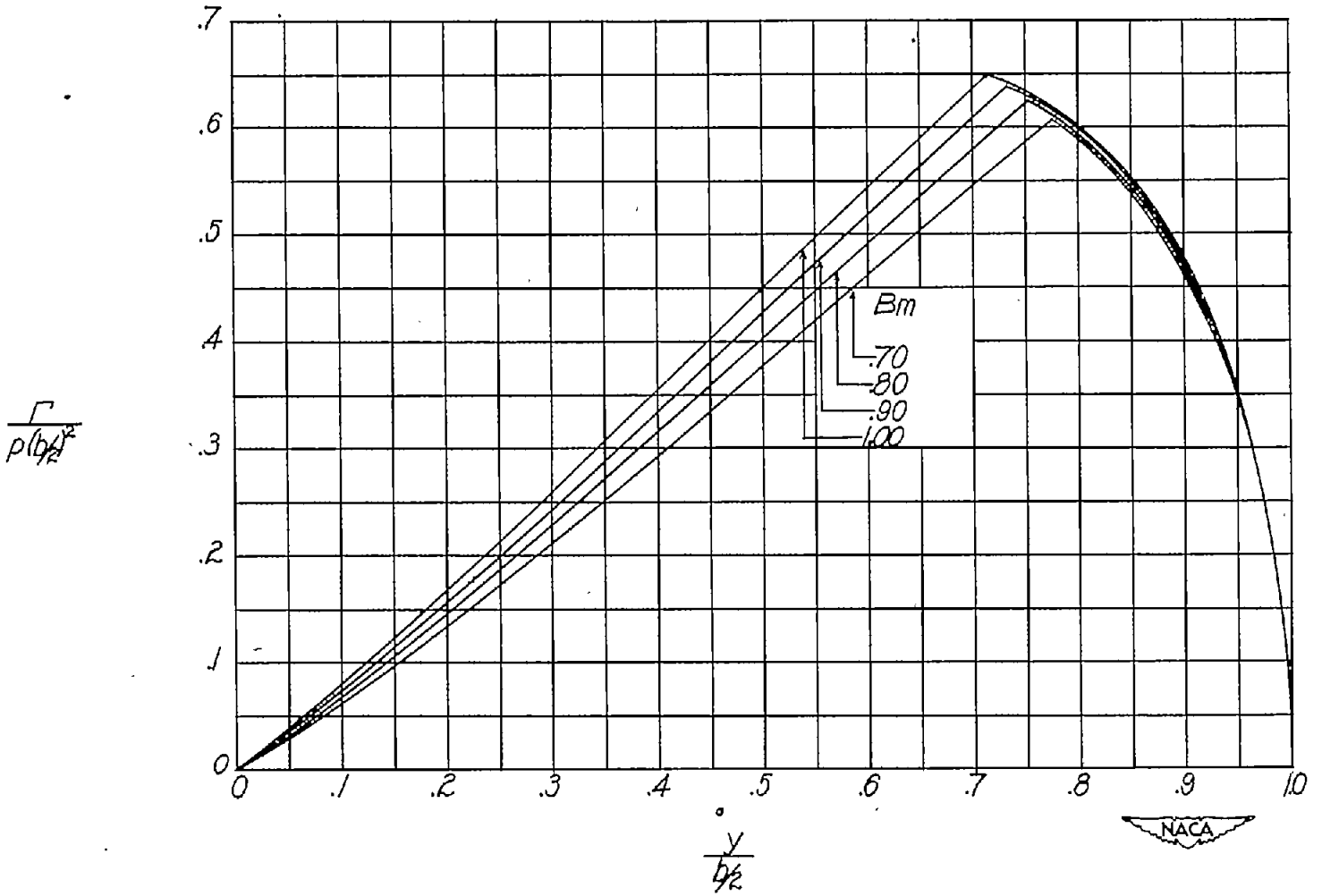

(b) AB = 3.

Figure 13.- Continued.

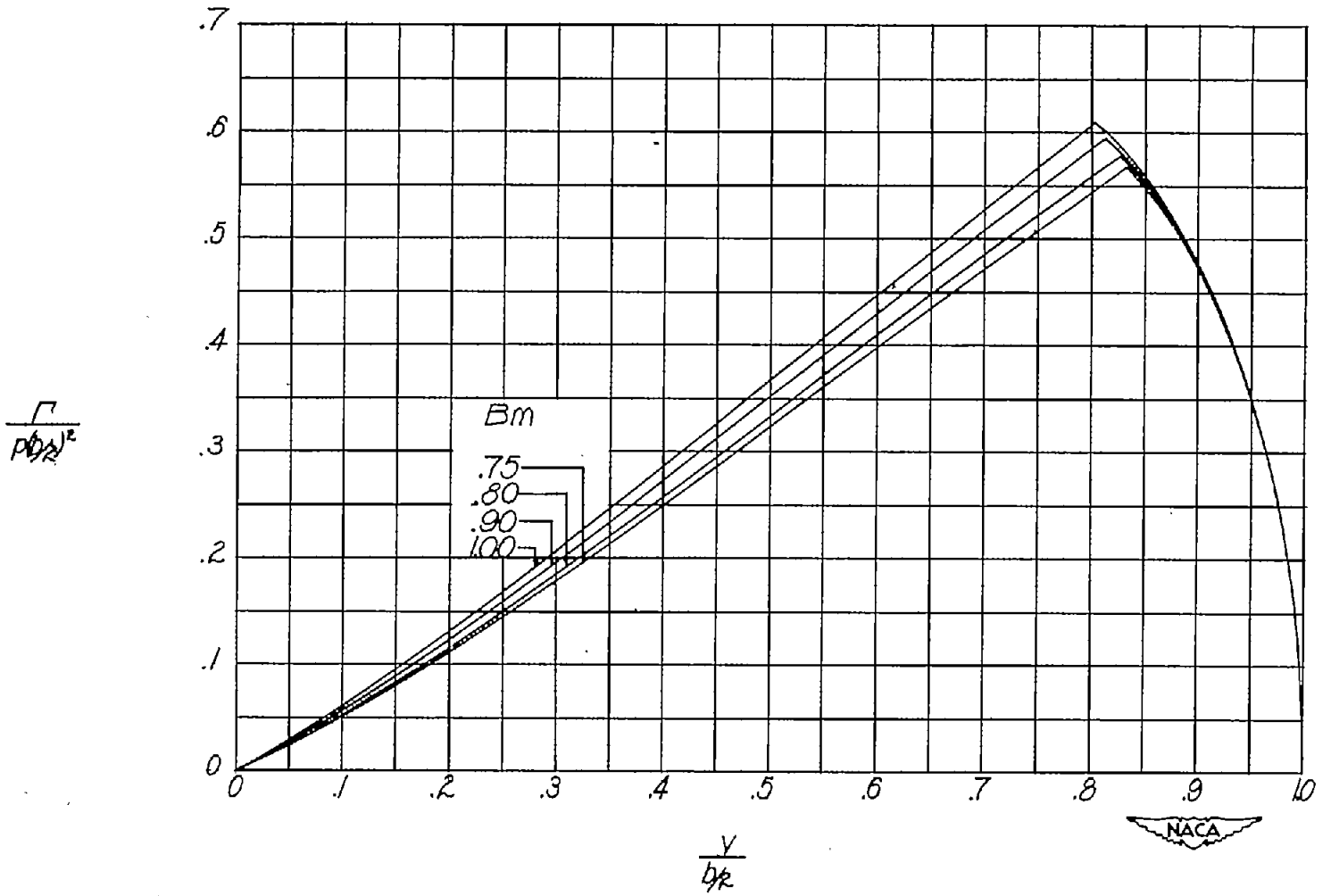

(c) AB = 4.

Figure 13.- Continued.

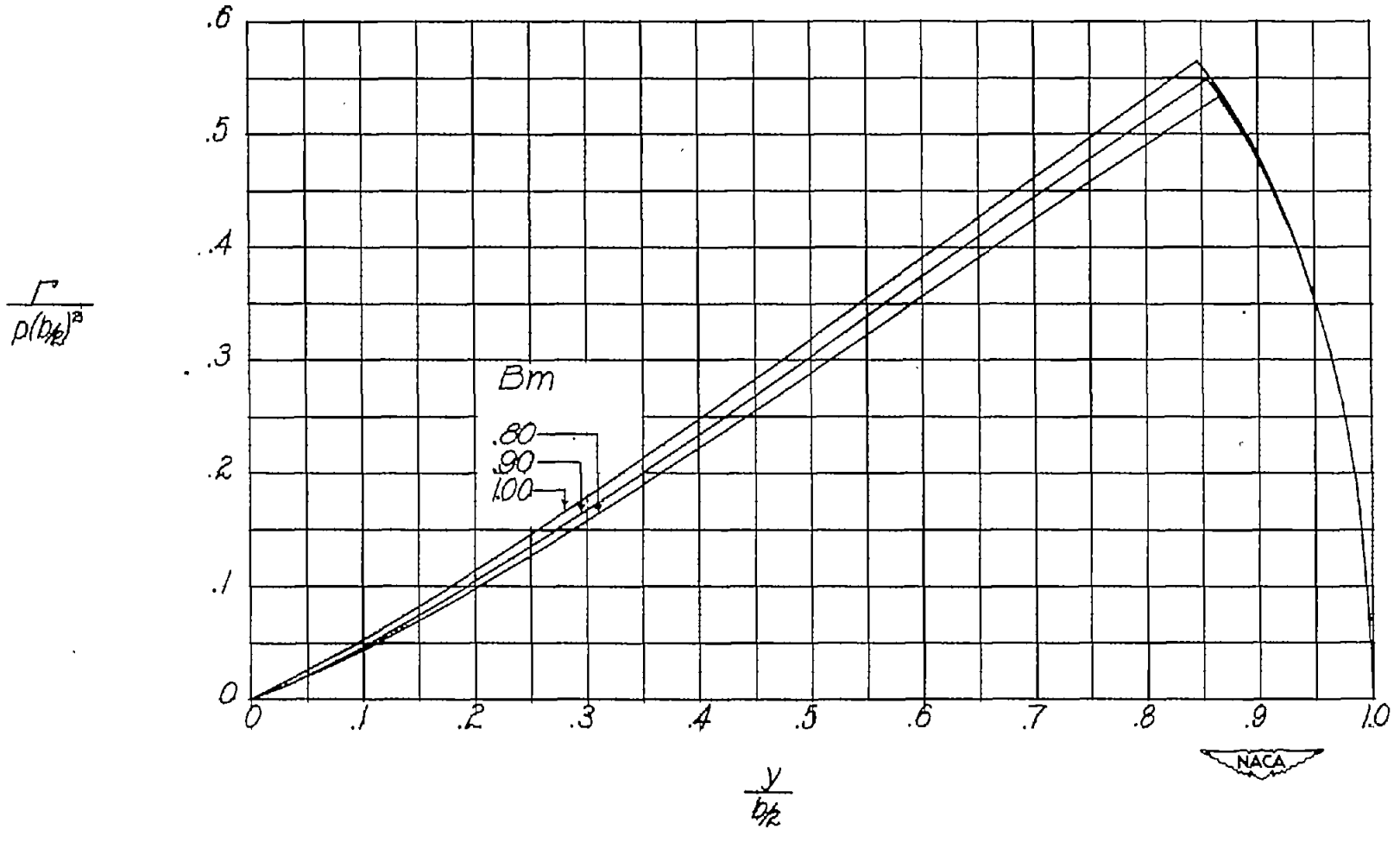

(d) AB = 5.

Figure 13.- Continued.

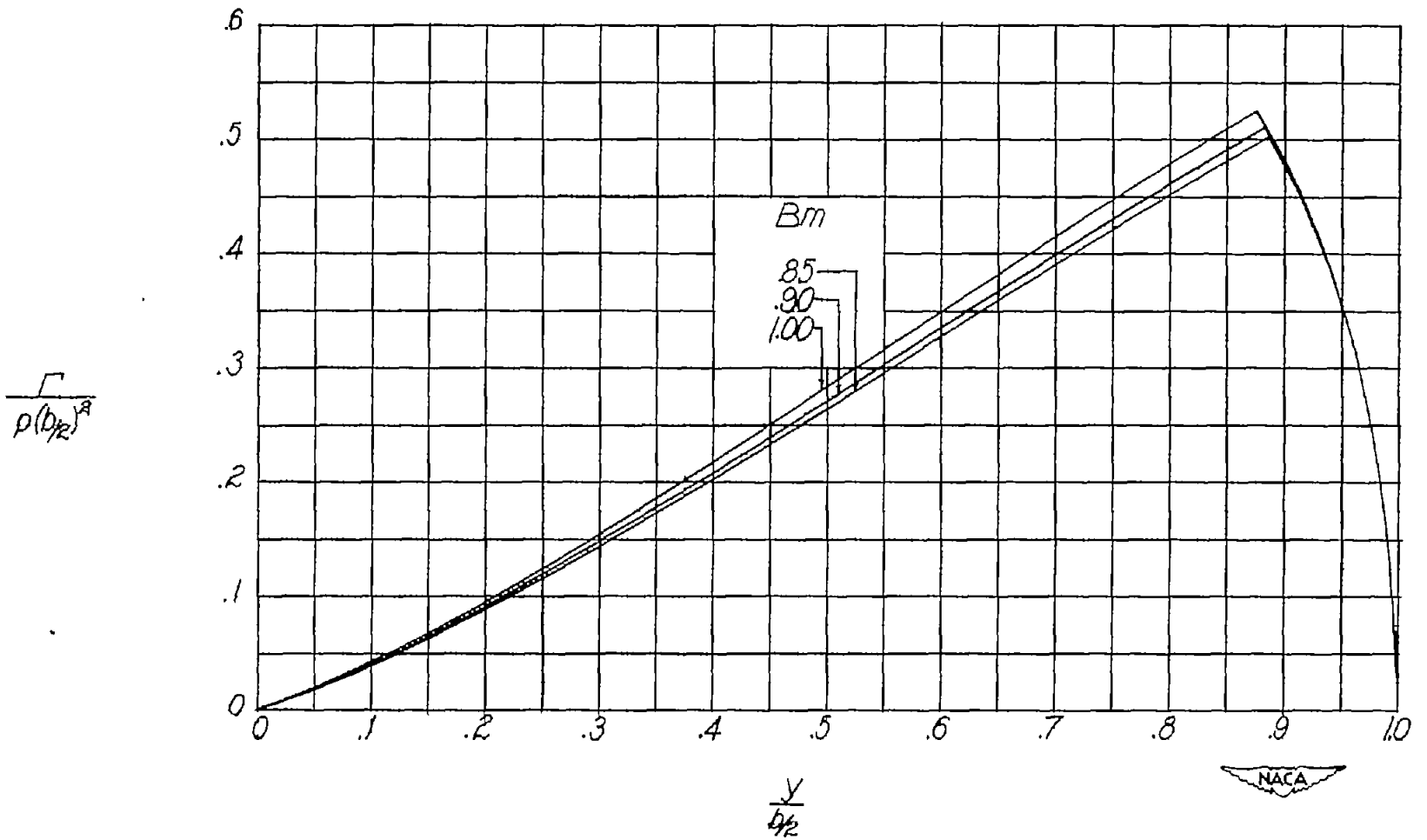

(e) AB = 6.

Figure 13.- Continued.

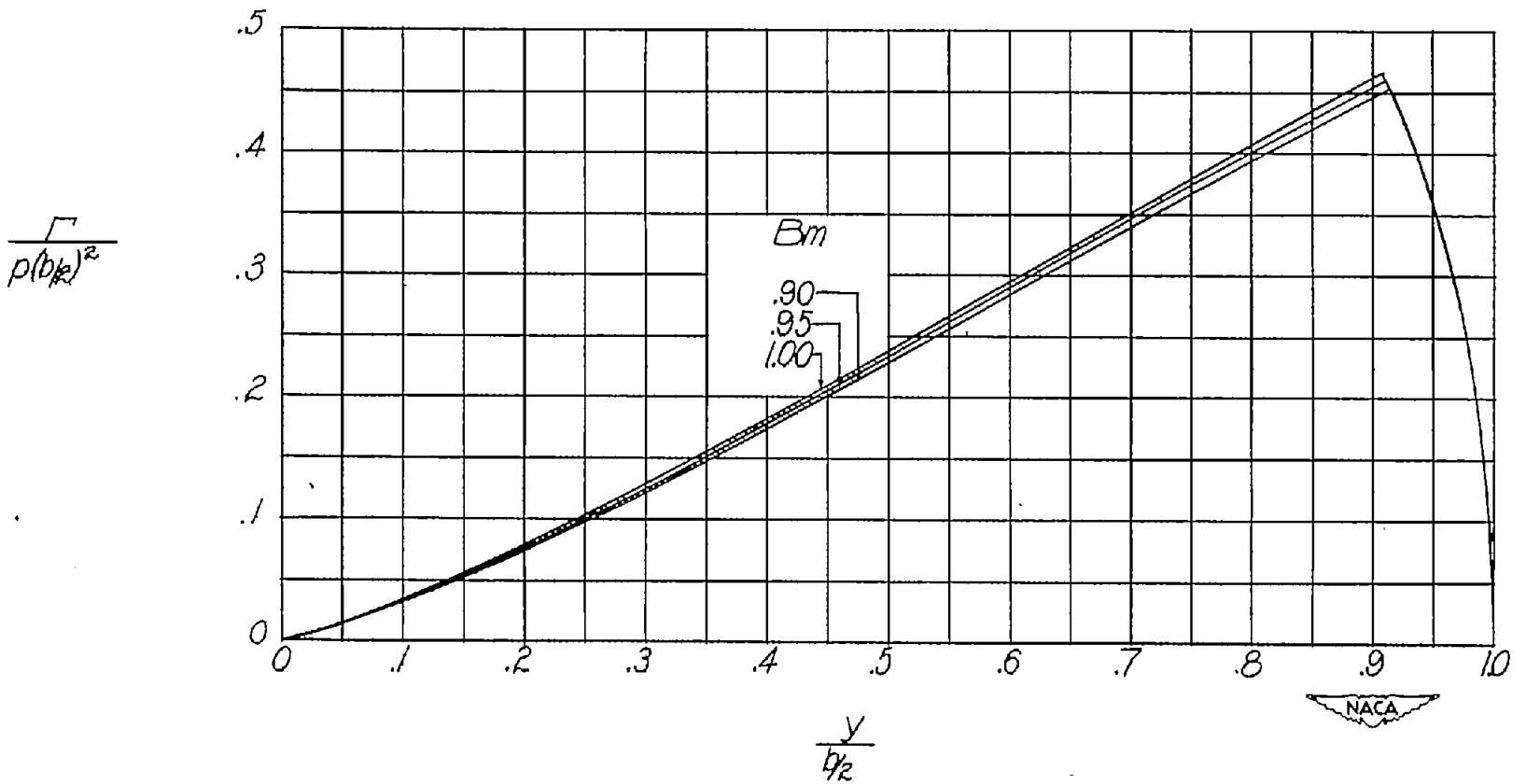

(f) AB = 8.

Figure 13.- Continued.

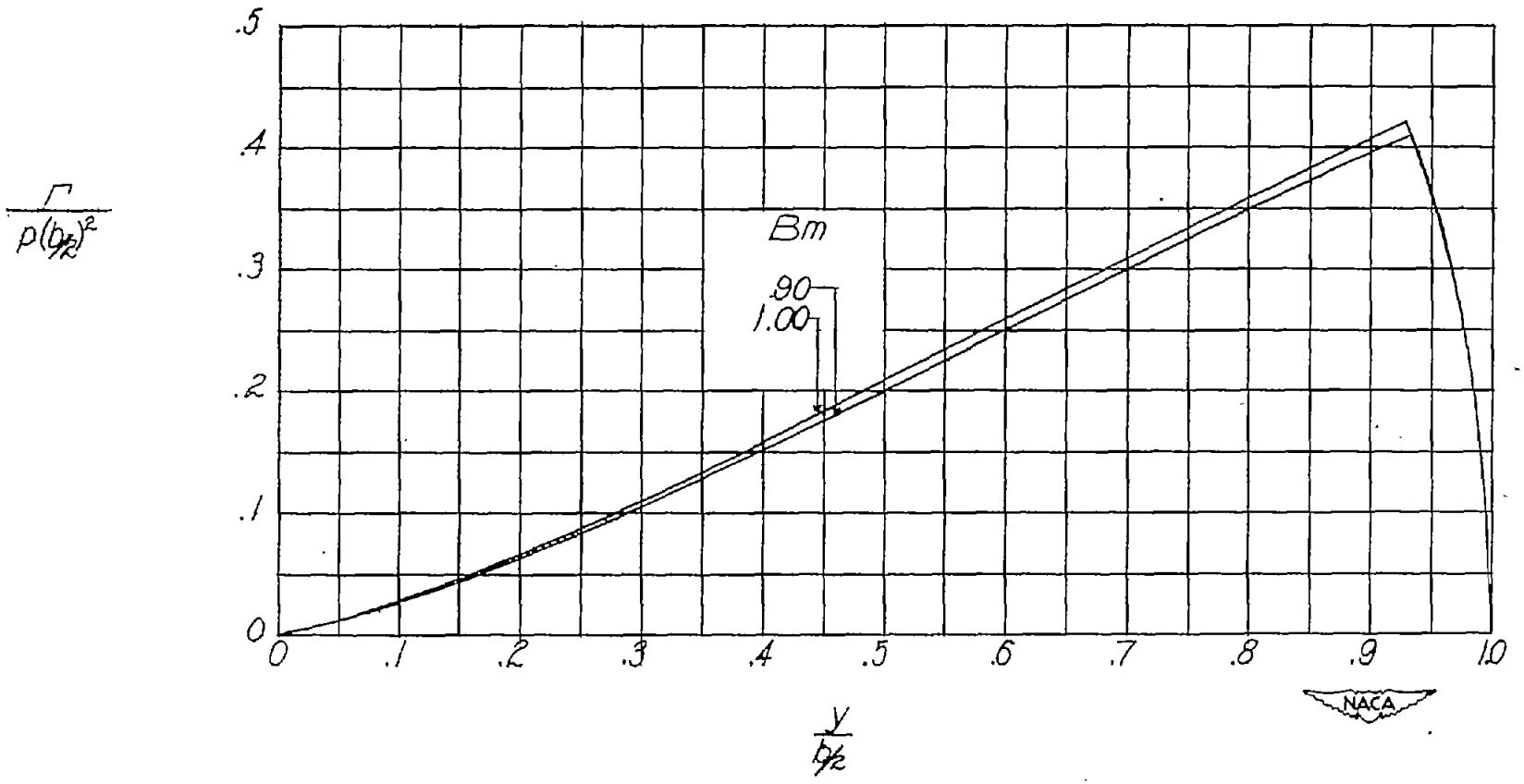

(g) AB = 10.

Figure 13.- Continued.

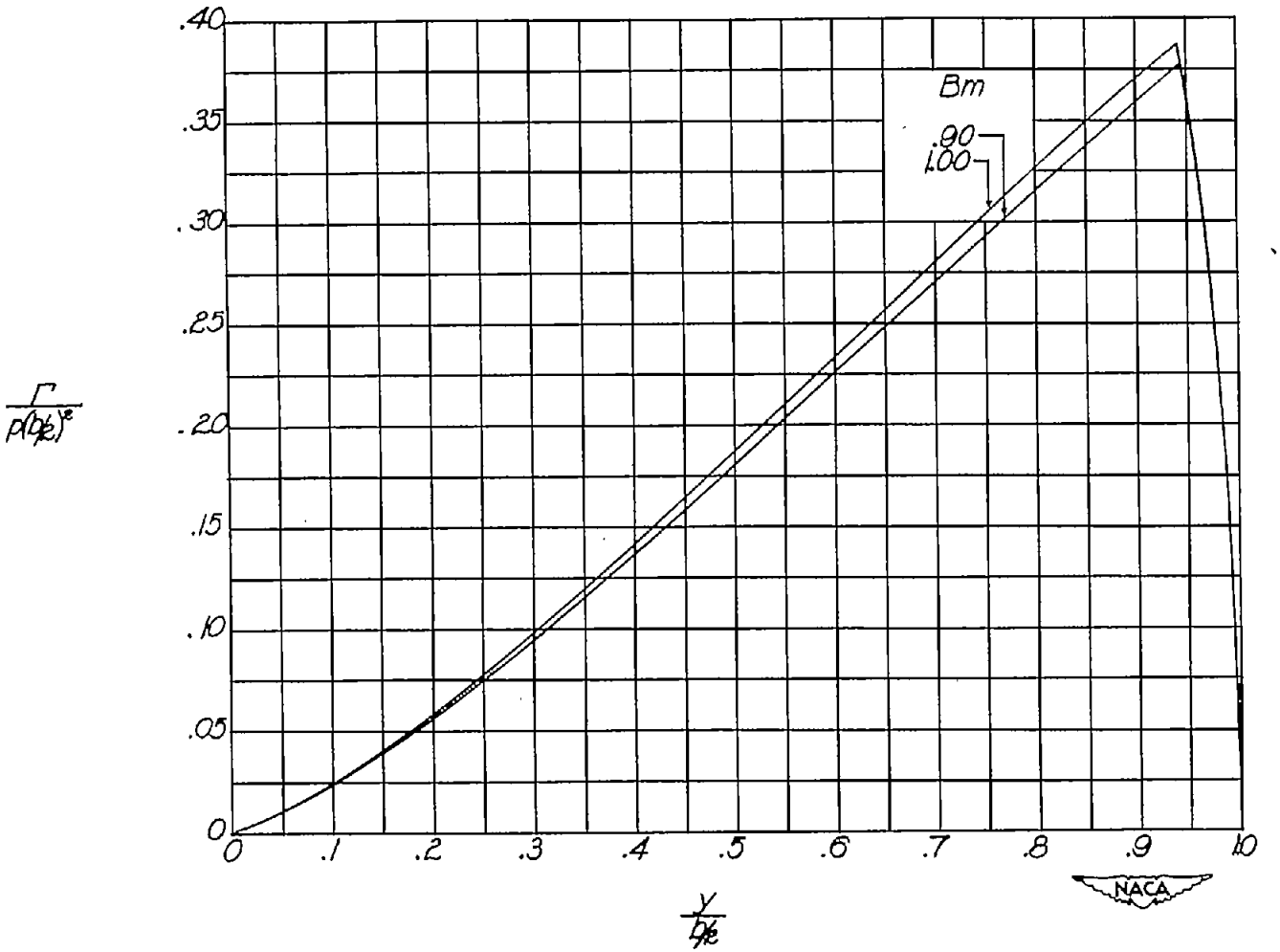

(h) AB = 12.

Figure 13.- Continued.

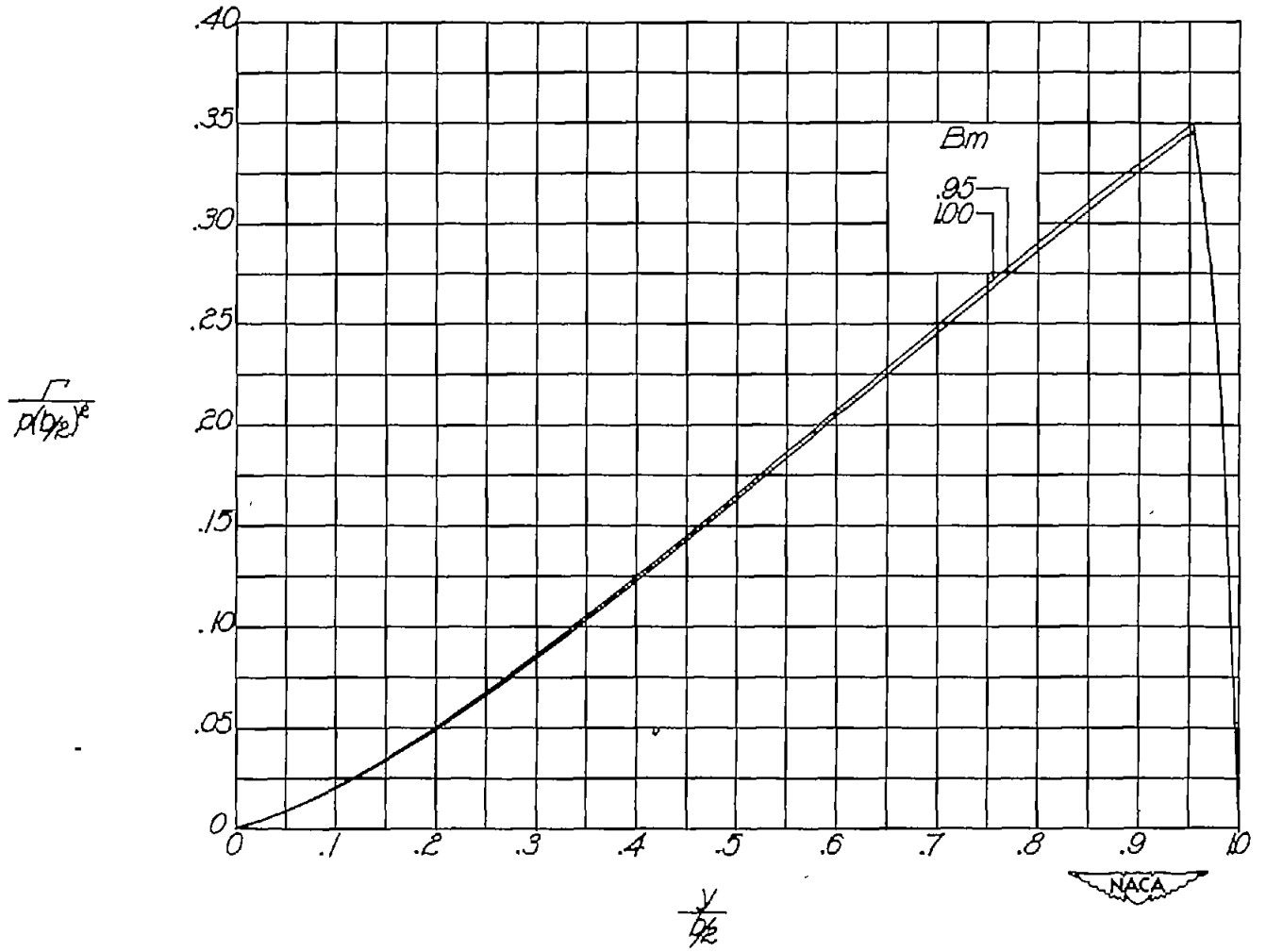

(i) AB = 15.

Figure 13.- Continued.

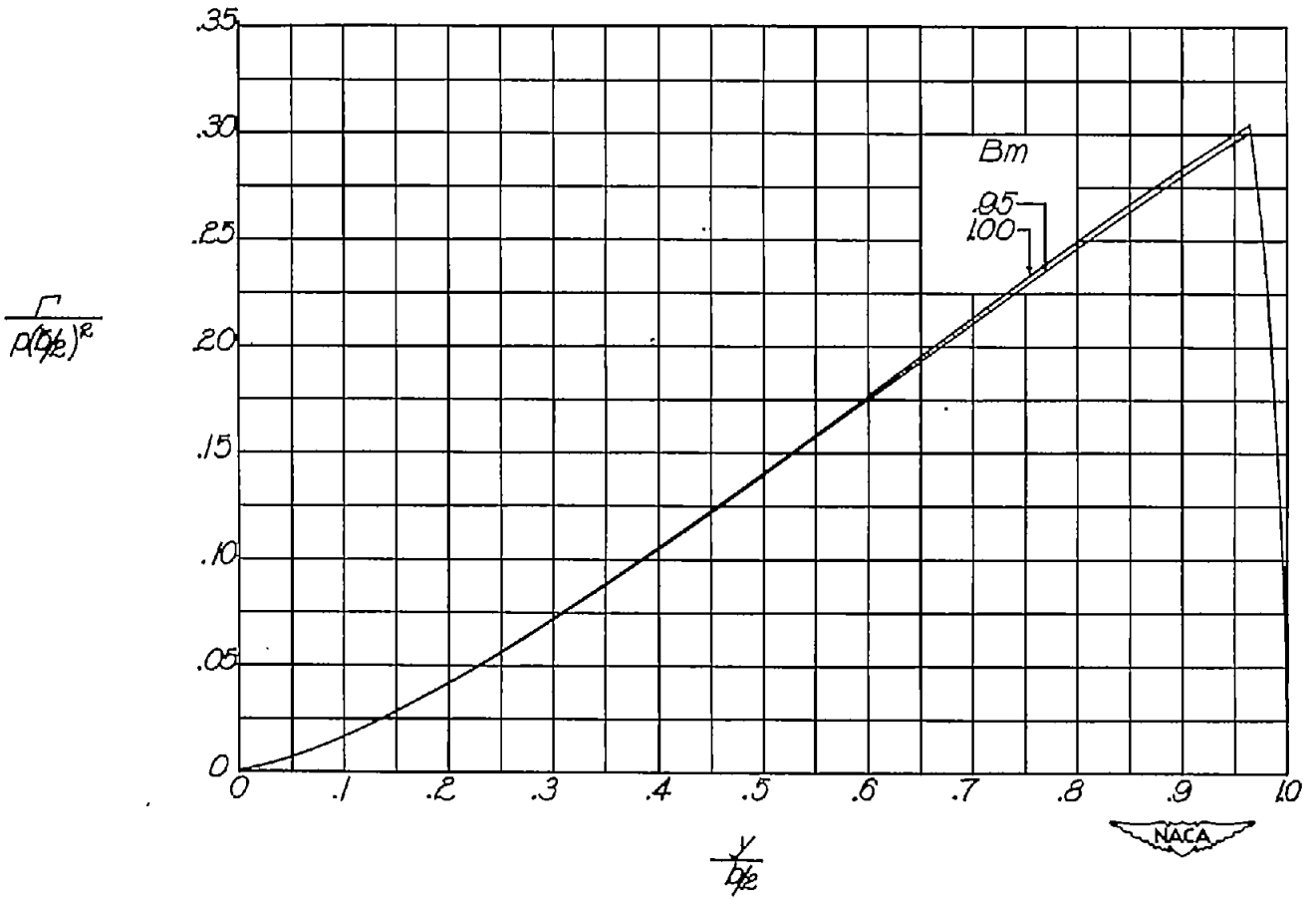

(j) AB = 20.

Figure 13.- Concluded.

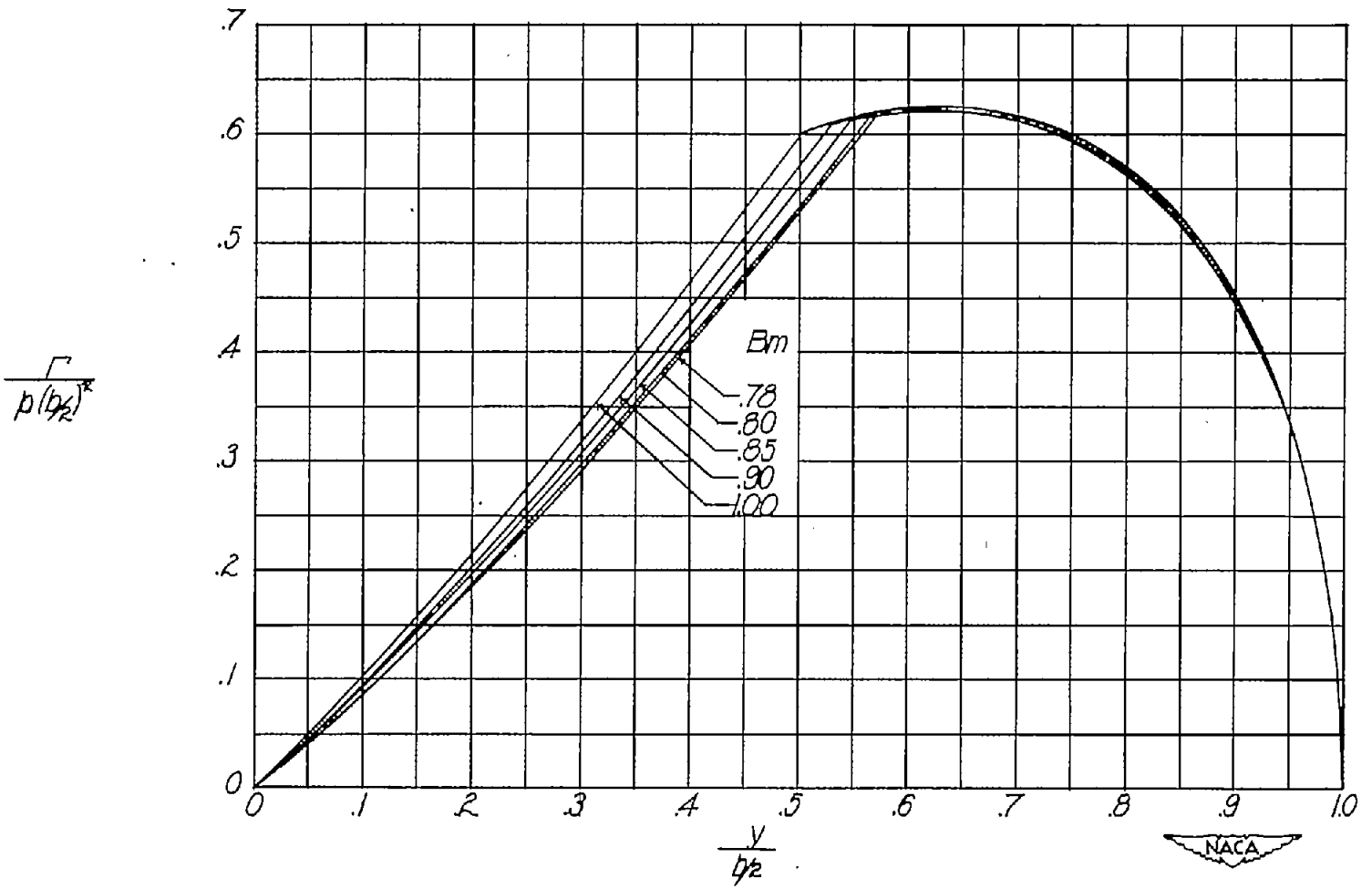

(a) AB = 2.

Figure 14.- Distribution of circulation along span for wings with steady rolling velocity with $\lambda = 0.75$.

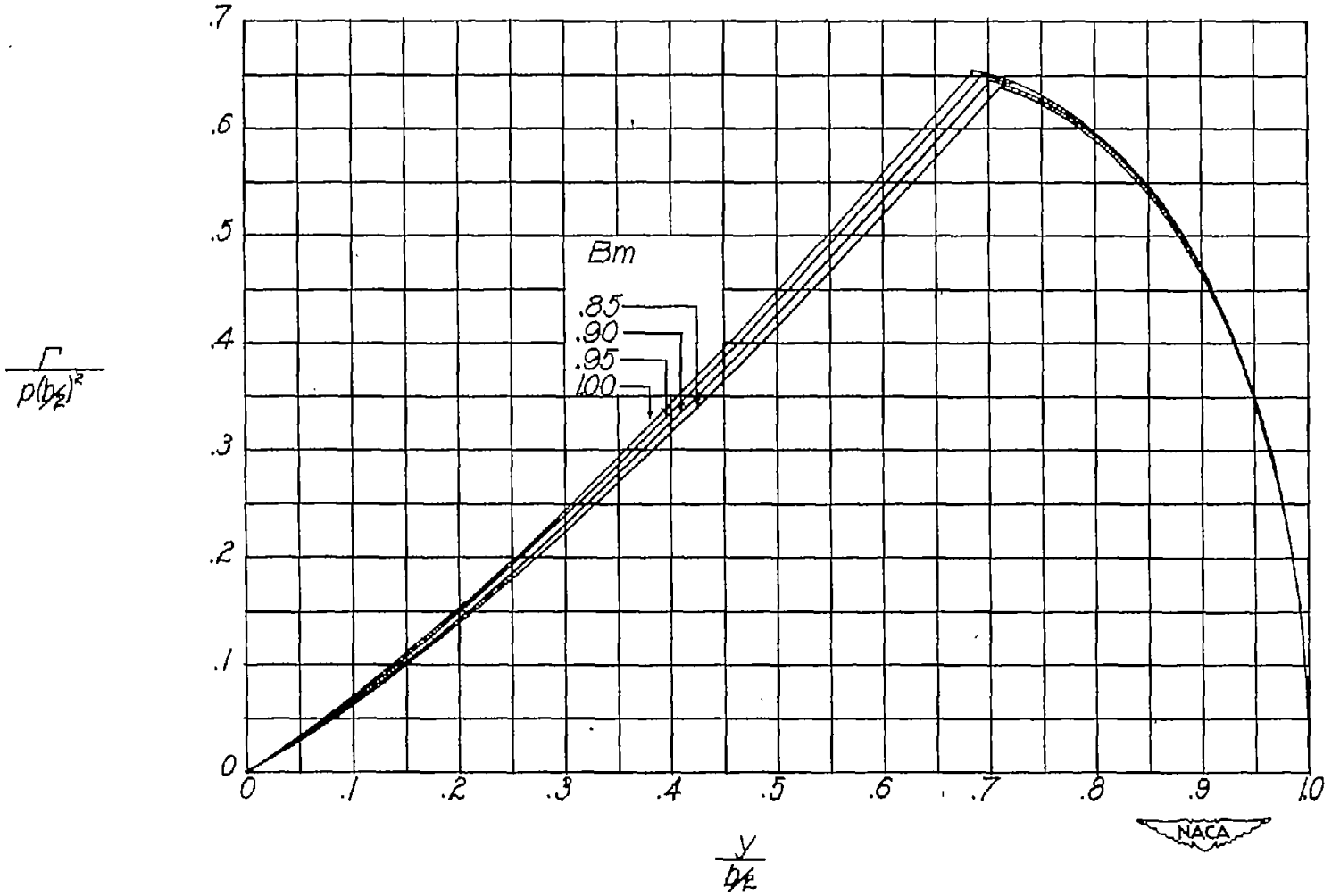

(b) AB = .3.

Figure 14.- Continued.

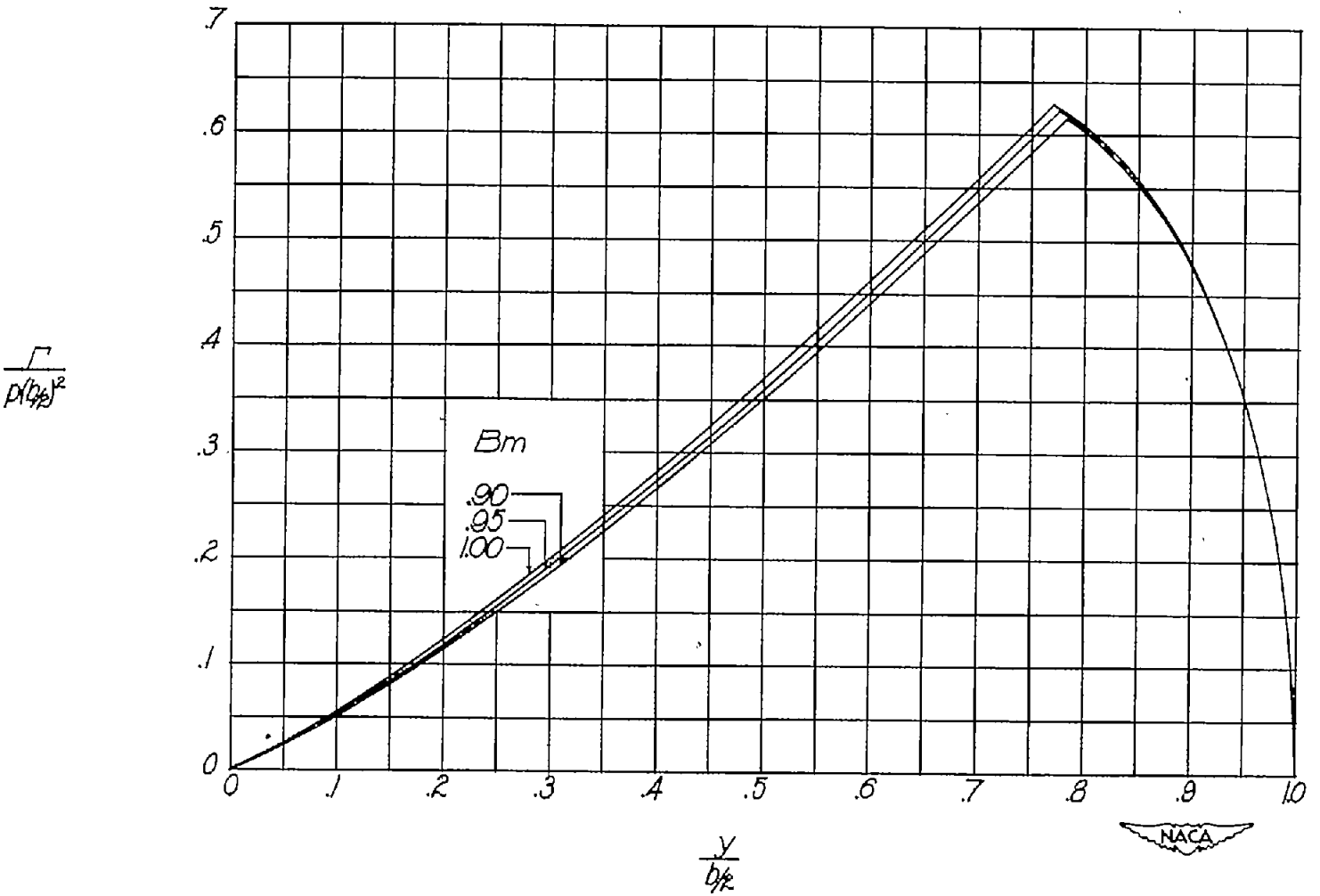

(c) AB = 4.

Figure 14.- Continued.

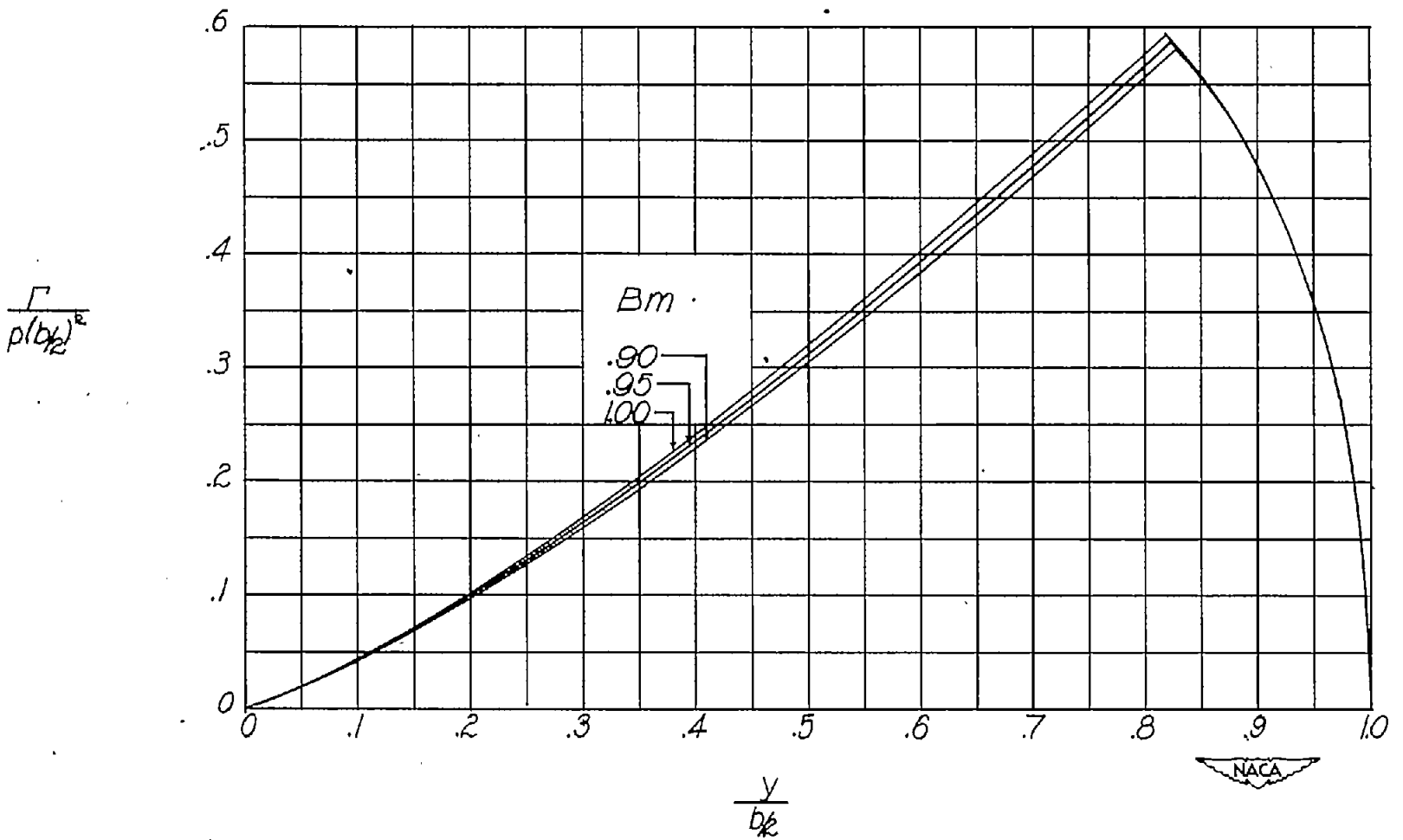

(d) AB = 5.

Figure 14.- Continued.

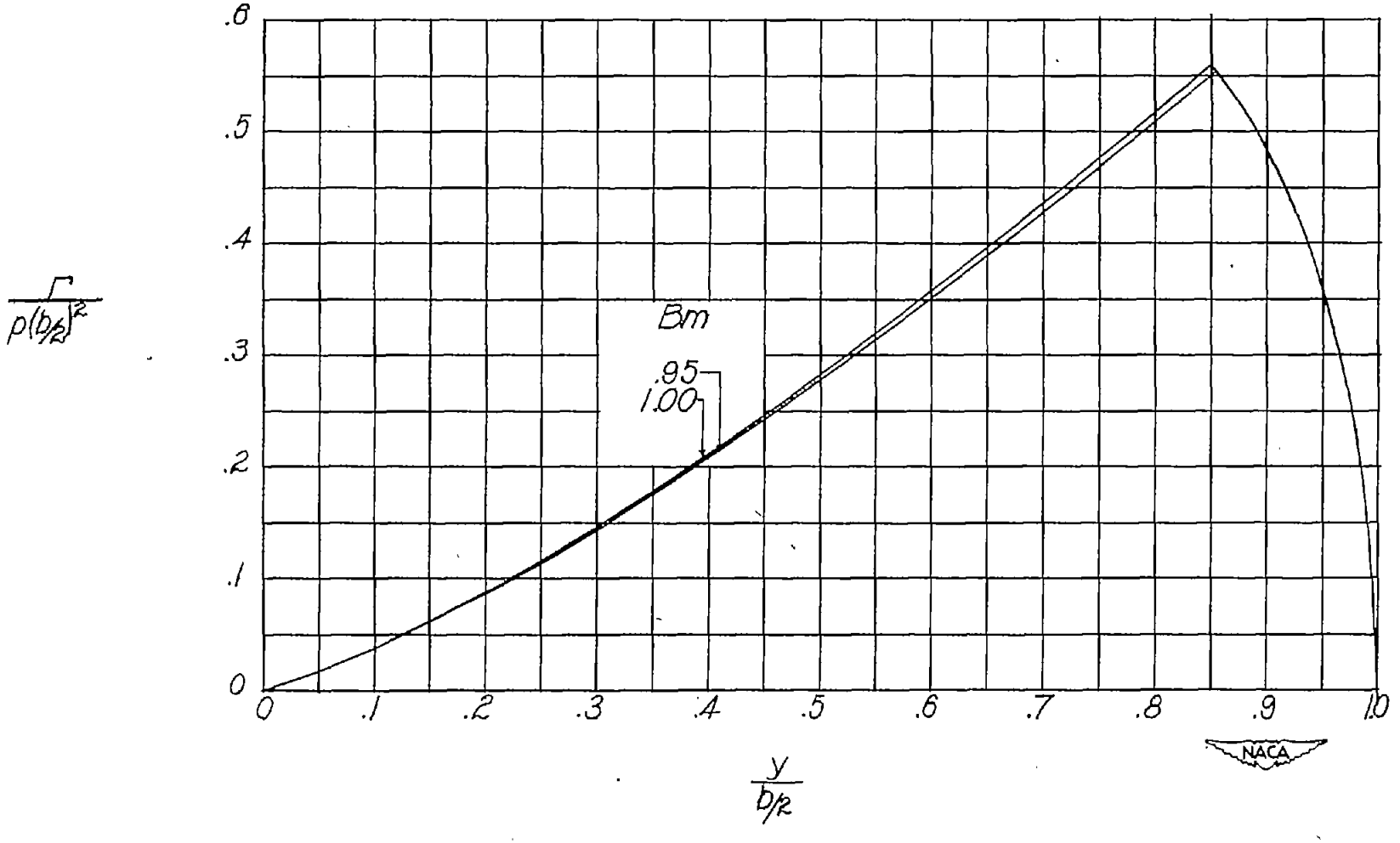

(e) AB = 6.

Figure 14.- Continued.

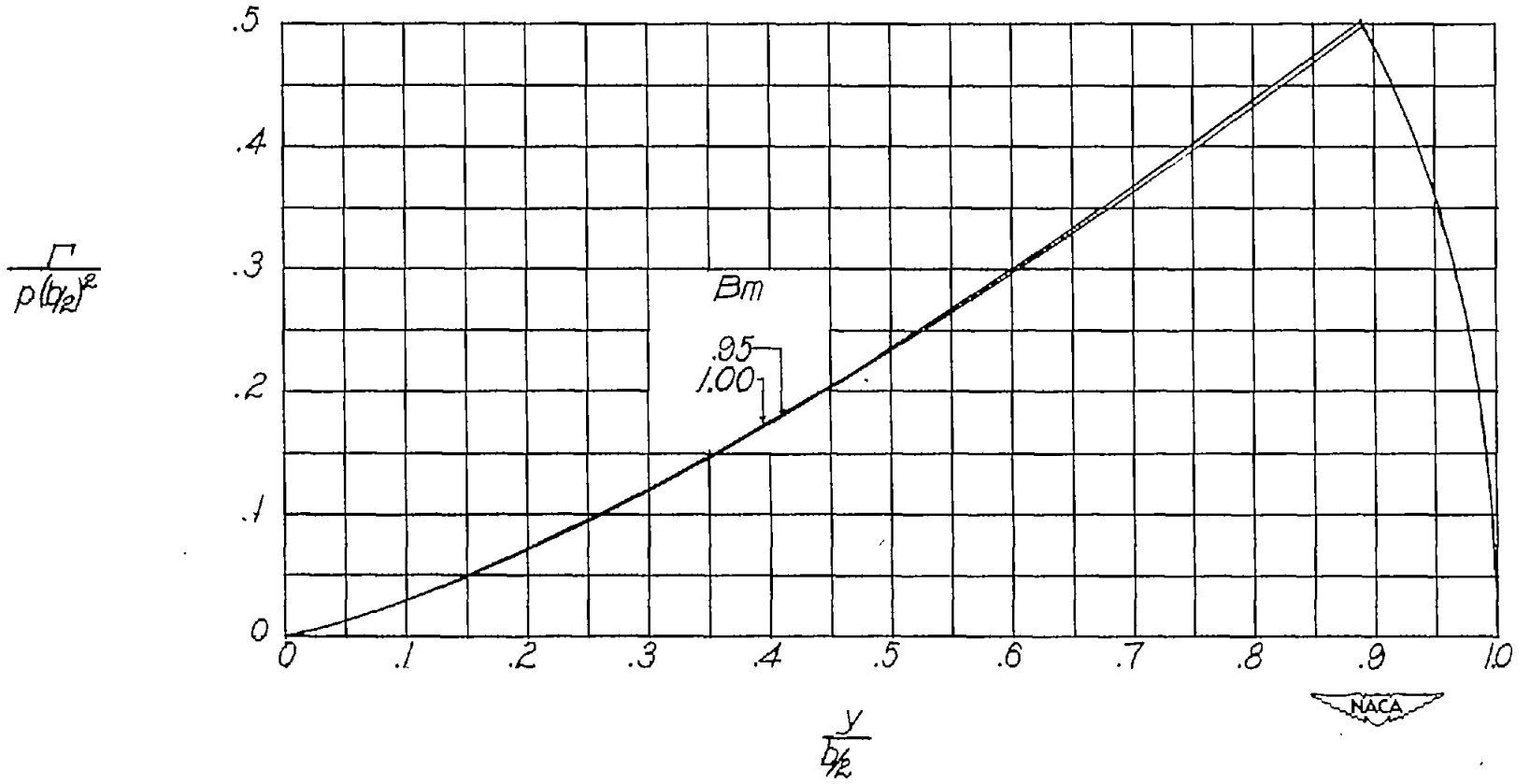

(f) AB = 8.

Figure 14.- Continued.

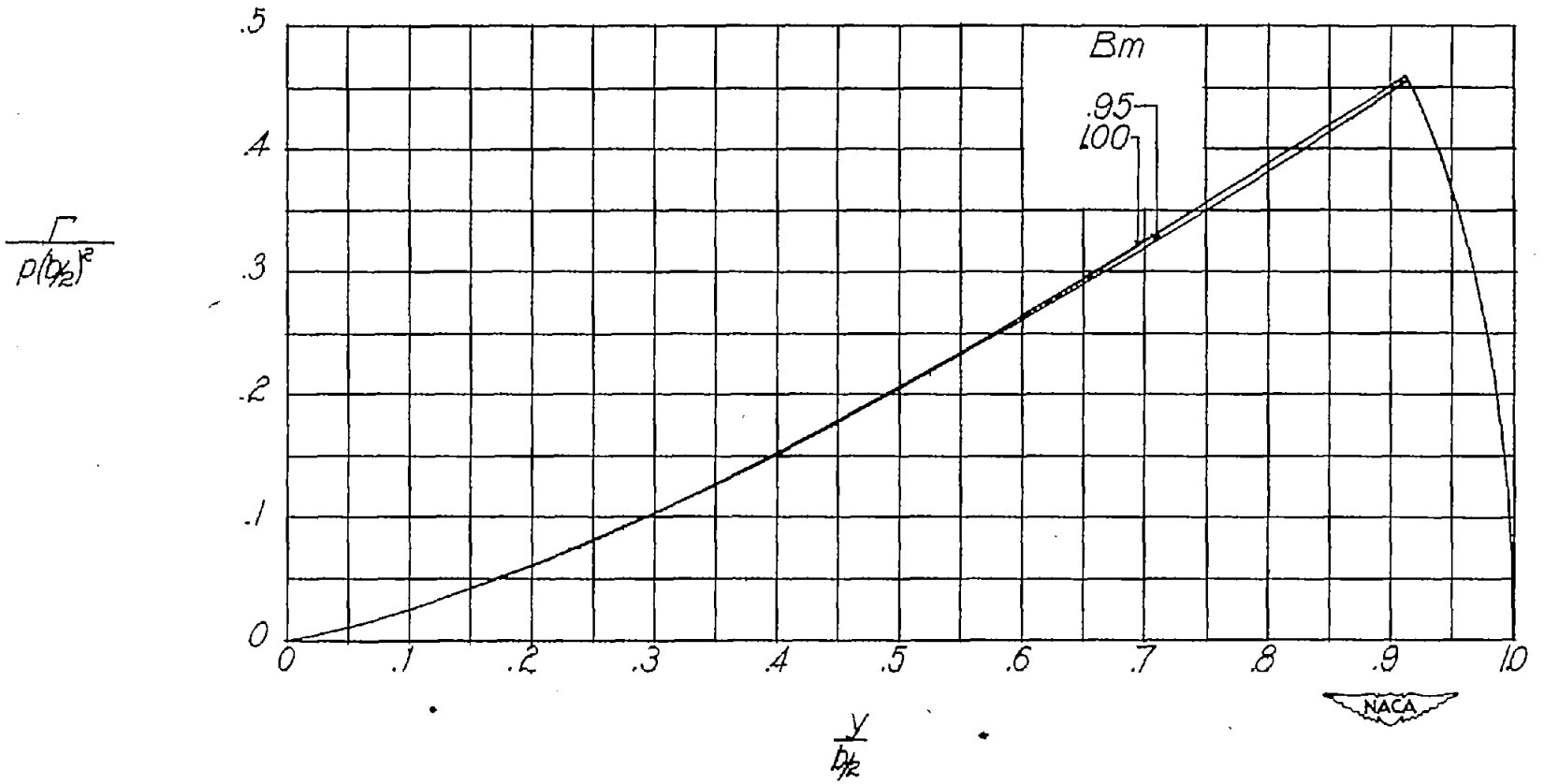

(g) AB = 10.

Figure 14.- Continued.

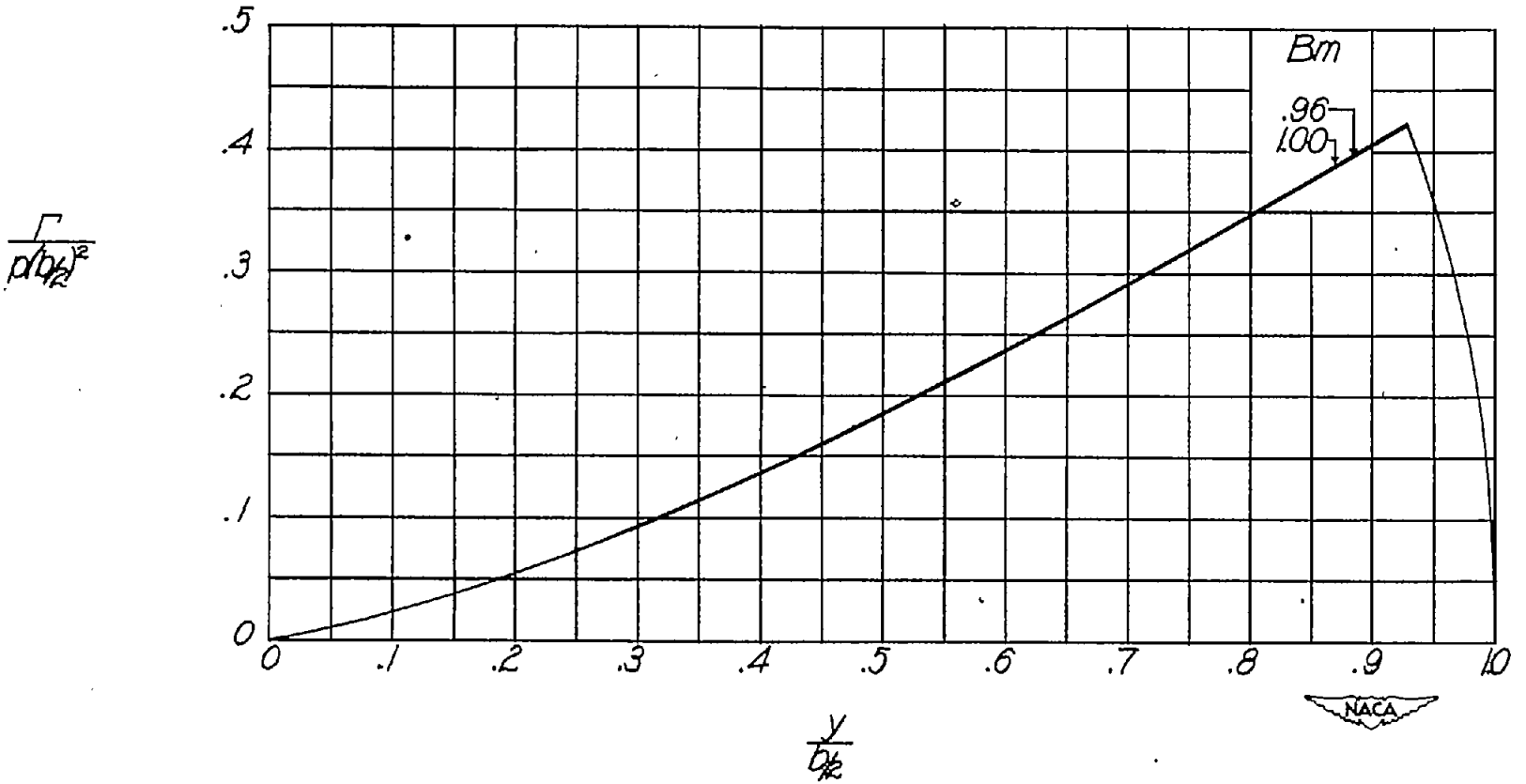

(h) AB = 12.

Figure 14.- Continued.

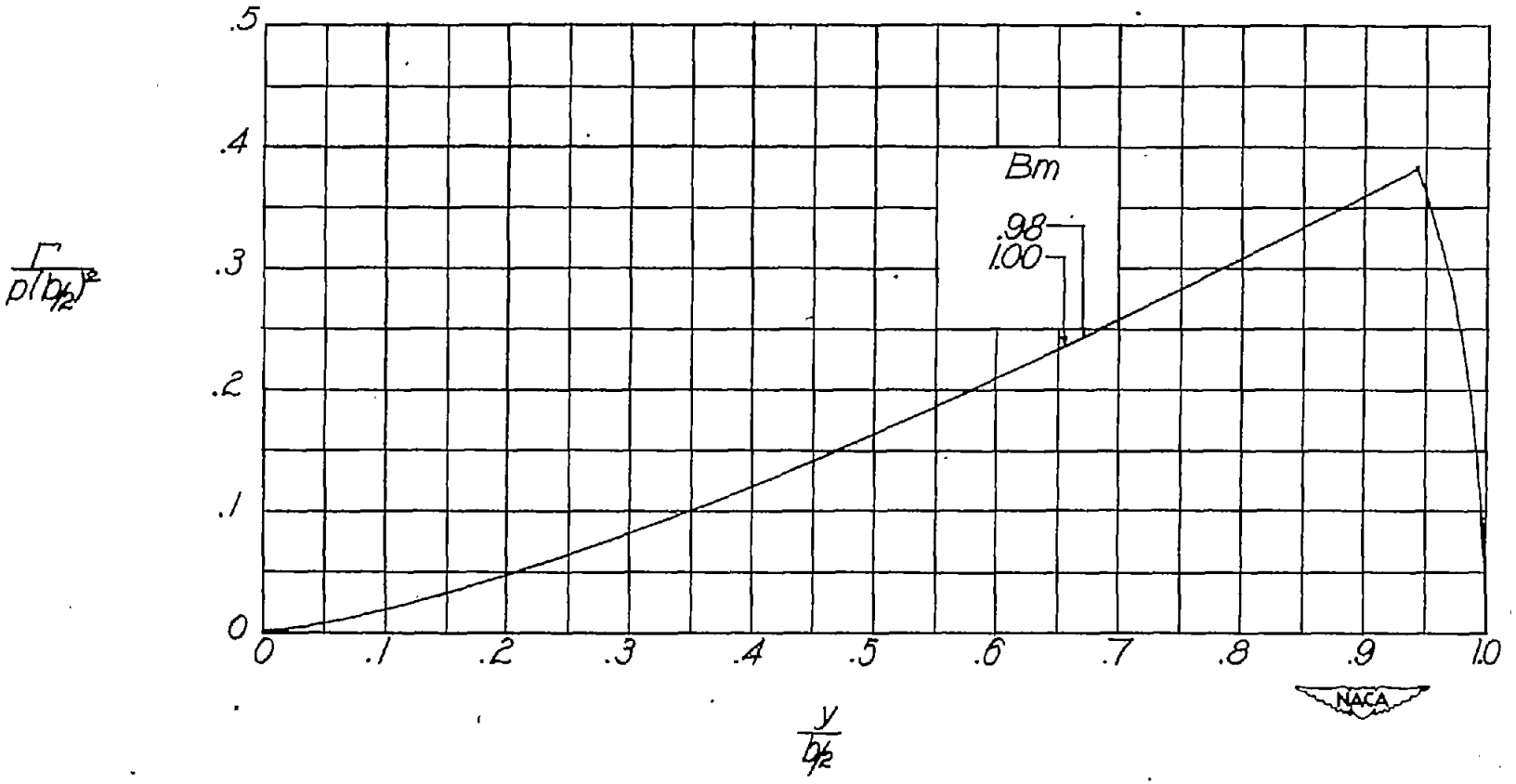

(i) AB = 15.

Figure 14.- Continued.

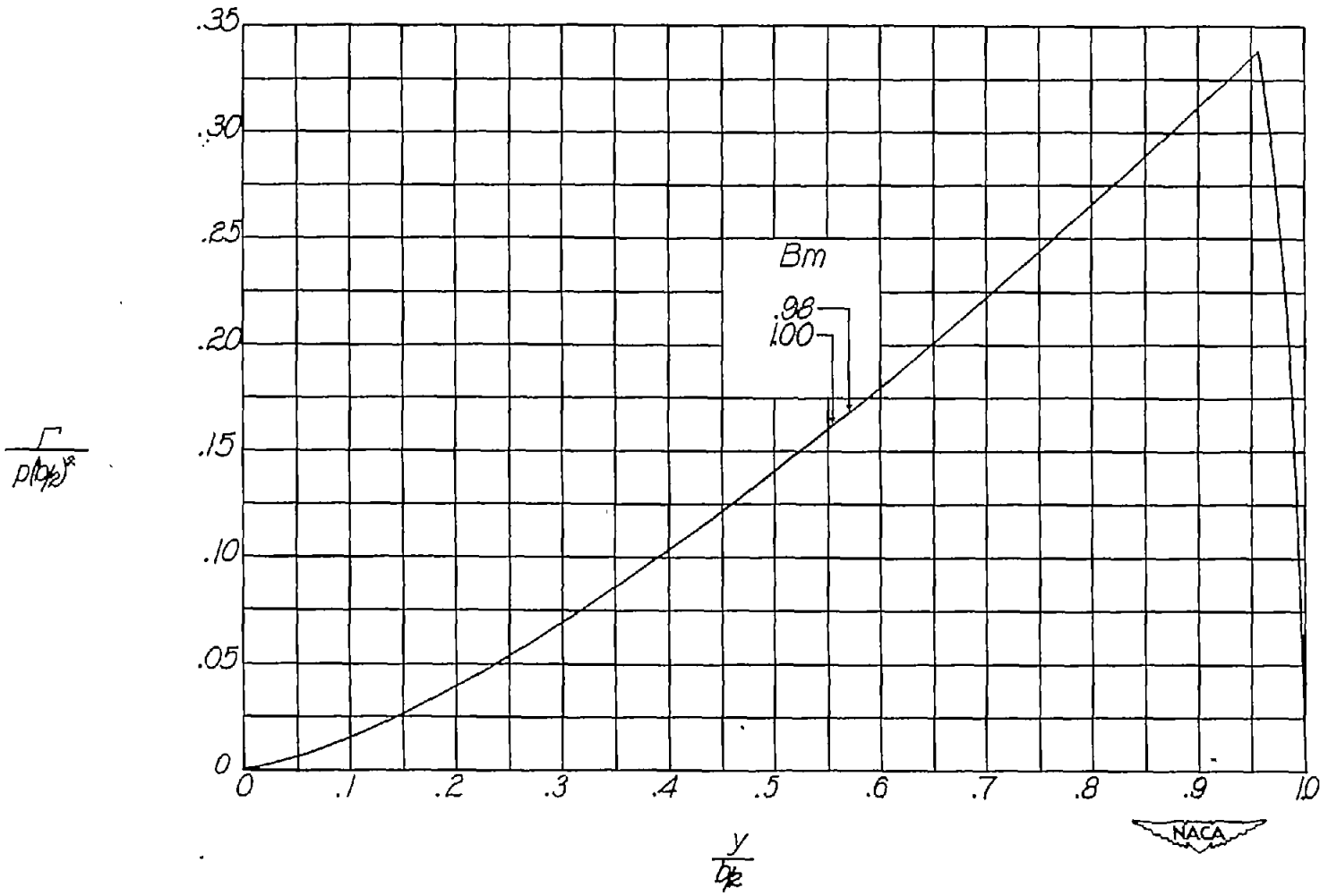

(j) AB = 20.

Figure 14.- Concluded.

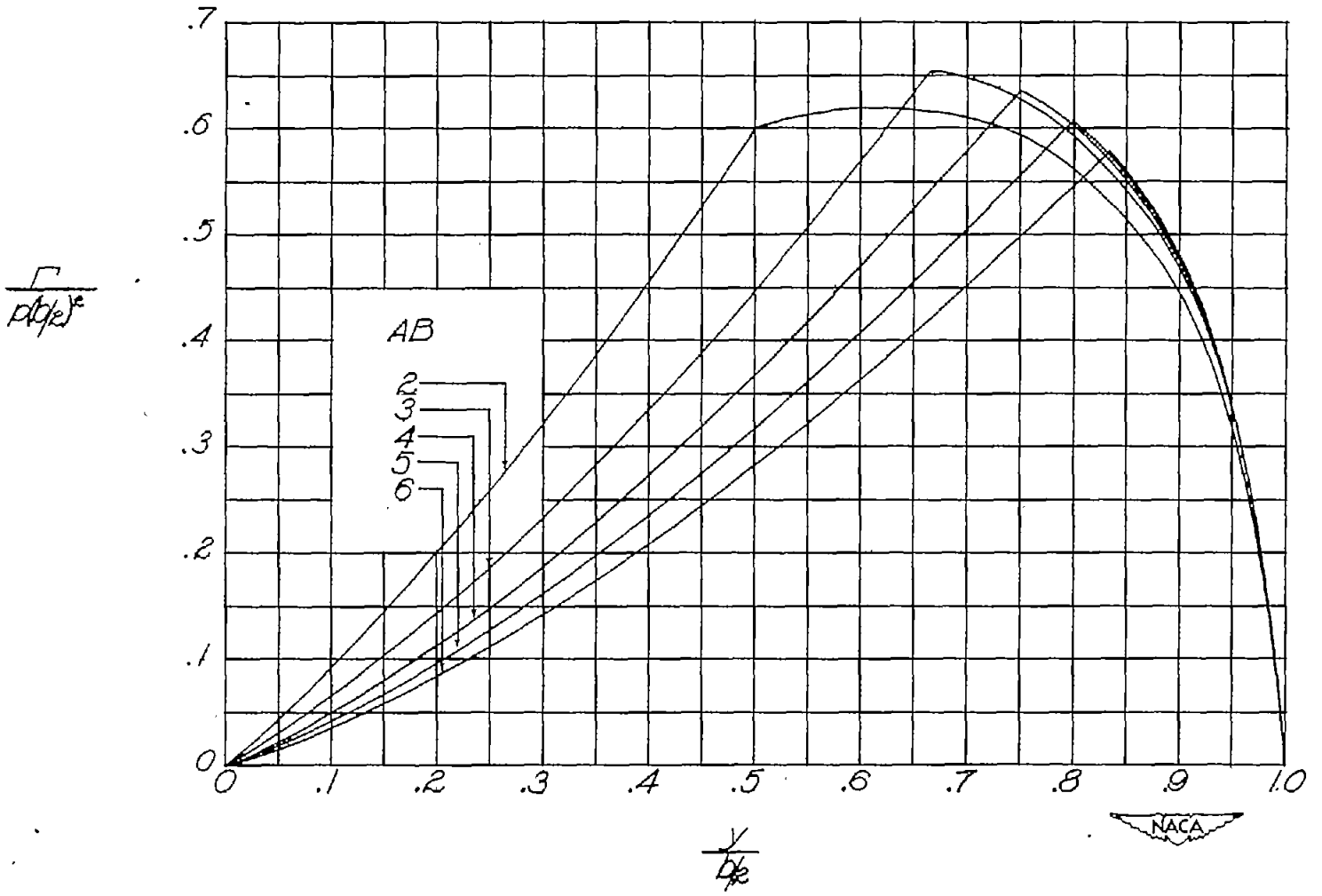

(a) AB = 2 to 6.

Figure 15.- Distribution of circulation along span for wings with steady rolling velocity with $\lambda = 1.00$. Bm = 1.00.

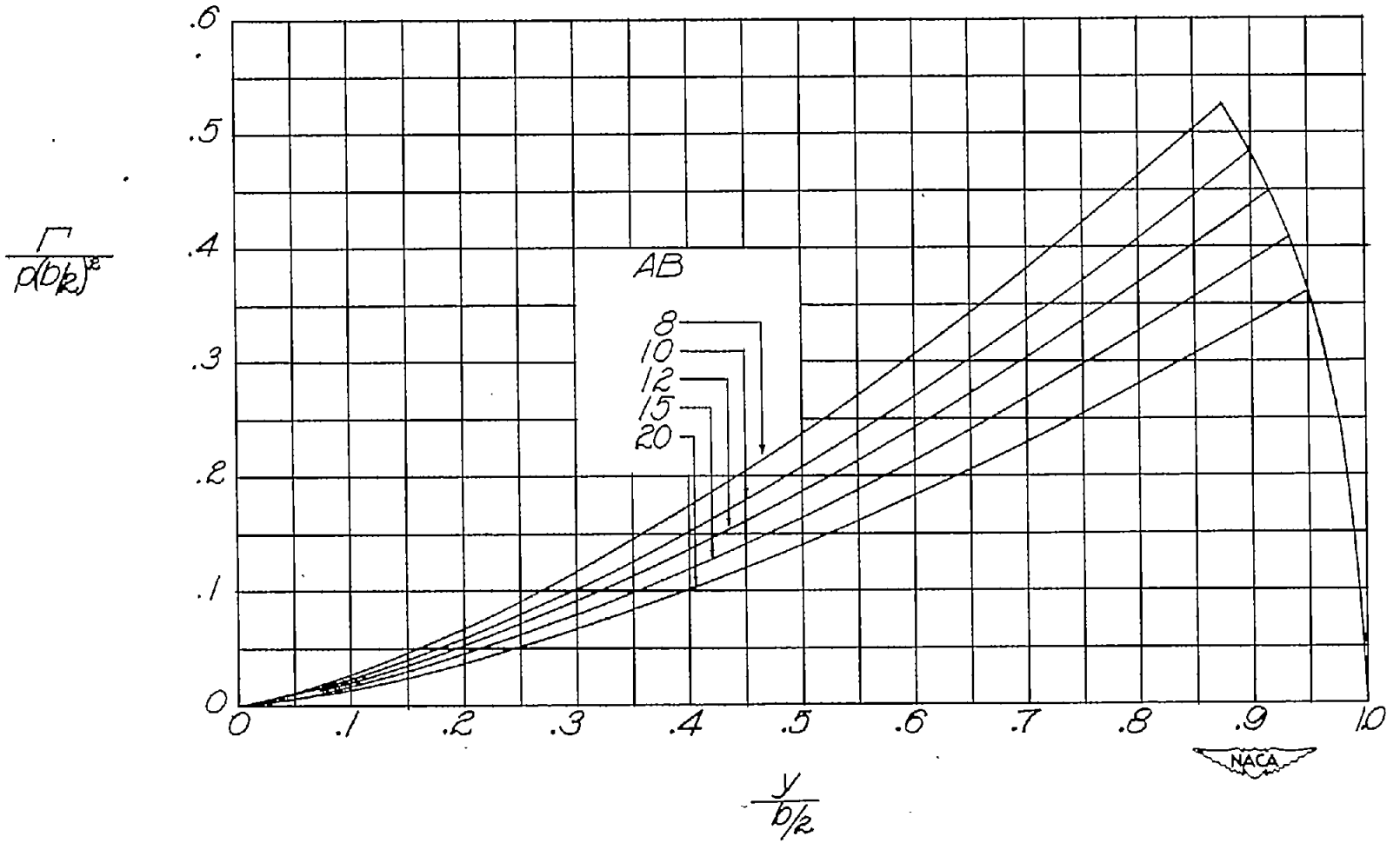

(b) AB = 8 to 20.

Figure 15.- Concluded.

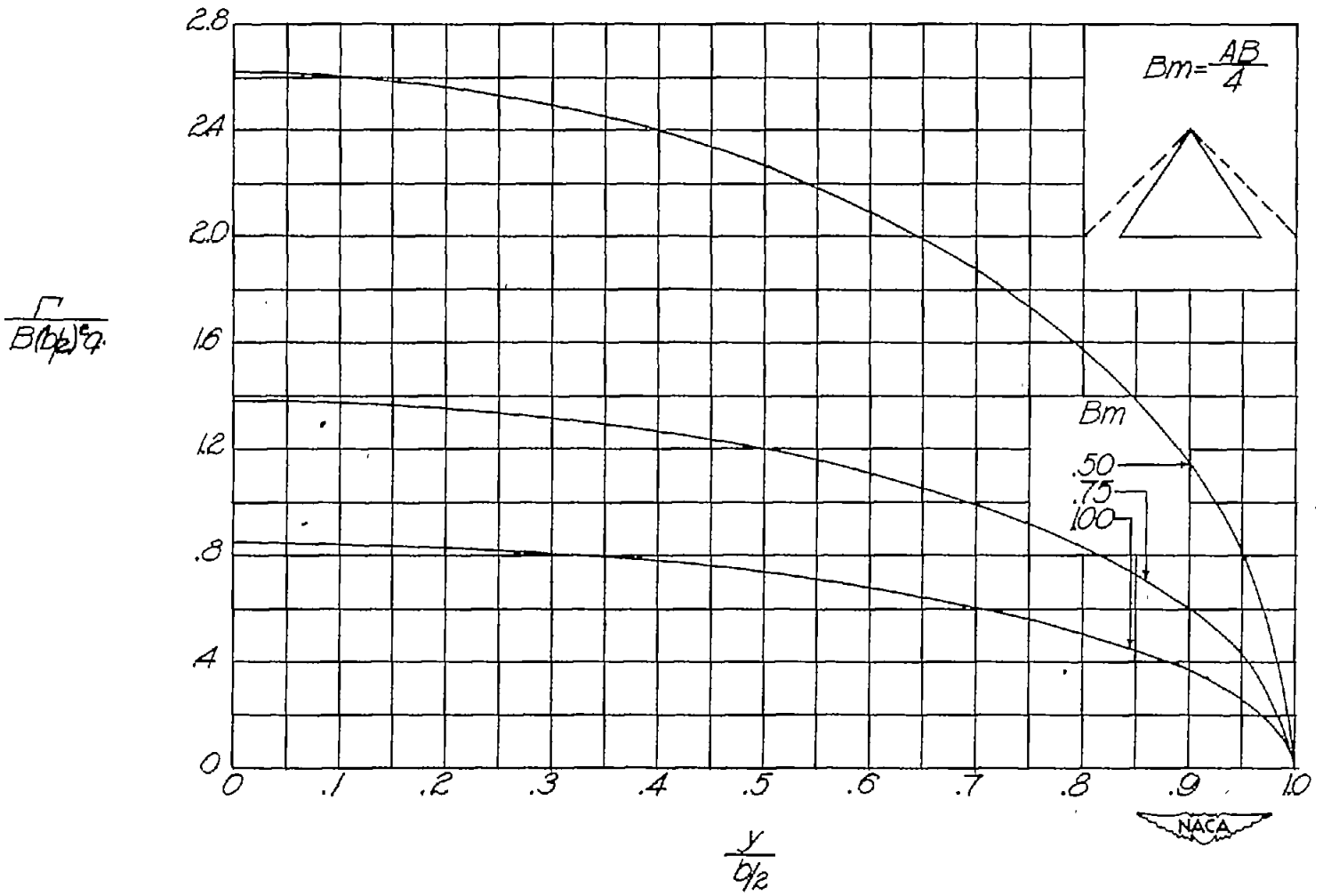

Figure 16.- Distribution of circulation along span for delta wings with steady pitching velocity. Wing pitching about apex.

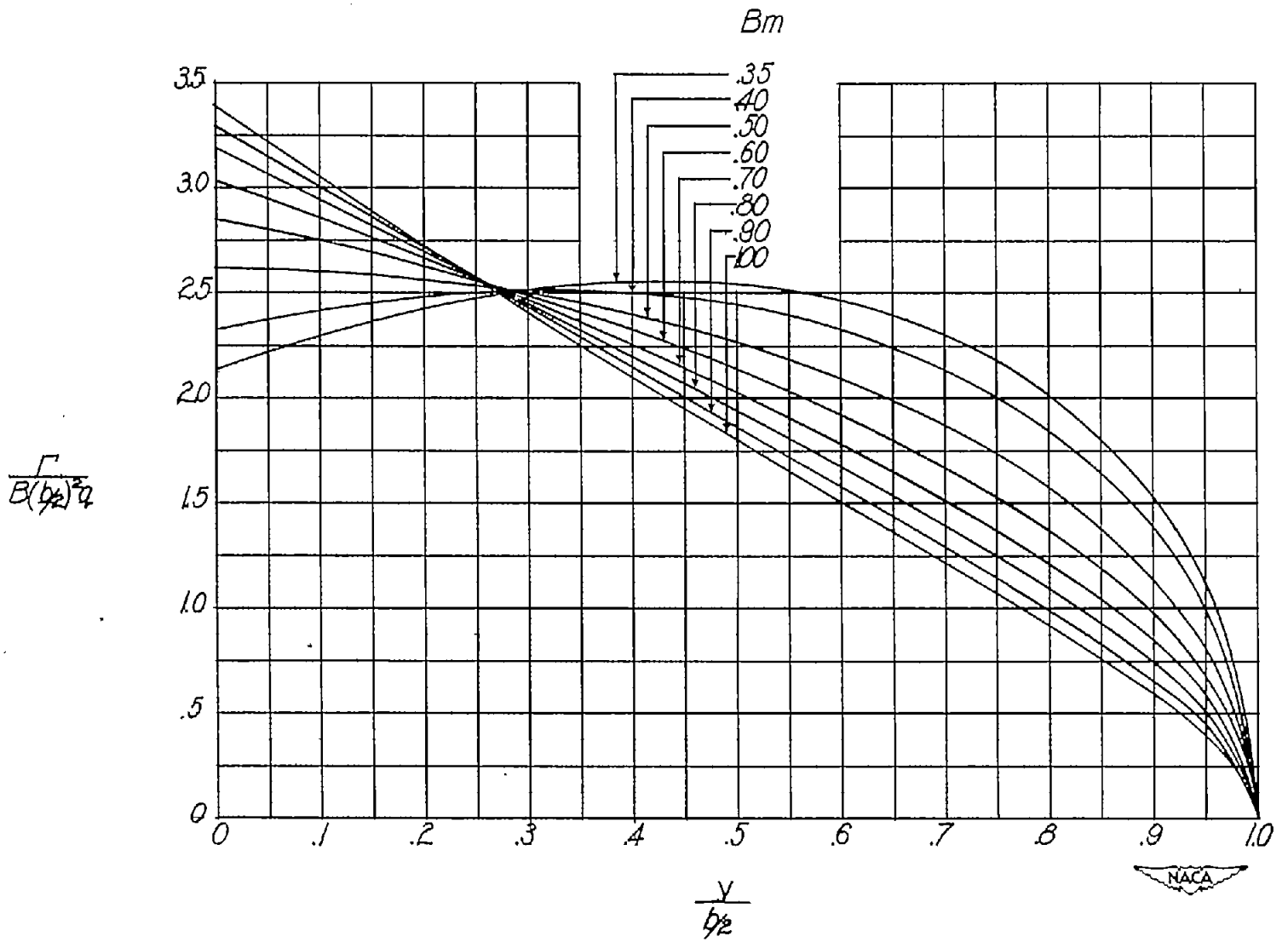

(a) AB = 2.

Figure 17.- Distribution of circulation along span for wings with steady pitching velocity with $\lambda = 0$. Wing pitching about apex.

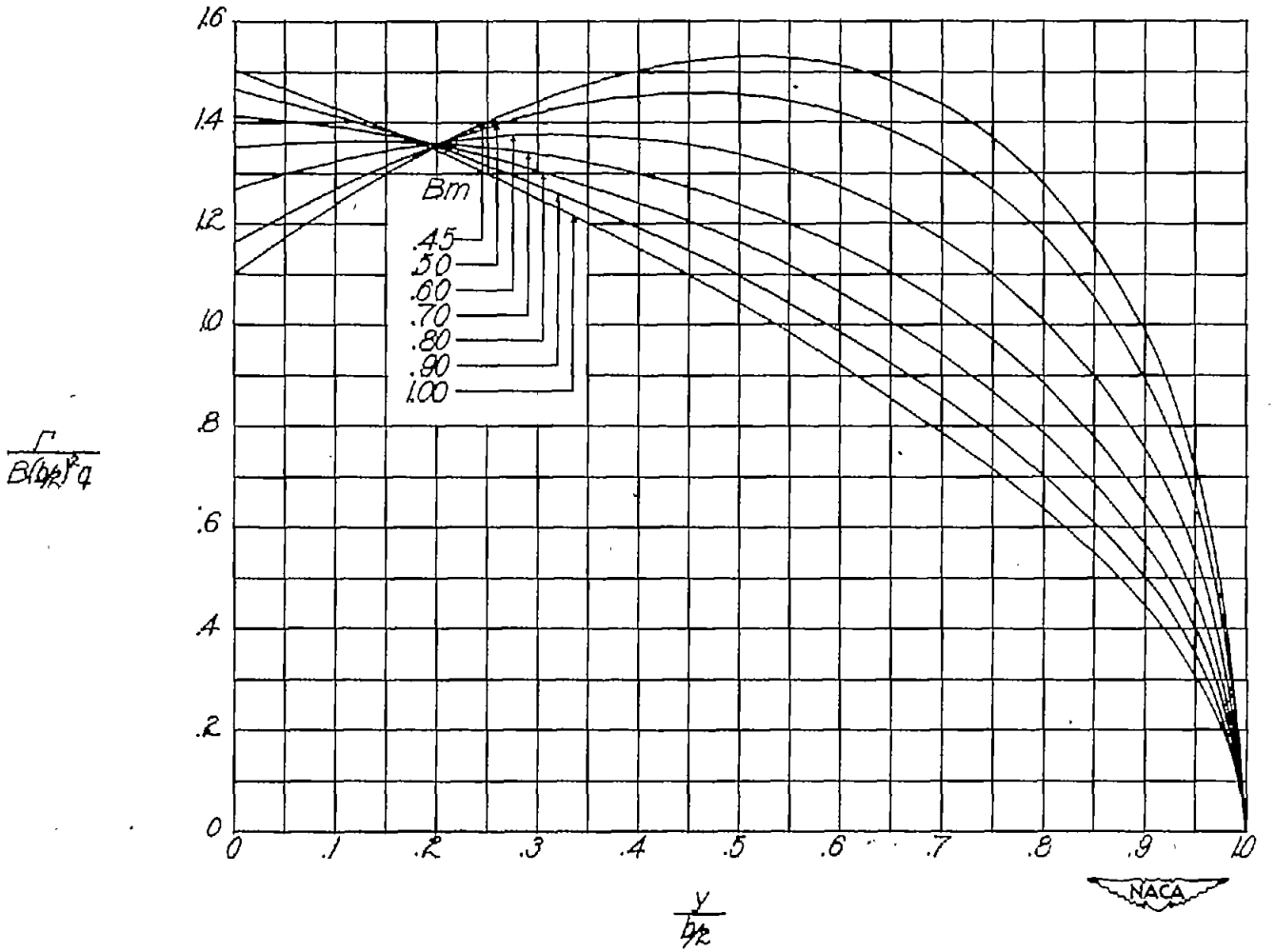

(b) AB = 3.

Figure 17.- Continued.

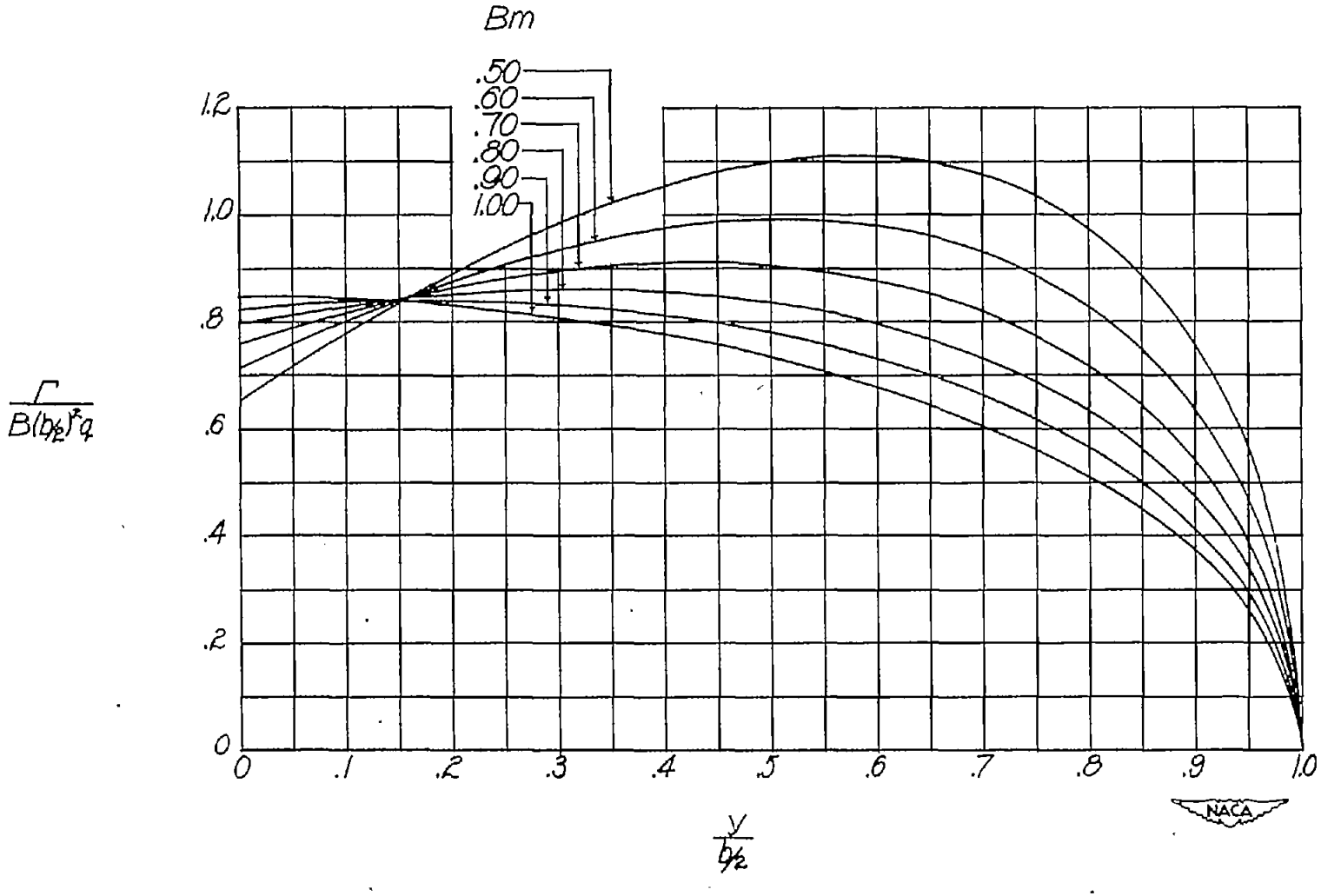

(c) AB = 4.

Figure 17.- Continued.

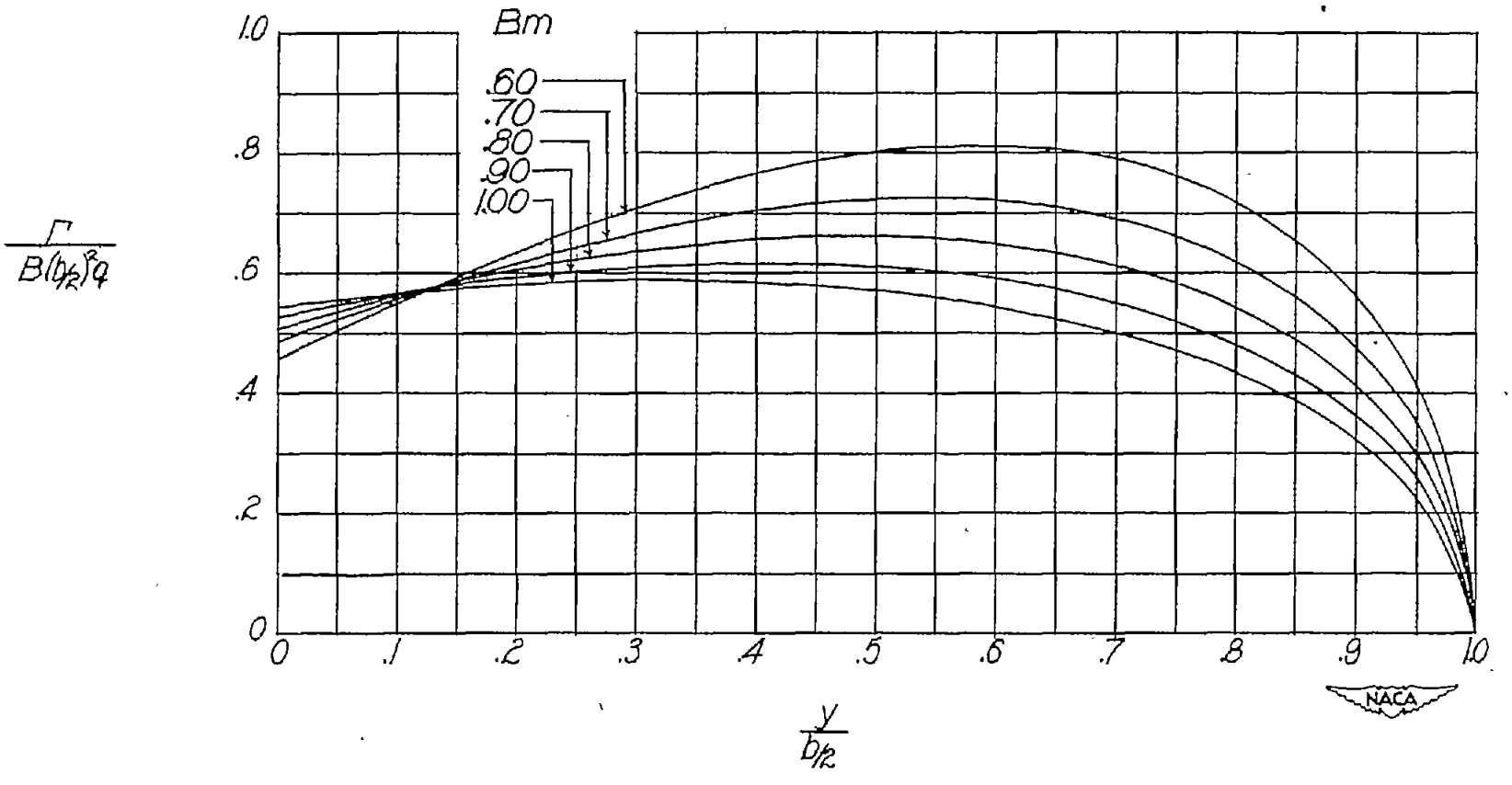

(d) AB = 5.

Figure 17.- Continued.

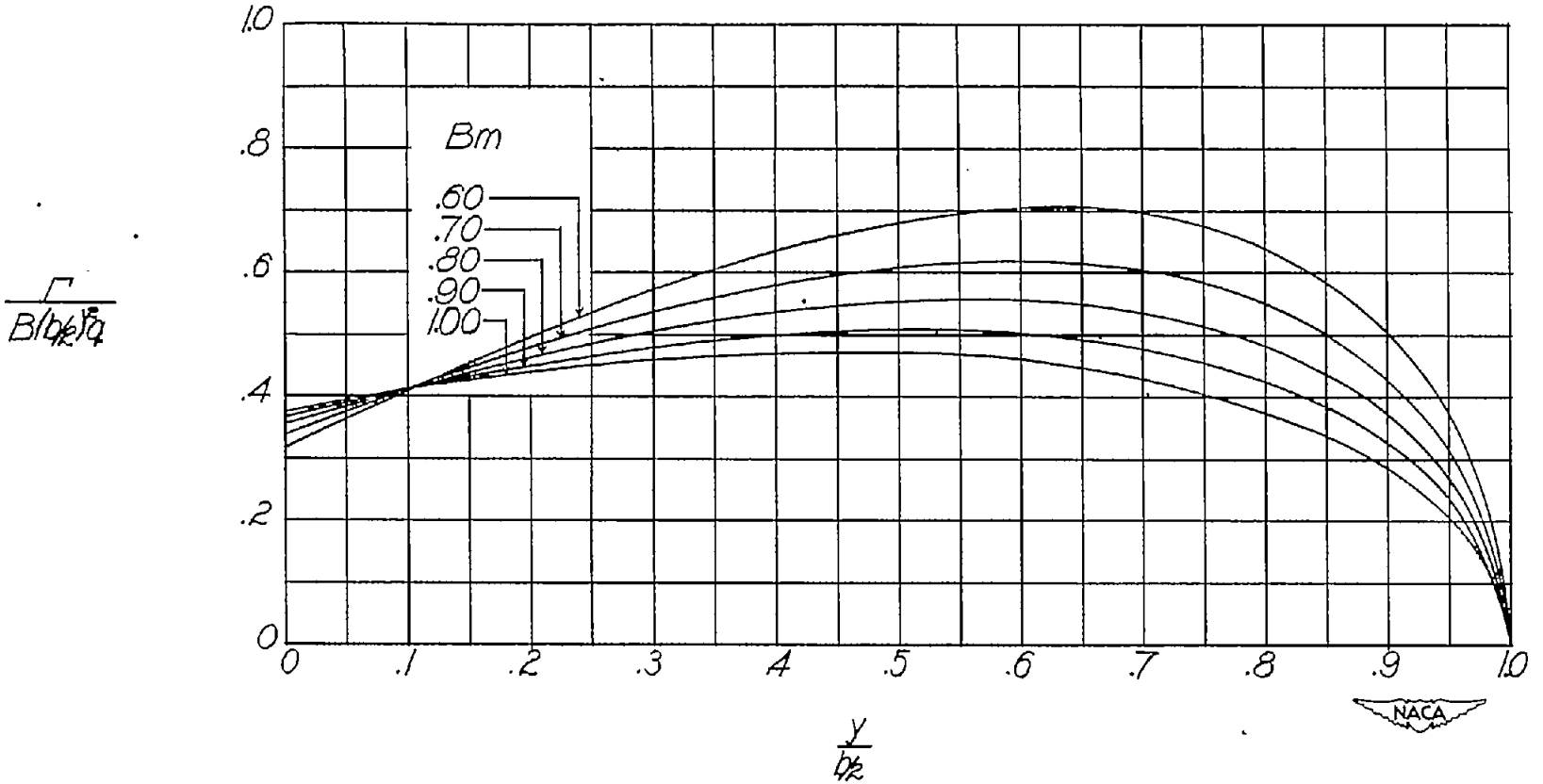

(e) AB = 6.

Figure 17.- Continued.

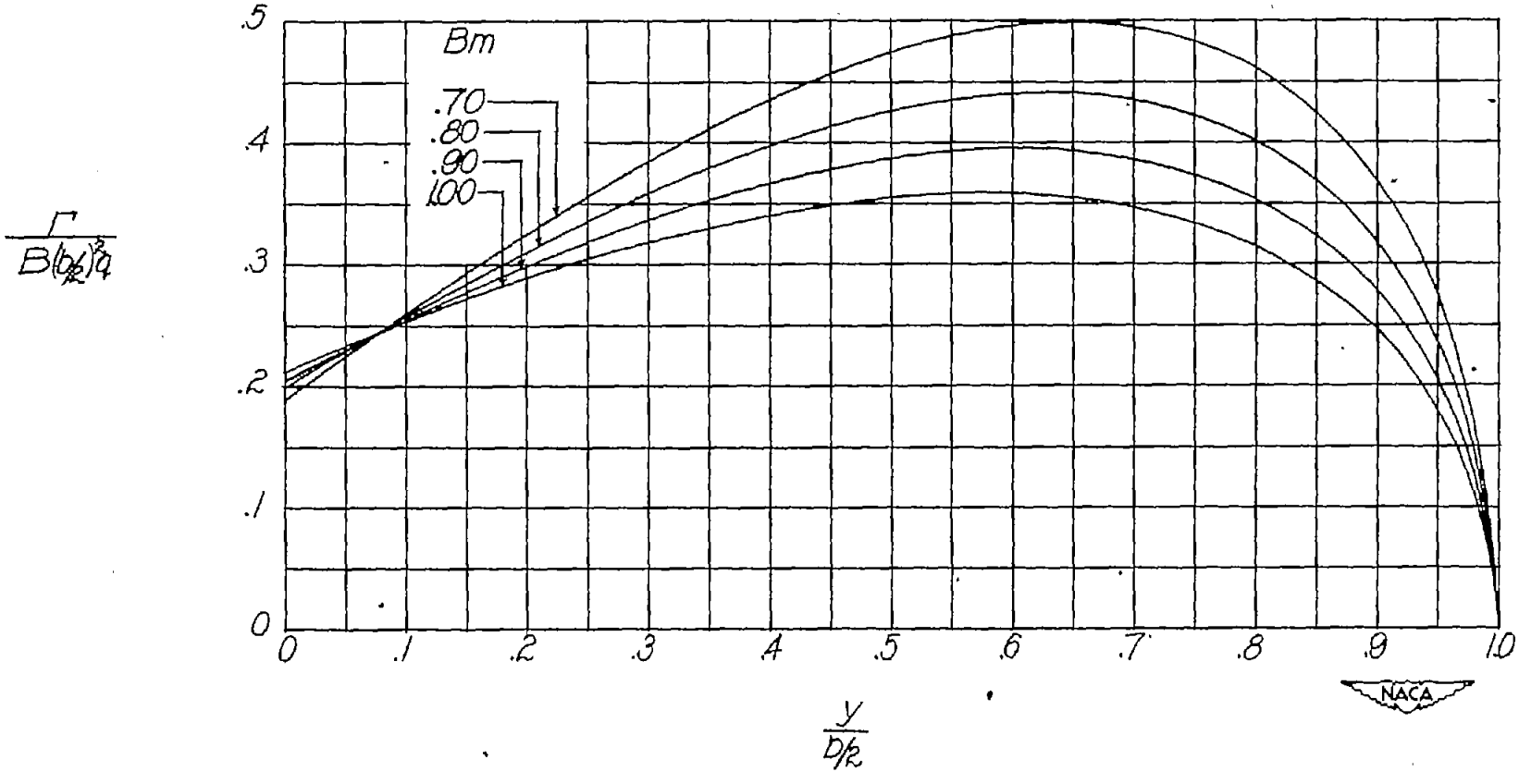

(f) AB = 8.

Figure 17.- Continued.

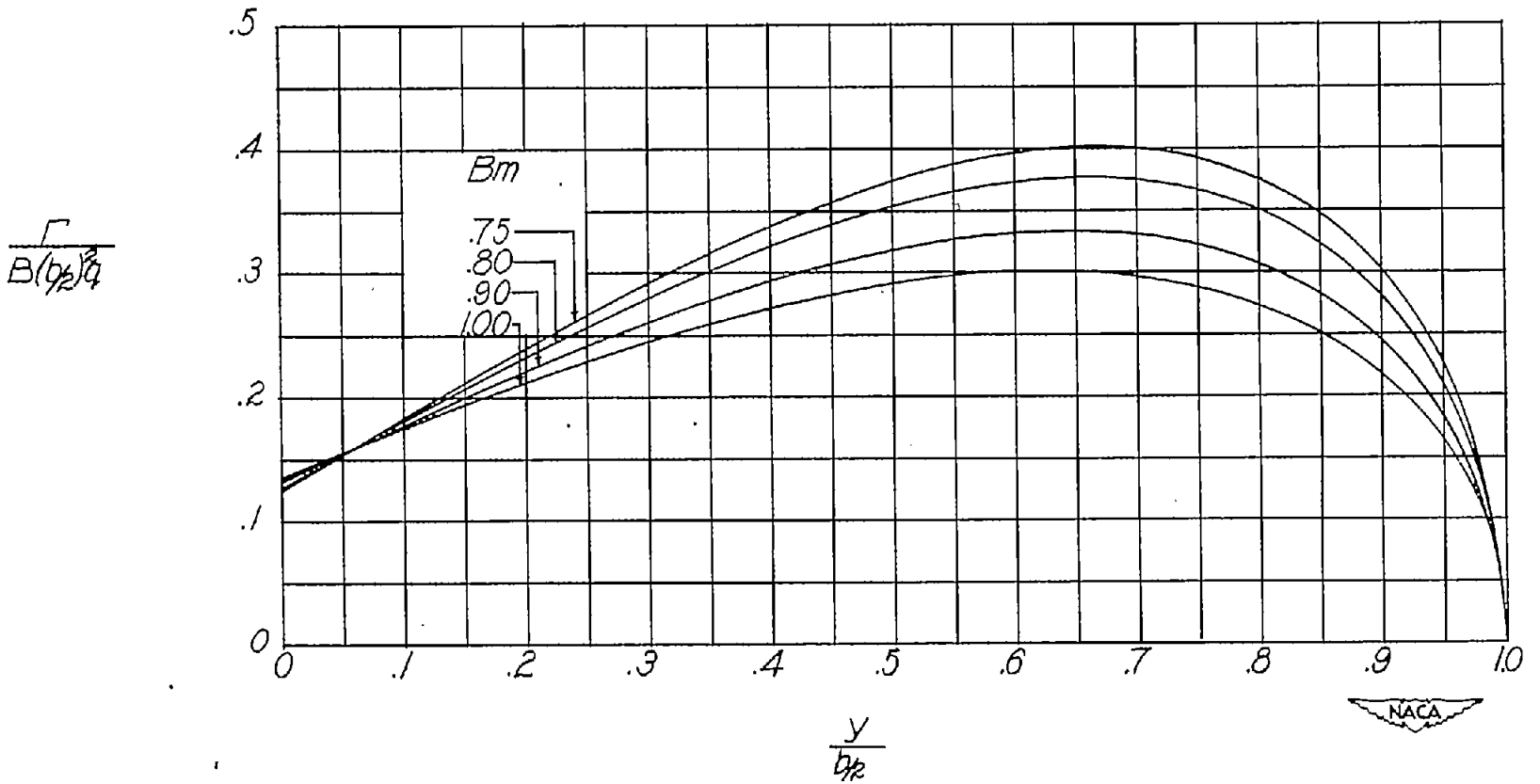

(g) AB = 10.

Figure 17.- Continued.

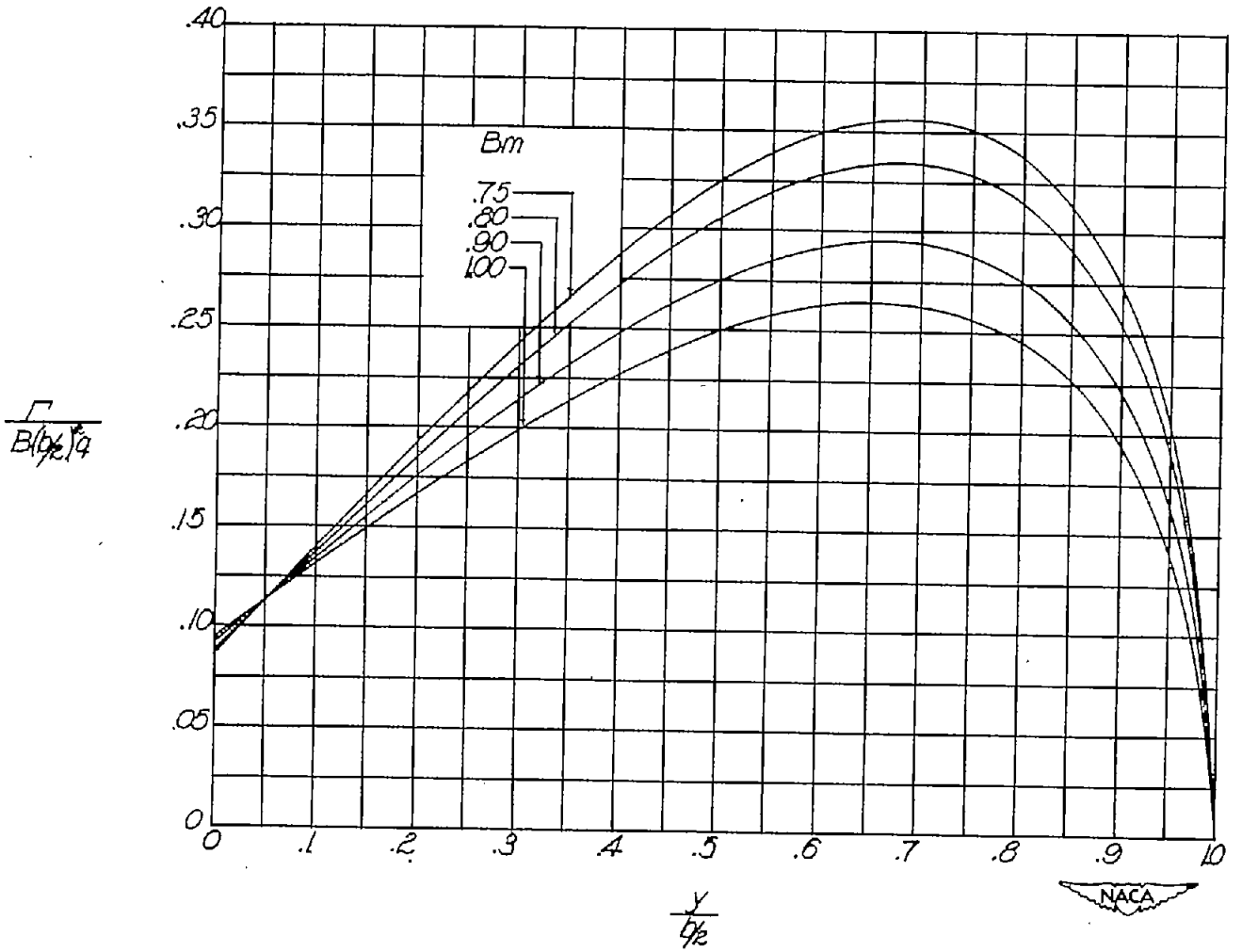

(h) AB = 12.

Figure 17.- Continued.

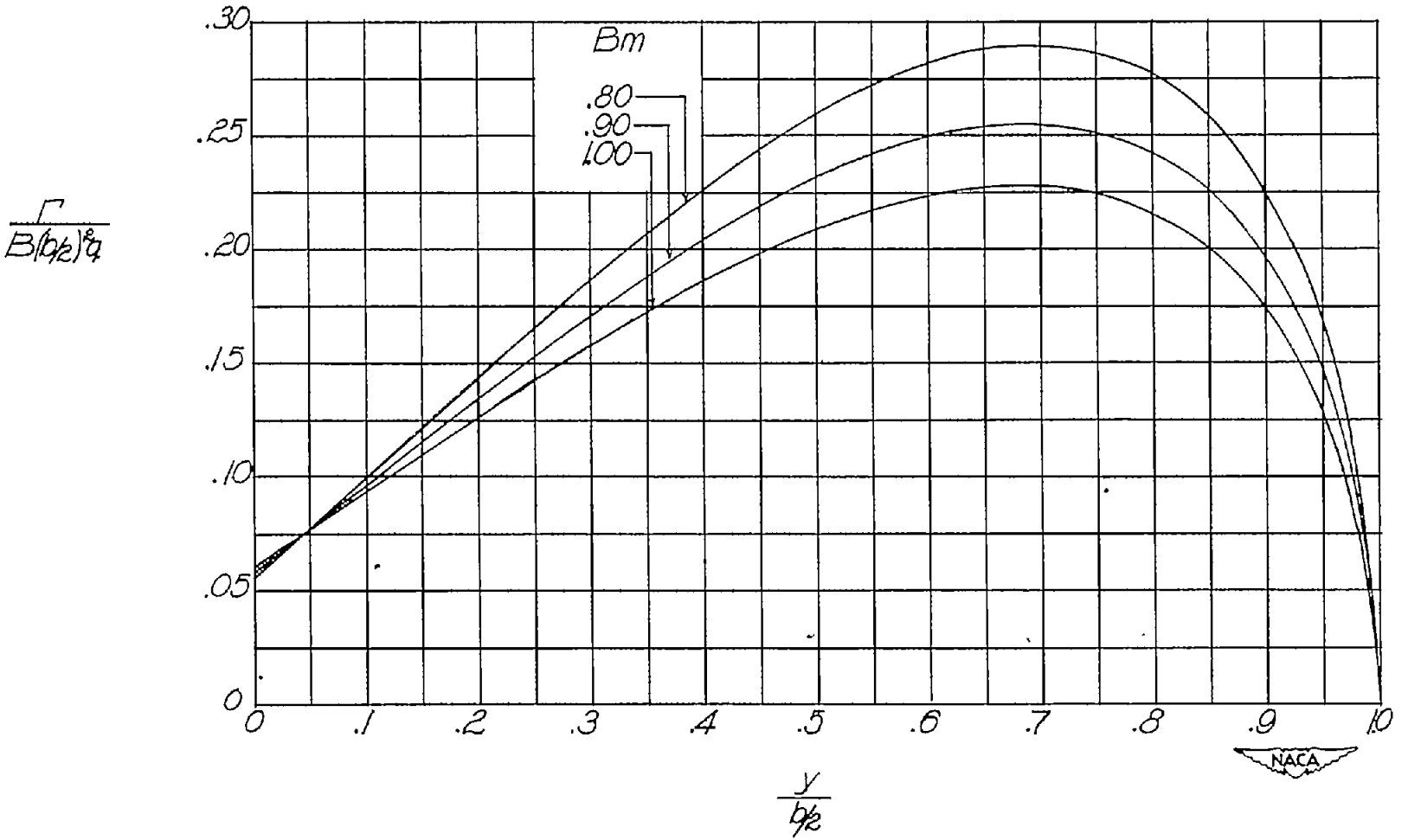

(i) AB = 15.

Figure 17.- Continued.

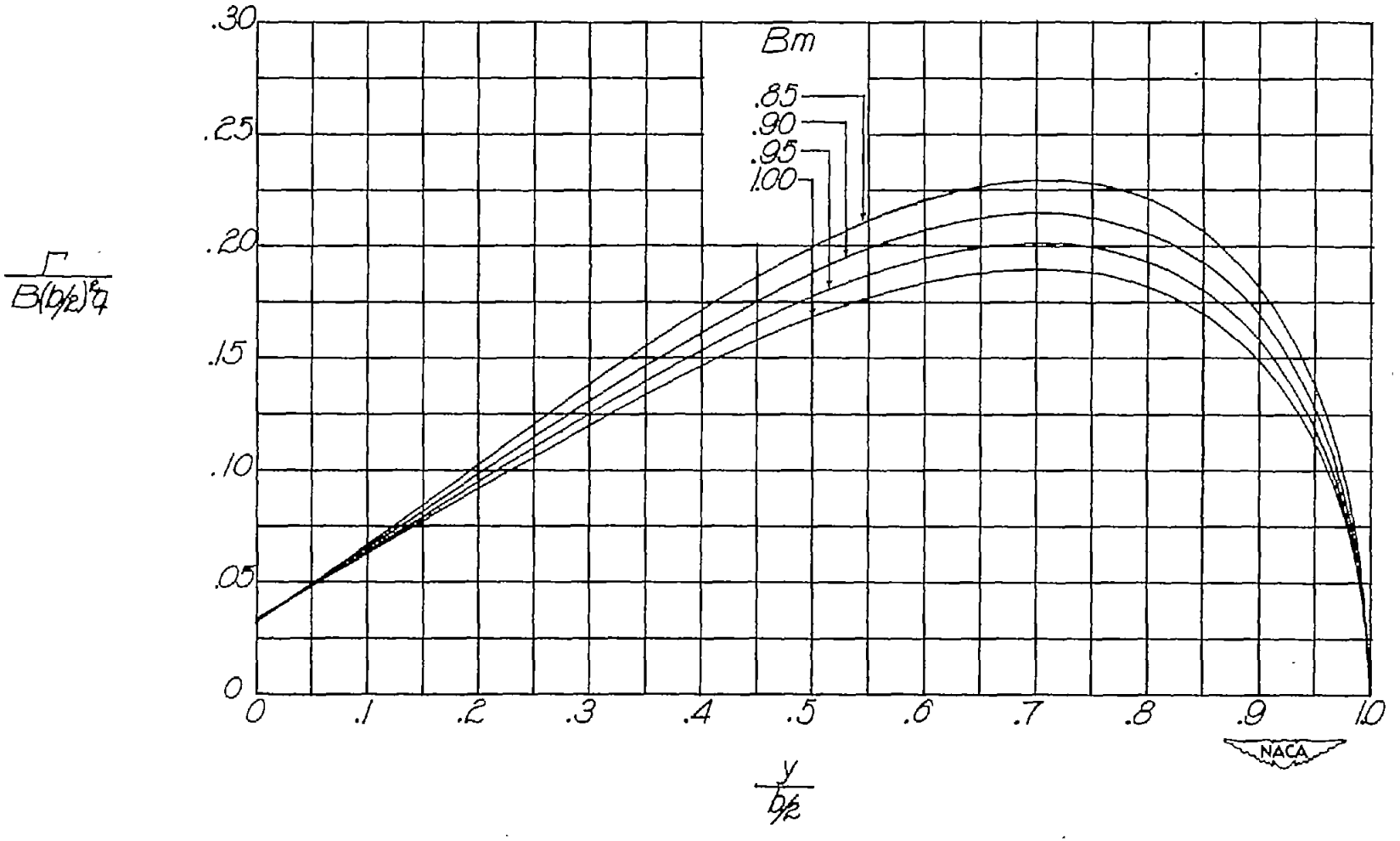

(j) AB = 20.

Figure 17.- Concluded.

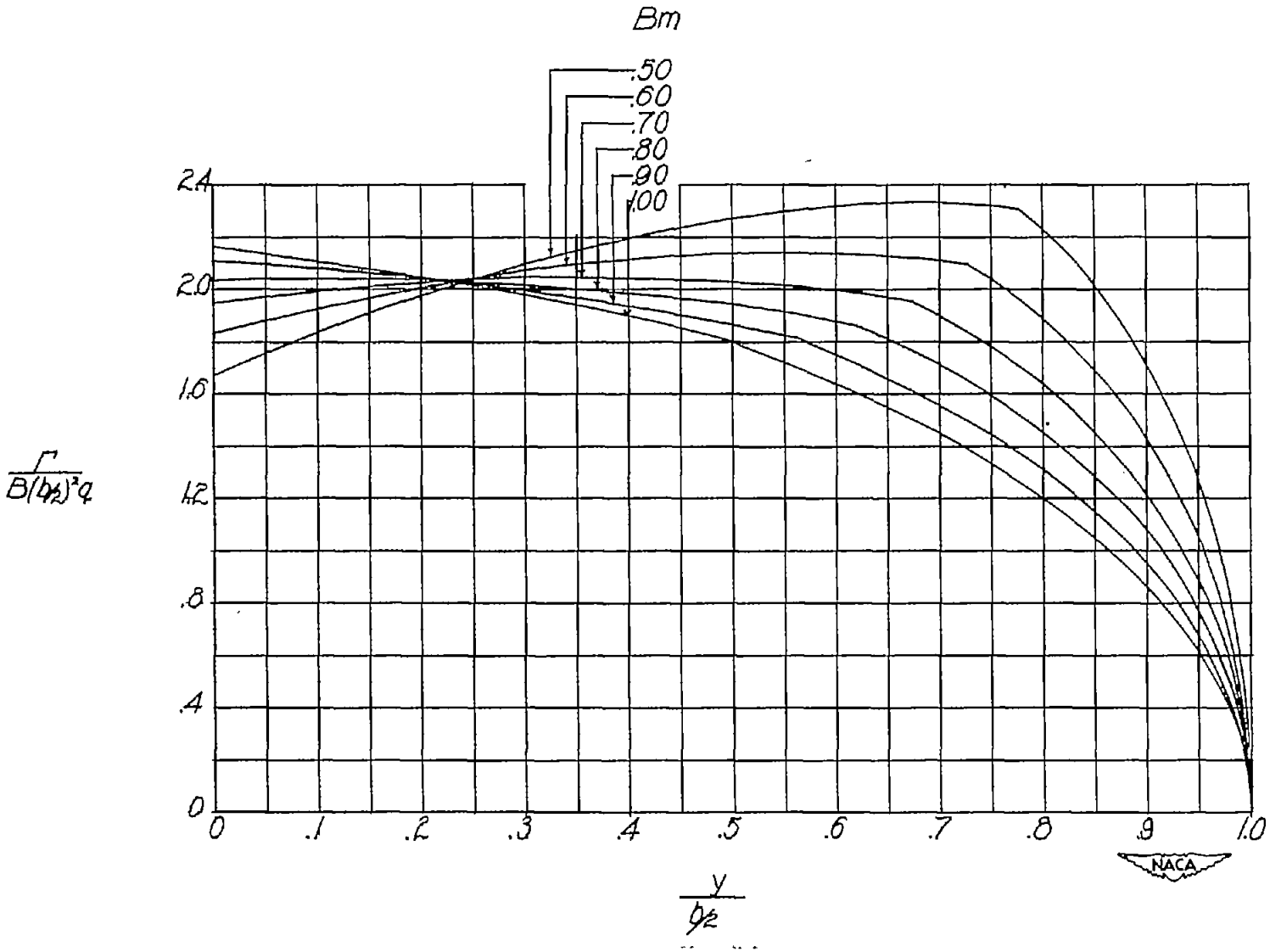

(a) AB = 2.

Figure 18.- Distribution of circulation along span for wing with steady pitching velocity with $\lambda = 0.25$. Wing pitching about apex.

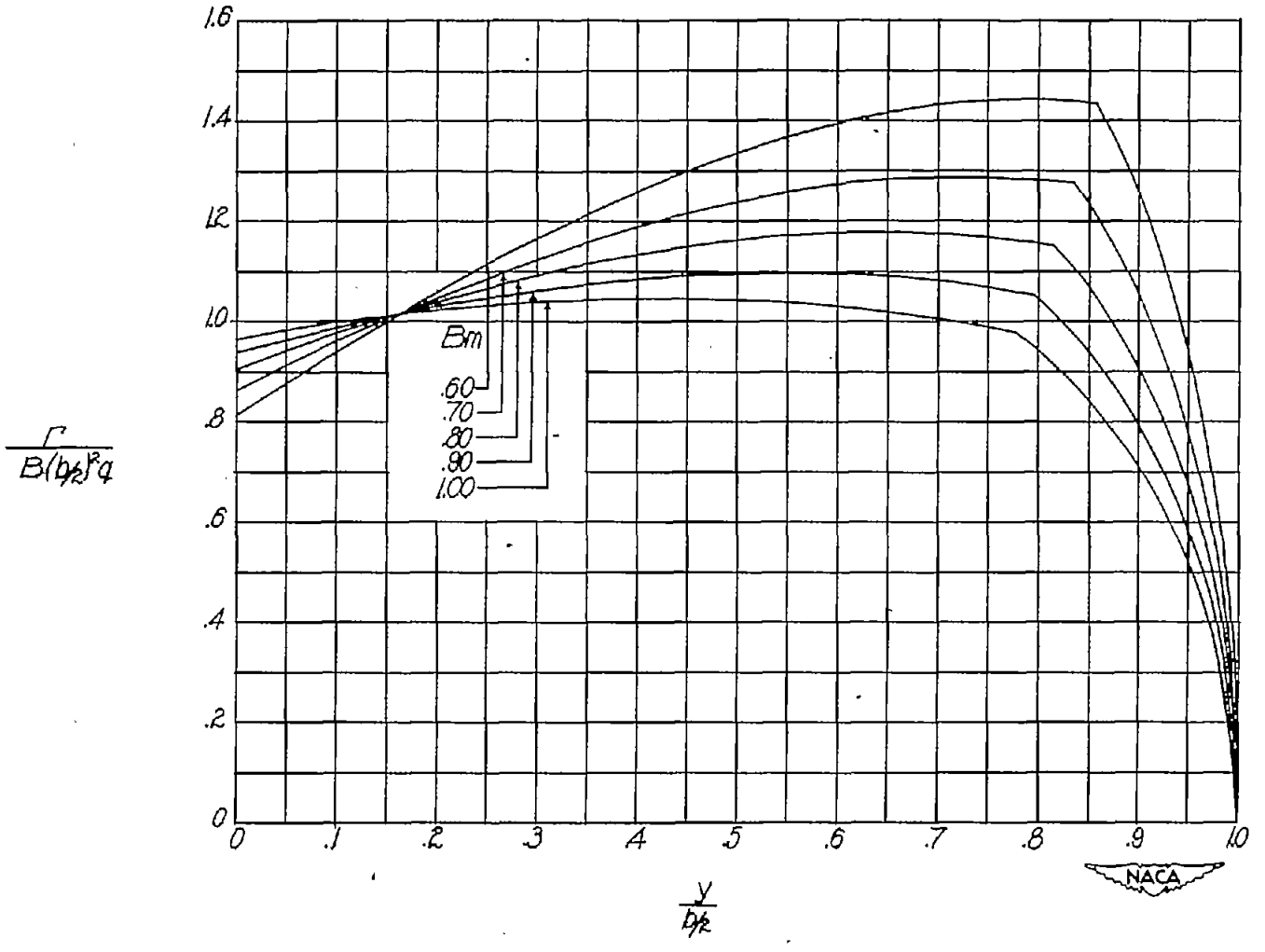

(b) AB = 3.

Figure 18.- Continued.

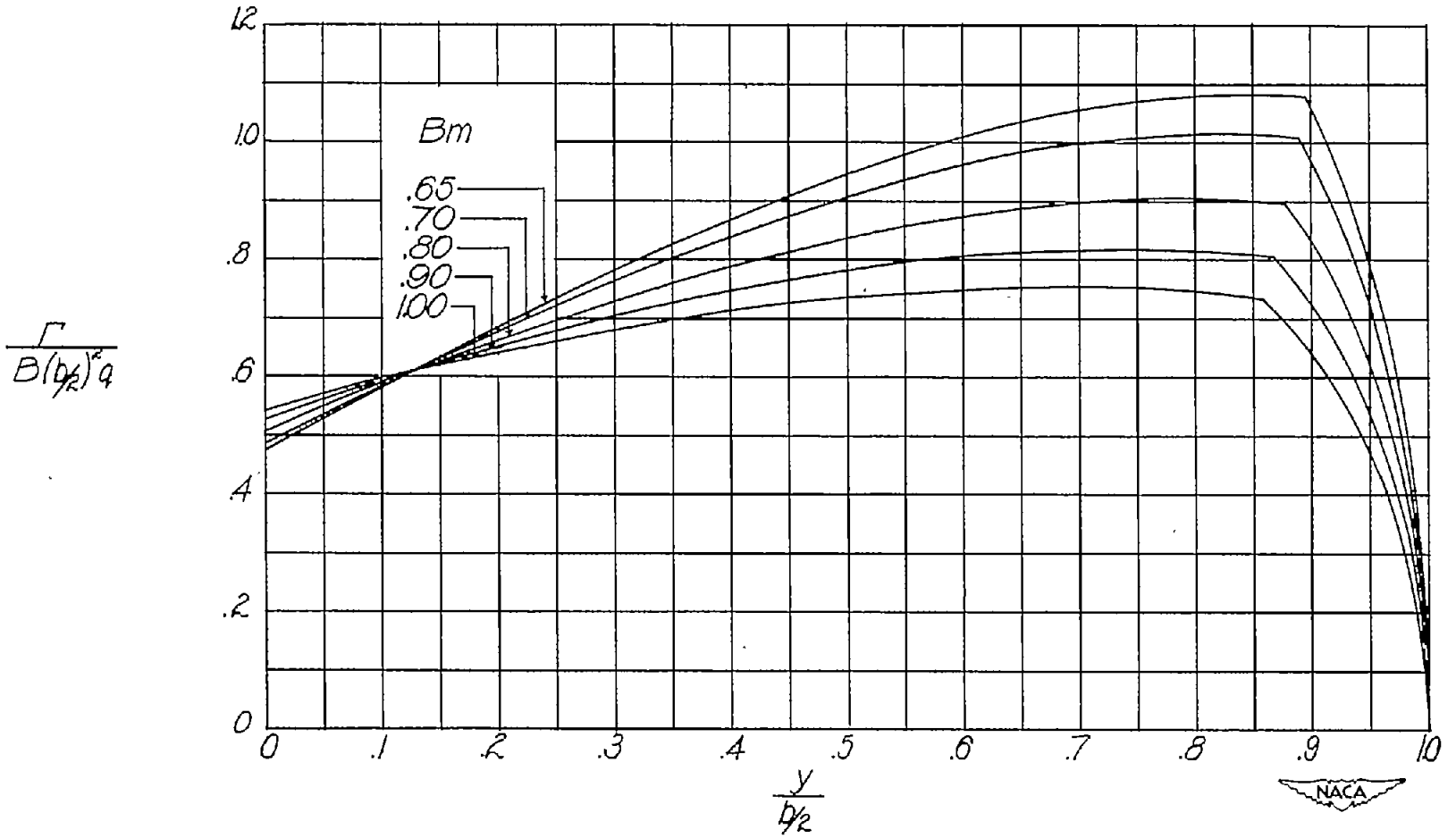

(c) AB = 4.

Figure 18.- Continued.

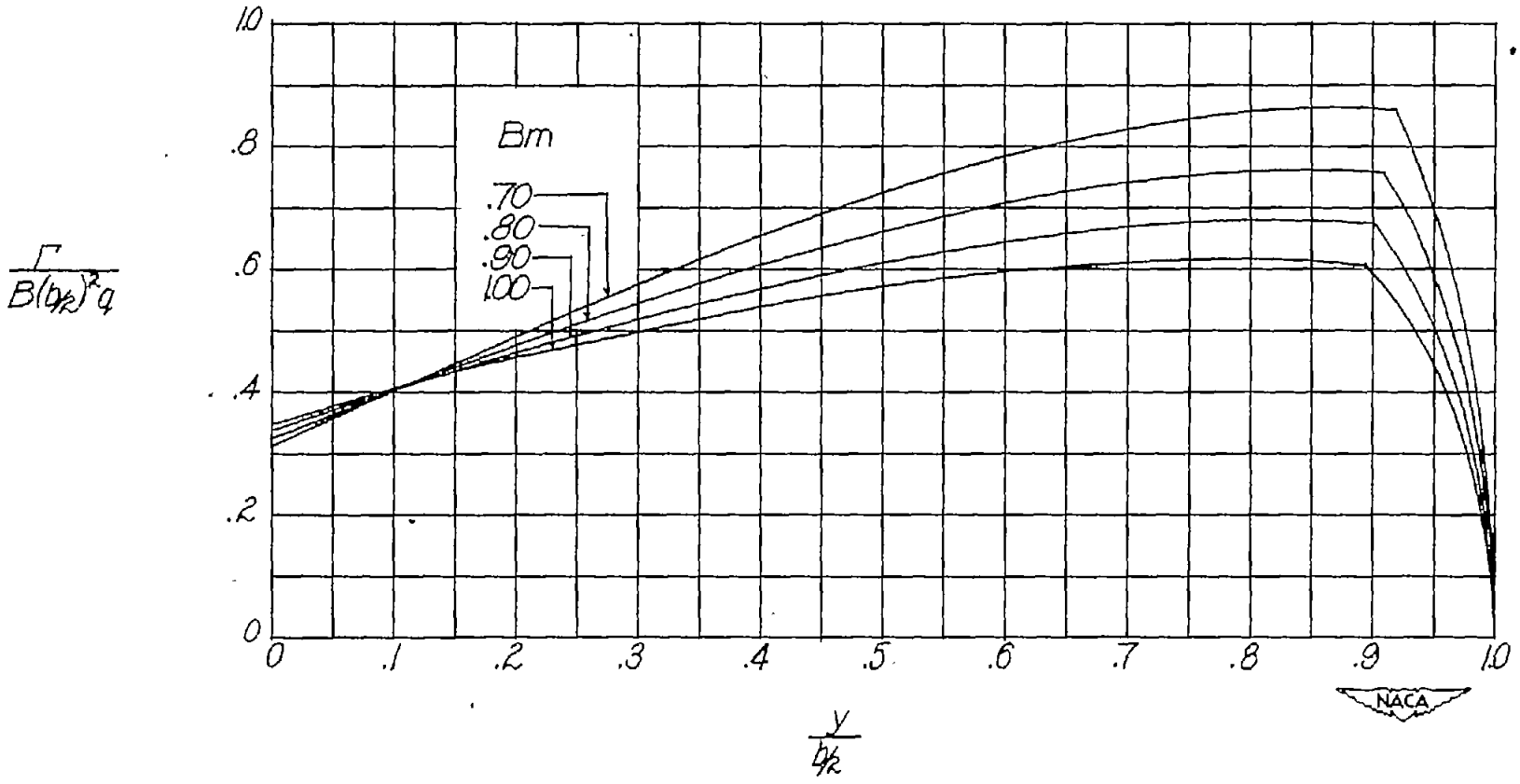

(d) AB = 5.

Figure 18.- Continued.

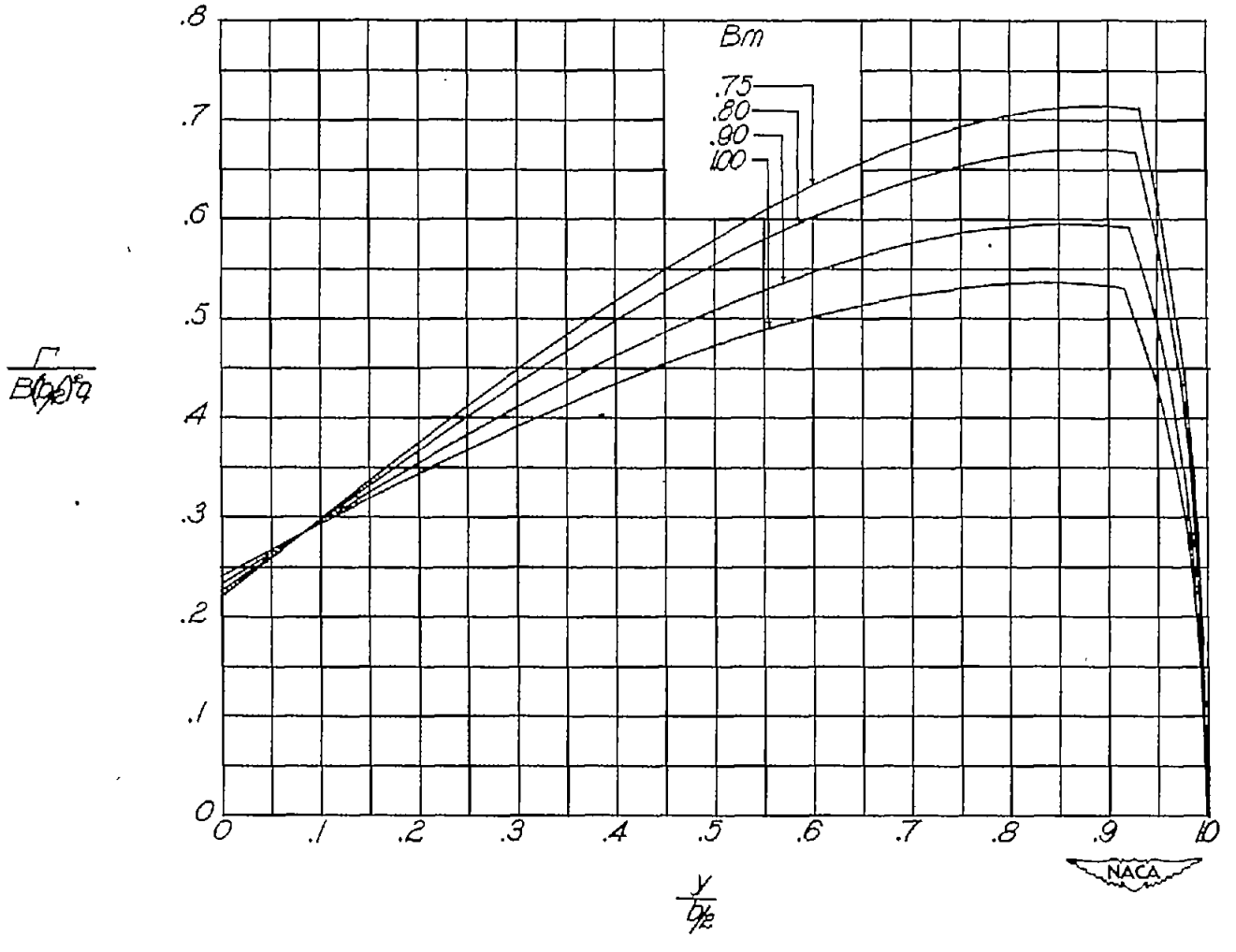

(e) AB = 6.

Figure 18.- Continued.

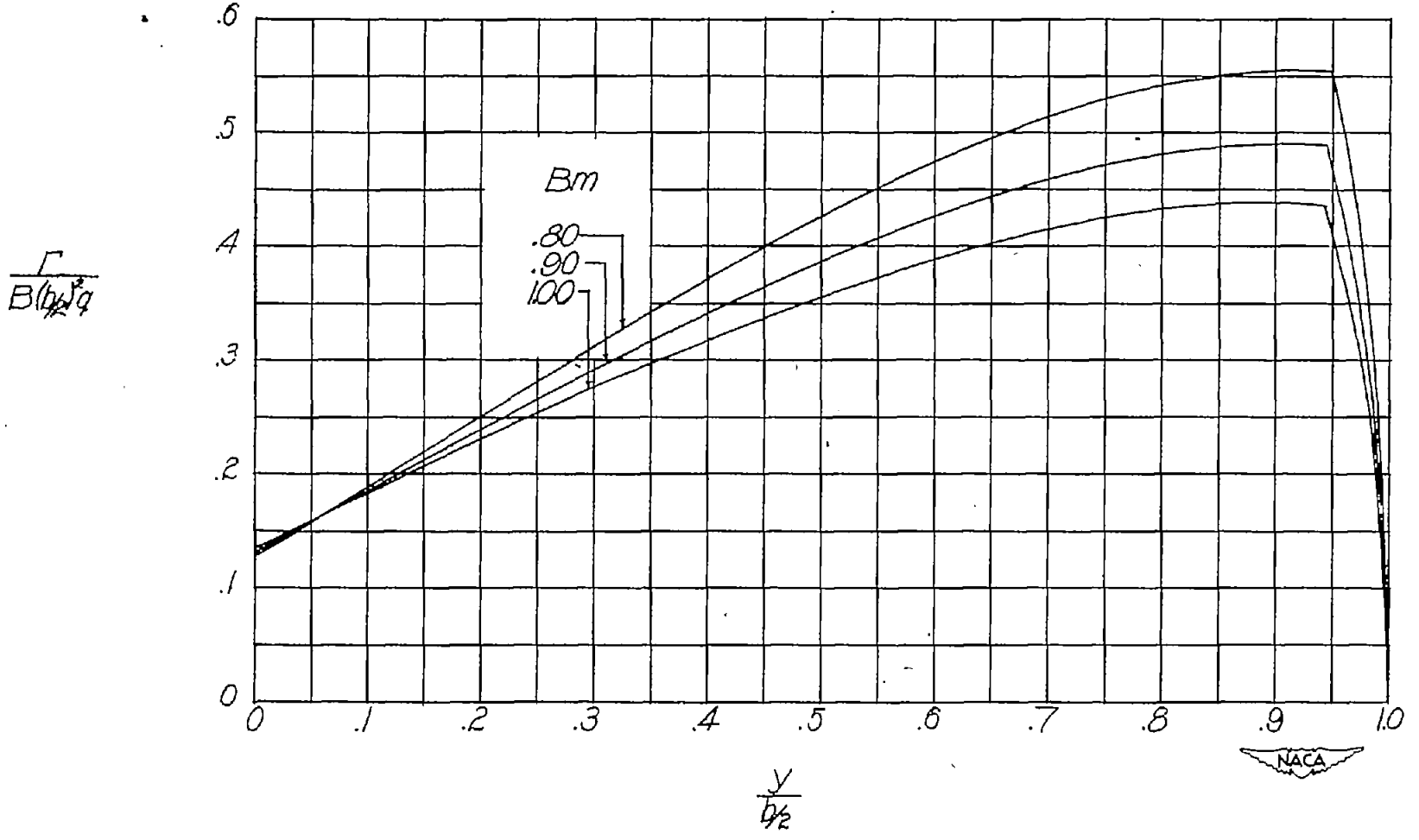

(f) AB = 8.

Figure 18.- Continued.

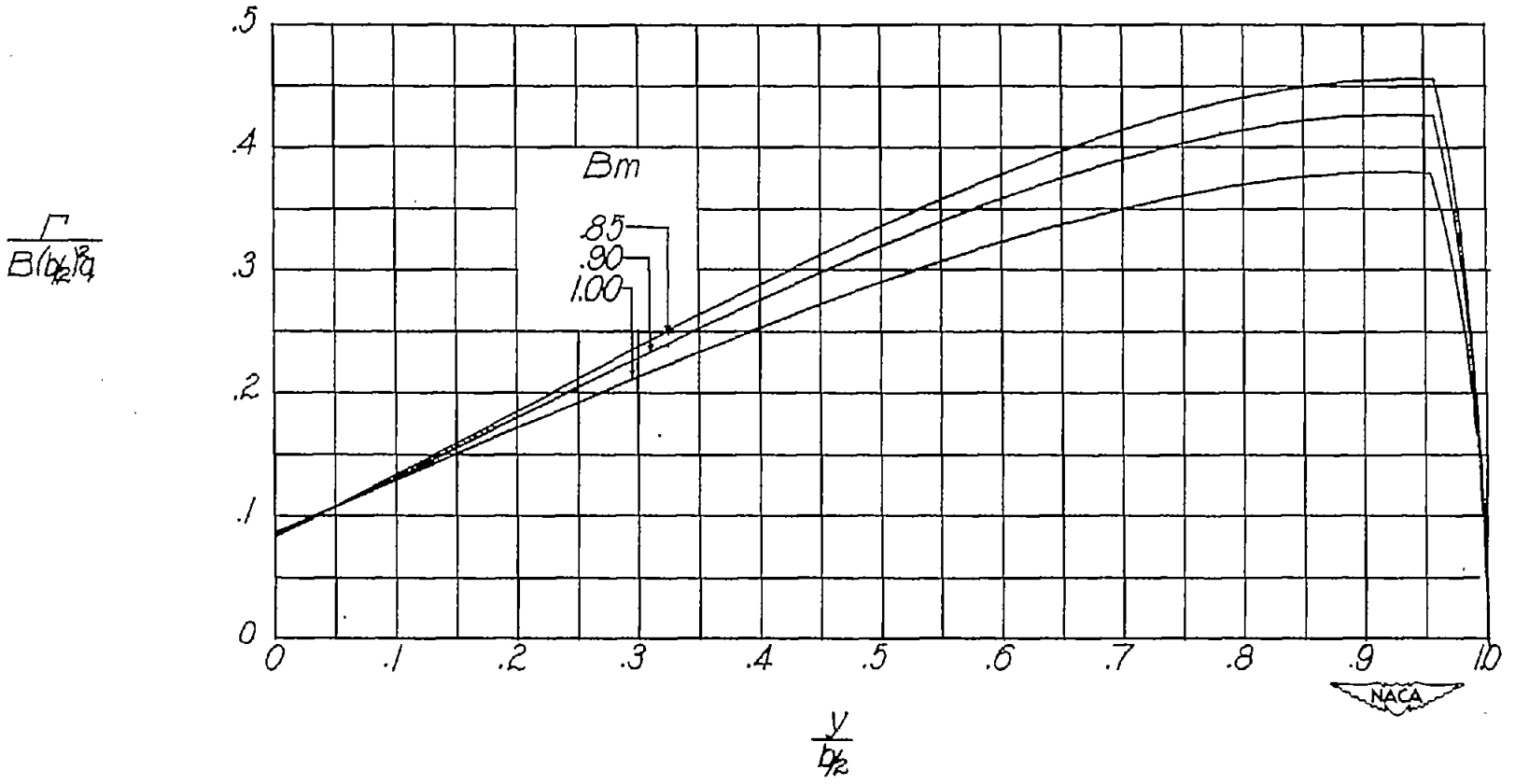

(g) AB = 10.

Figure 18.- Continued.

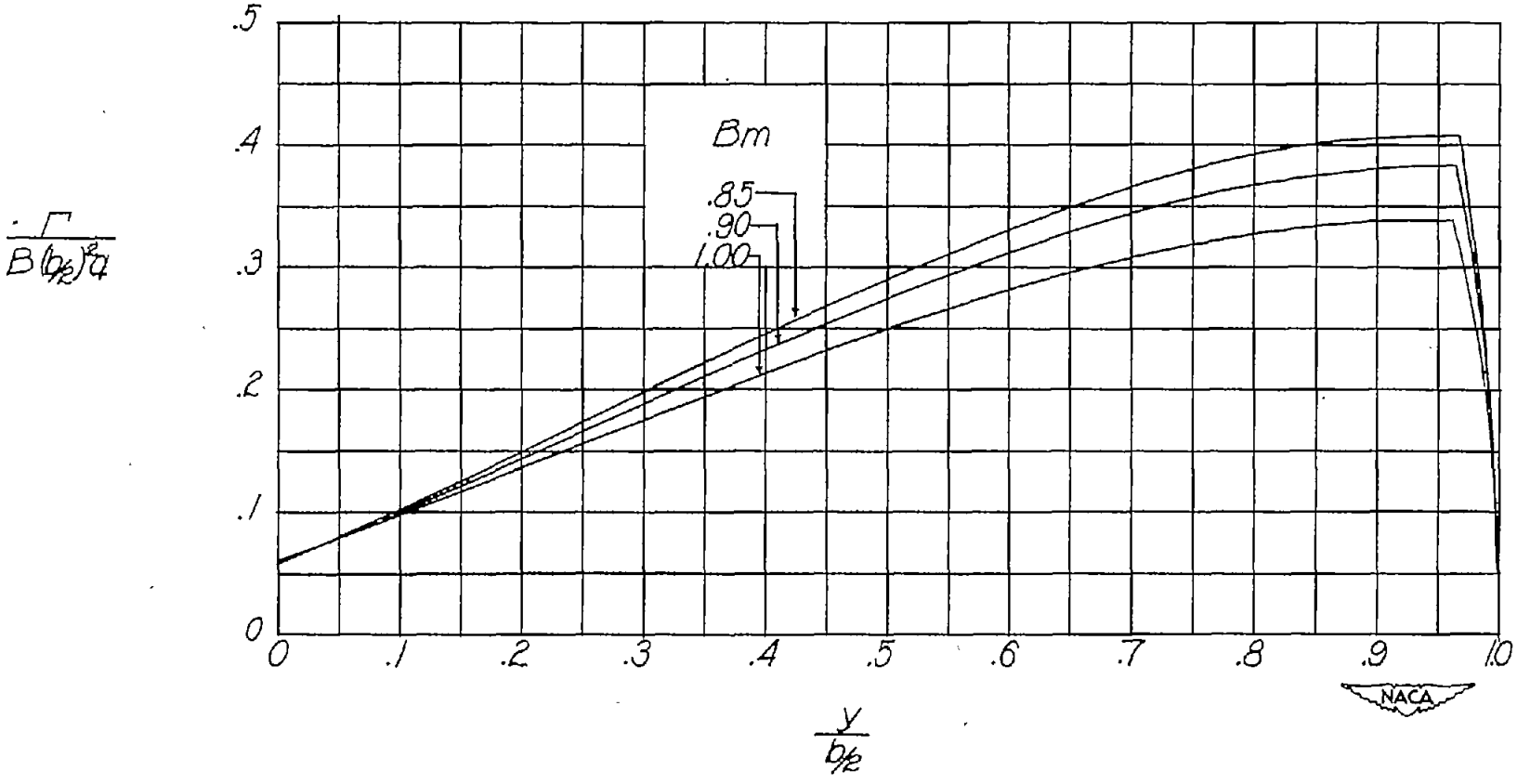

(h) AB = 12.

Figure 18.- Continued.

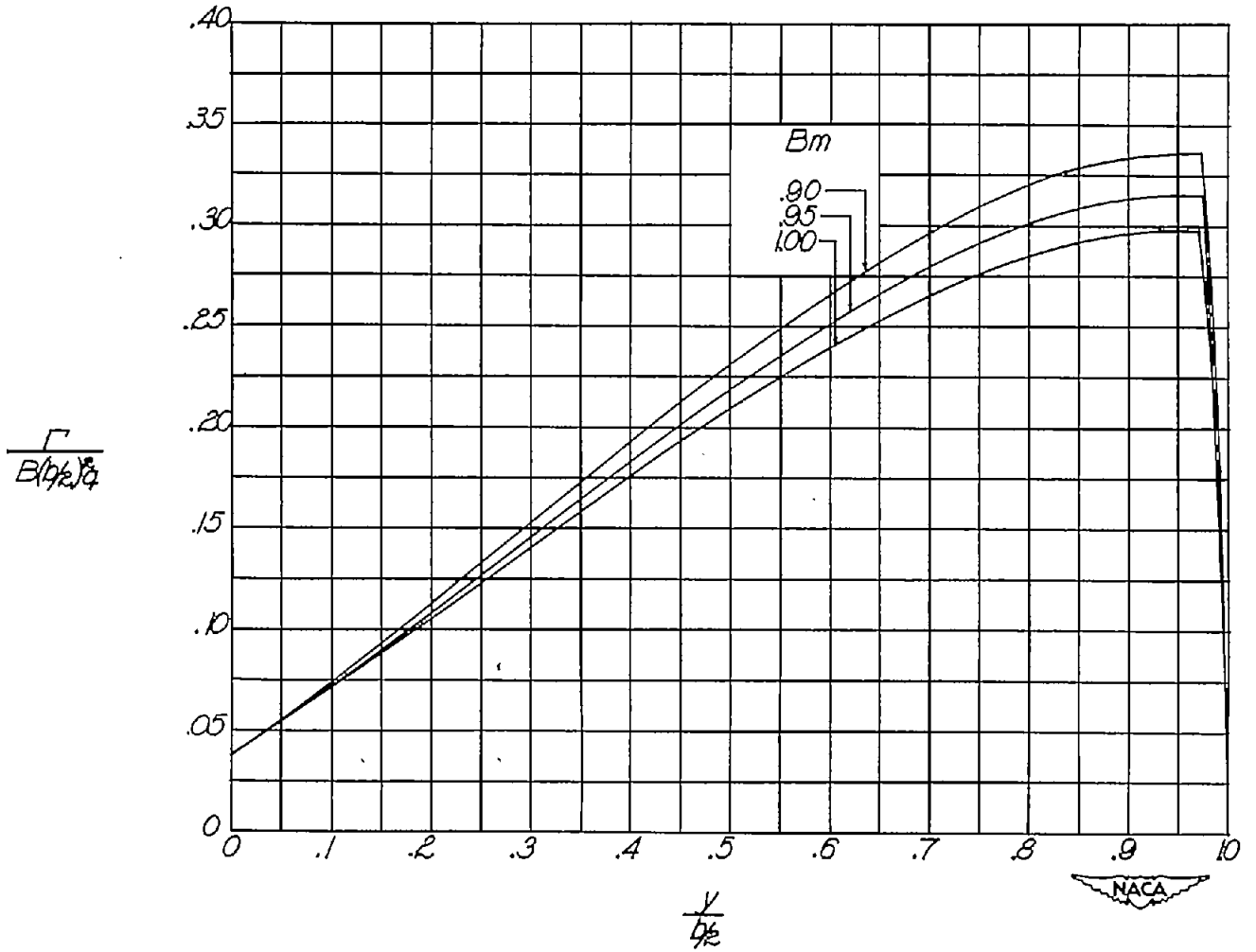

(i) AB = 15.

Figure 18.- Continued.

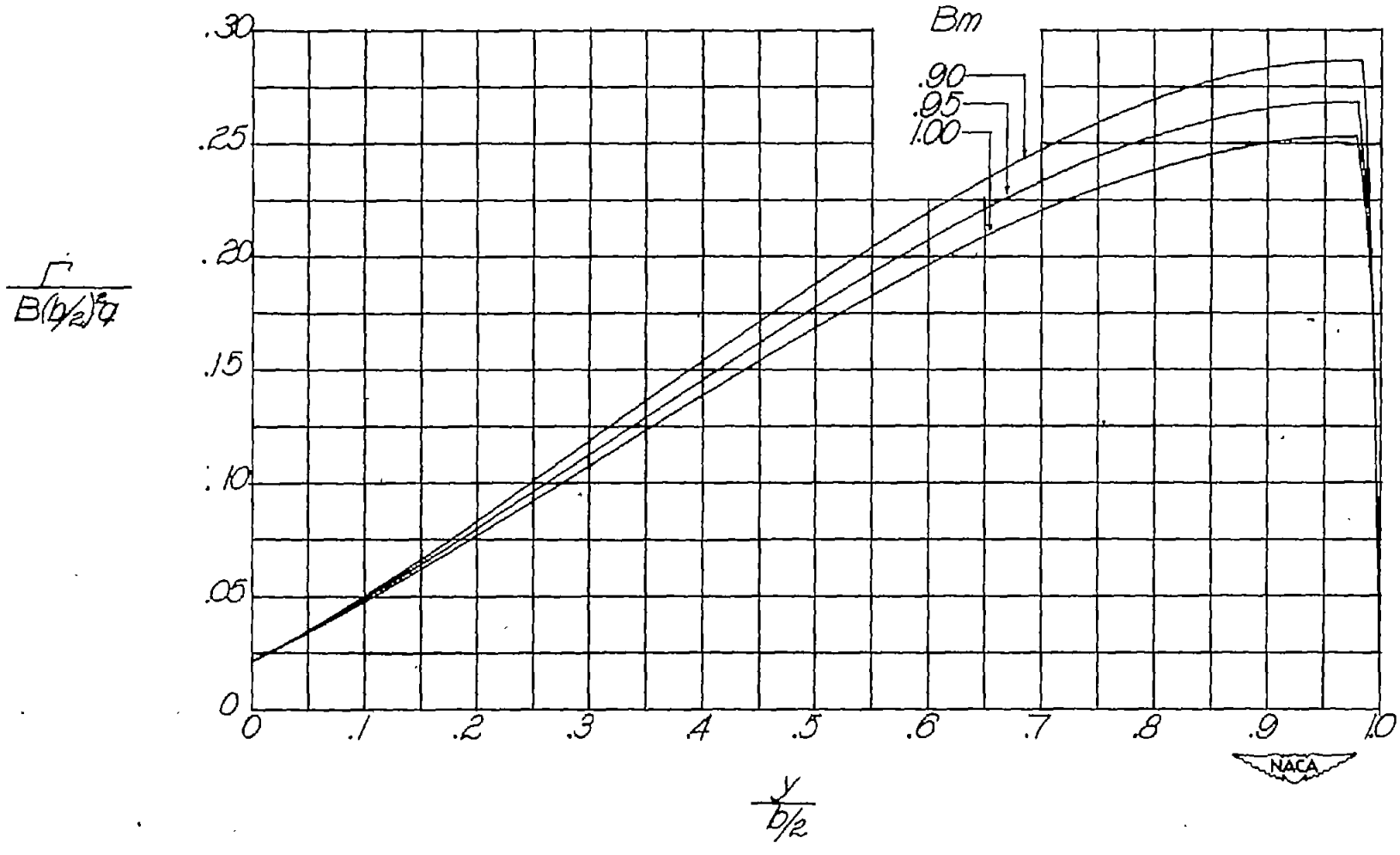

(j) AB = 20.

Figure 18.- Concluded.

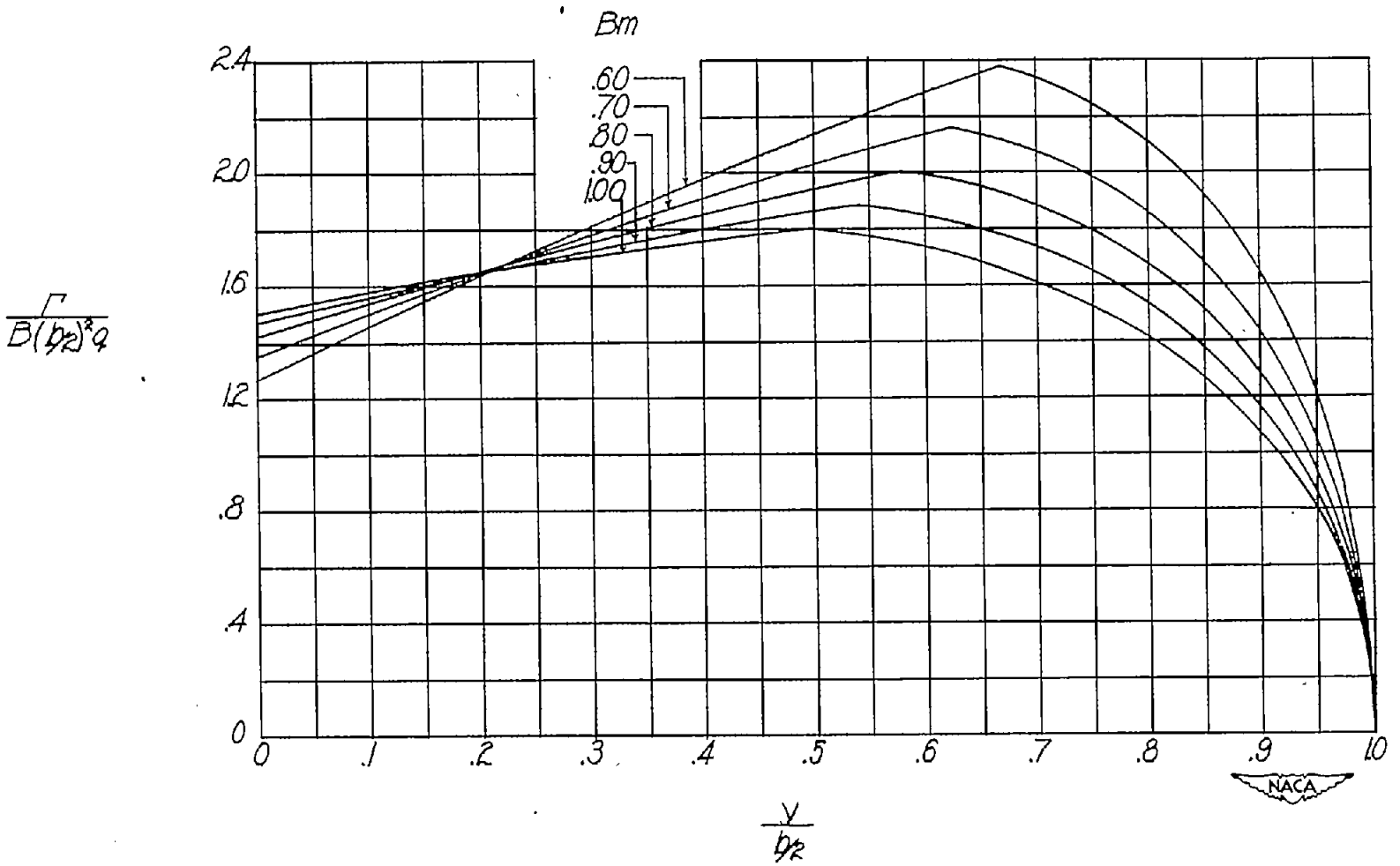

(a) AB = 2.

Figure 19.- Distribution of circulation along span for wings with steady pitching velocity with $\lambda = 0.50$. Wing pitching about apex.

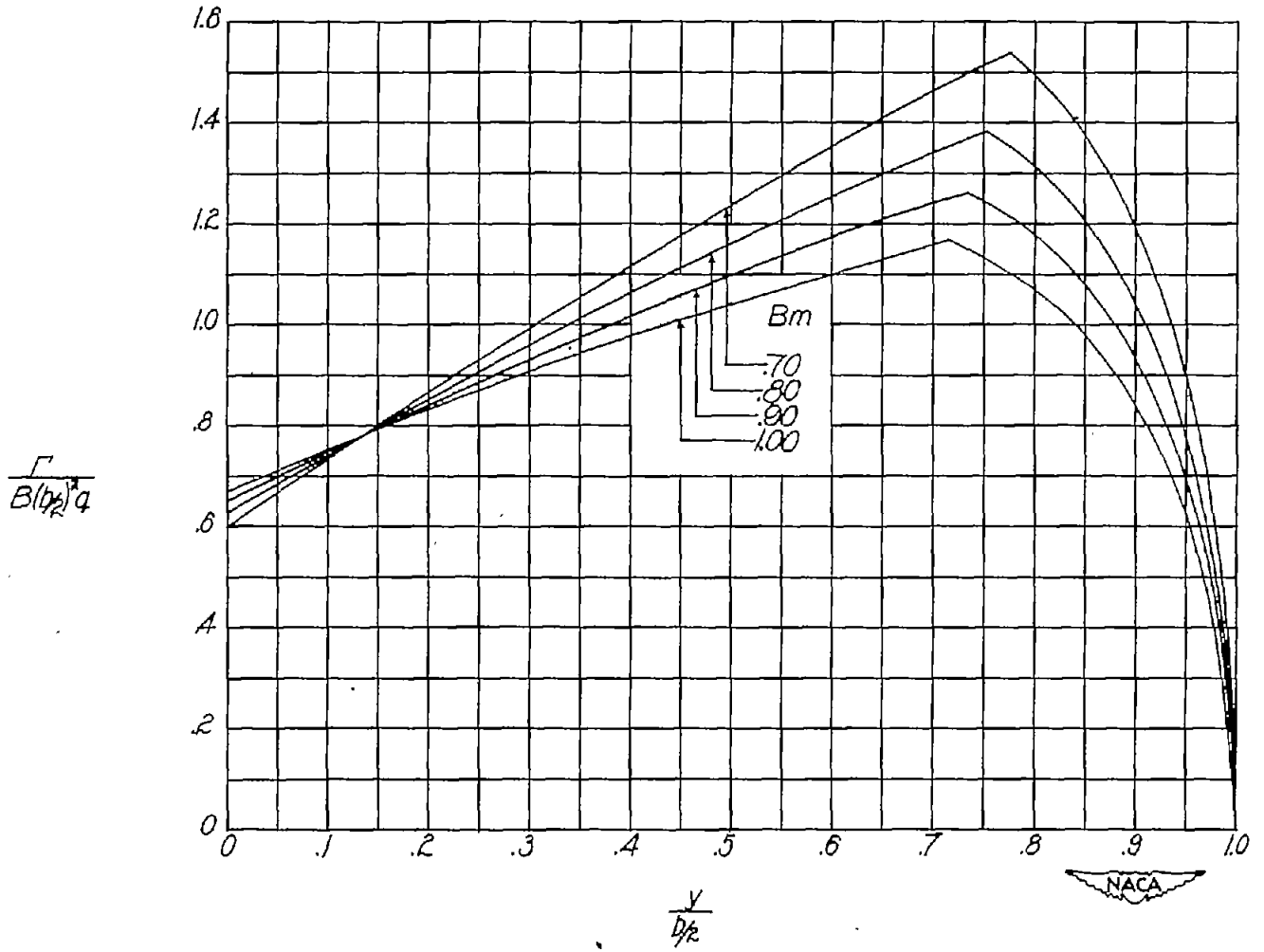

(b) AB = 3.

Figure 19.- Continued.

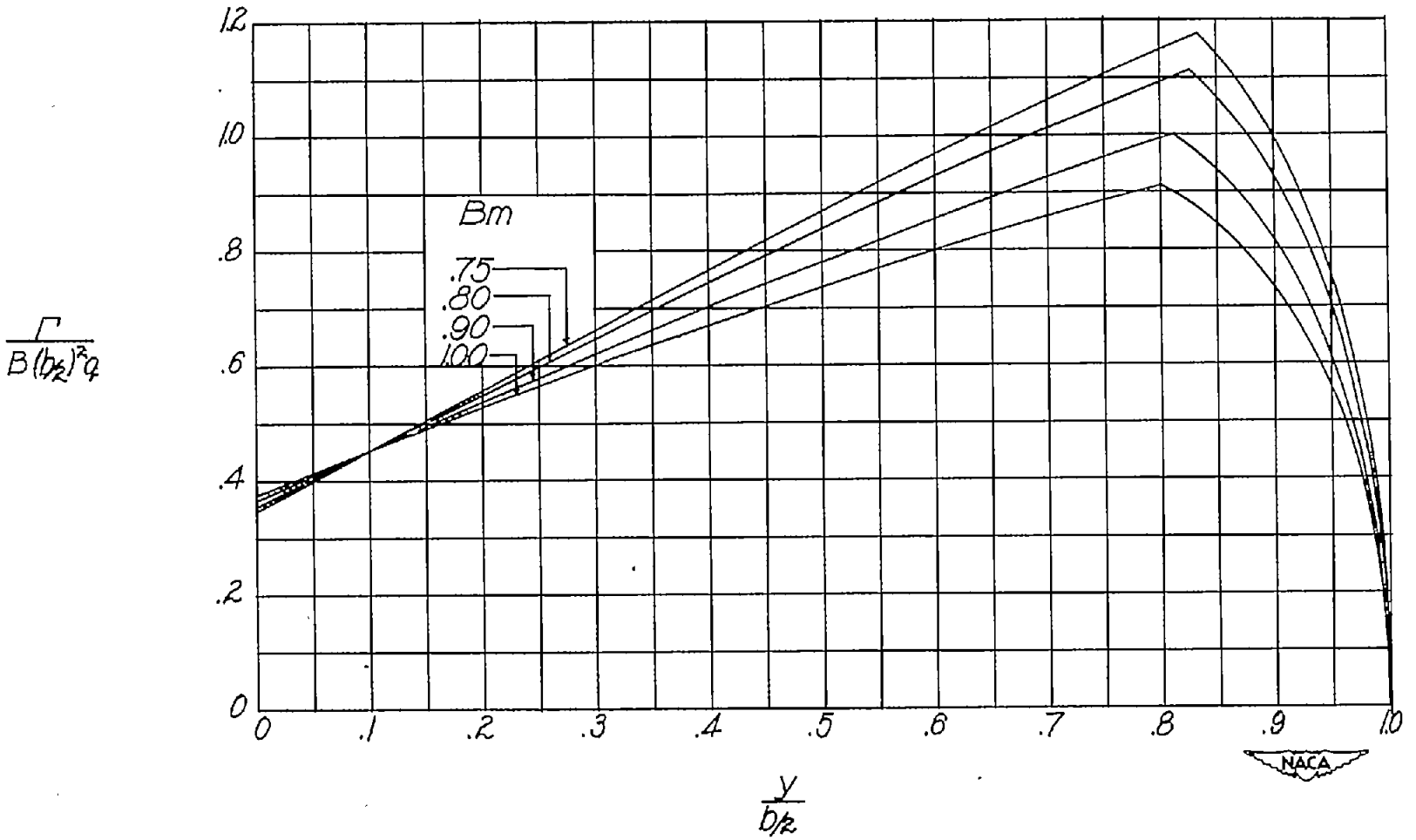

(c) AB = 4.

Figure 19.- Continued.

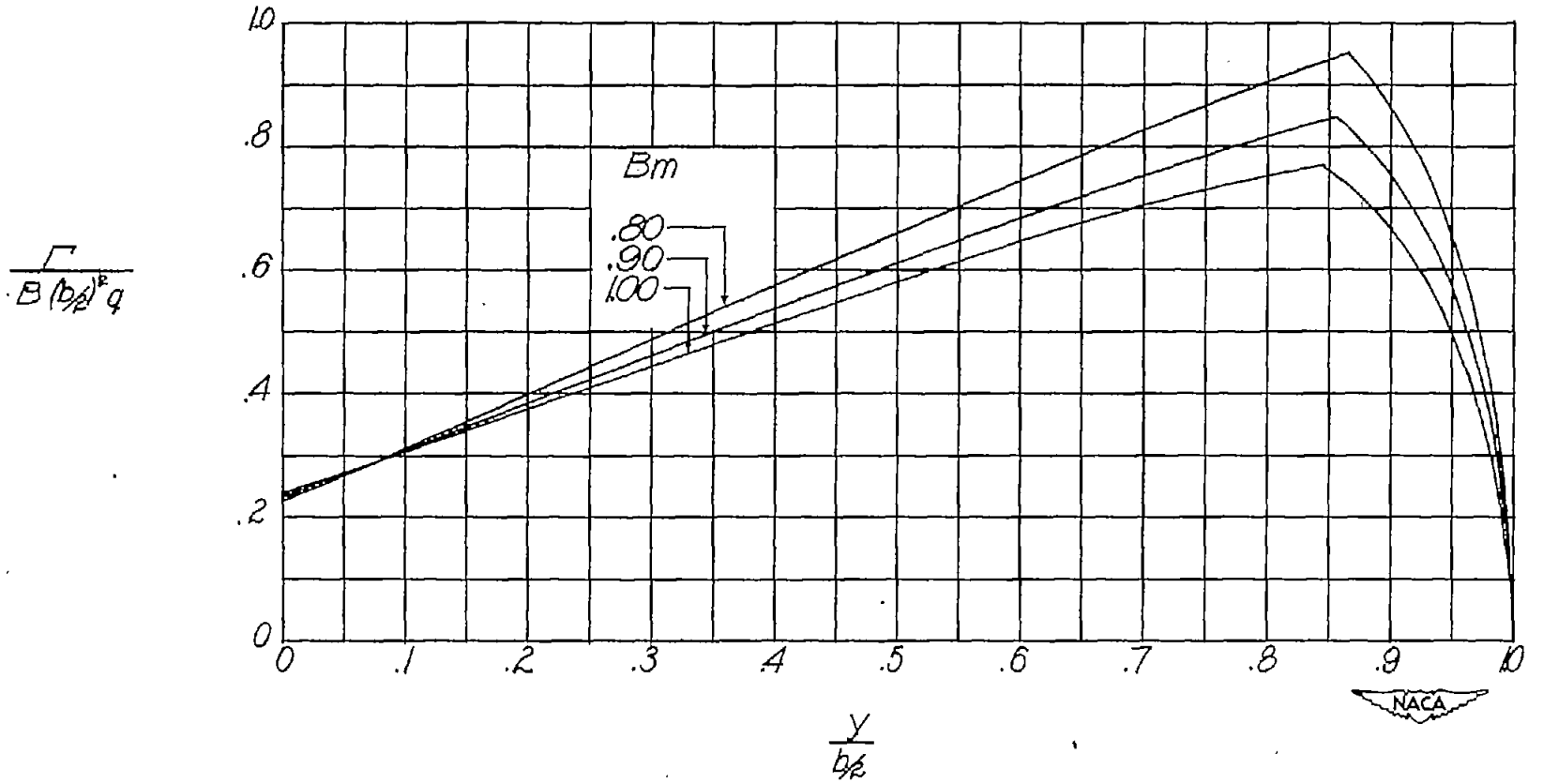

(d) AB = 5.

Figure 19.- Continued.

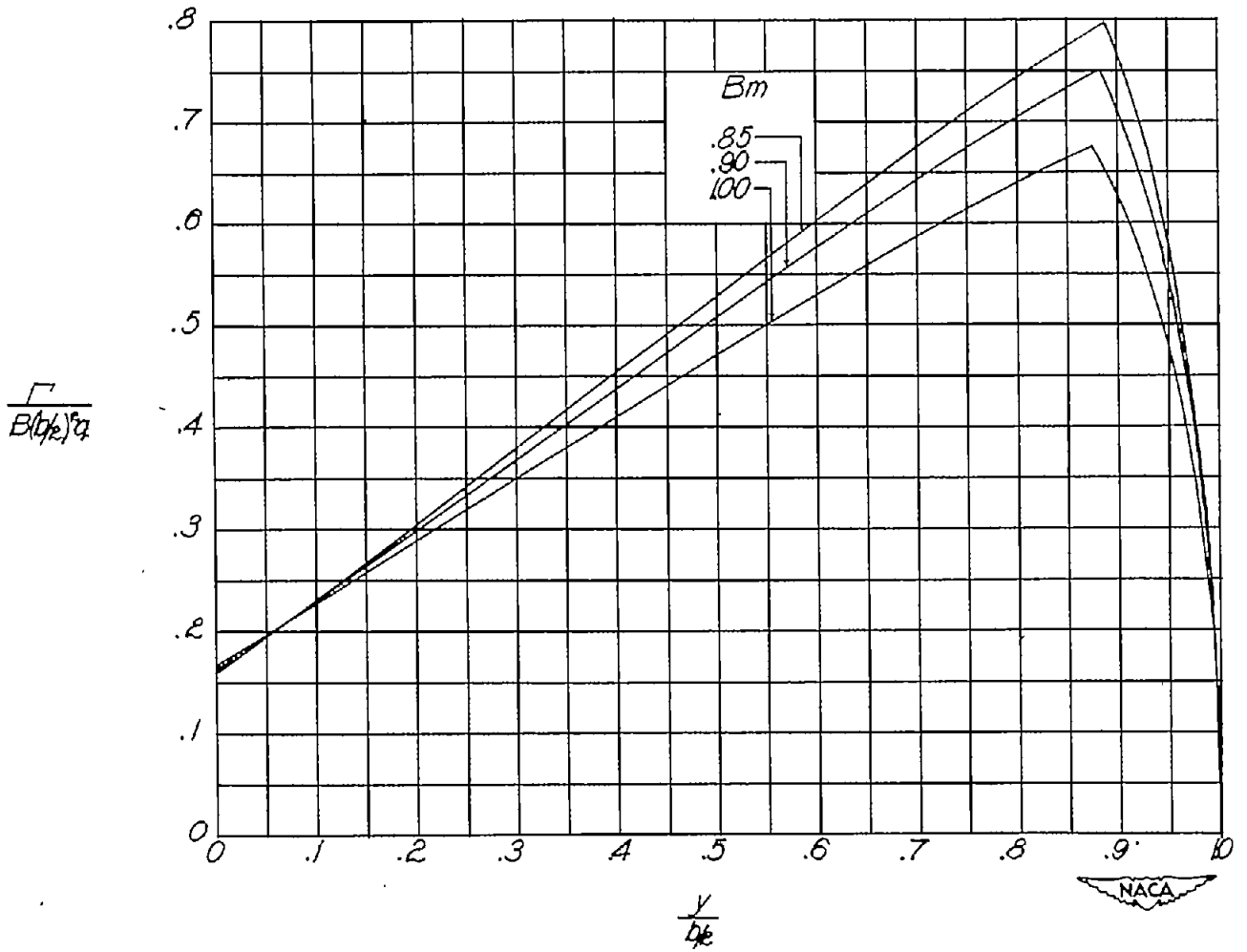

(e) AB = 6.

Figure 19.- Continued.

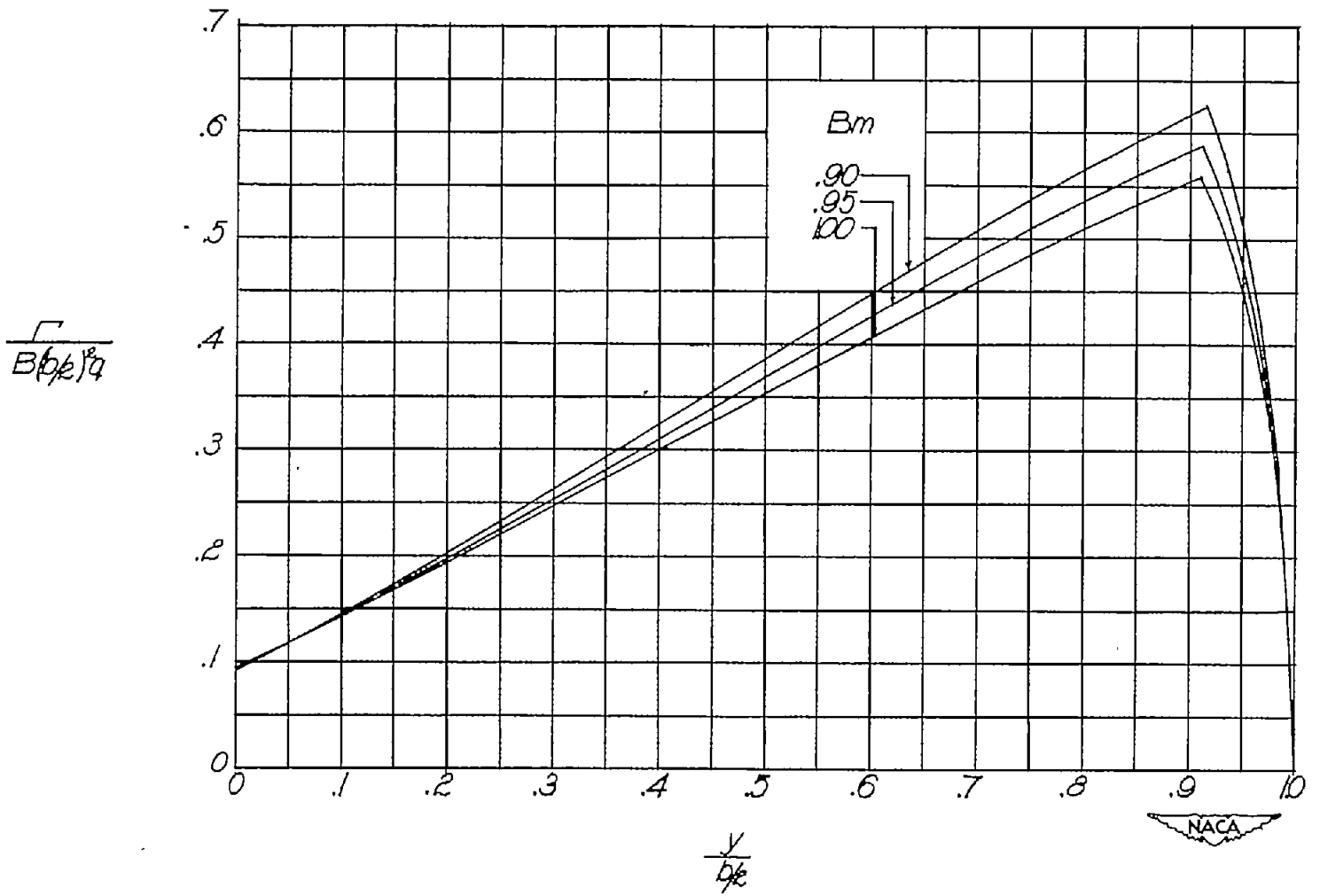

(f) AB = 8.

Figure 19.- Continued.

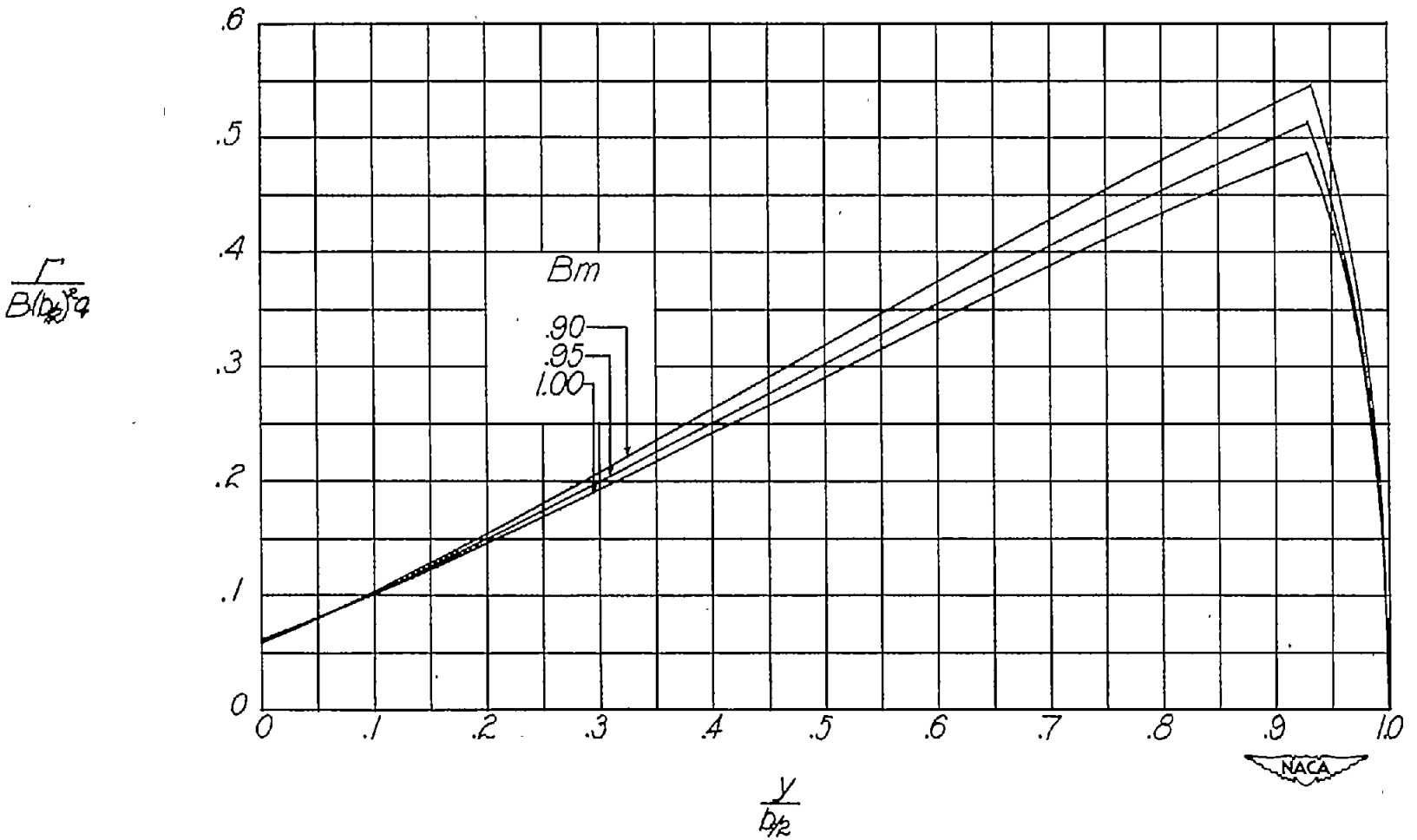

(g) AB = 10.

Figure 19.- Continued.

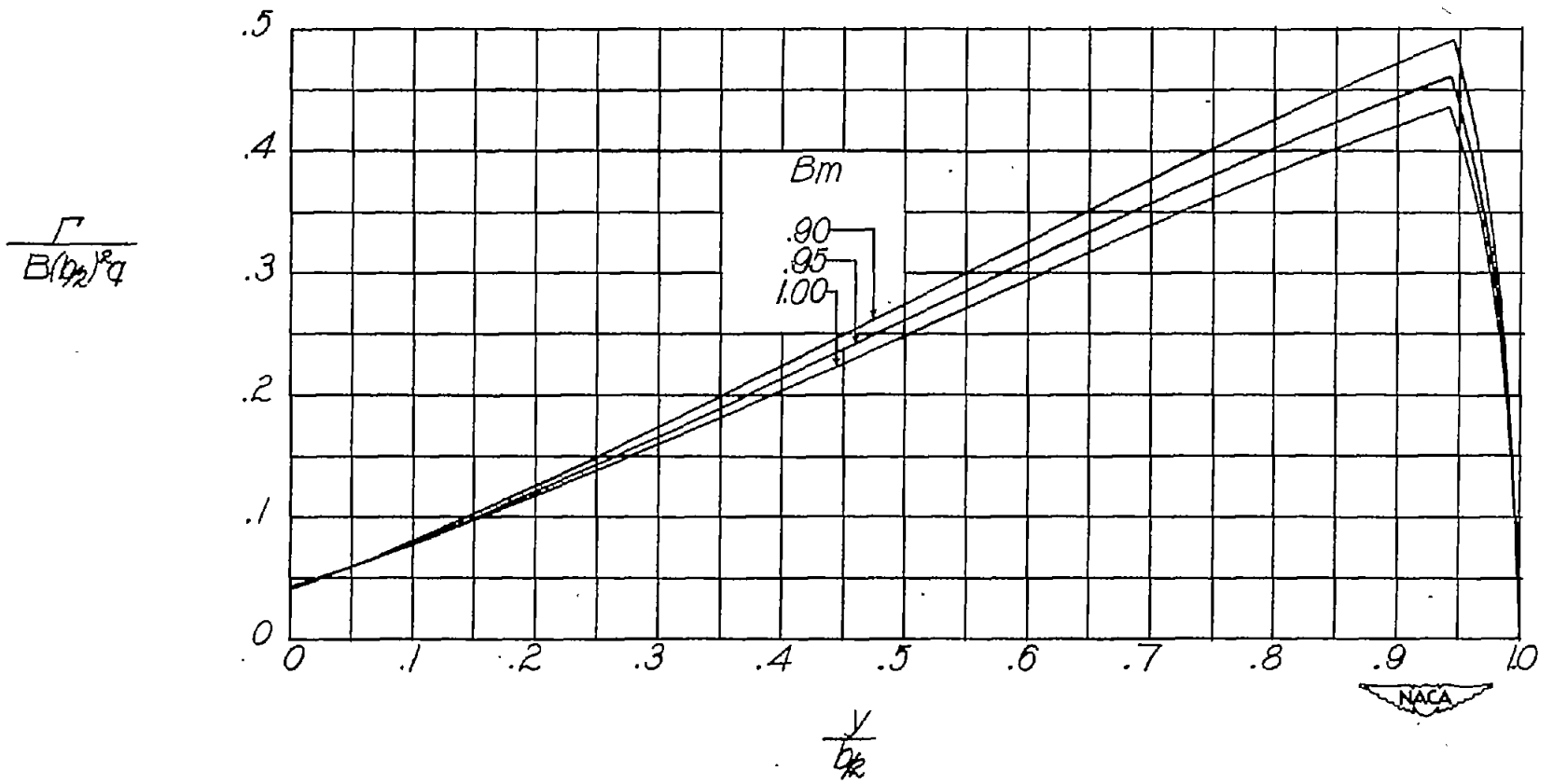

(h) AB = 12.

Figure 19.- Continued.

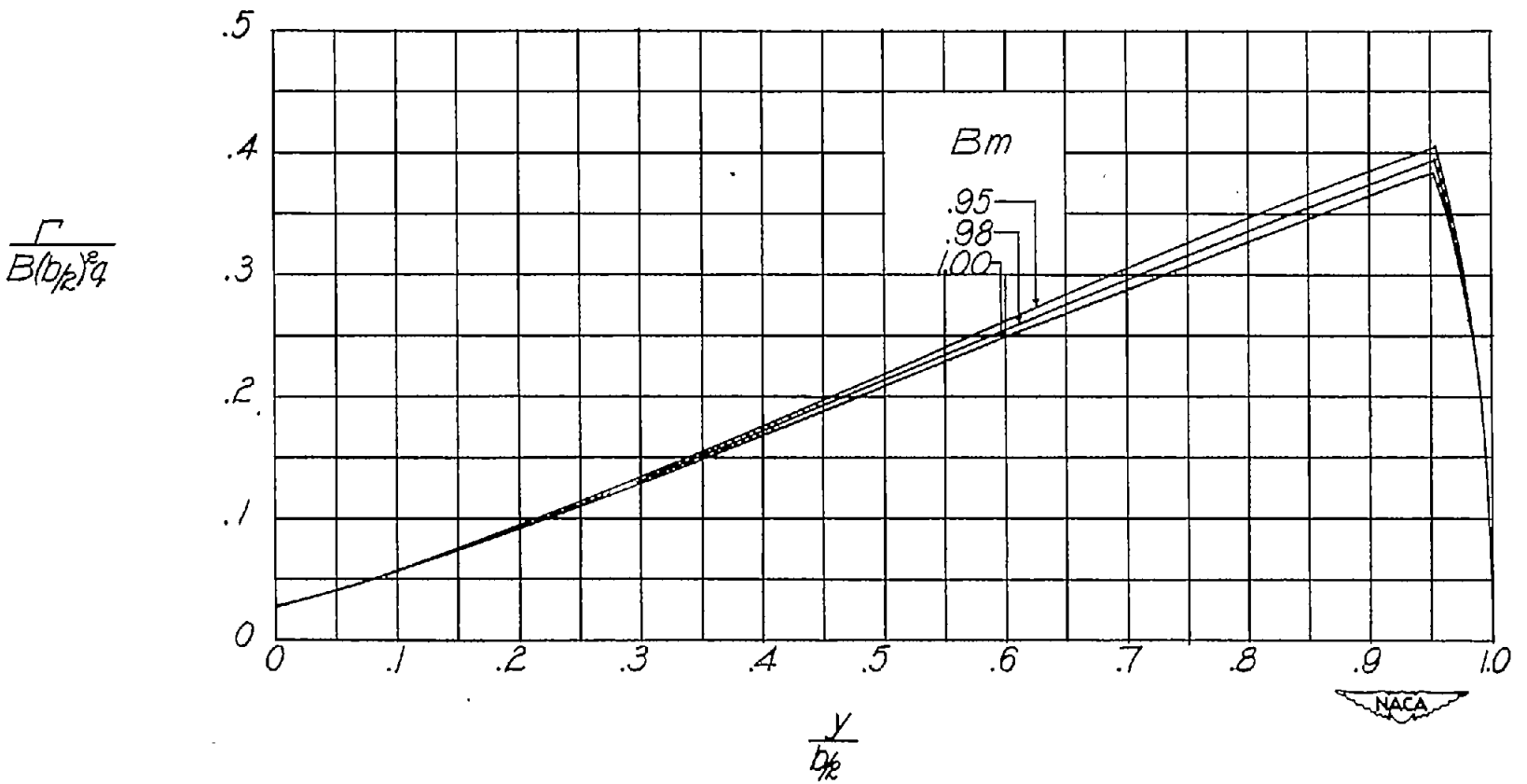

(i) AB = 15.

Figure 19.- Continued.

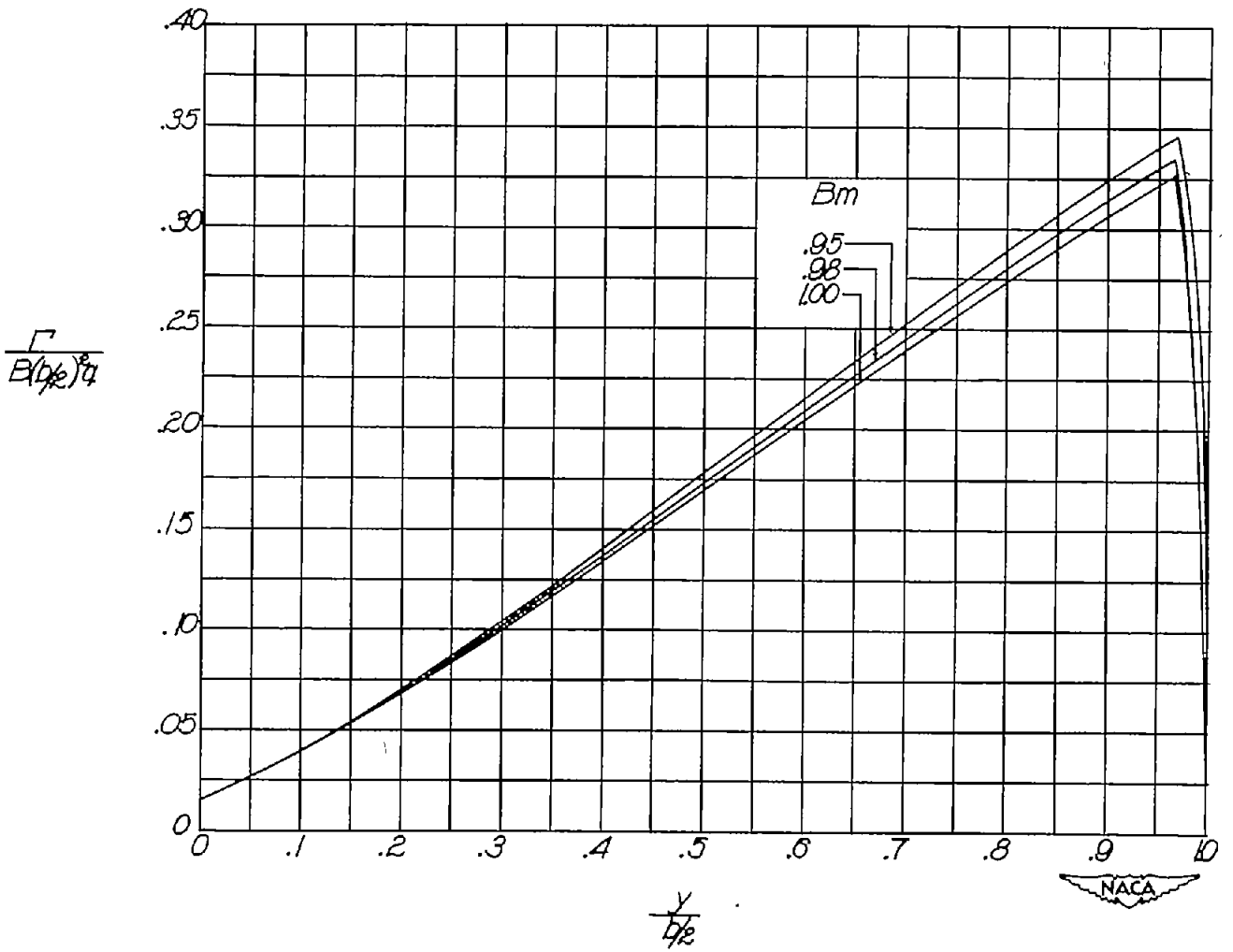

(j) AB = 20.

Figure 19.- Concluded.

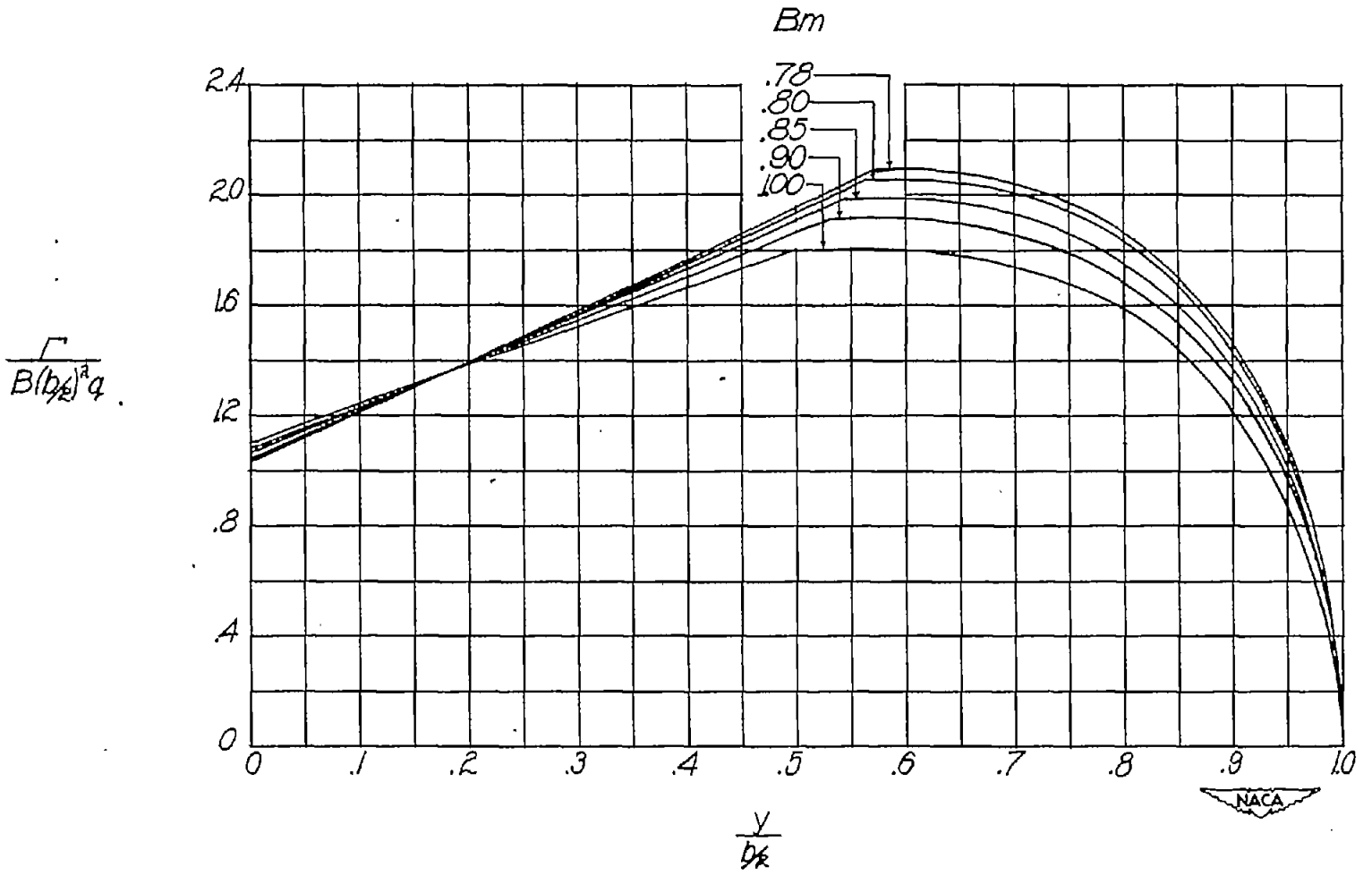

(a) AB = 2.

Figure 20.- Distribution of circulation along span for wings with steady pitching velocity with $\lambda = 0.75$. Wing pitching about apex.

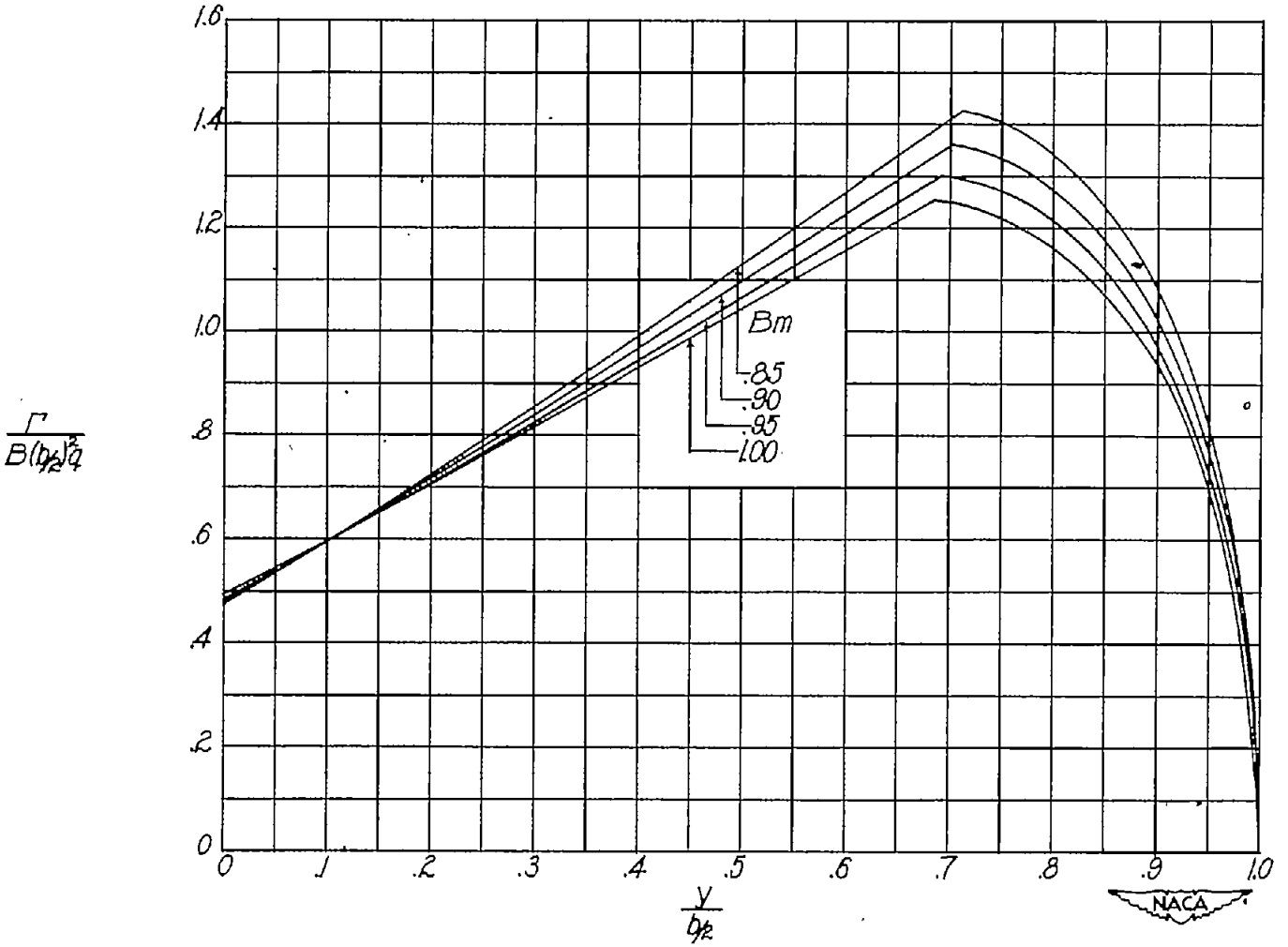

(b) AB = 3.

Figure 20.- Continued.

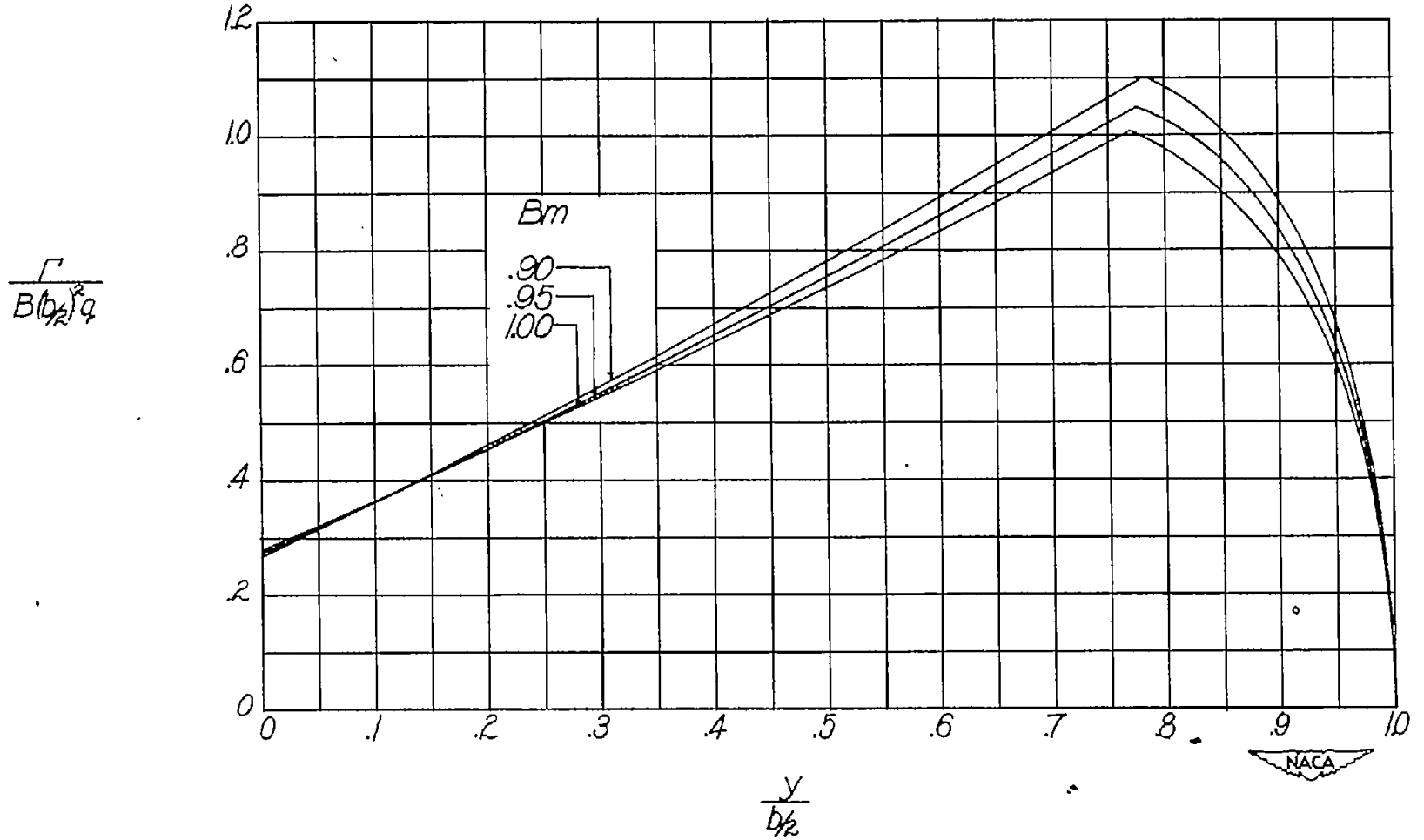

(c) AB = 4.

Figure 20.- Continued.

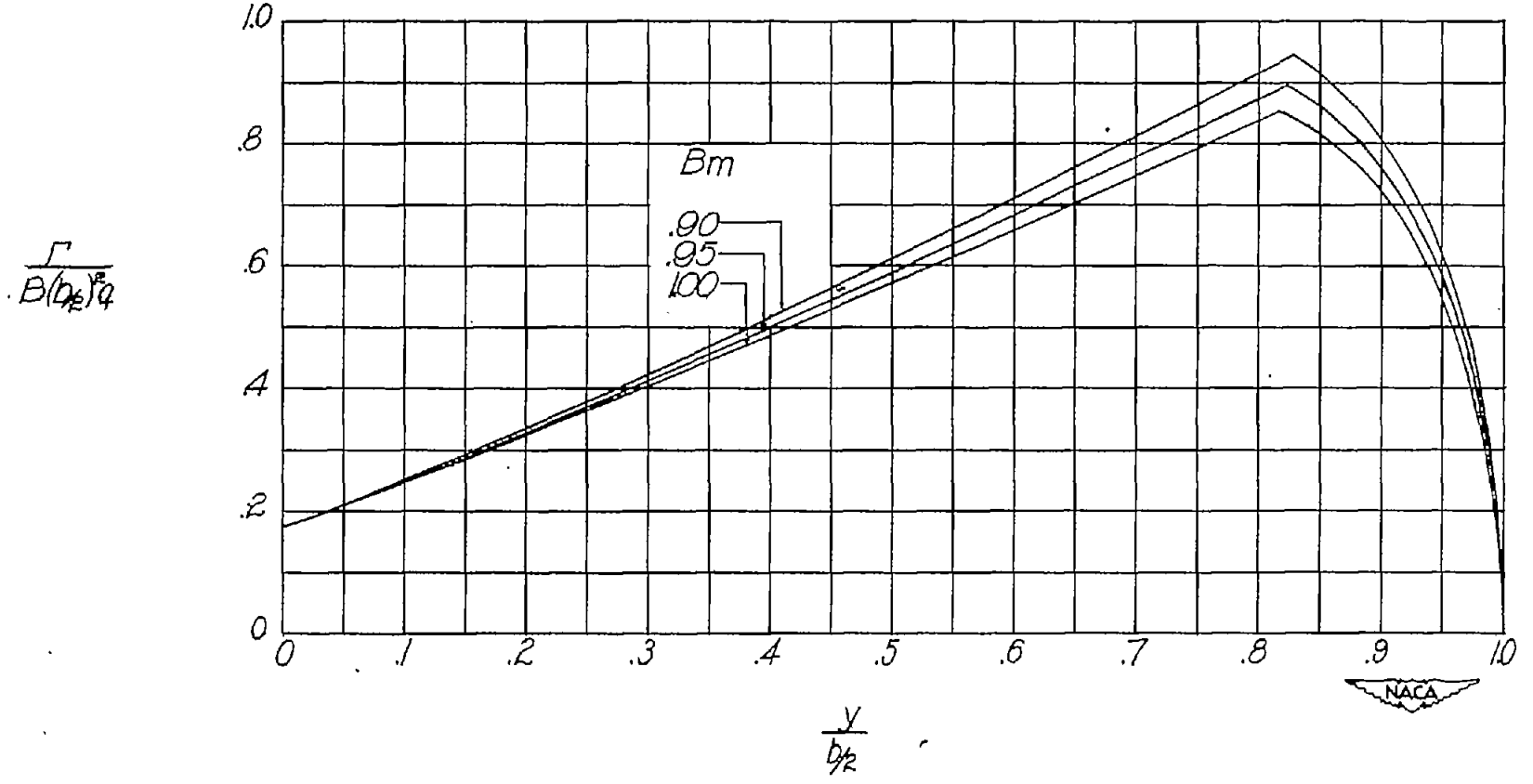

(d) AB = 5.

Figure 20.- Continued.

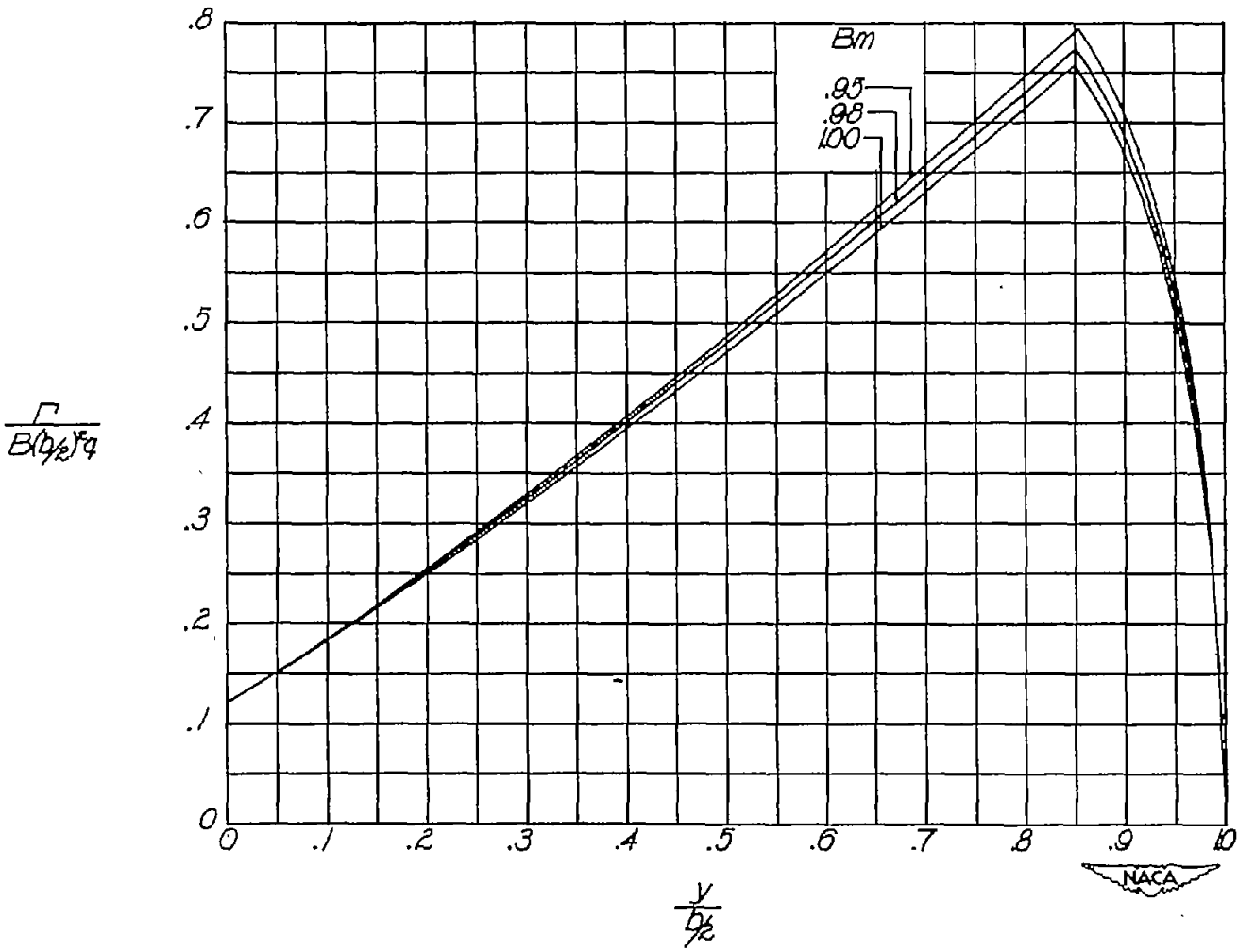

(e) AB = 6.

Figure 20.- Continued.

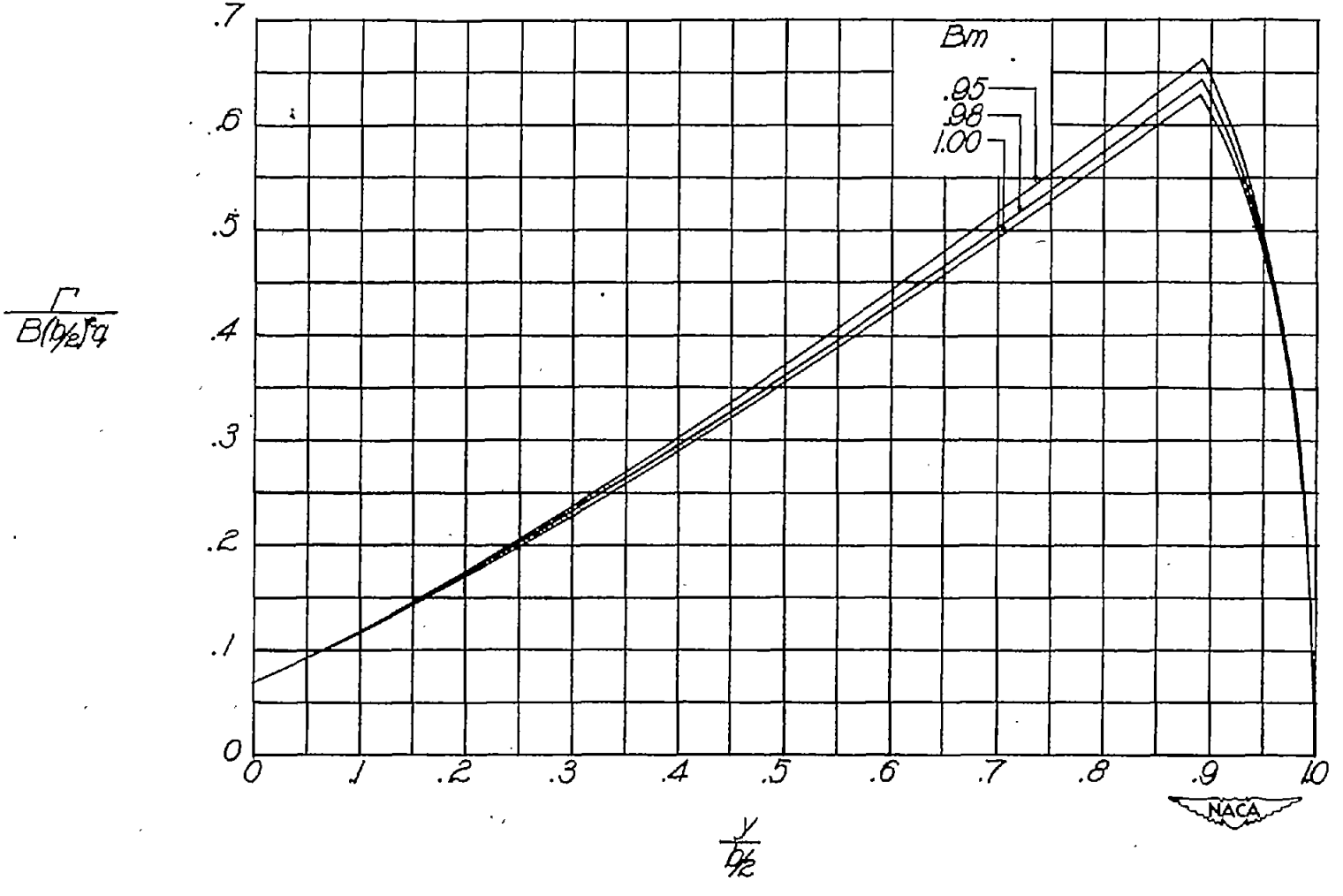

(f) AB = 8.

Figure 20.- Continued.

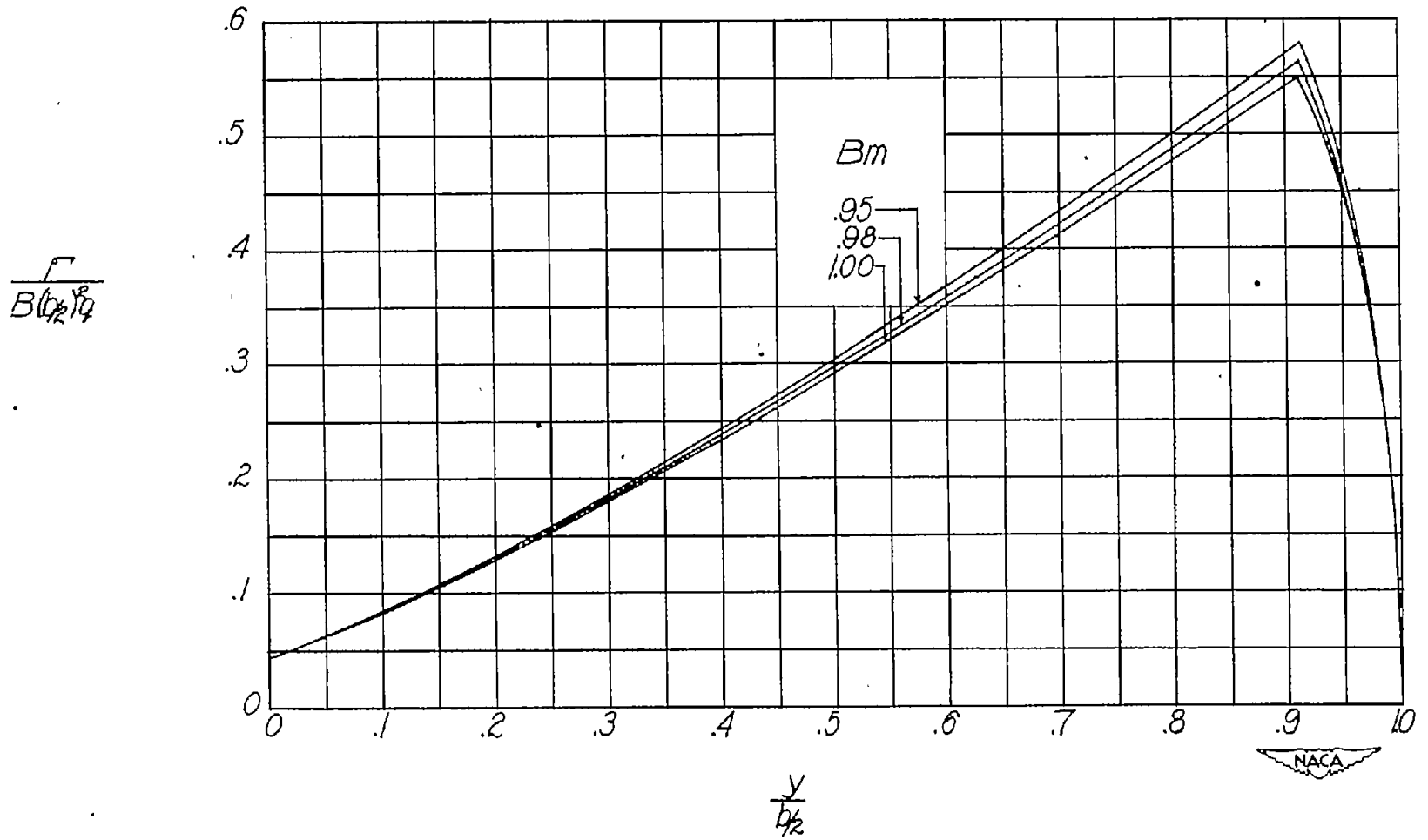

(g) AB = 10.

Figure 20.- Continued.

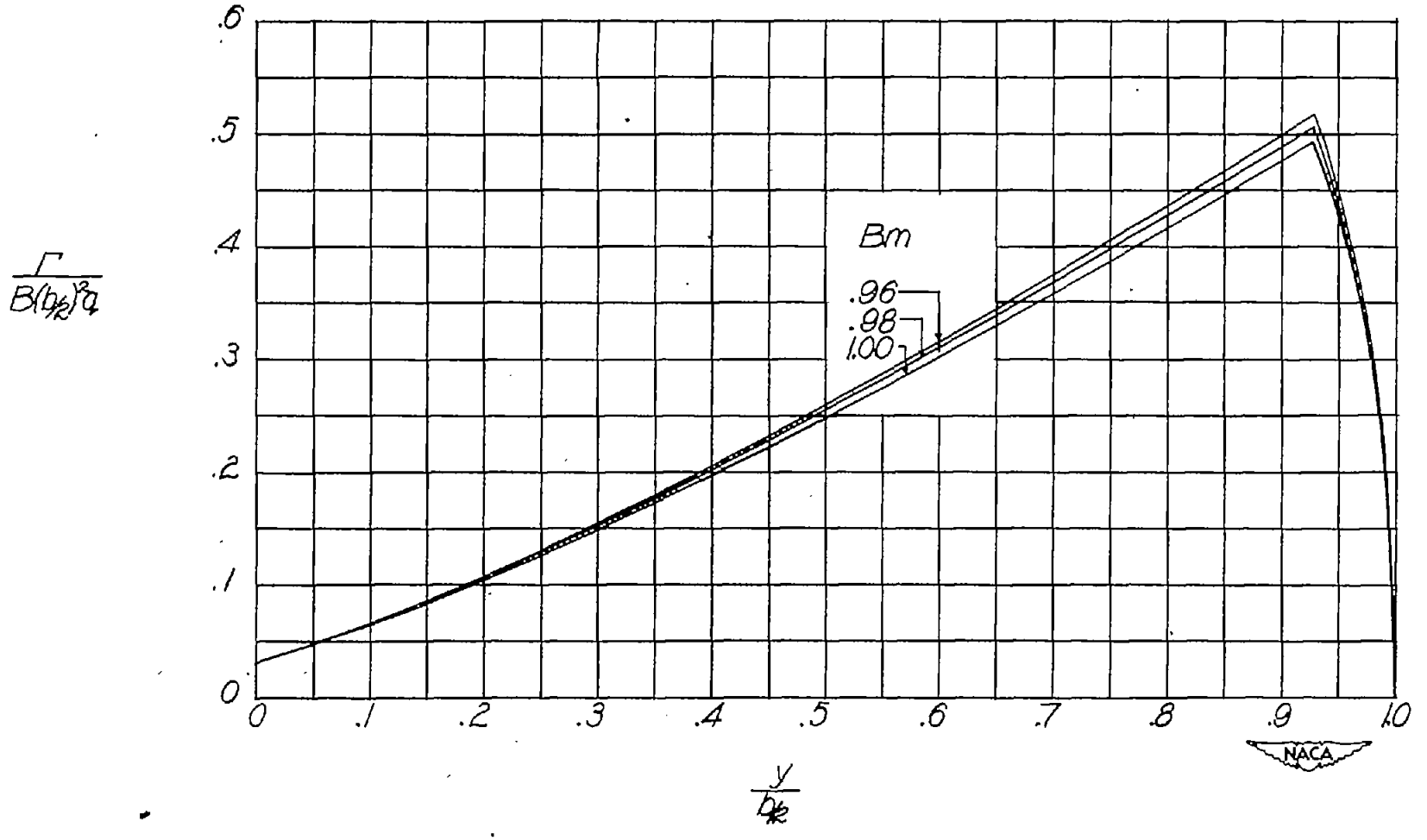

(h) AB = 12.

Figure 20.- Continued.

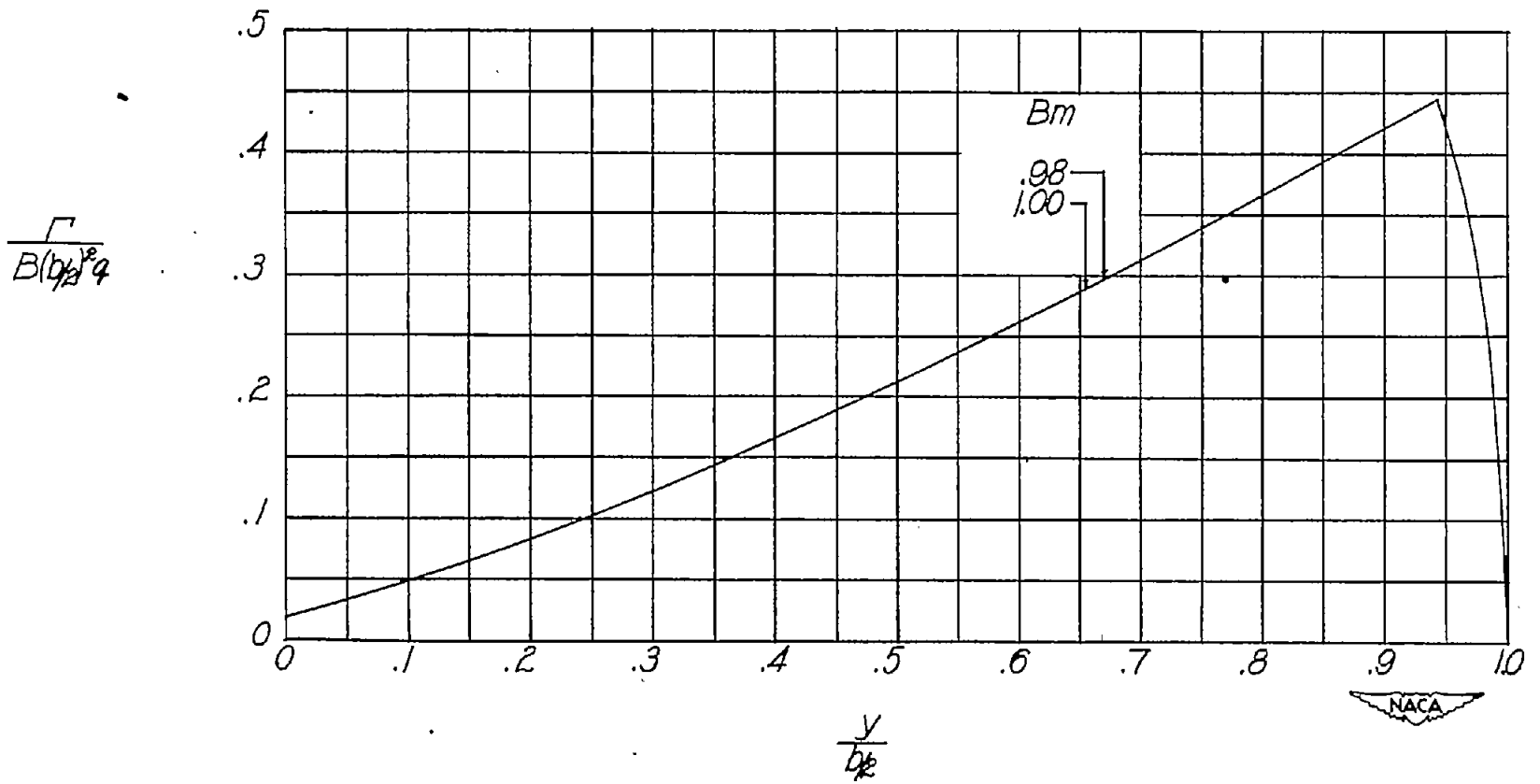

(i) AB = 15.

Figure 20.- Continued.

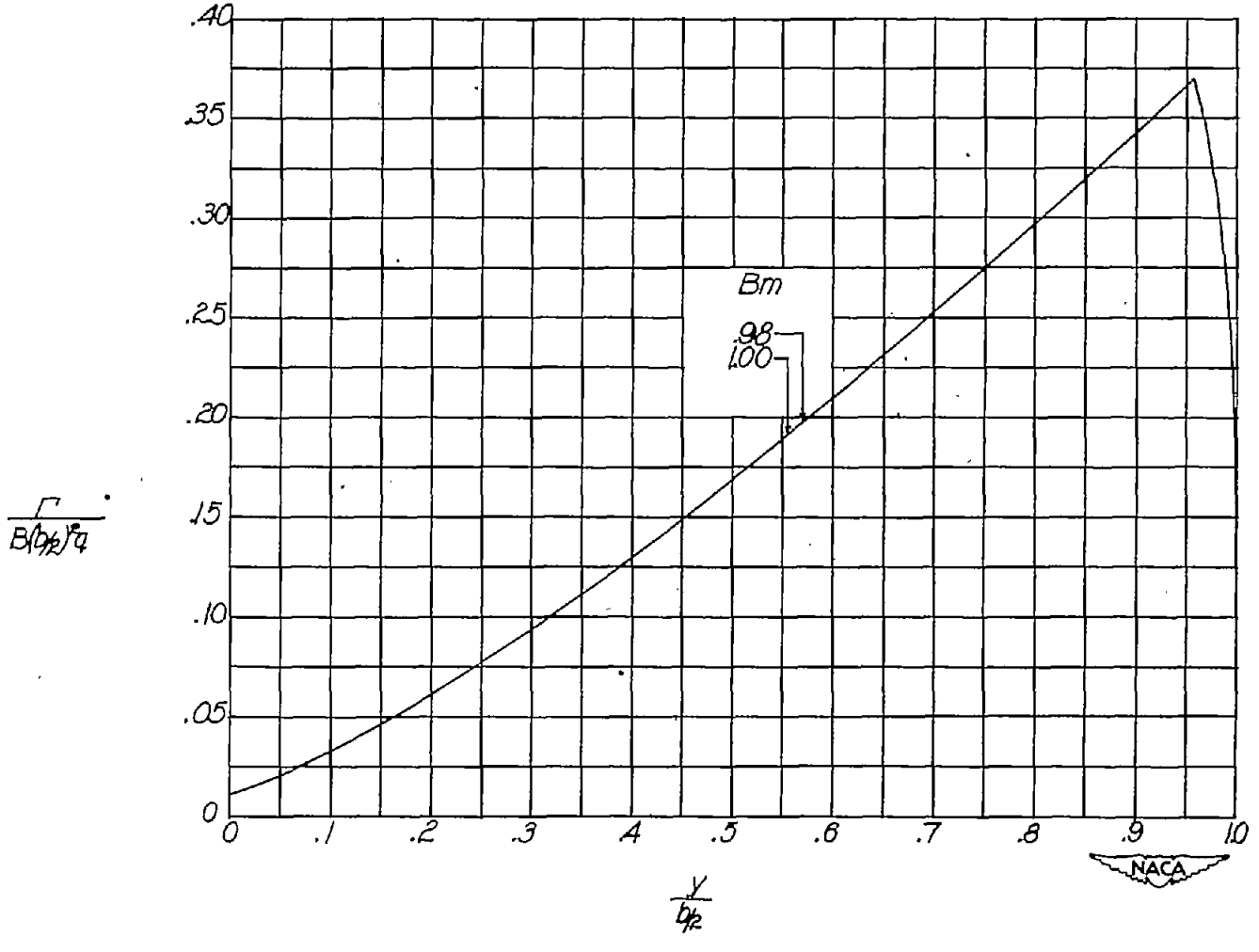

(j) AB = 20.

Figure 20.- Concluded.

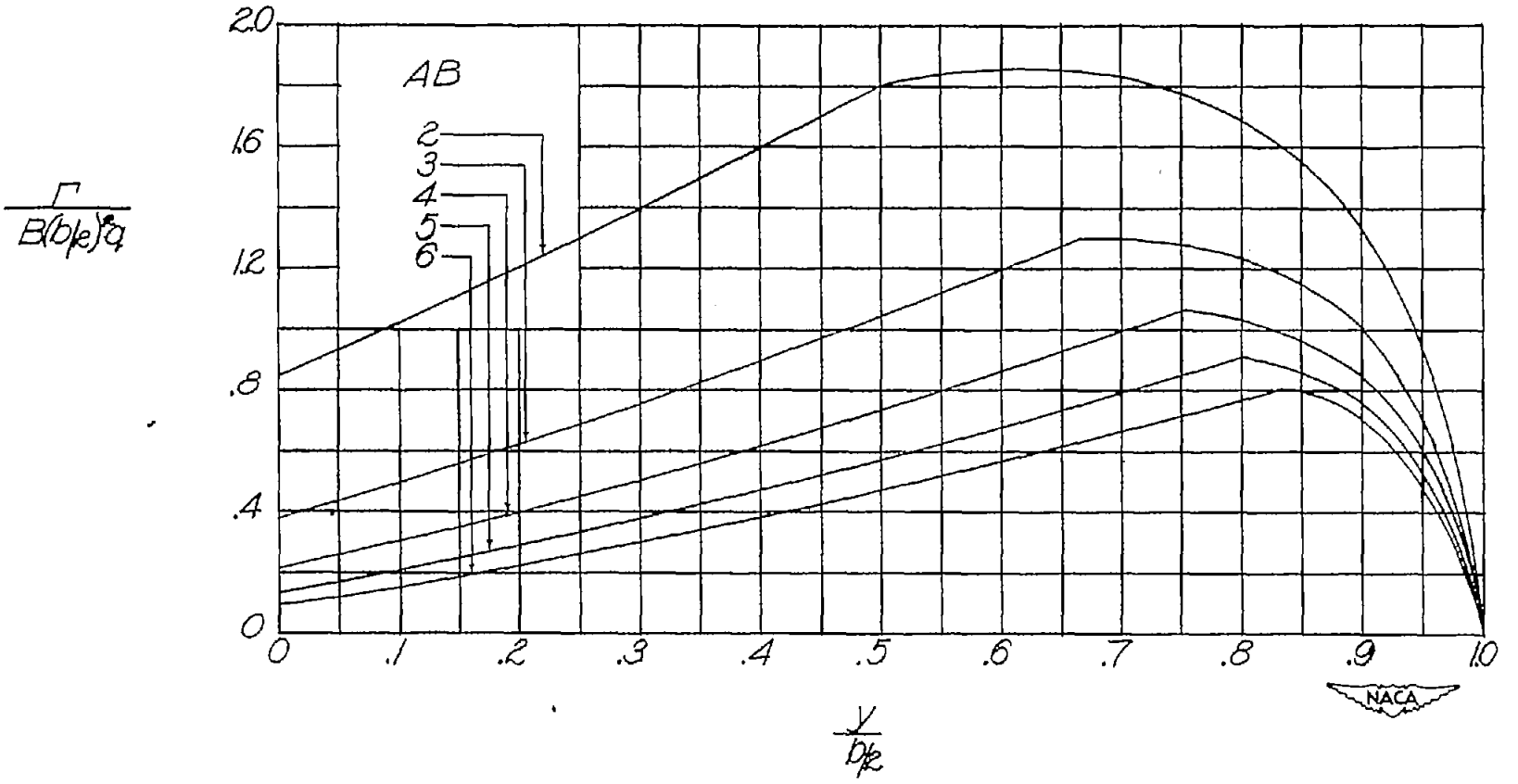

(a) AB = 2 to 6.

Figure 21.- Distribution of circulation along span for wings with steady pitching velocity with $\lambda = 1.00$. Bm = 1.00. Wing pitching about apex.

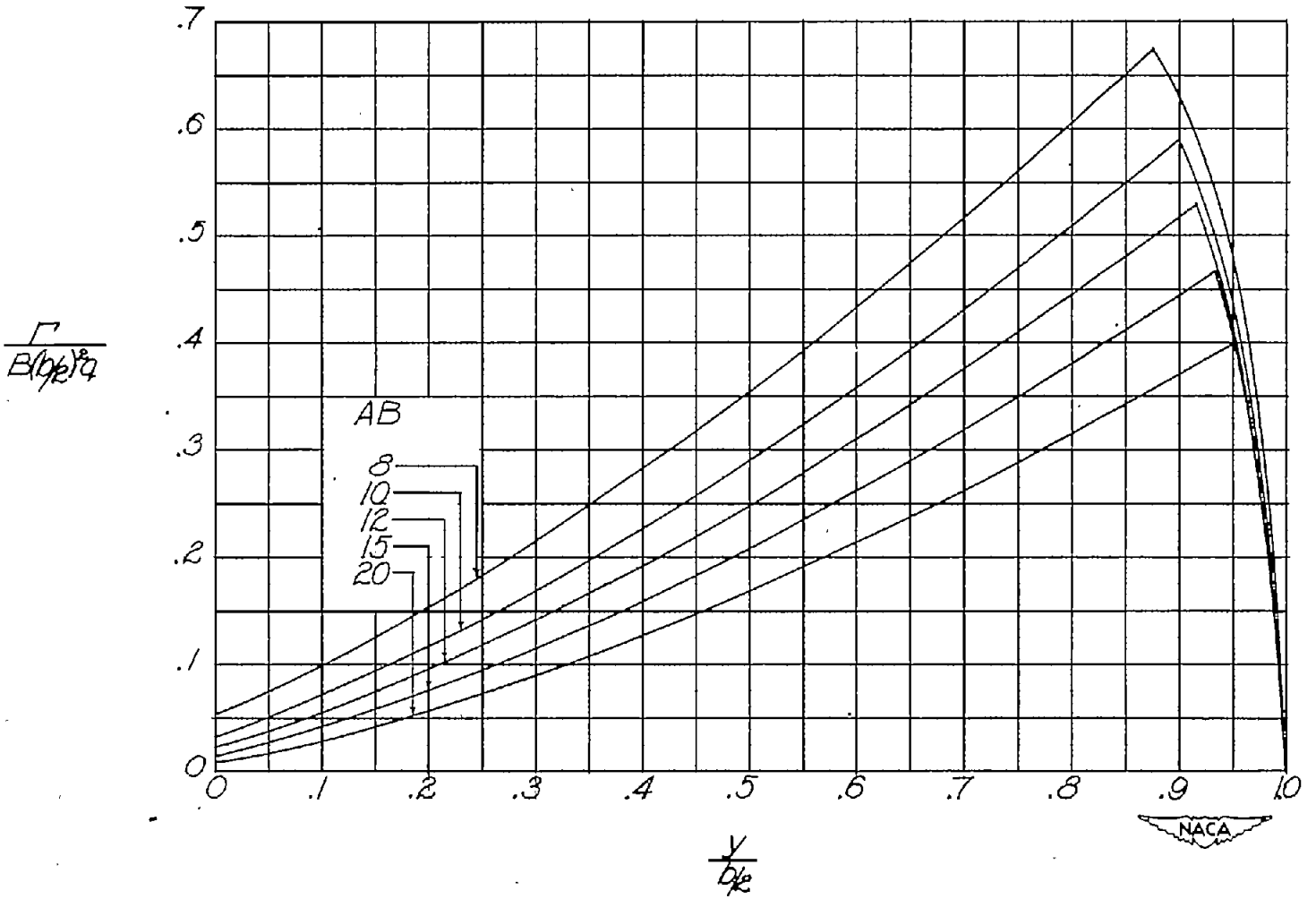

(b) AB = 8 to 20.

Figure 21.- Concluded.

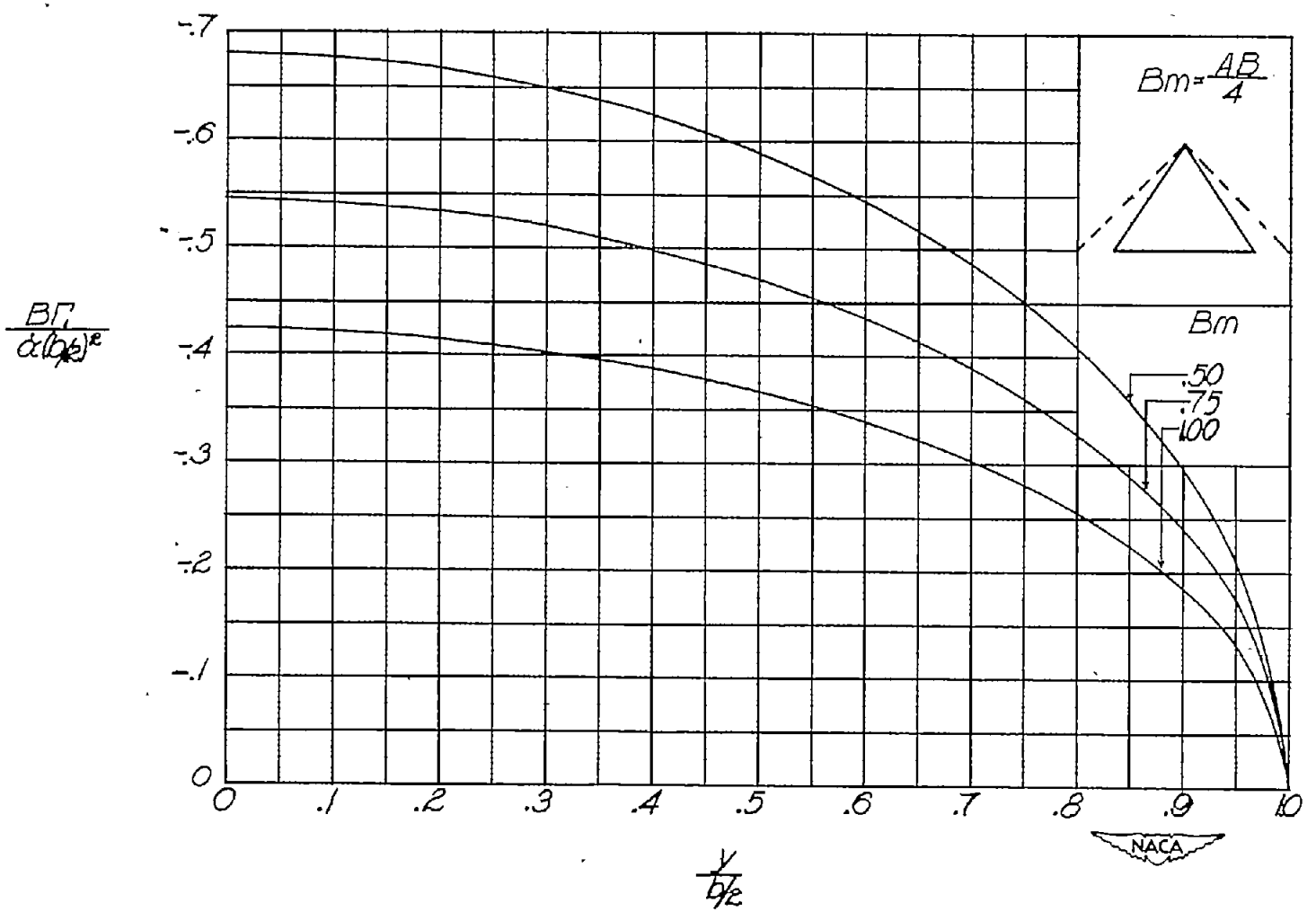

Figure 22.- Distribution of circulation along span for delta wings with constant vertical accleration. $\Gamma = \Gamma_1 + \Gamma_2$.

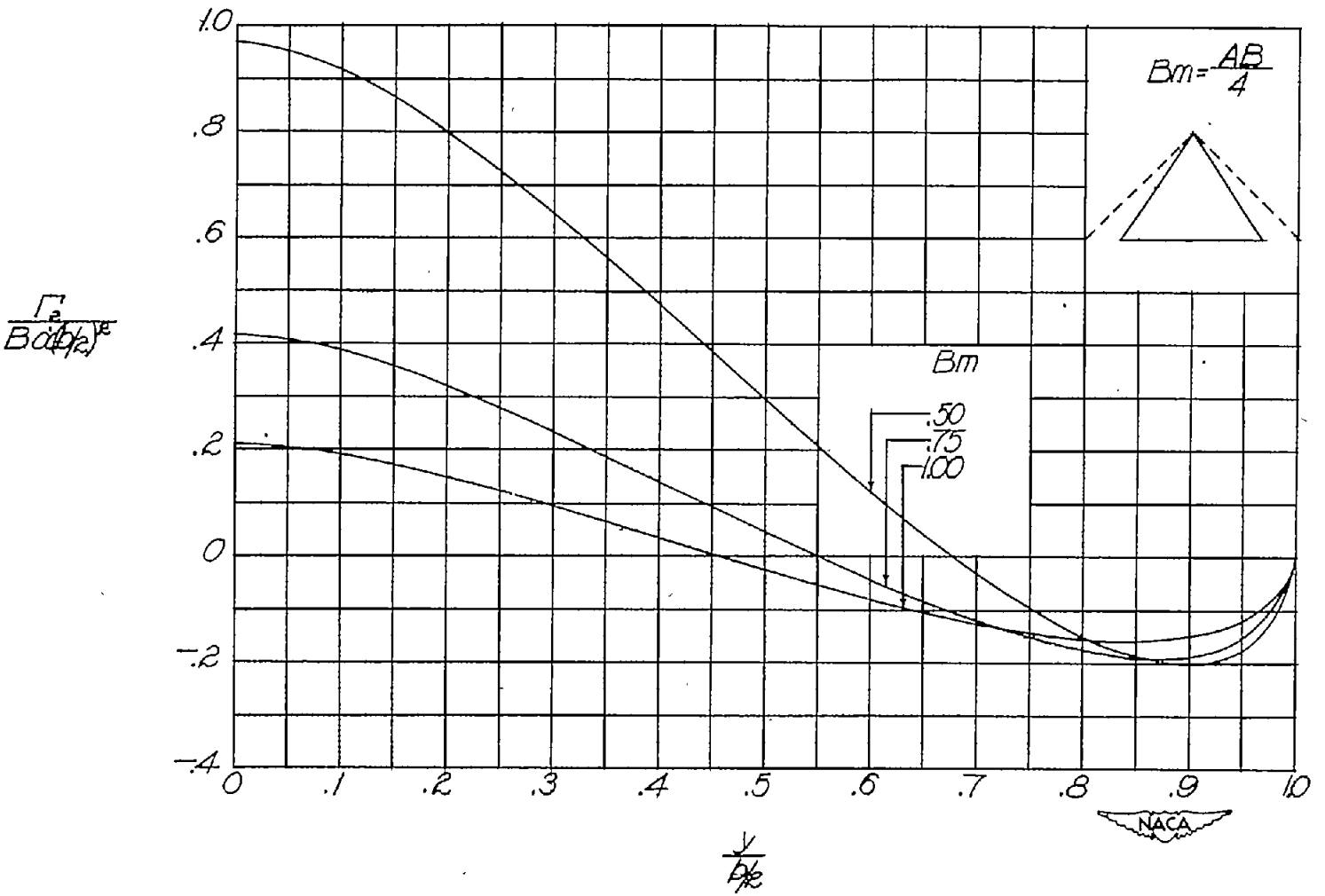

Figure 22.- Concluded.

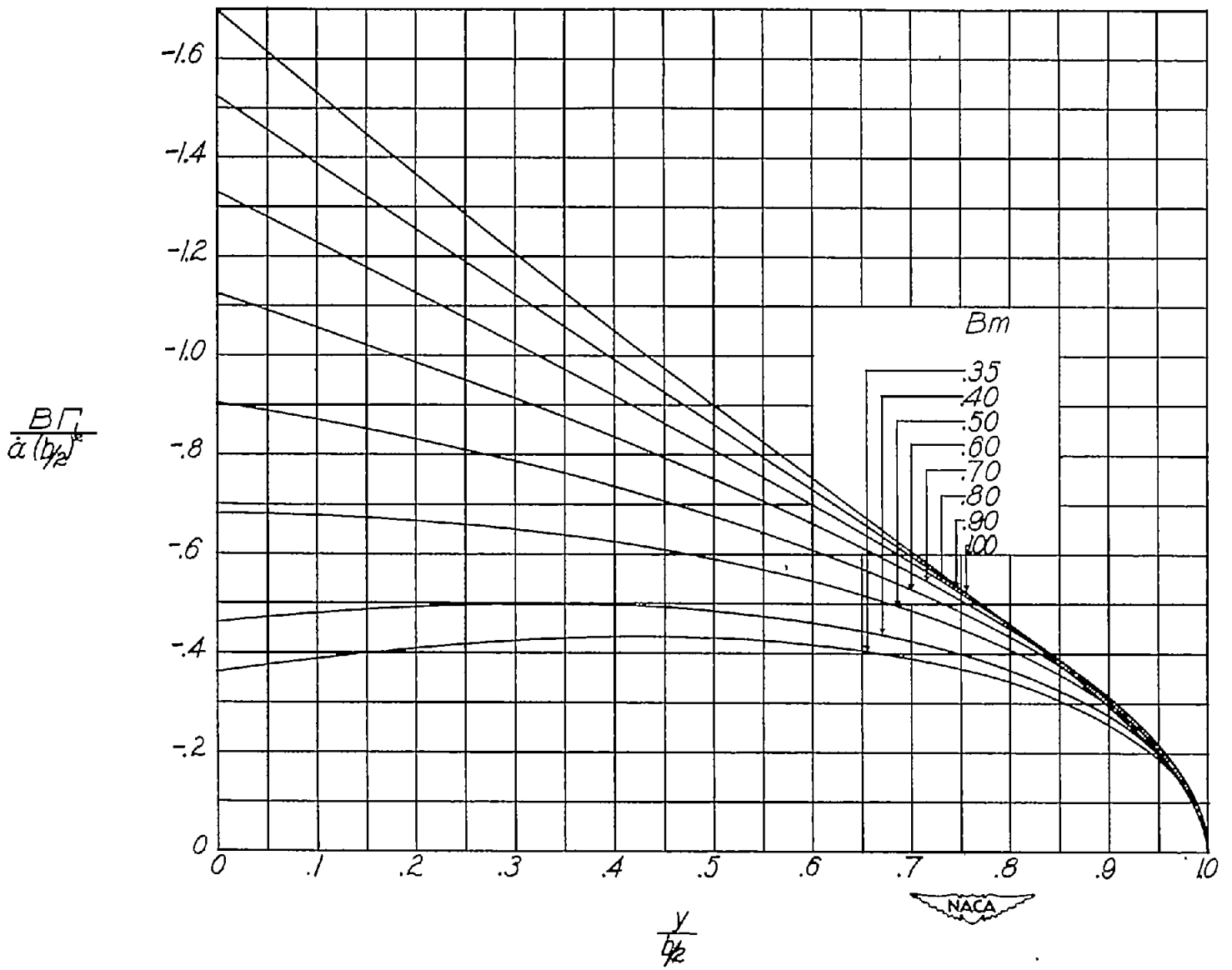

(a) AB = 2.

Figure 23.- Distribution of circulation along span for wings with constant vertical acceleration with $\lambda = 0$. $\Gamma = \Gamma_1 + \Gamma_2$.

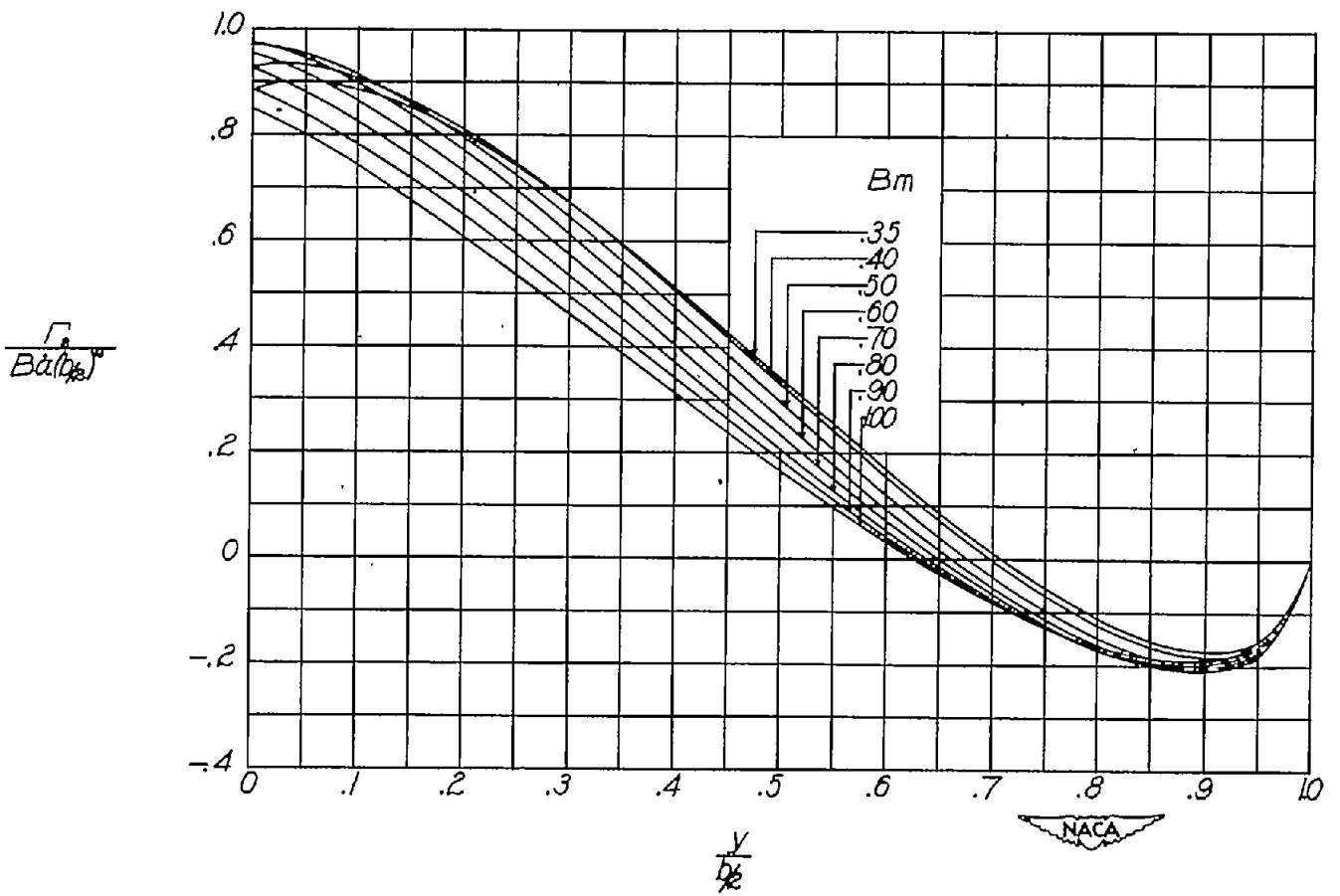

(a) AB = 2. Concluded.

Figure 23.- Continued.

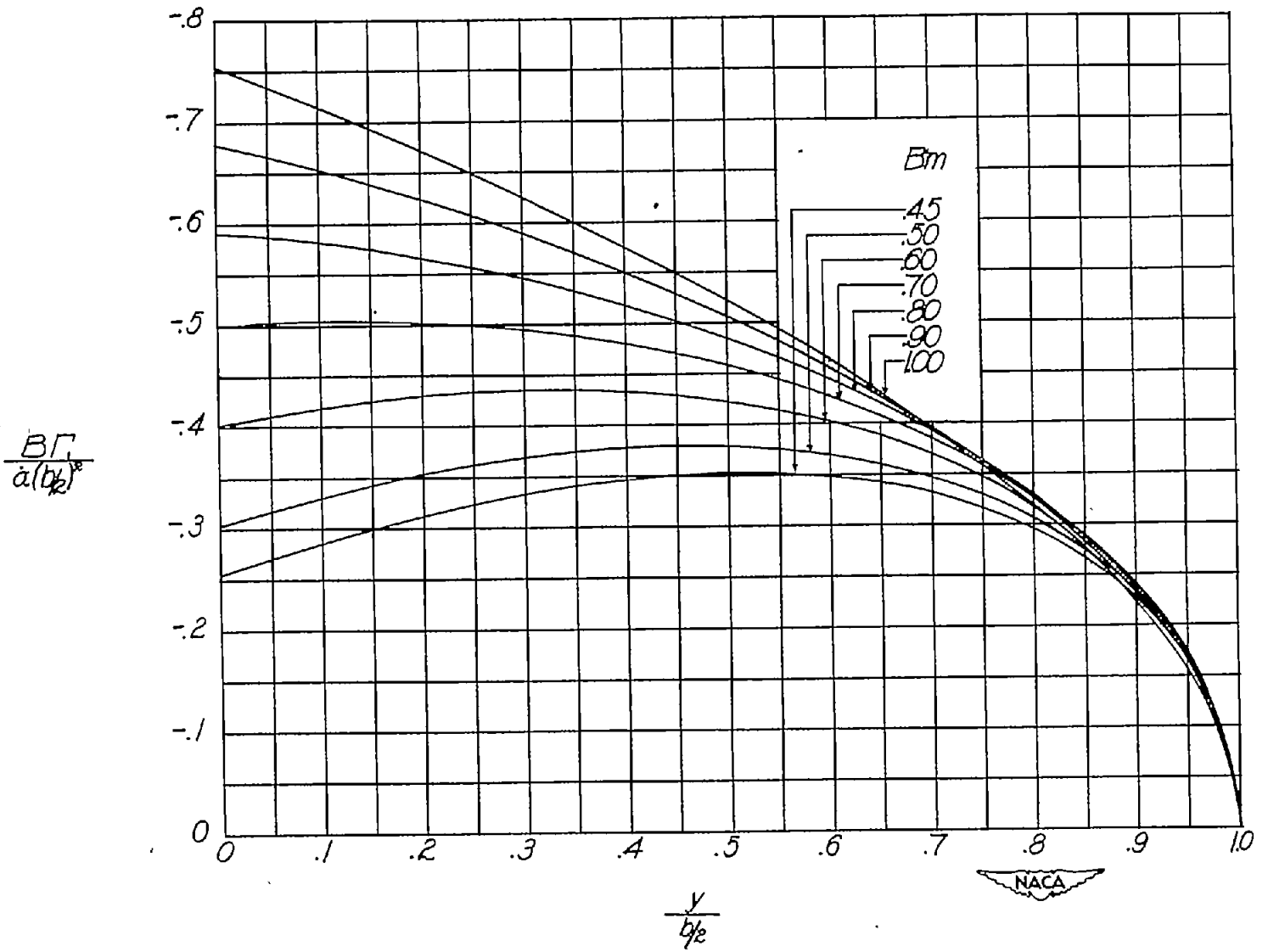

(b) AB = 3.

Figure 23.- Continued.

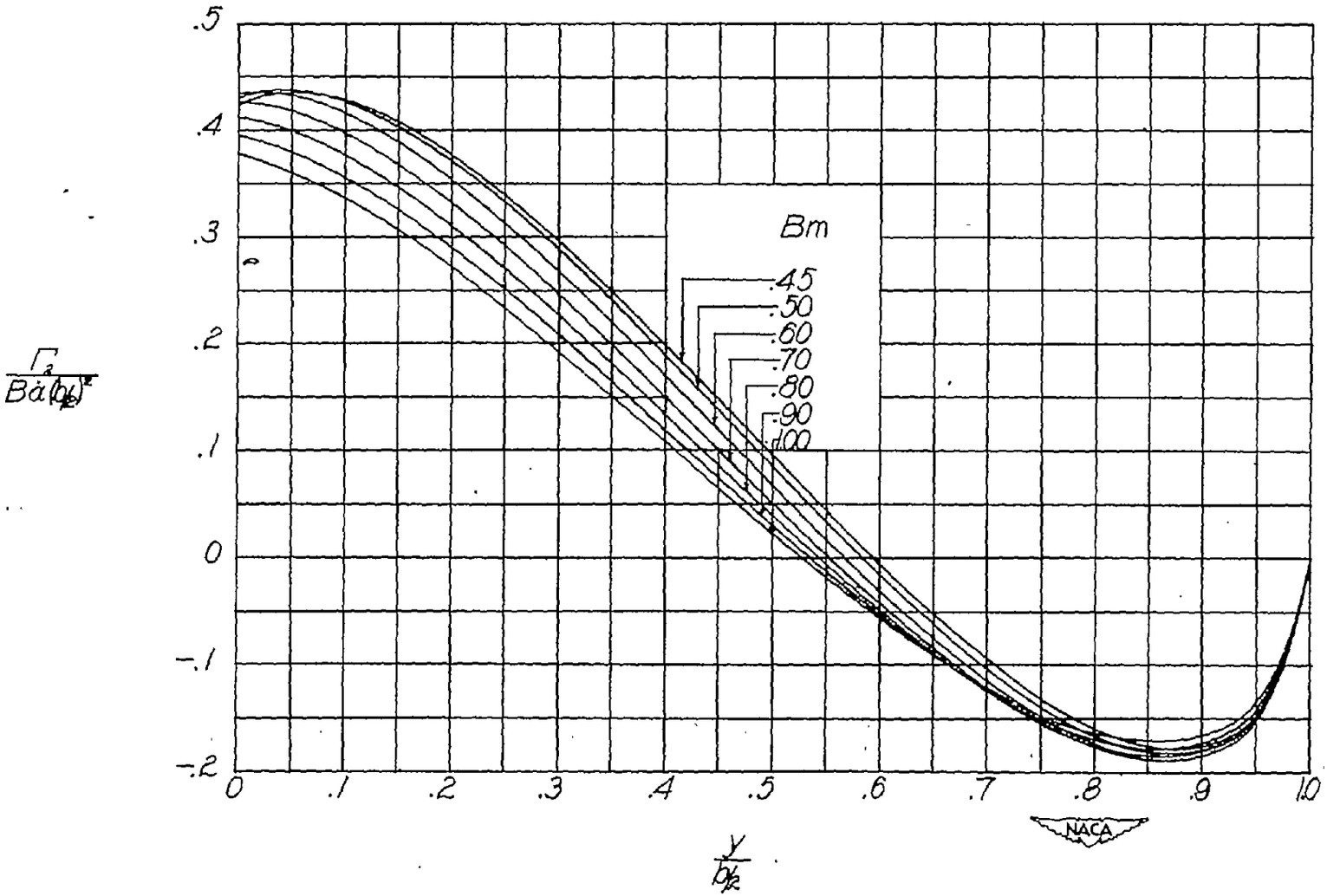

(b) AB = 3. Concluded.

Figure 23.- Continued.

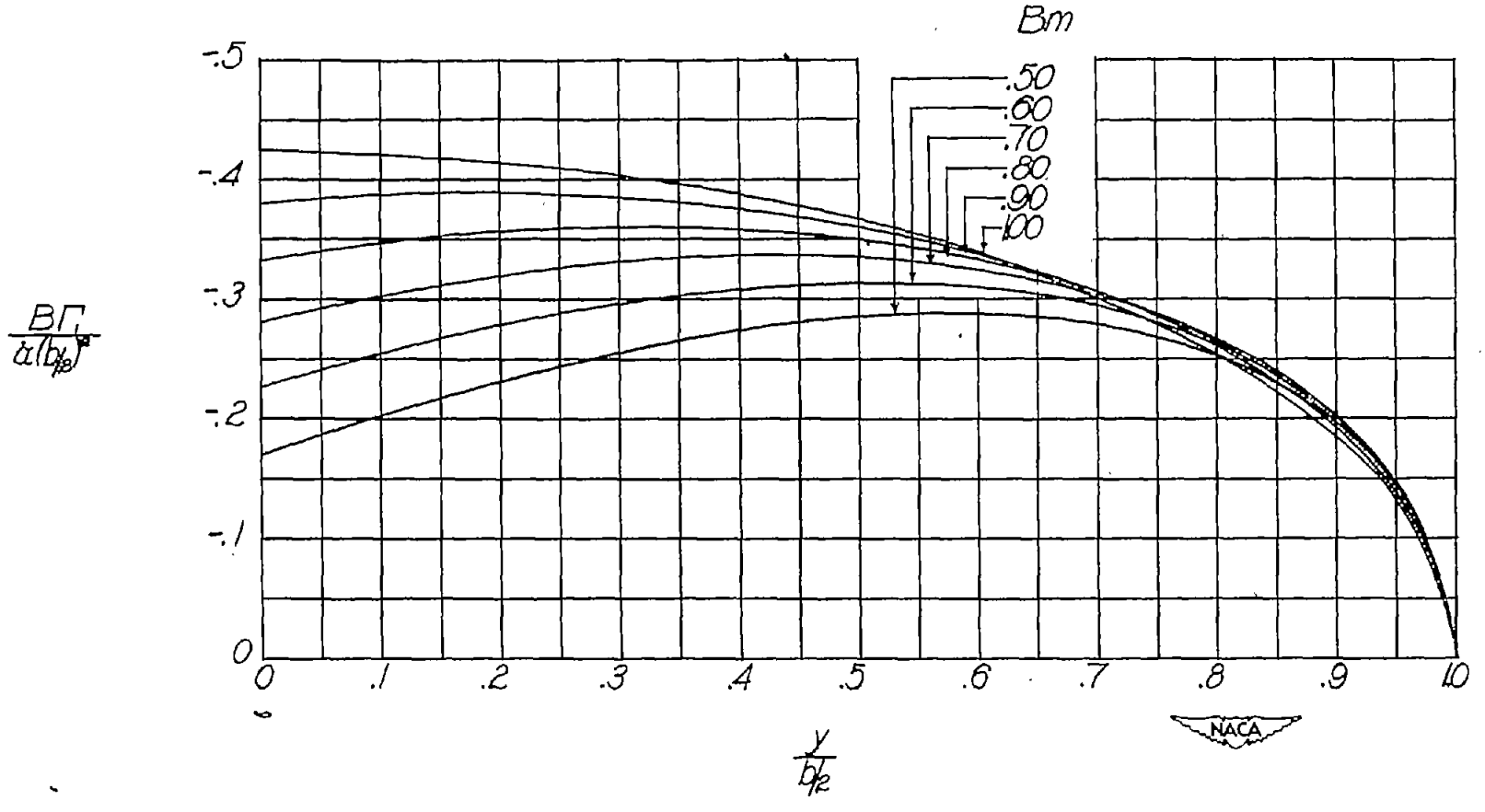

(c) AB = 4.

Figure 23.- Continued.

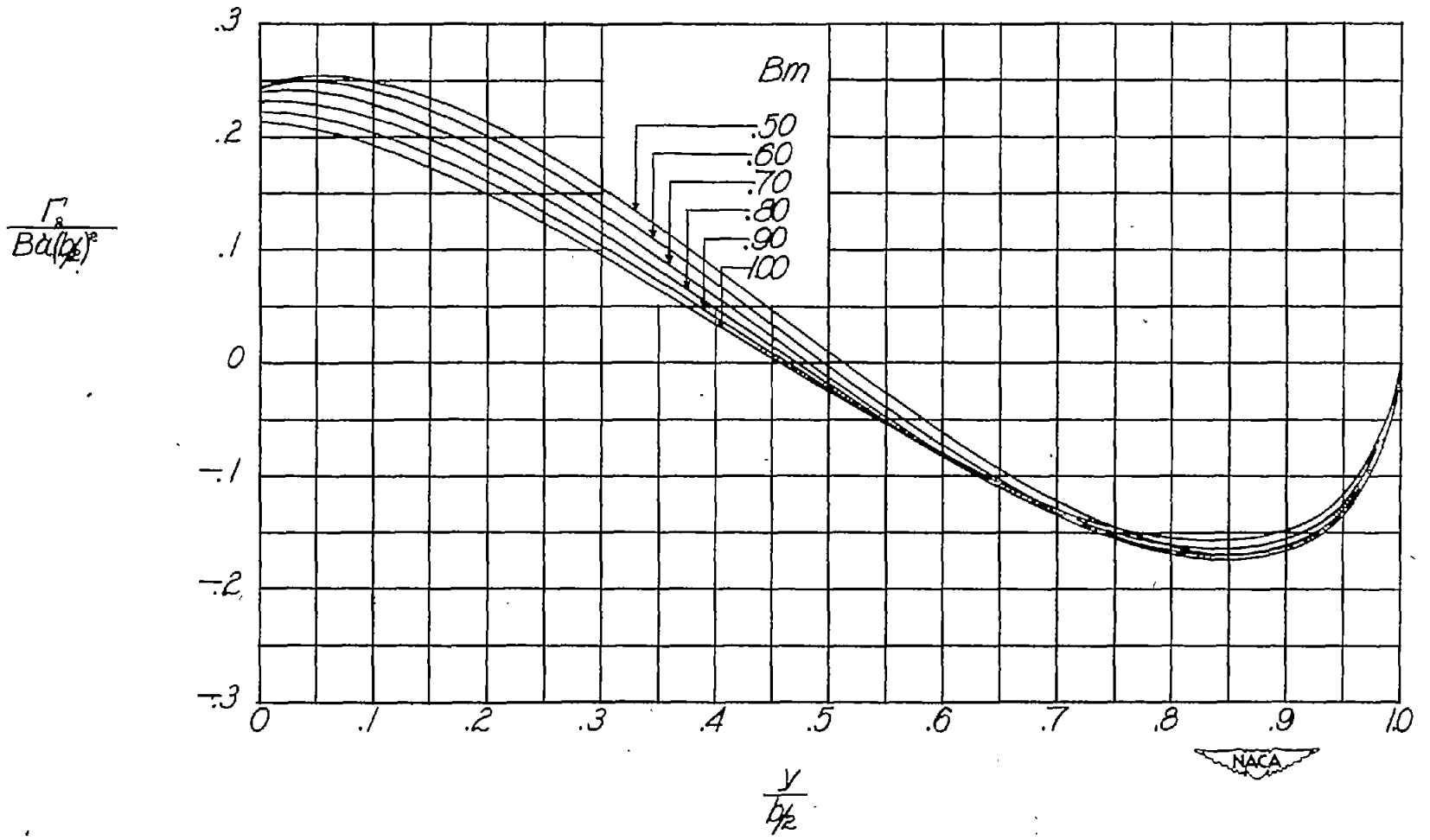

(c) AB = 4. Concluded.

Figure 23.- Continued.

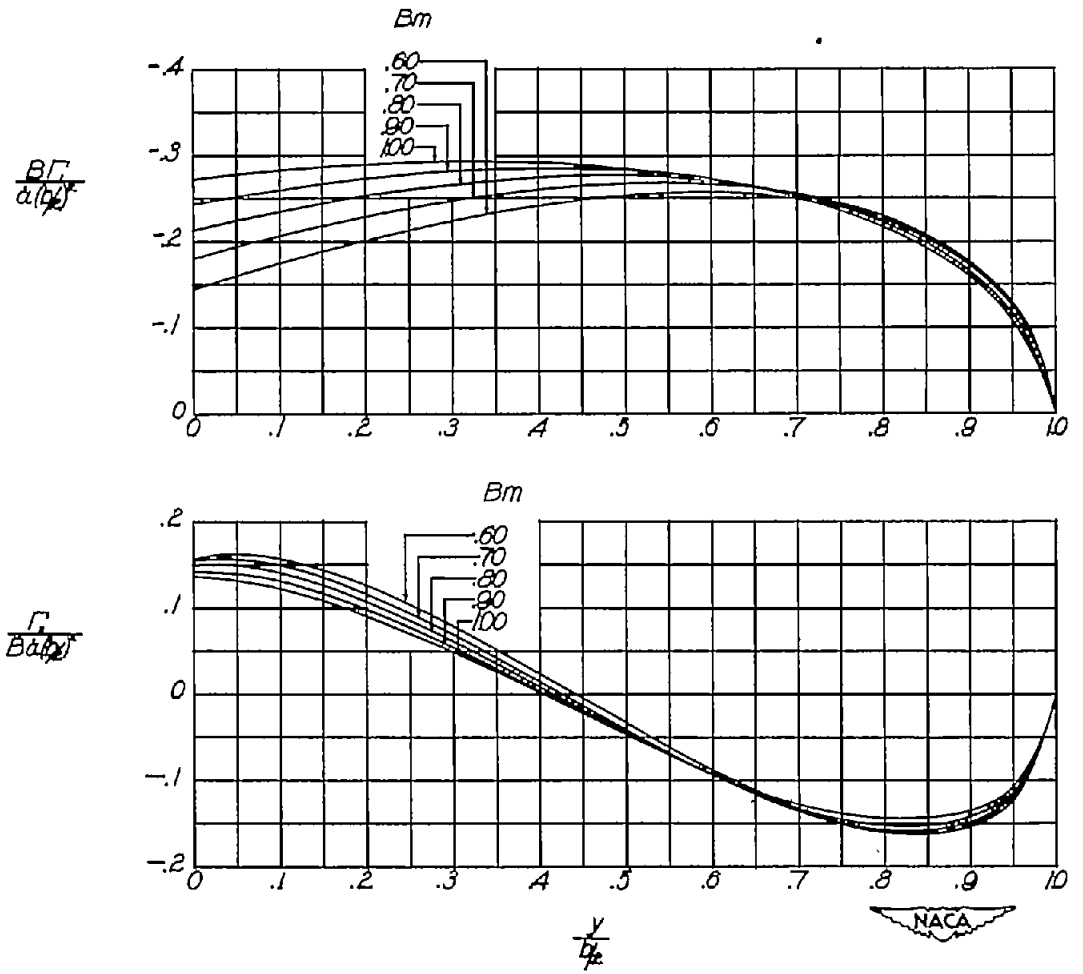

(d) AB = 5.

Figure 23.- Continued.

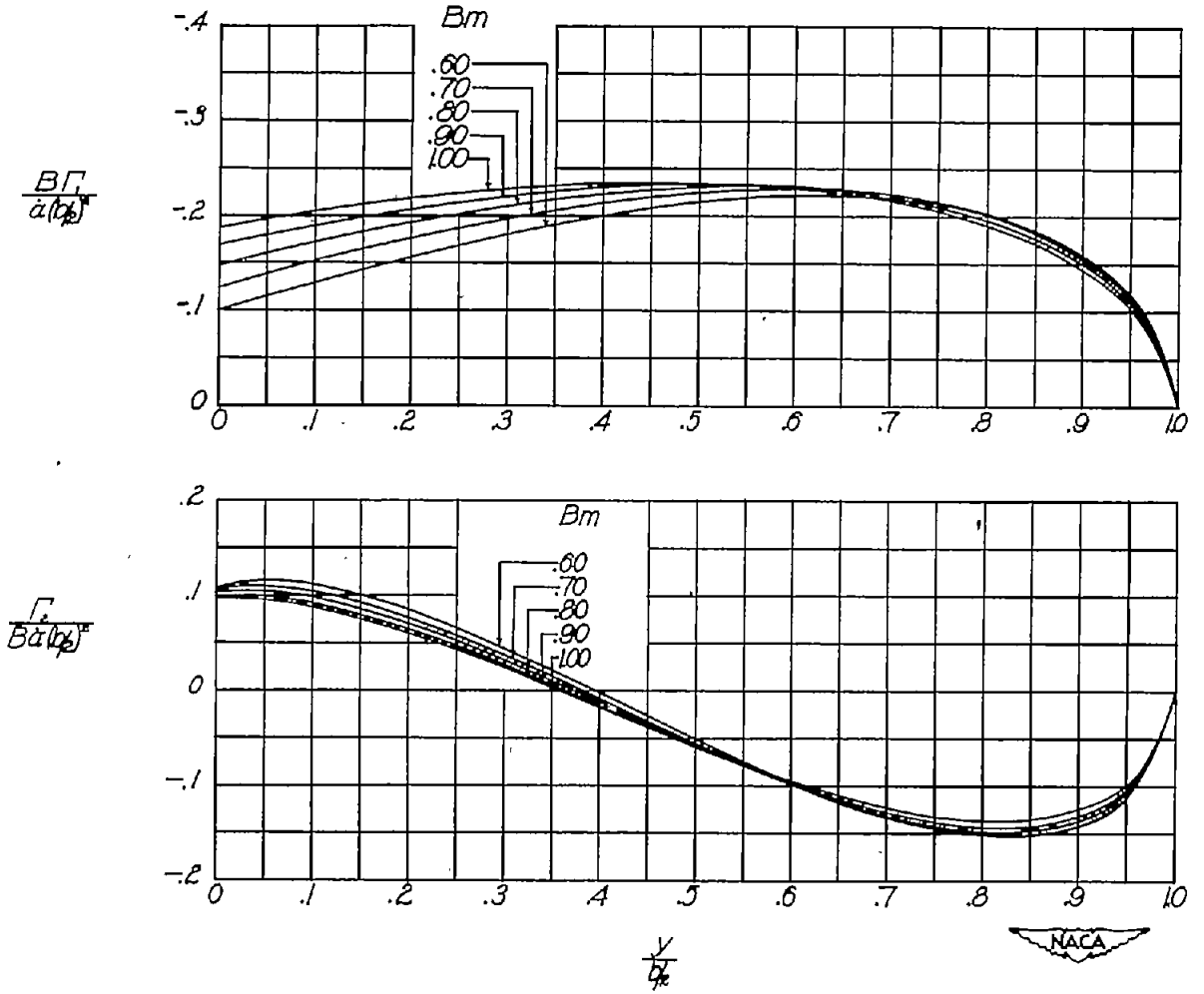

(e) AB = 6.

Figure 23.- Continued.

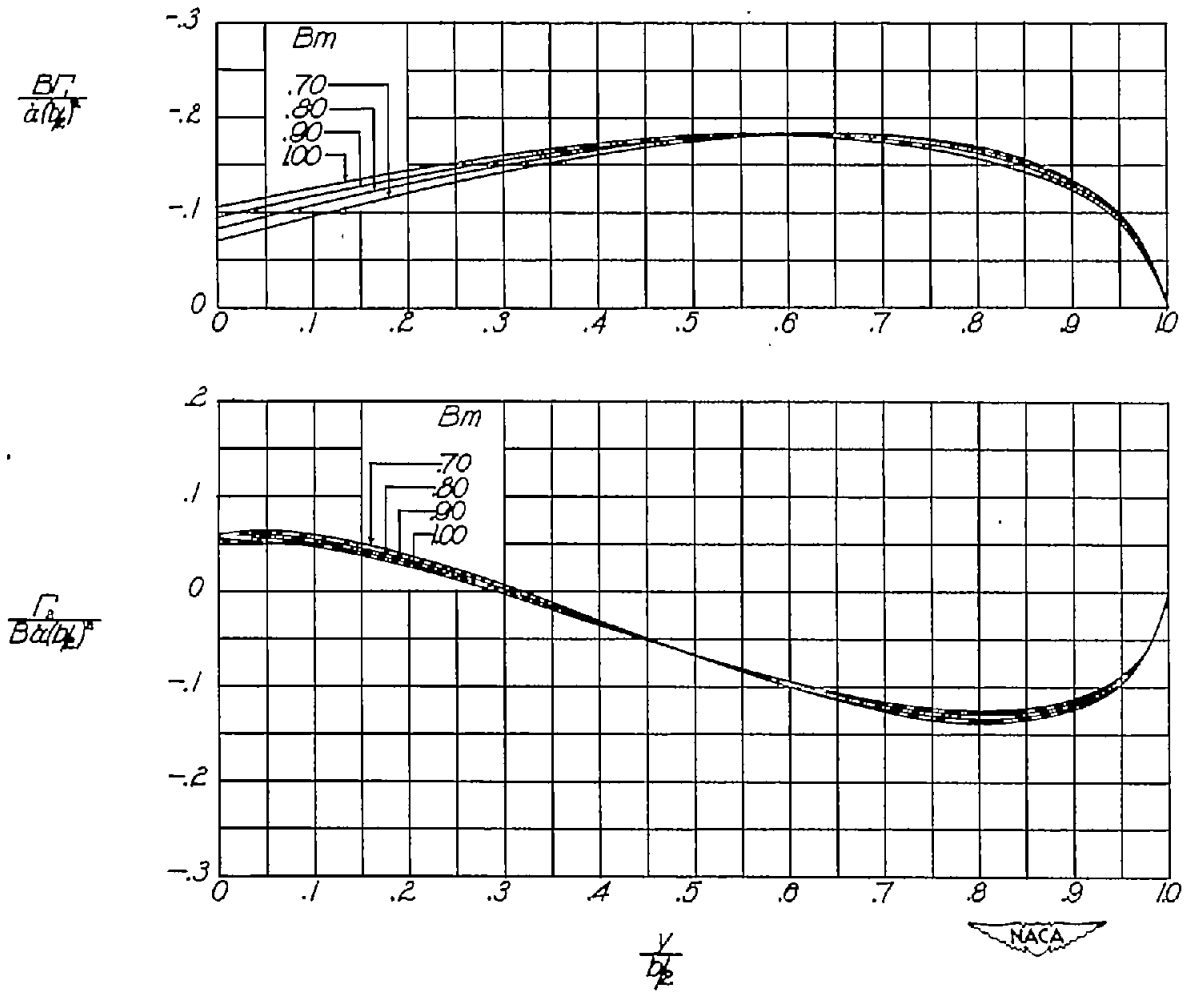

(f) AB = 8.

Figure 23.- Continued.

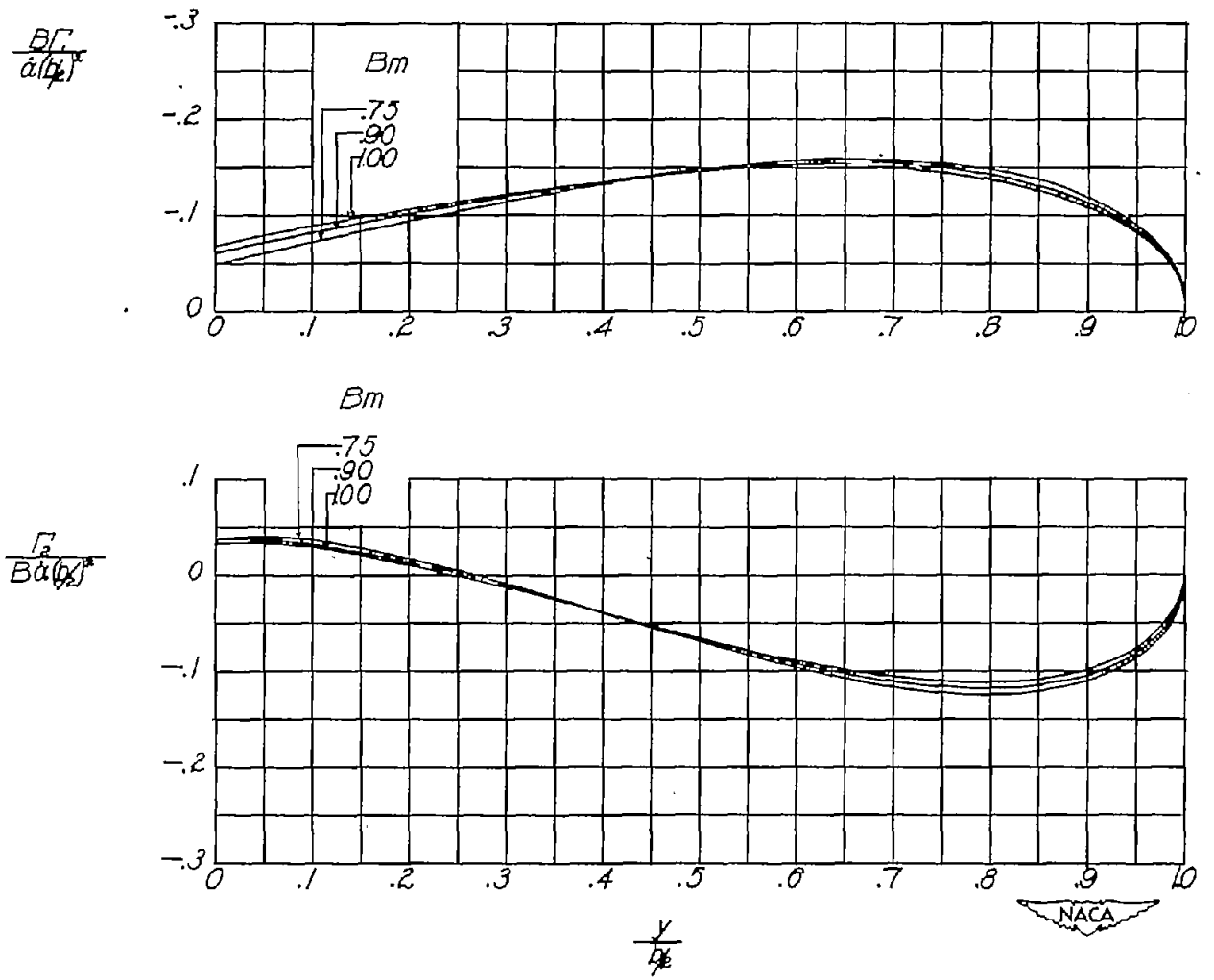

(g) AB = 10.

Figure 23.- Continued.

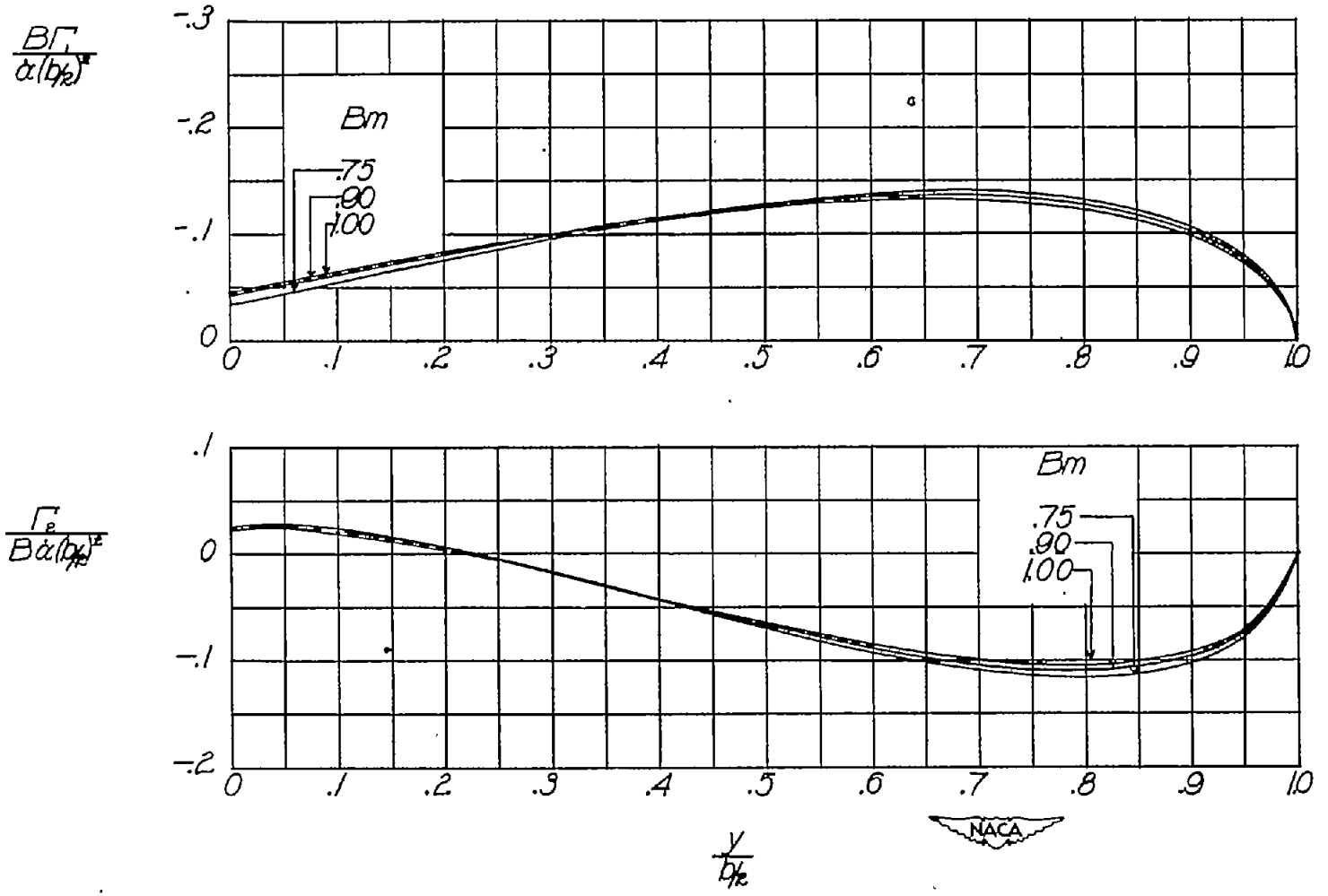

(h) AB = 12.

Figure 23.- Continued.

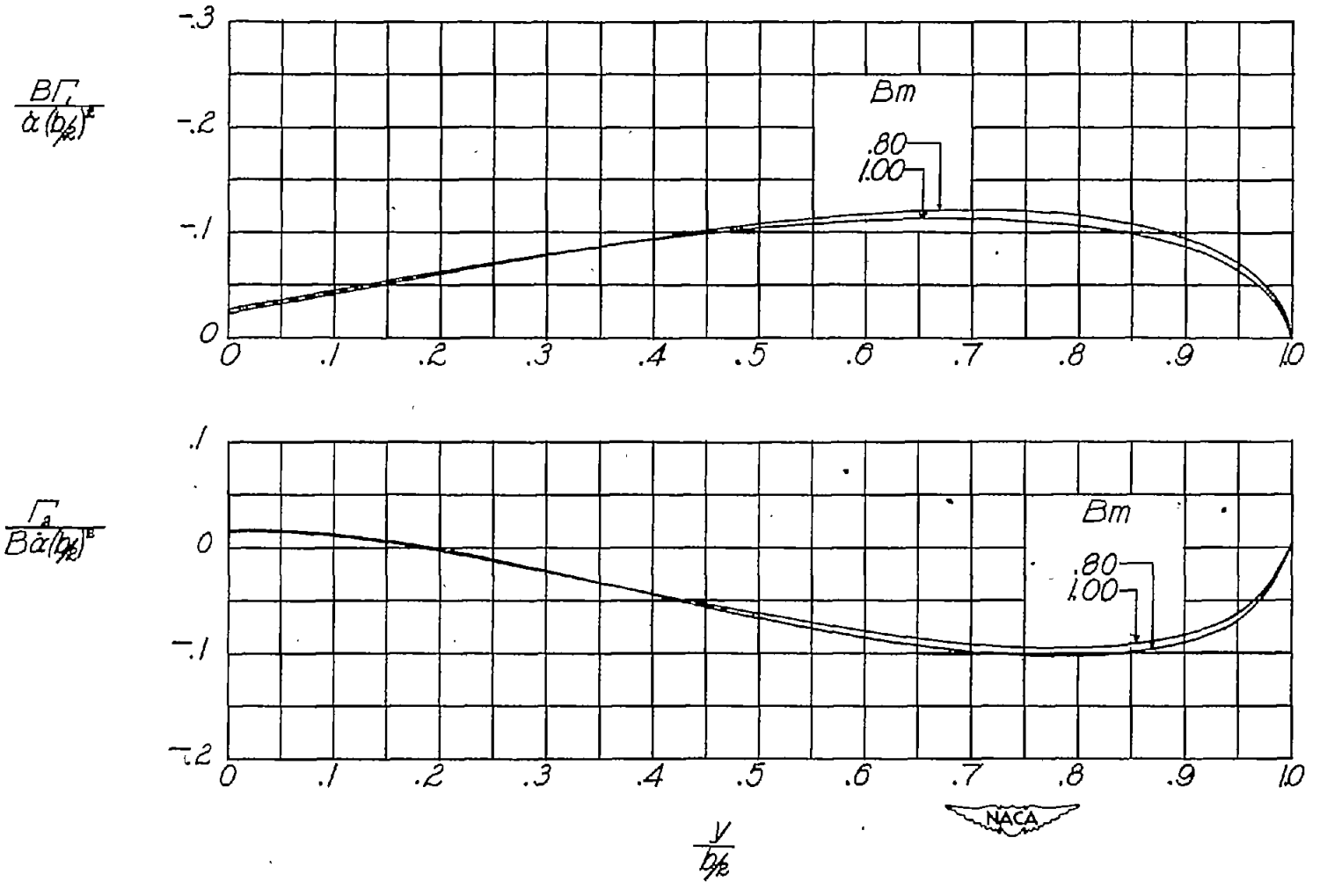

(i) AB = 15.

Figure 23.- Continued.

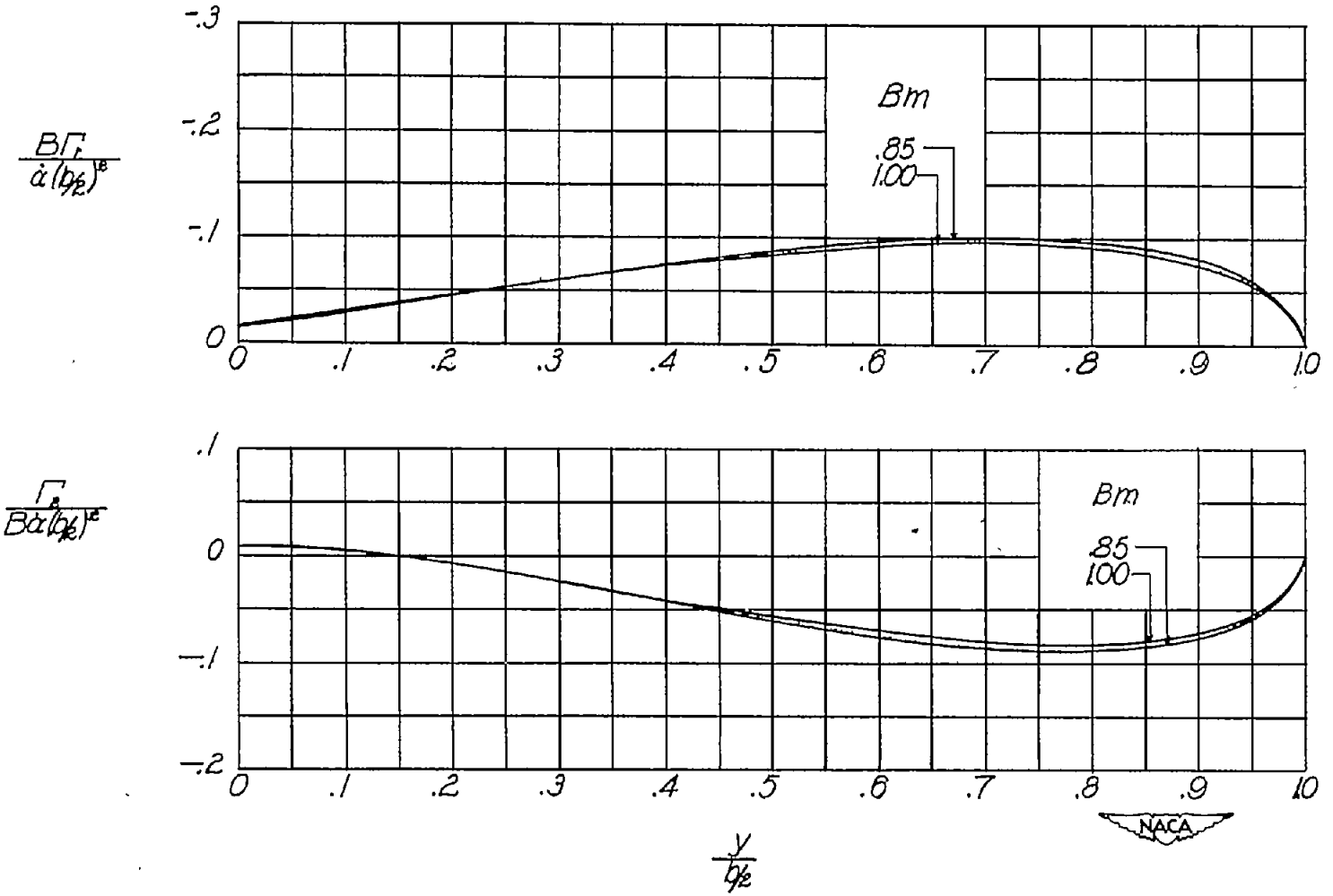

(j) AB = 20.

Figure 23.- Concluded.

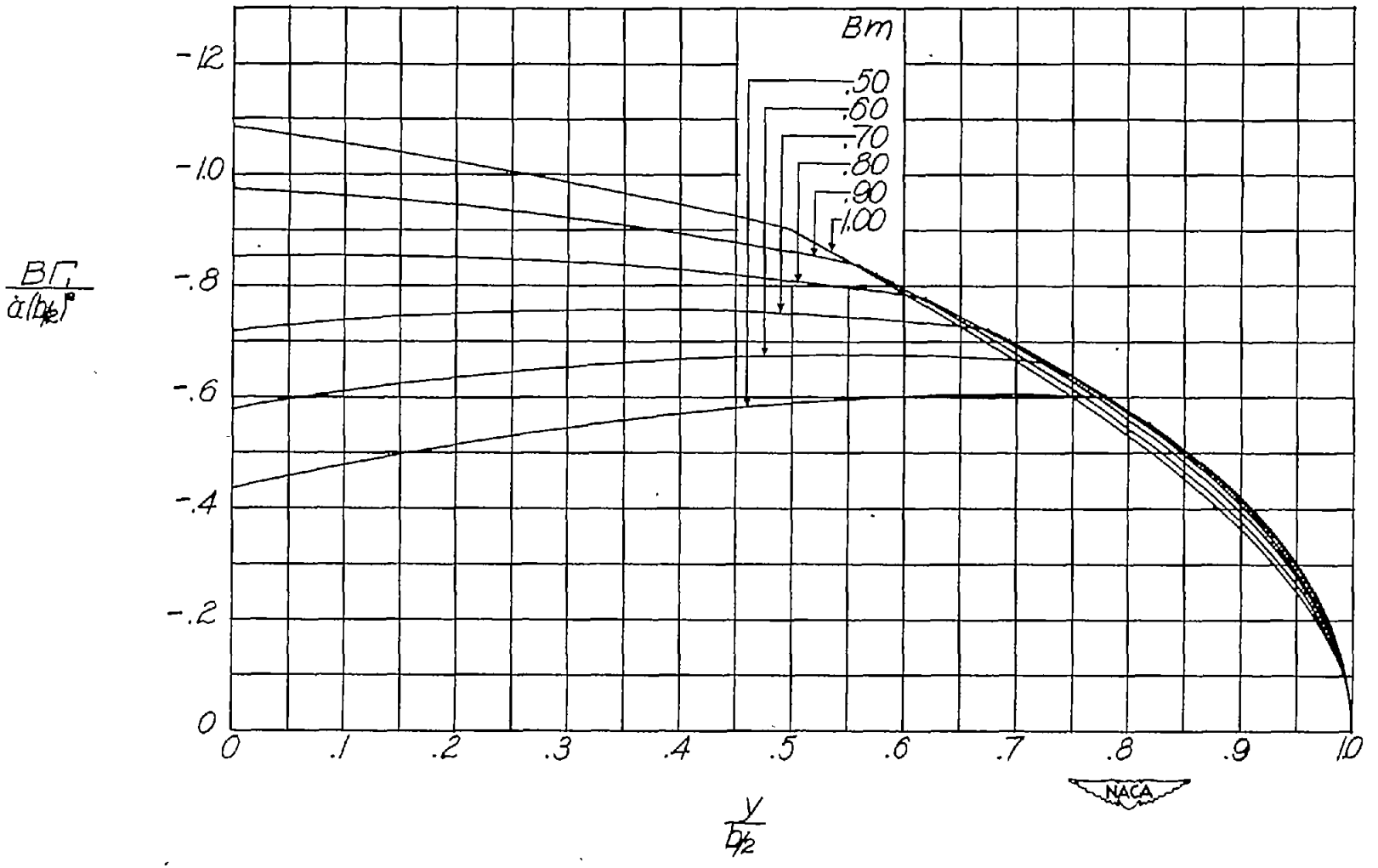

(a) AB = 2.

Figure 24.- Distribution of circulation along span for wings with constant vertical acceleration with $\lambda = 0.25$. $\Gamma = \Gamma_1 + \Gamma_2$.

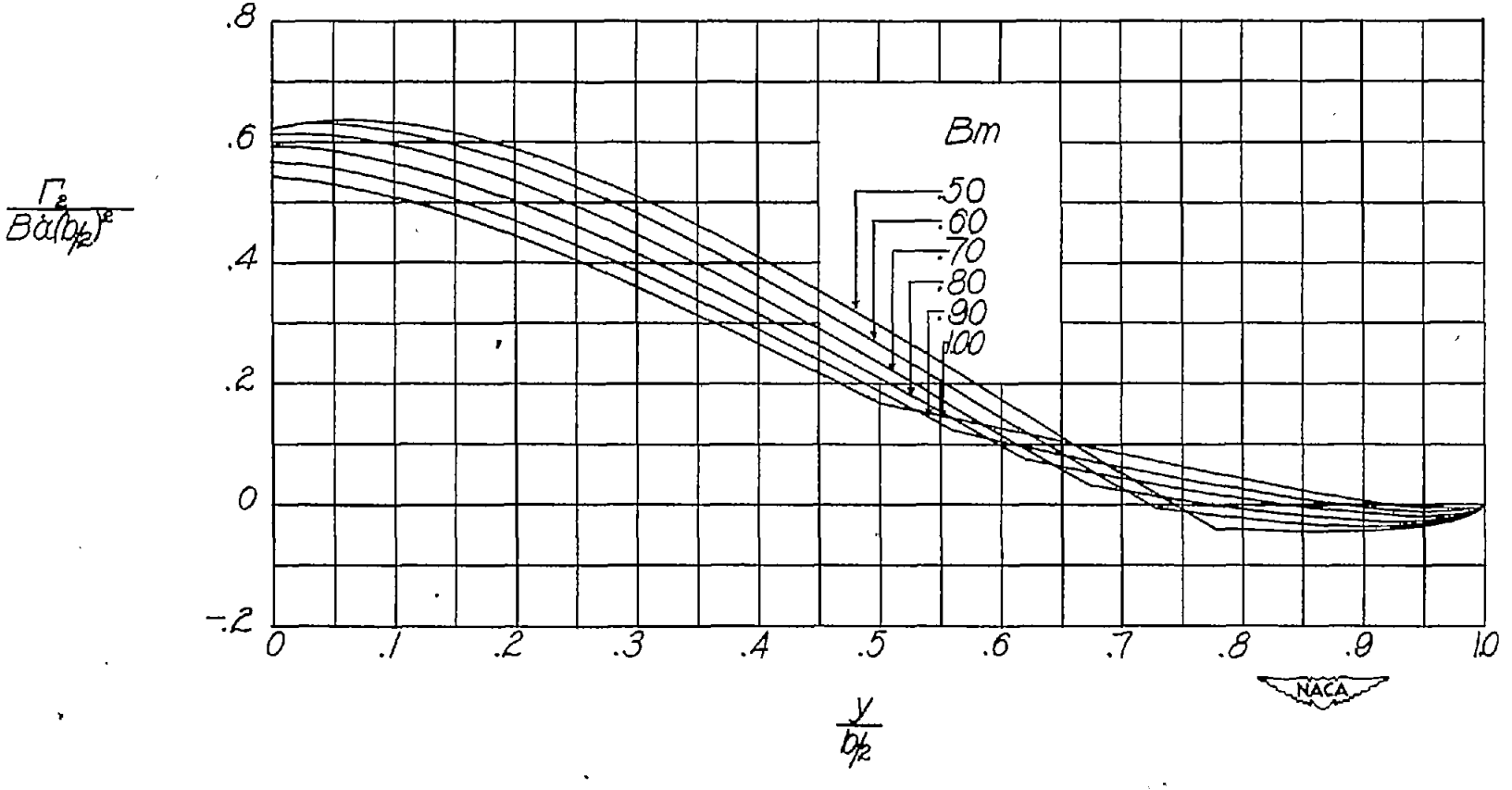

(a) AB = 2. Concluded.

Figure 24.- Continued.

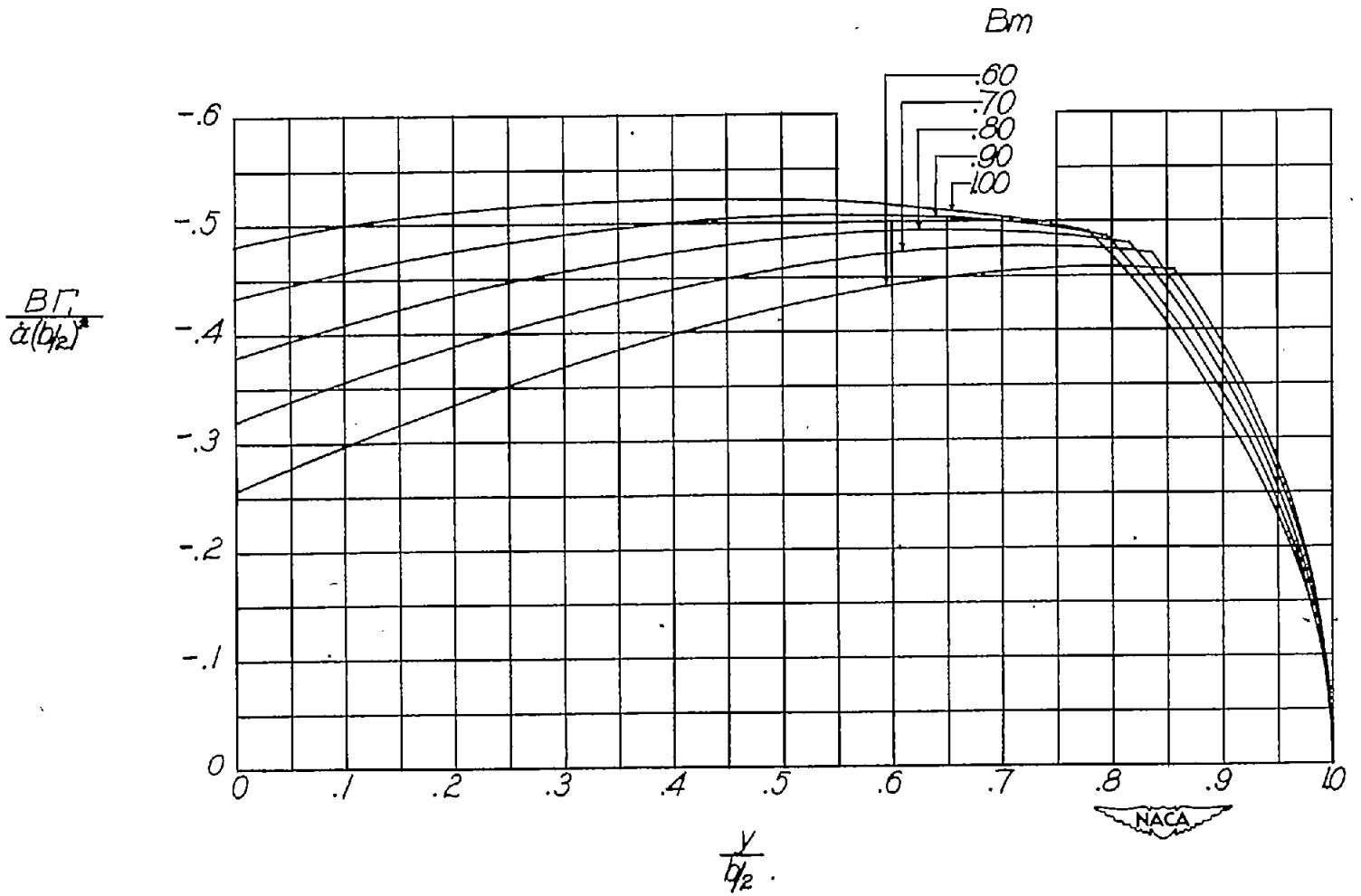

(b) AB = 3.

Figure 24.- Continued.

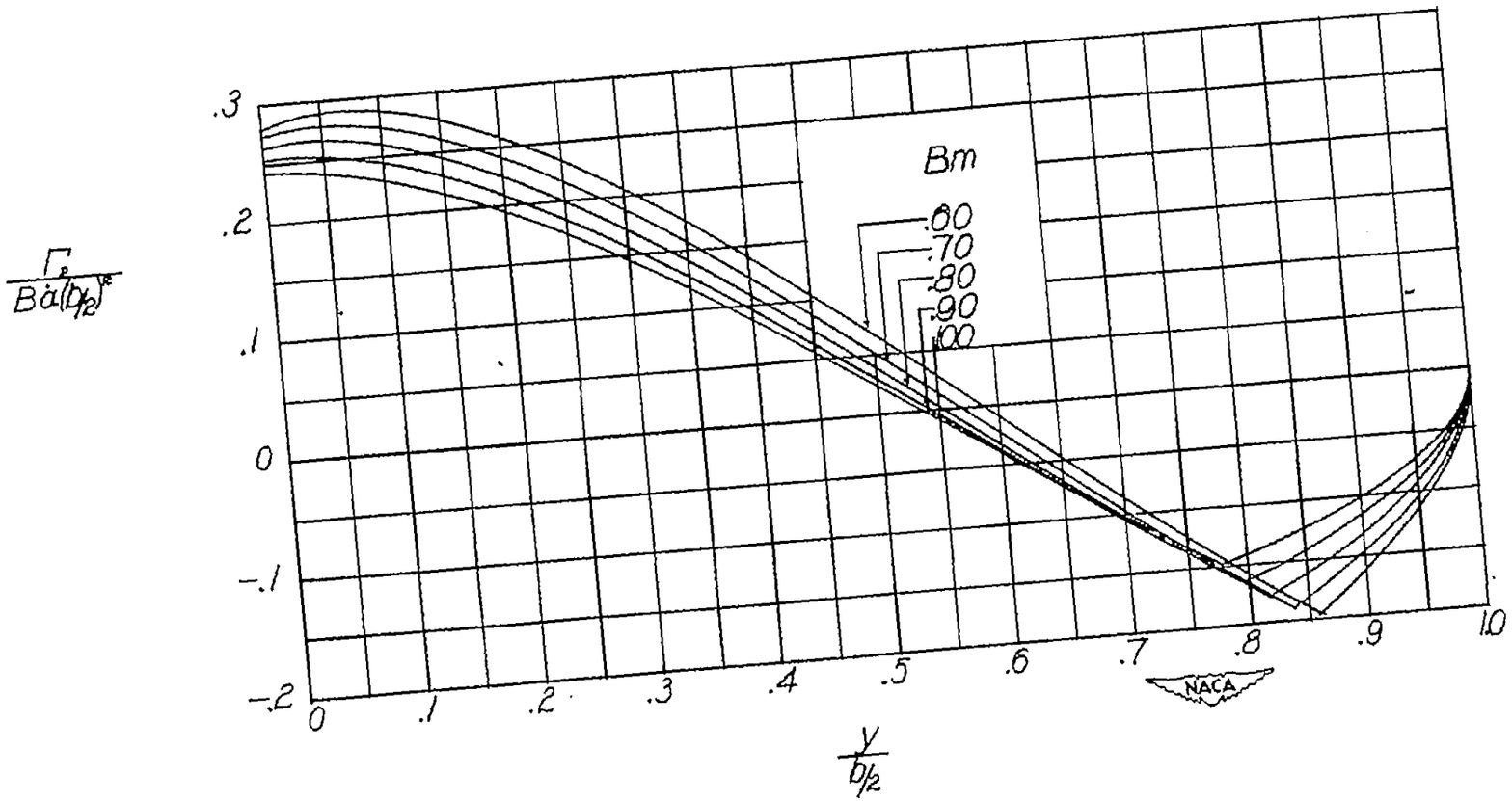

(b) AB = 3. Concluded.

Figure 24.- Continued.

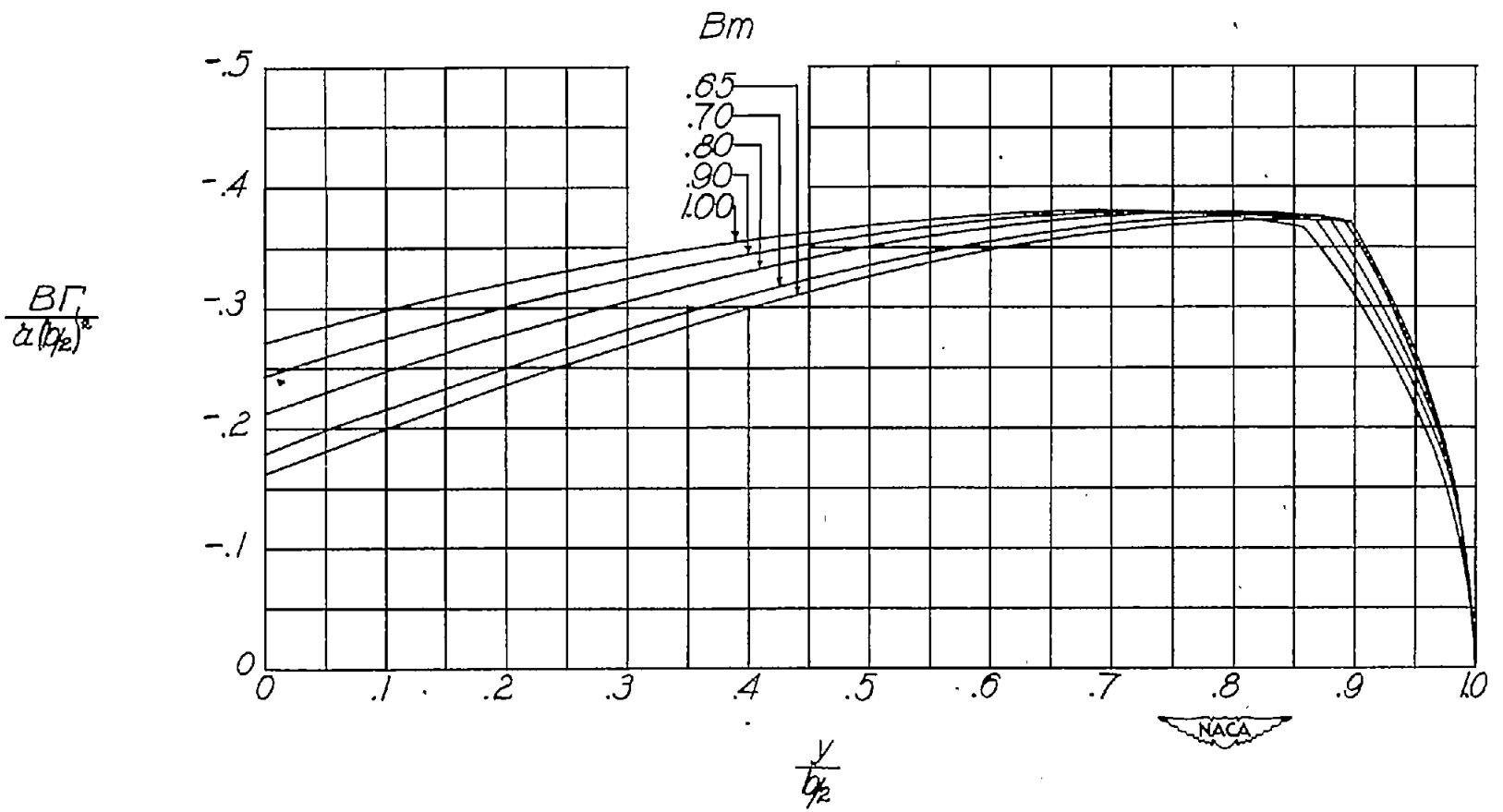

(c) AB = 4.

Figure 24.- Continued.

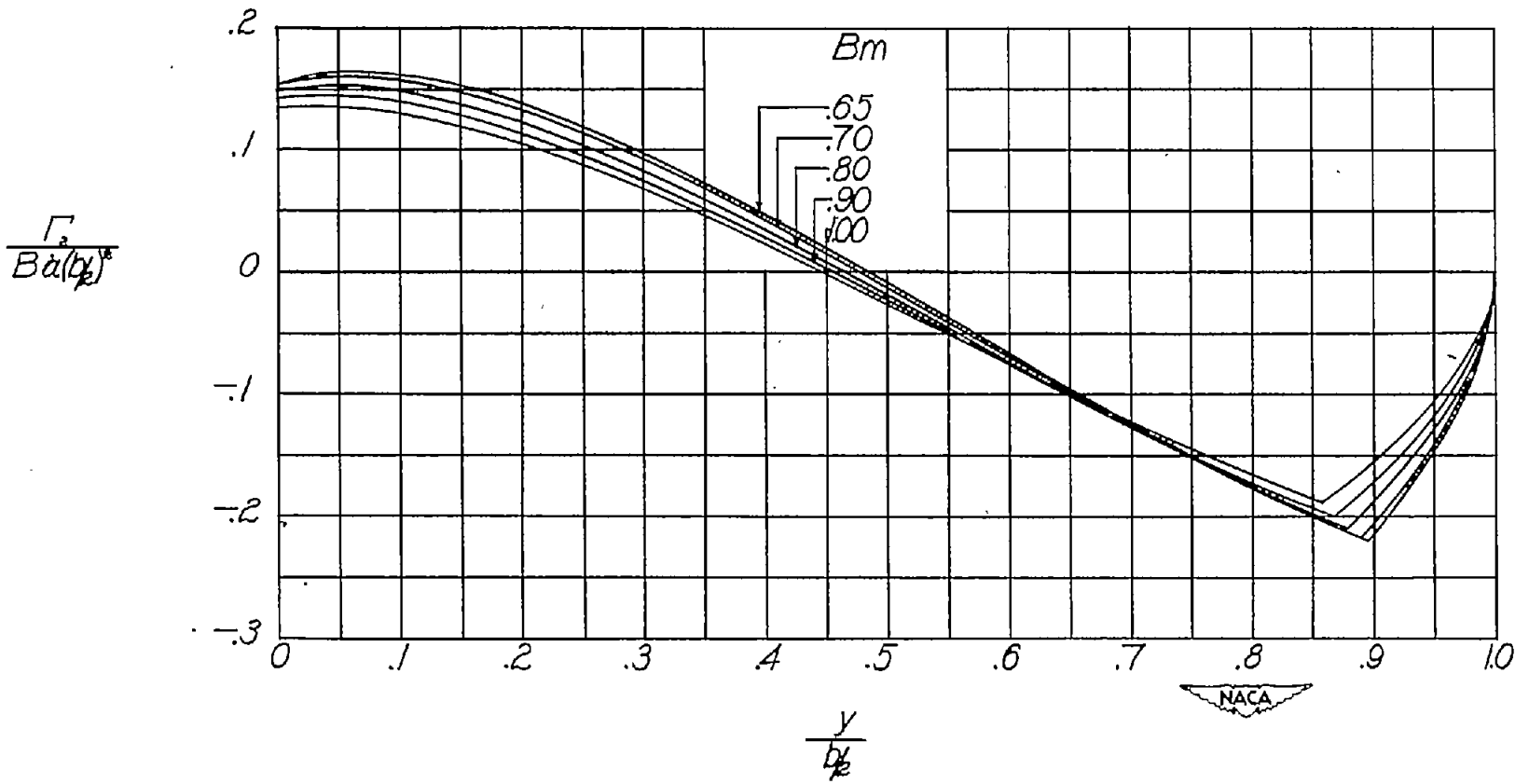

(c) AB = 4. Concluded.

Figure 24.- Continued.

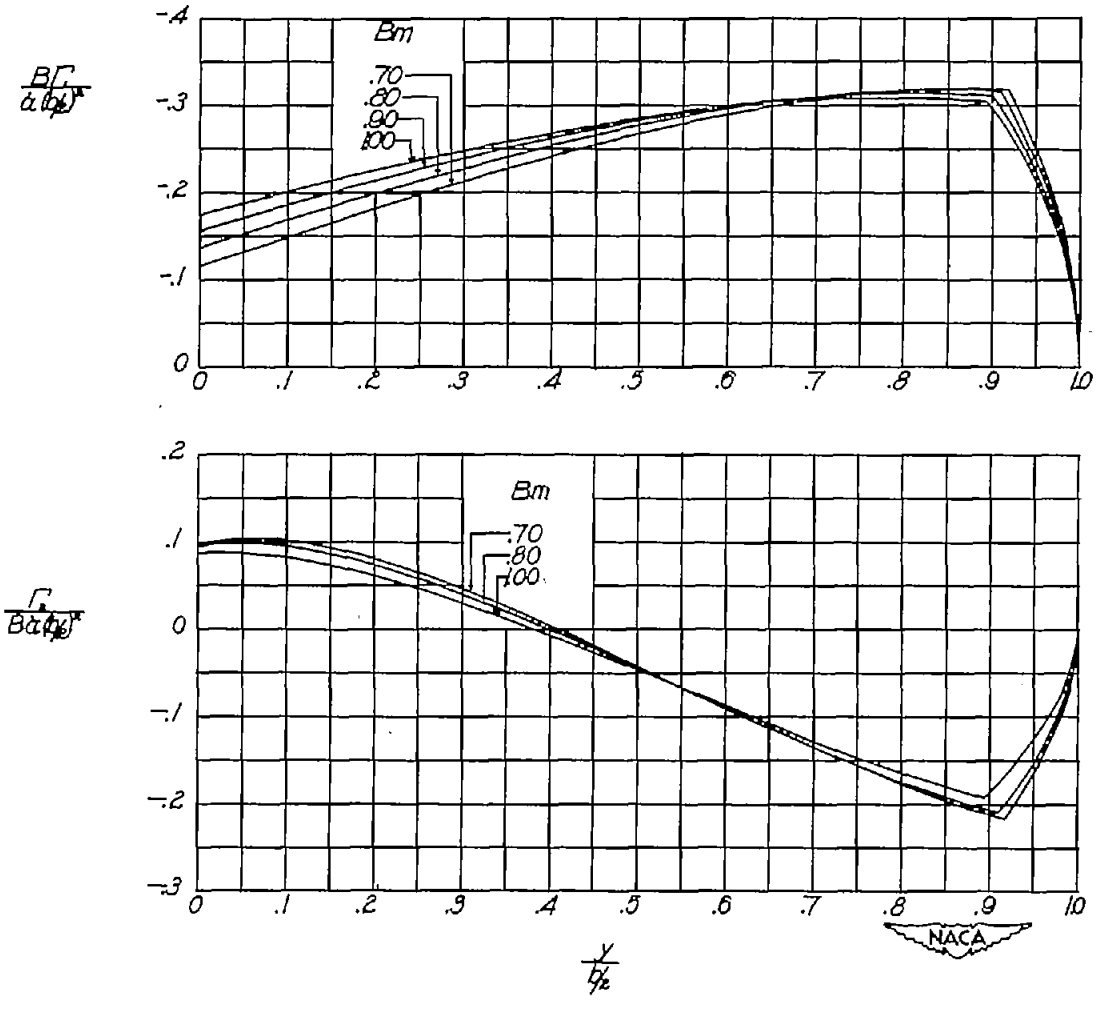

(d) AB = 5.

Figure 24.- Continued.

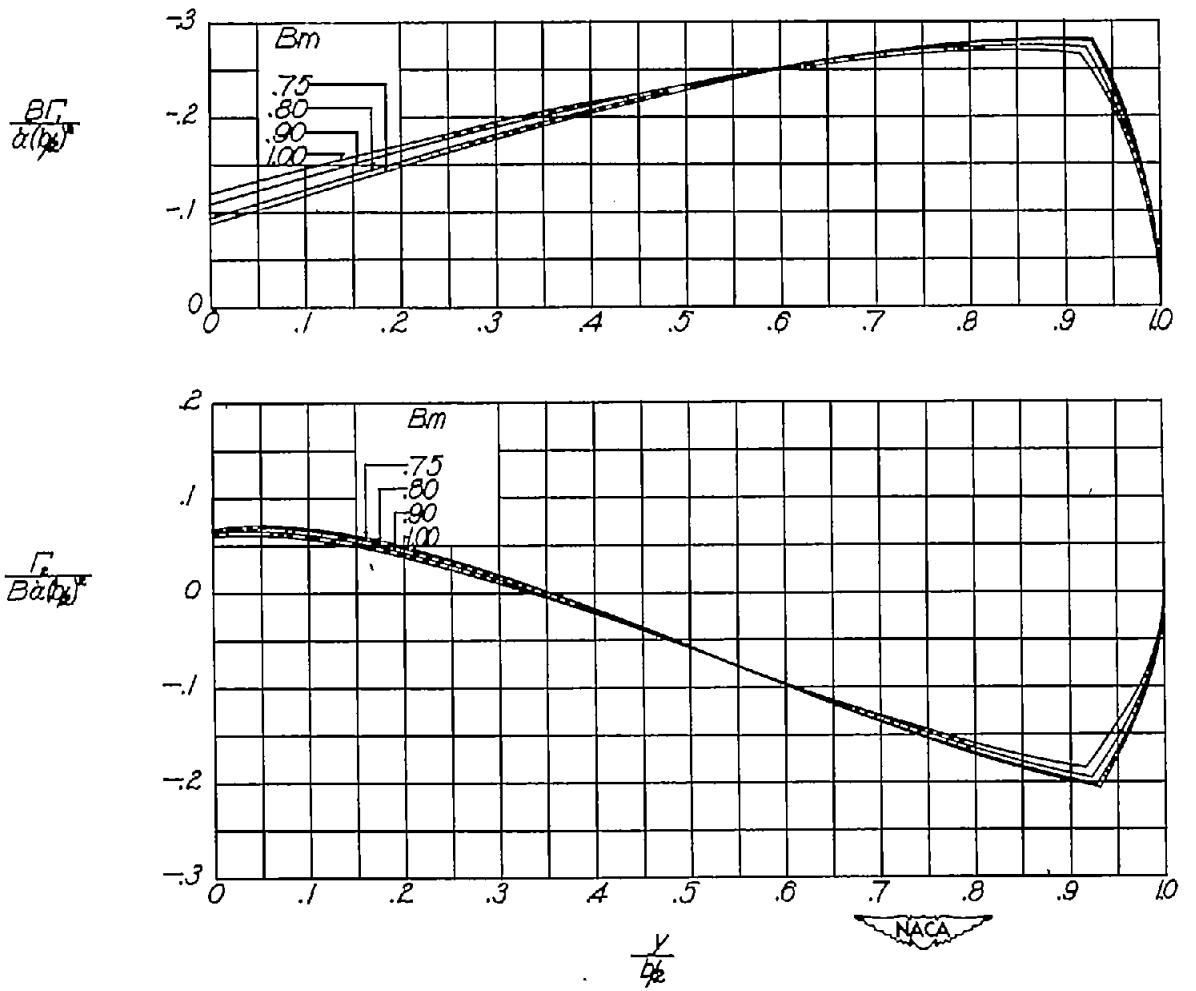

(e) AB = 6.

Figure 24.- Continued.

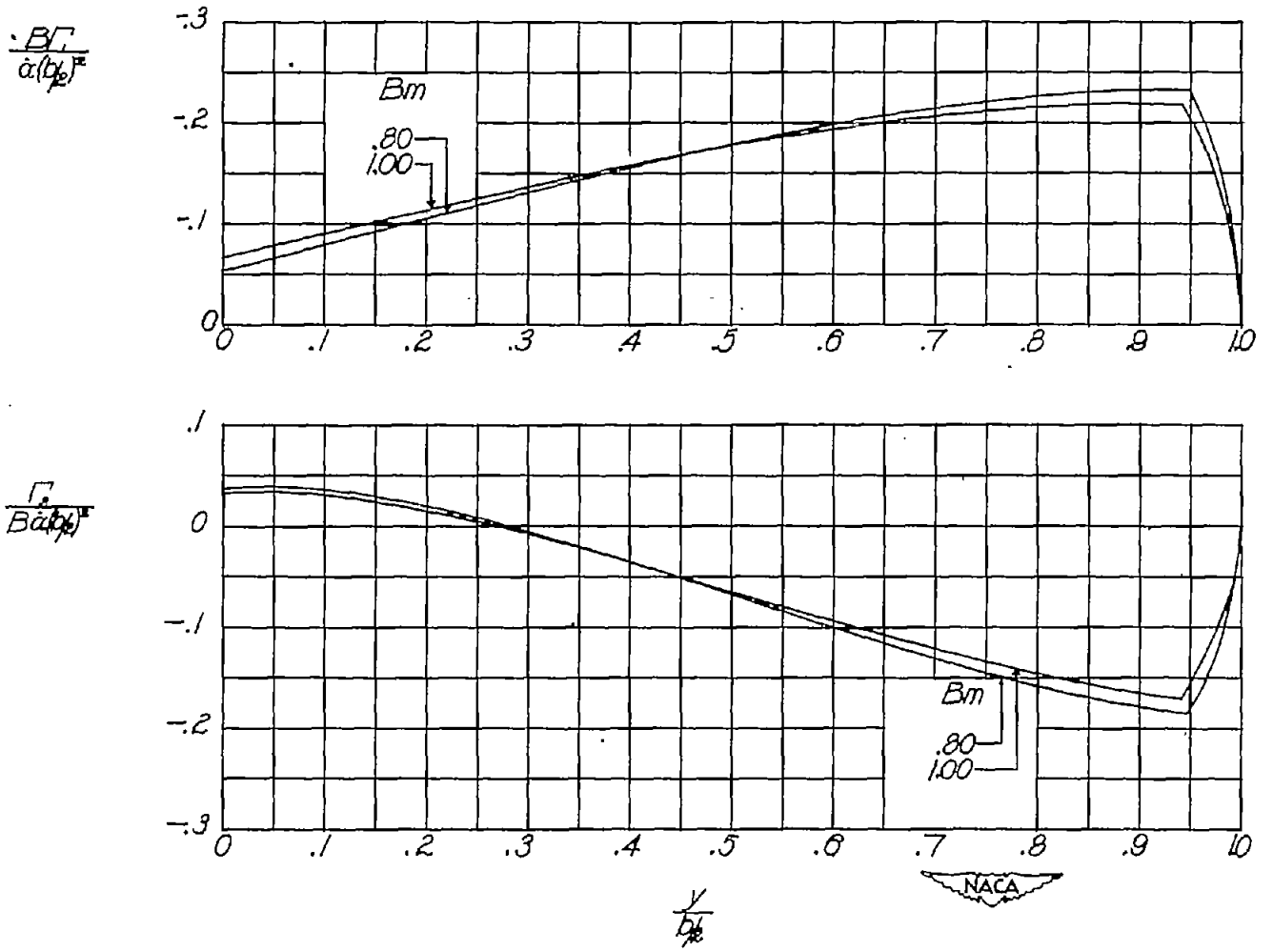

(f) AB = 8.

Figure 24.- Continued.

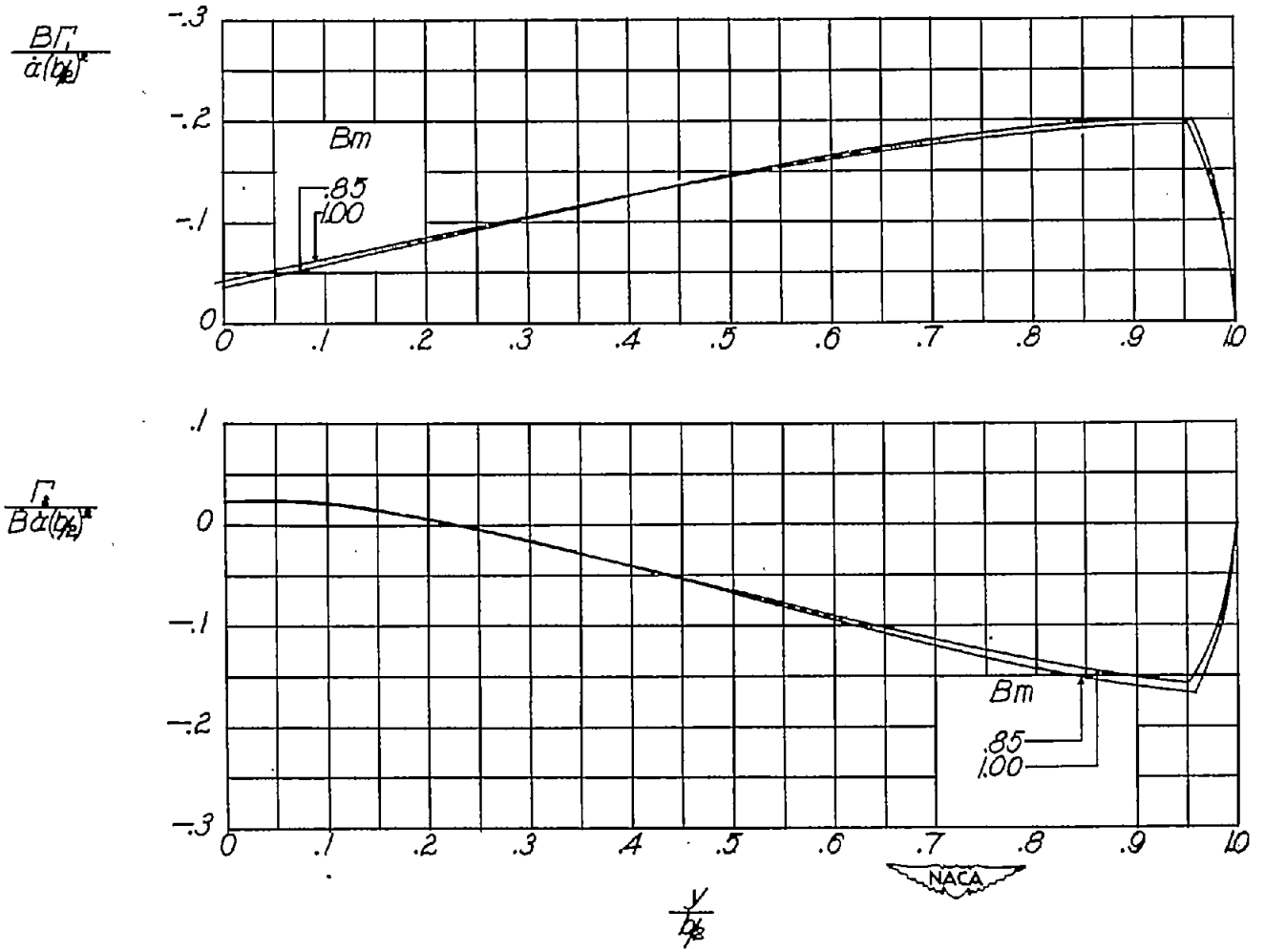

(g) AB = 10.

Figure 24.- Continued.

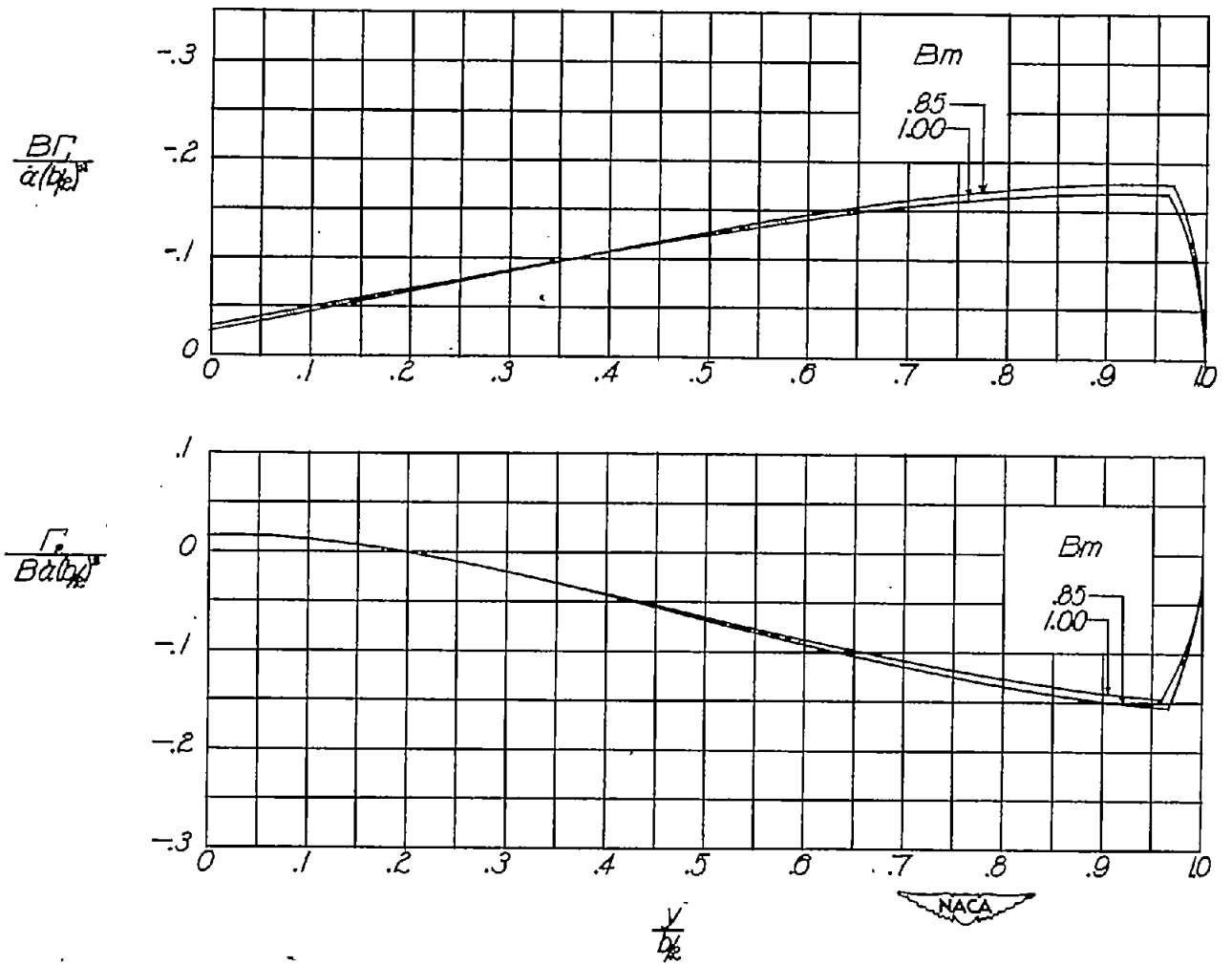

(h) AB = 12.

Figure 24.- Continued.

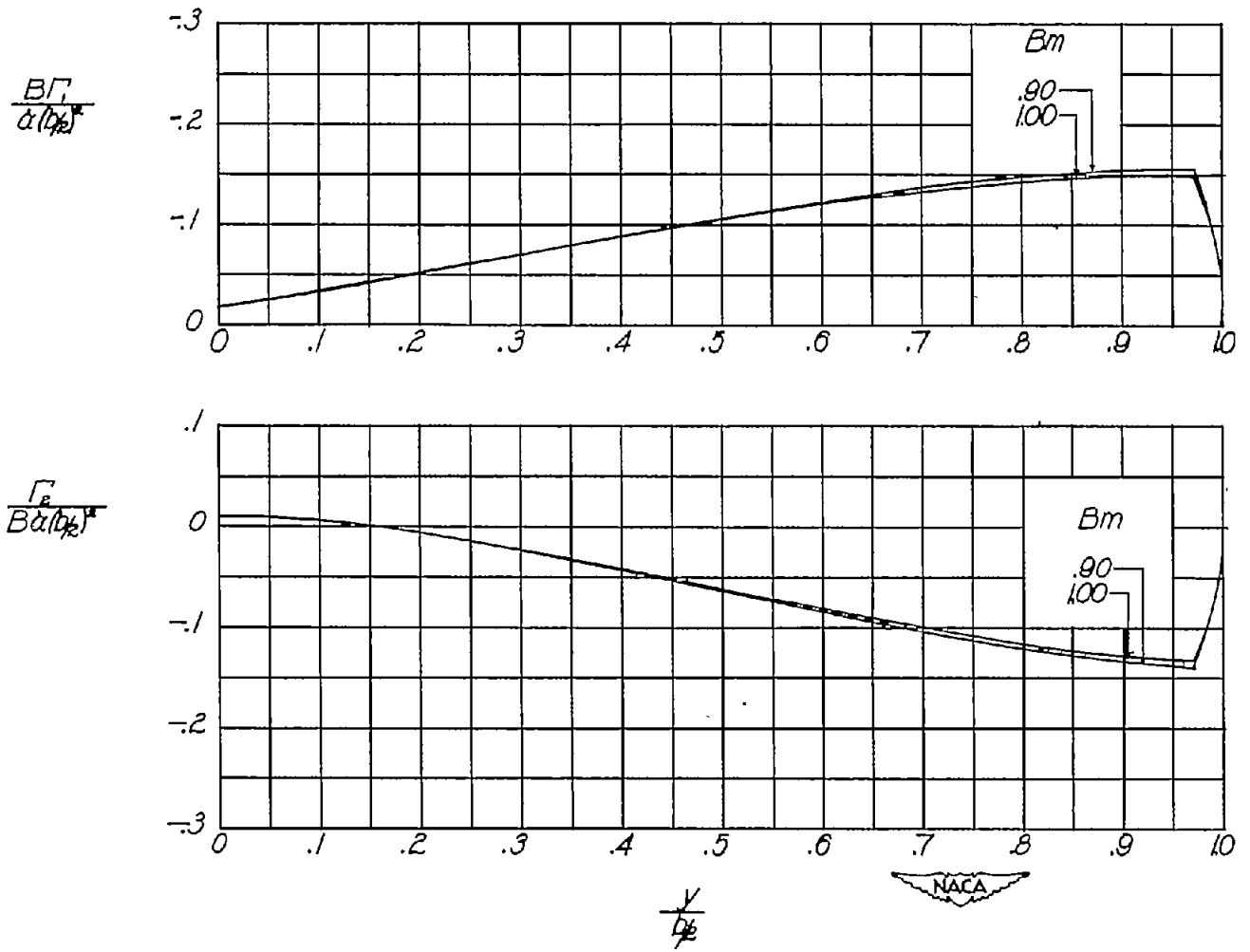

(i) AB = 15.

Figure 24.- Continued.

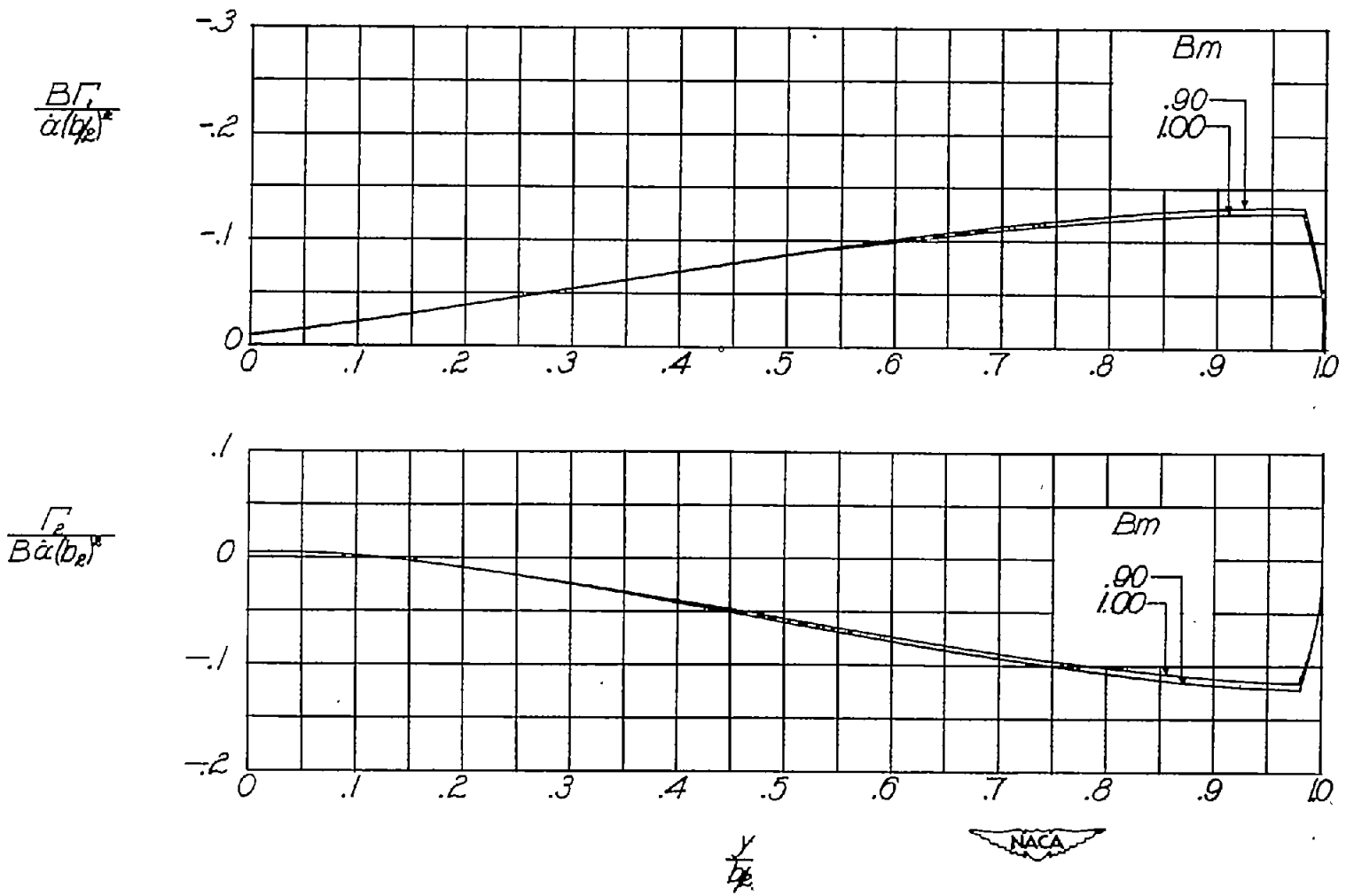

(j) AB = 20.

Figure 24.- Concluded.

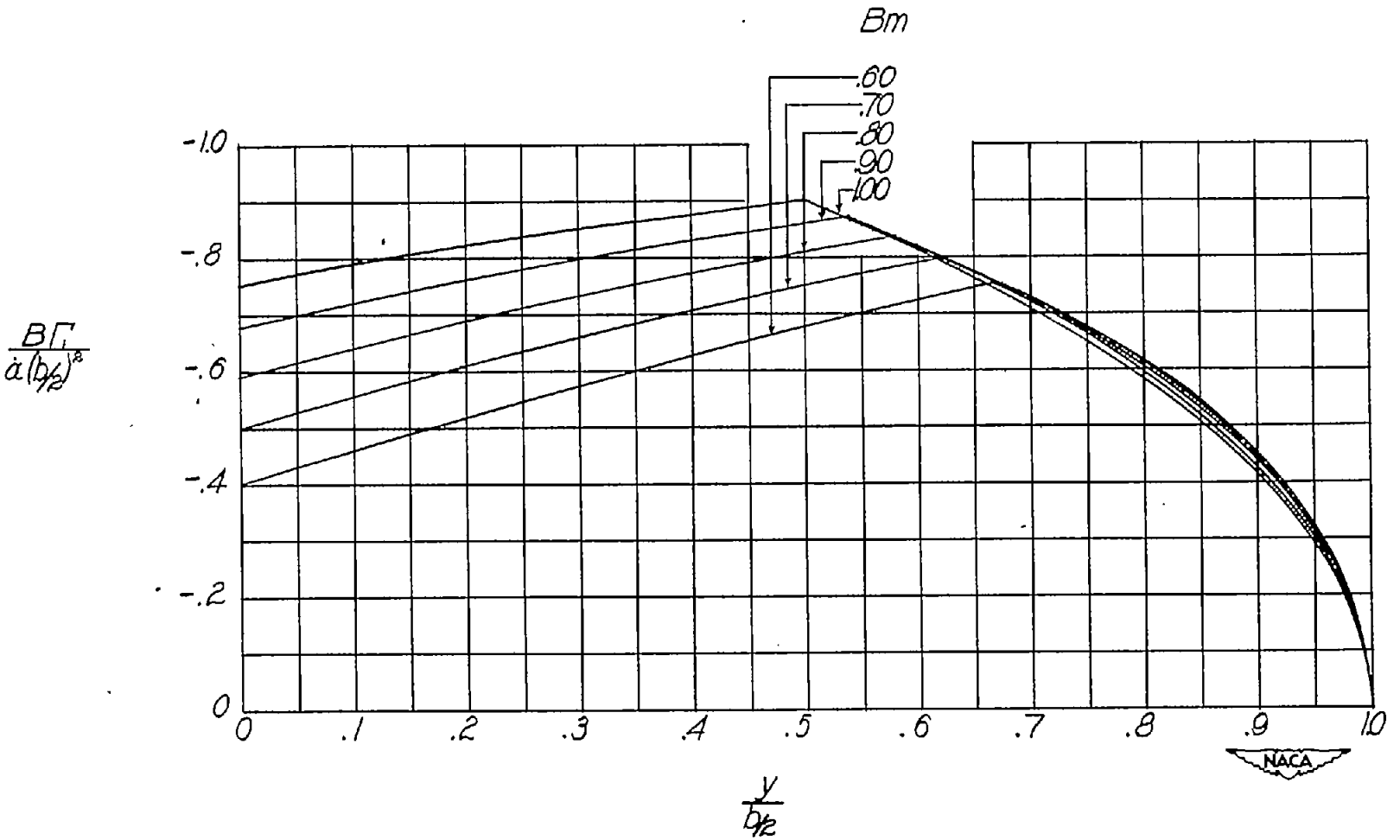

(a) AB = 2.

Figure 25.- Distribution of circulation along span for wings with constant vertical acceleration with $\lambda = 0.50$. $\Gamma = \Gamma_1 + \Gamma_2$.

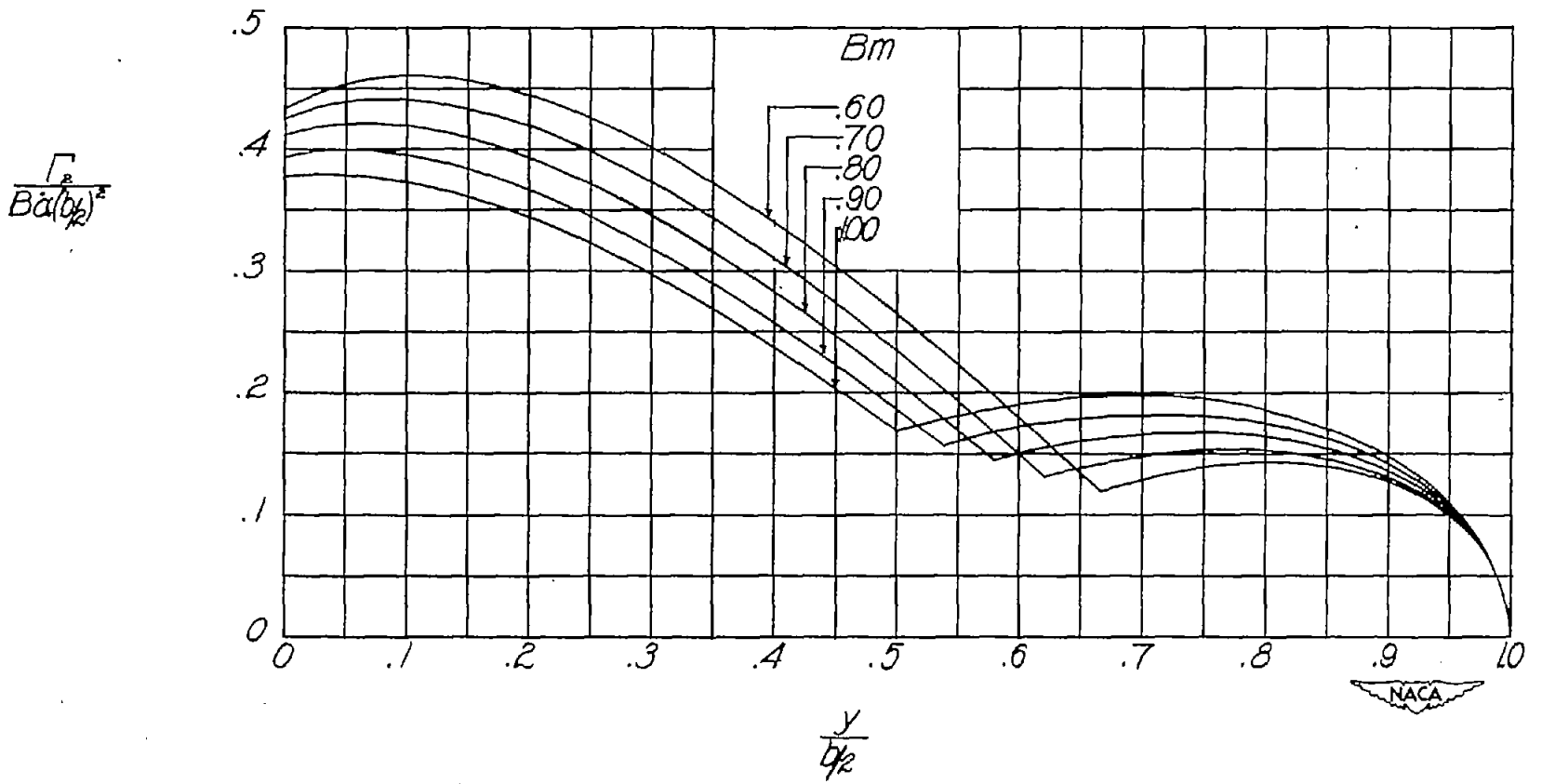

(a) AB = 2. Concluded.

Figure 25.- Continued.

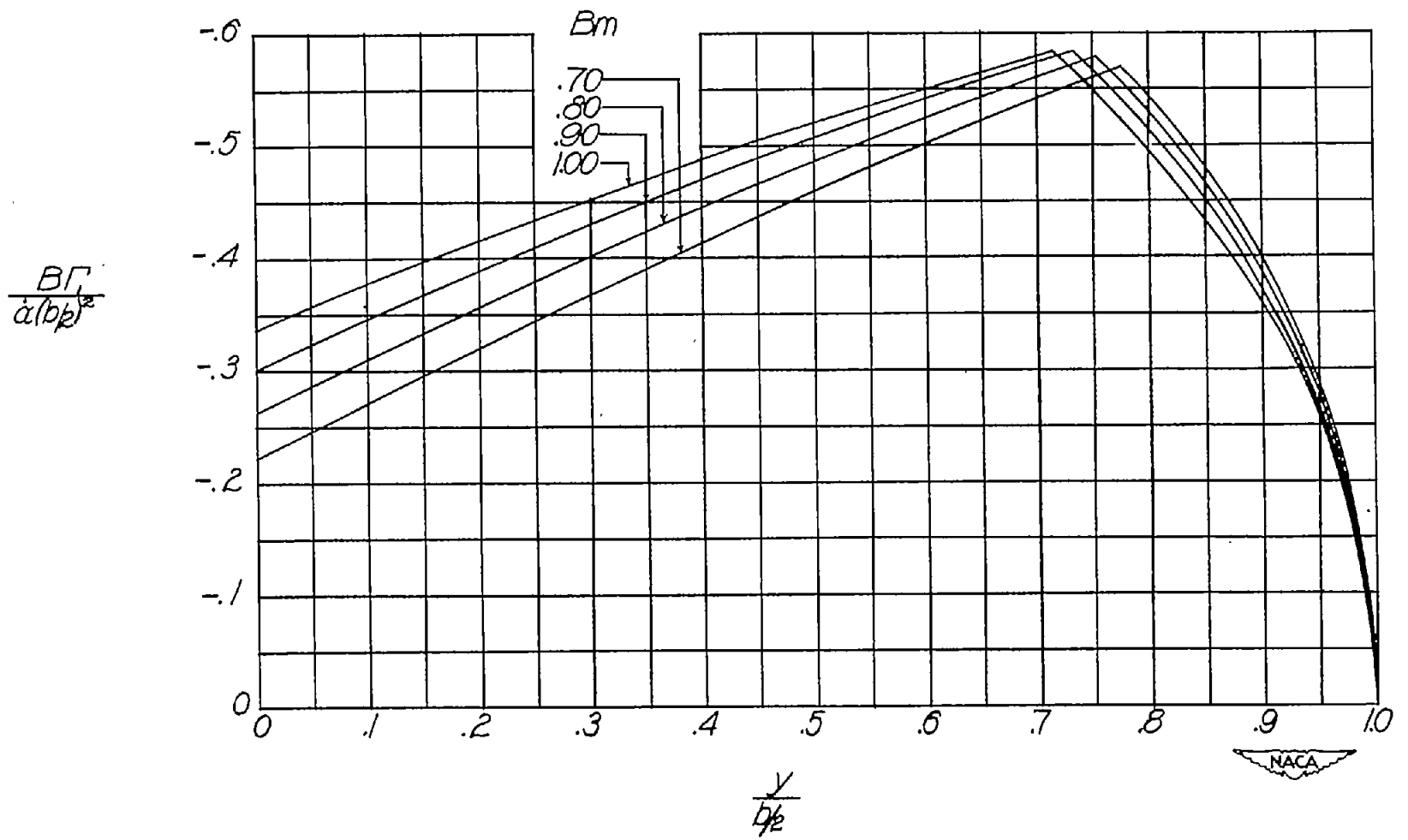

(b) AB = 3.

Figure 25.- Continued.

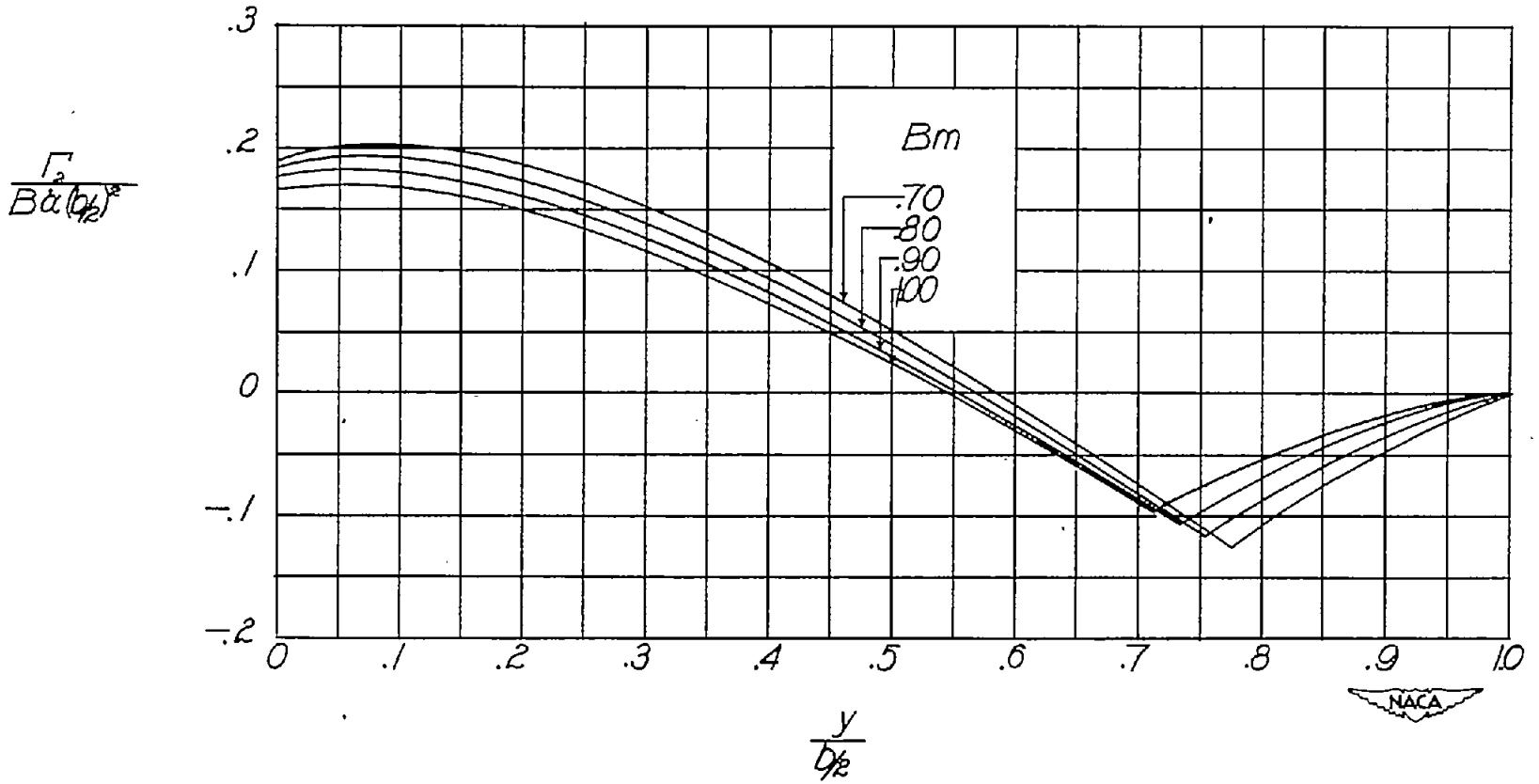

(b) AB = 3. Concluded.

Figure 25.- Continued.

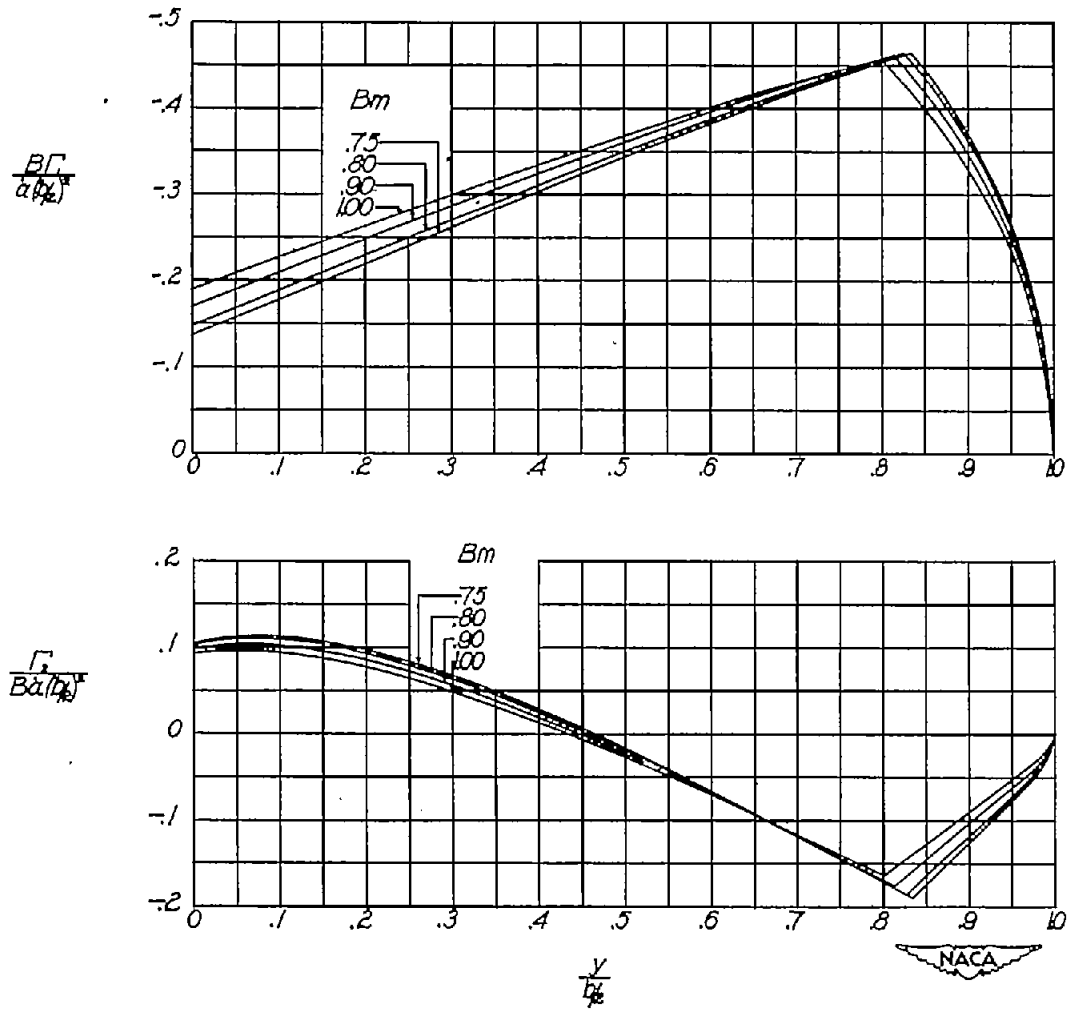

(c) AB = 4.

Figure 25.- Continued.

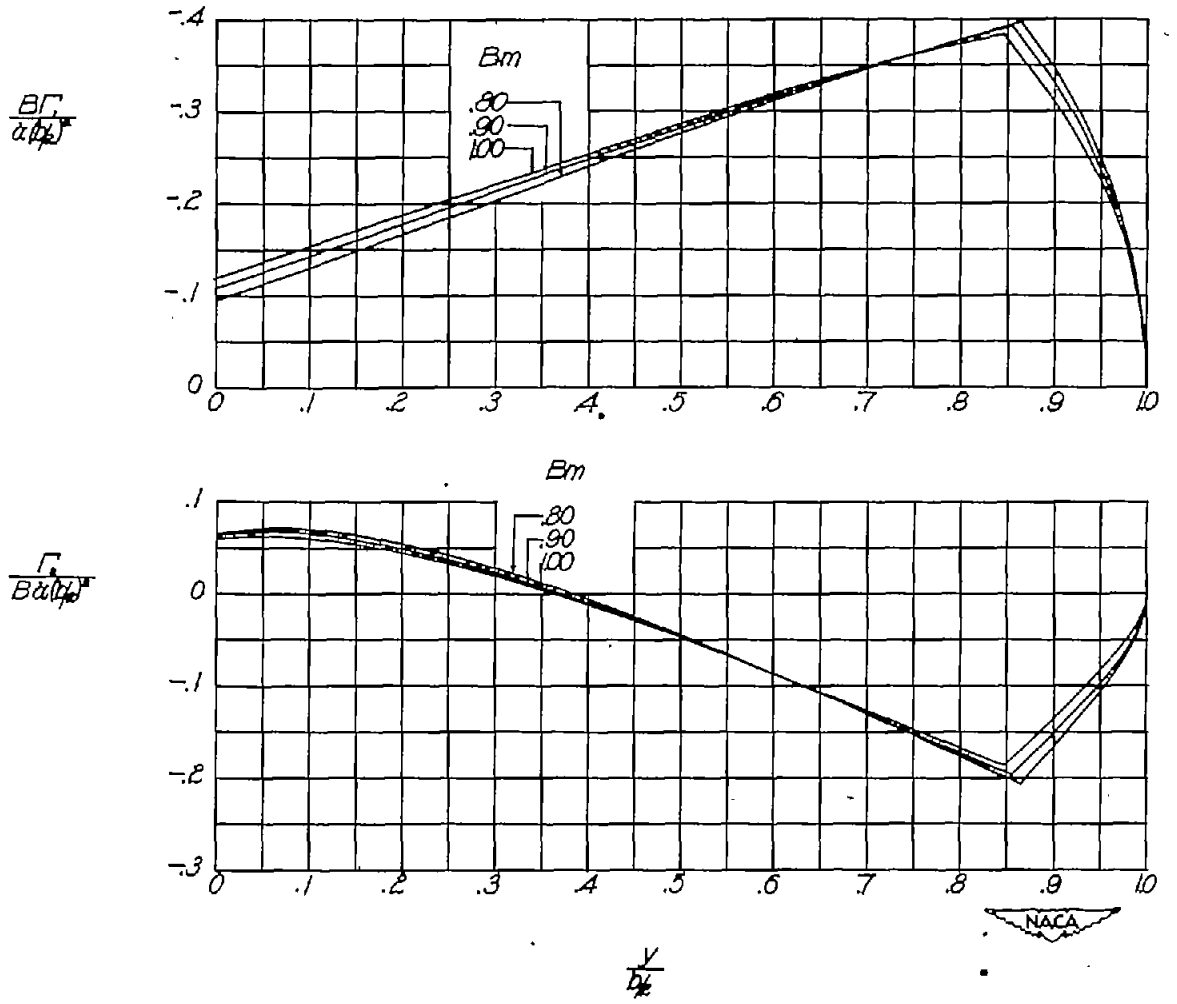

(d) AB = 5.

Figure 25.- Continued.

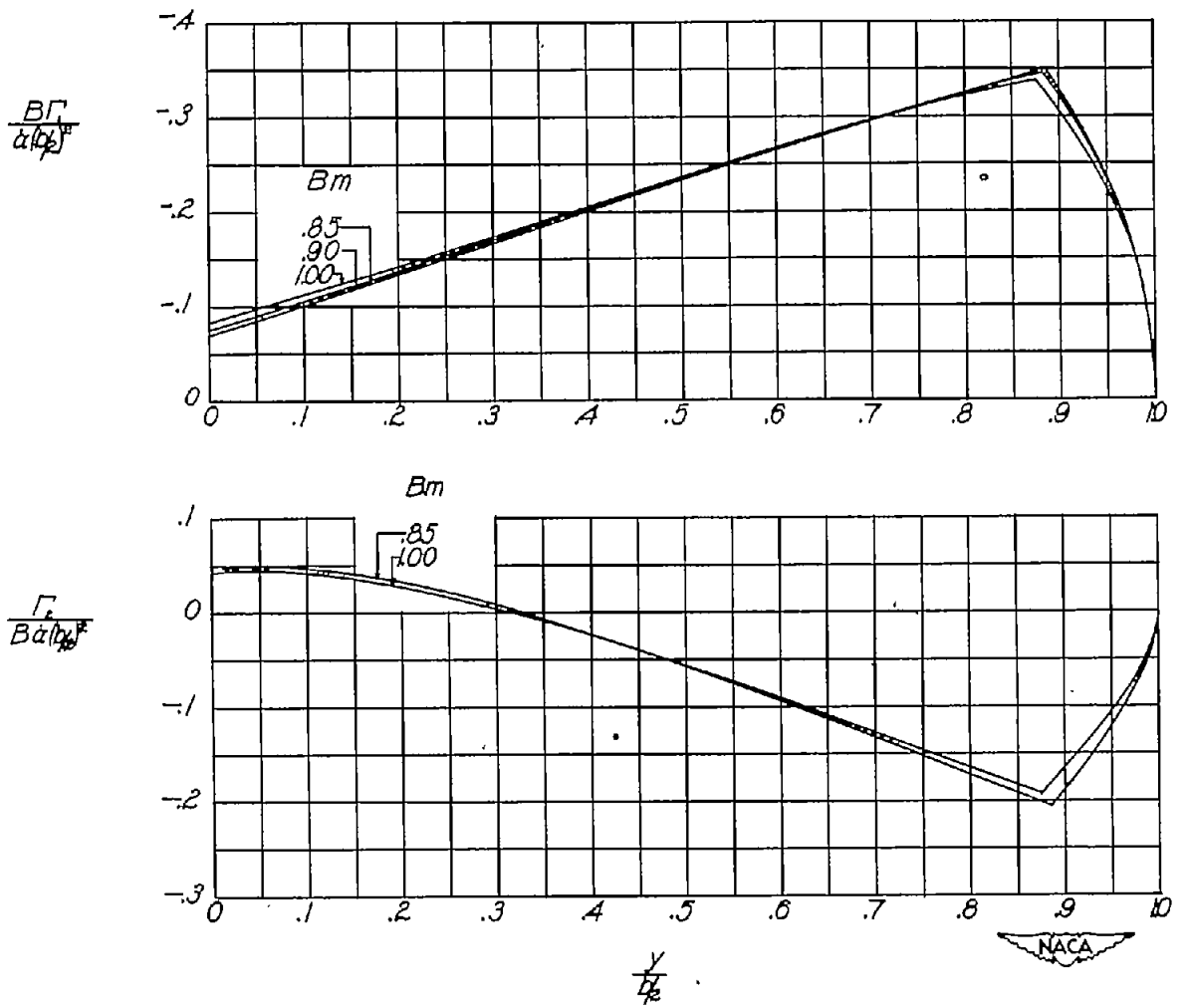

(e) AB = 6.

Figure 25.- Continued.

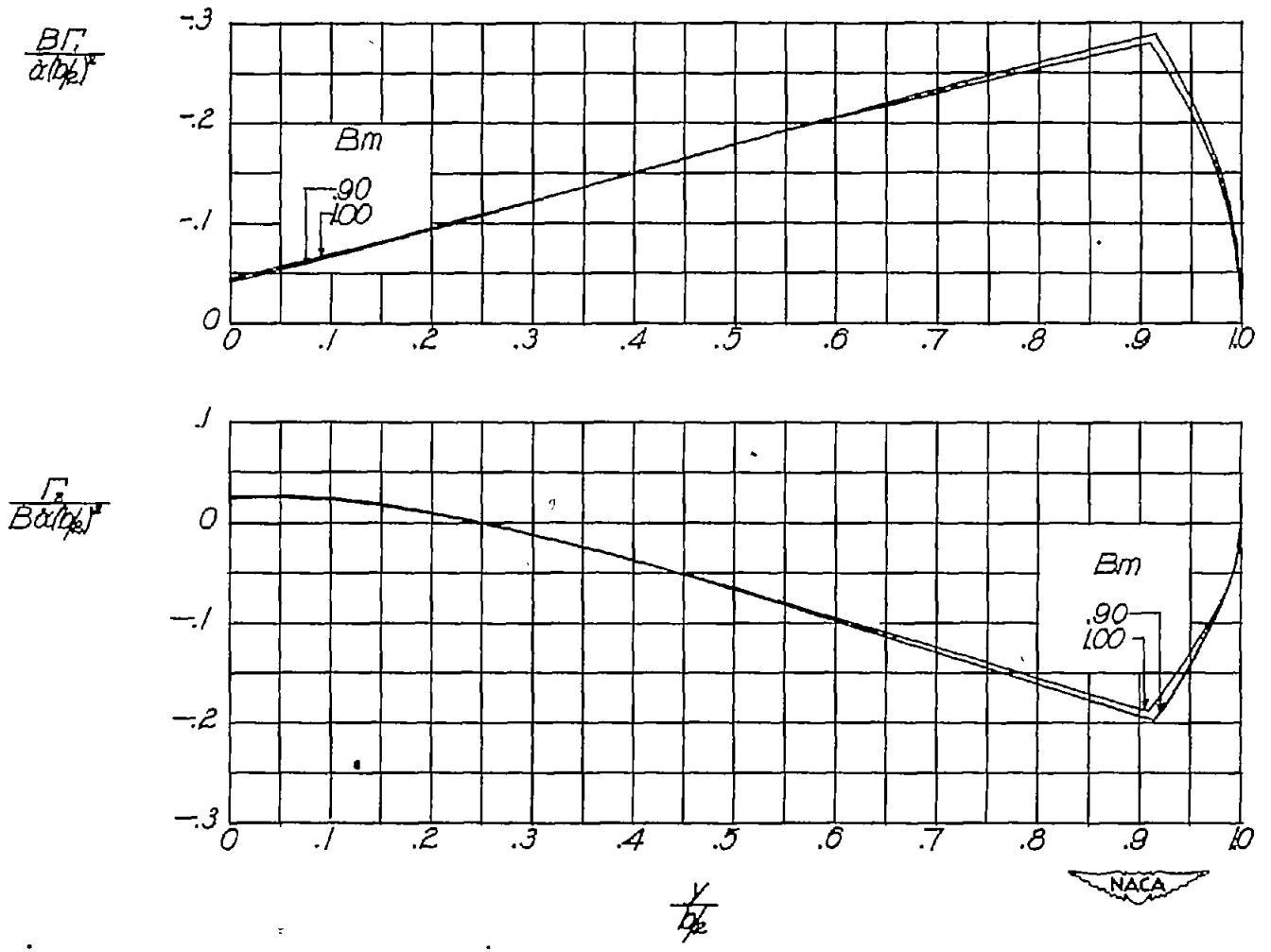

(f) AB = 8.

Figure 25.- Continued.

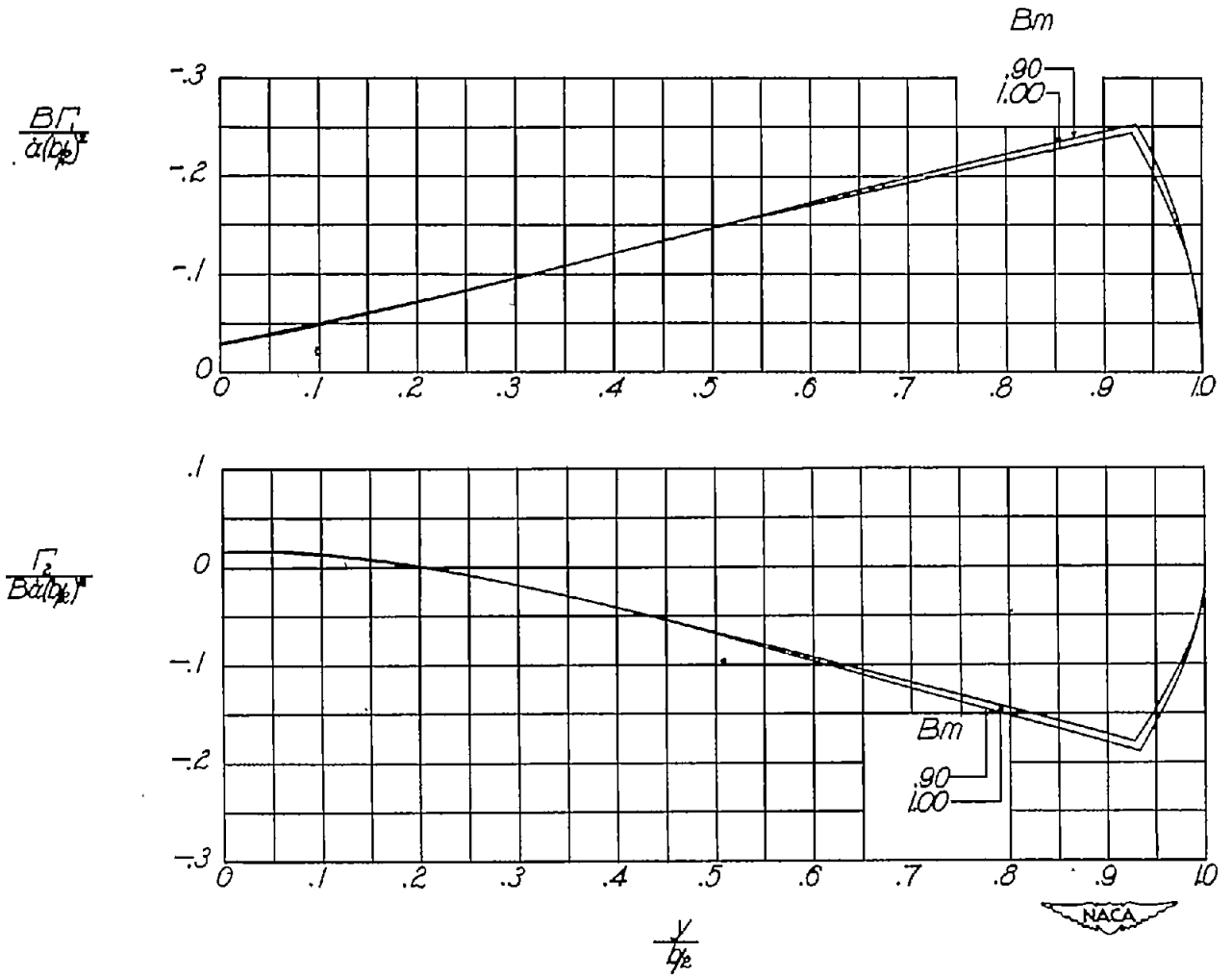

(g) AB = 10.

Figure 25.- Continued.

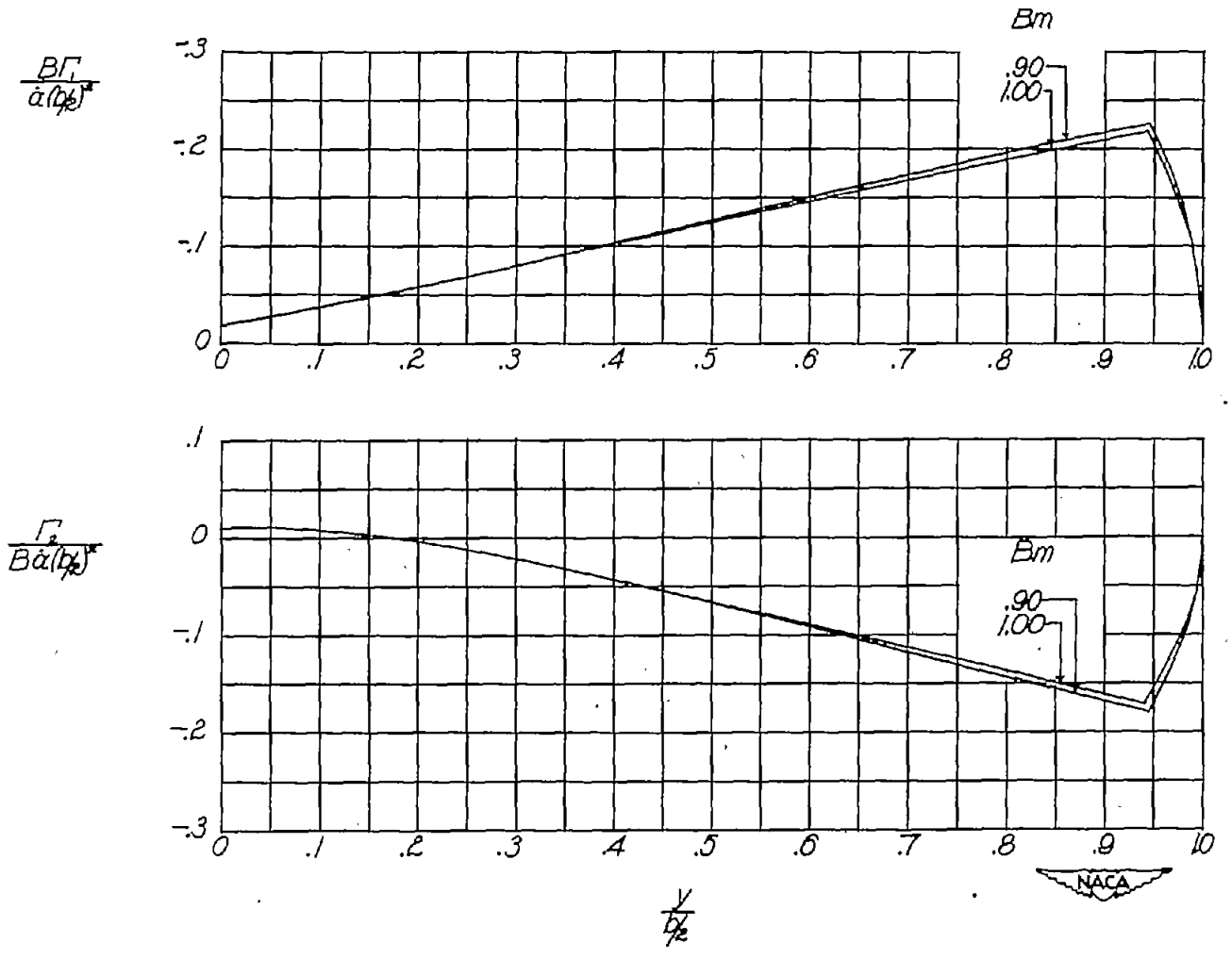

(h) AB = 12.

Figure 25.- Continued.

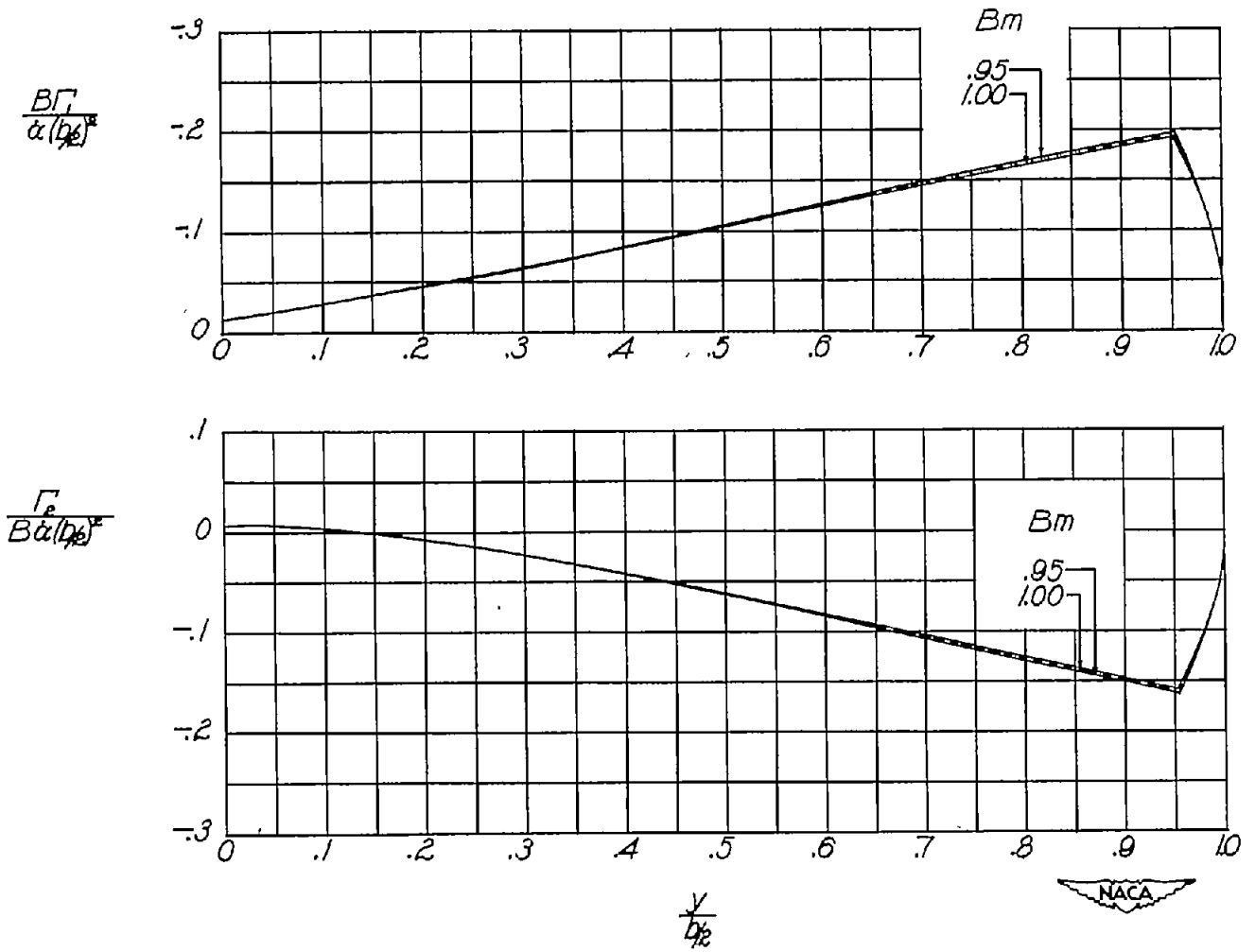

(i) AB = 15.

Figure 25.- Continued.

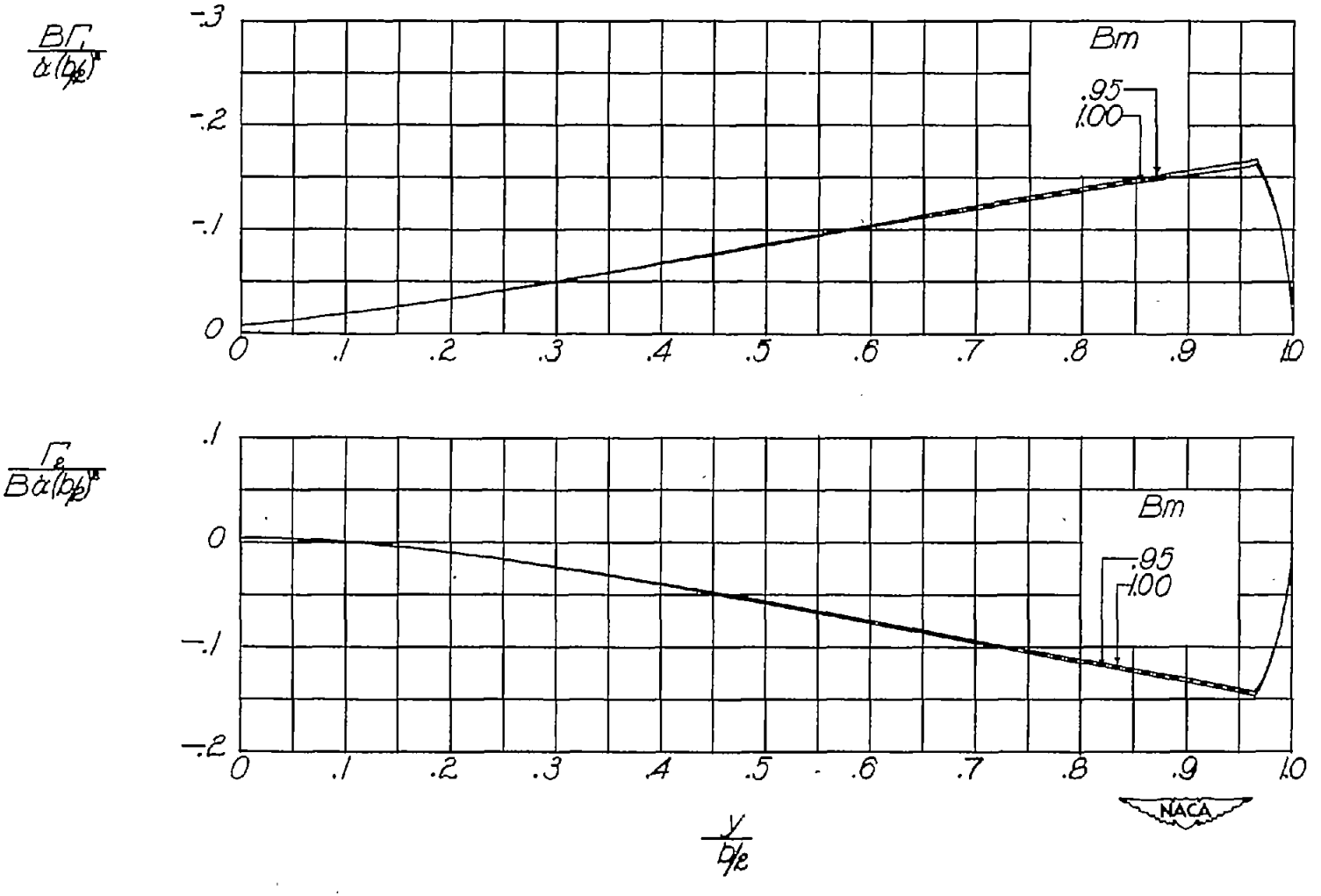

(j) AB = 20.

Figure 25.- Concluded.

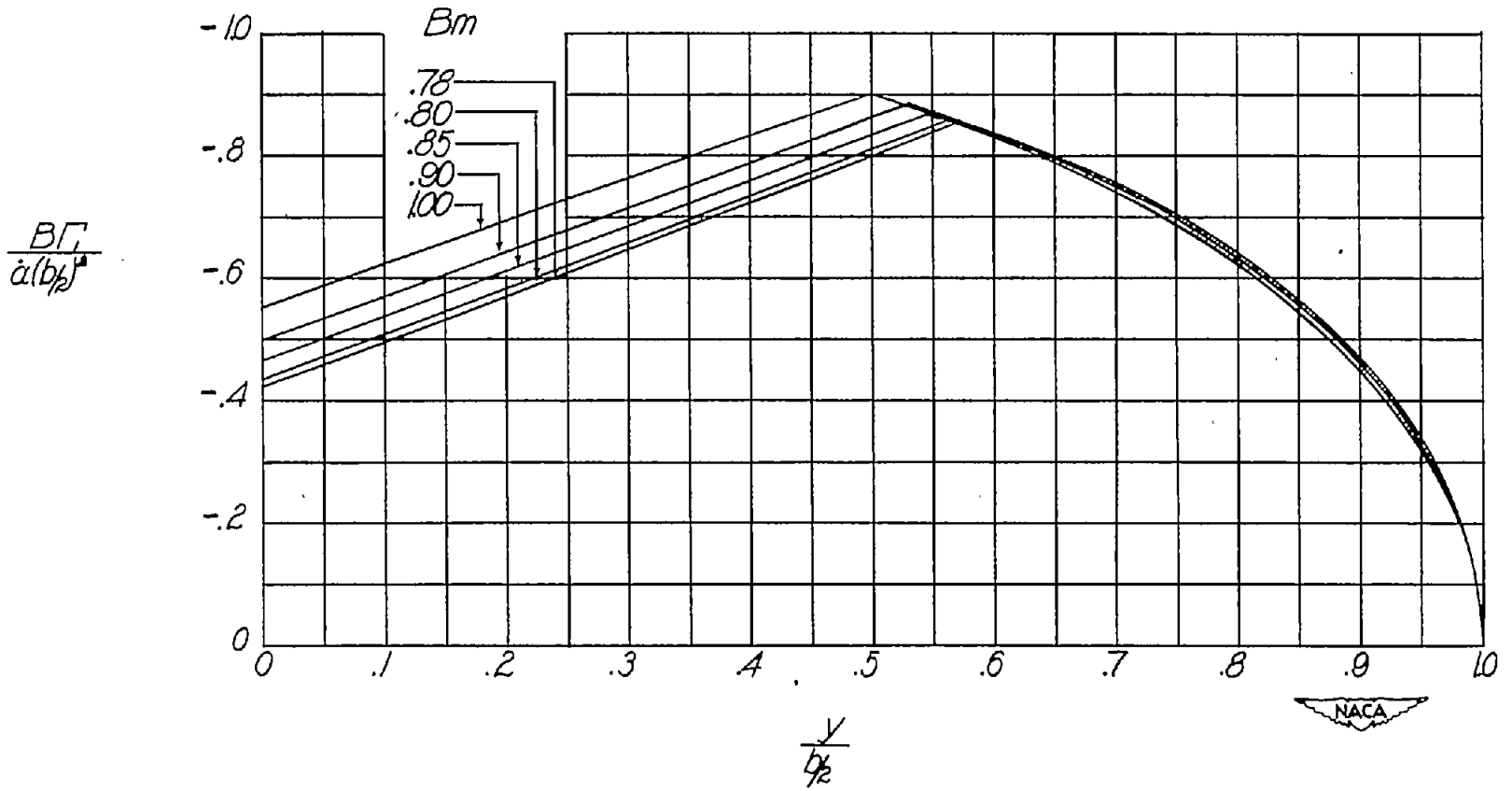

(a) AR = 2.

Figure 26.- Distribution of circulation along span for wings with constant vertical acceleration with $\lambda = 0.75$. $\Gamma = \Gamma_1 + \Gamma_2$.

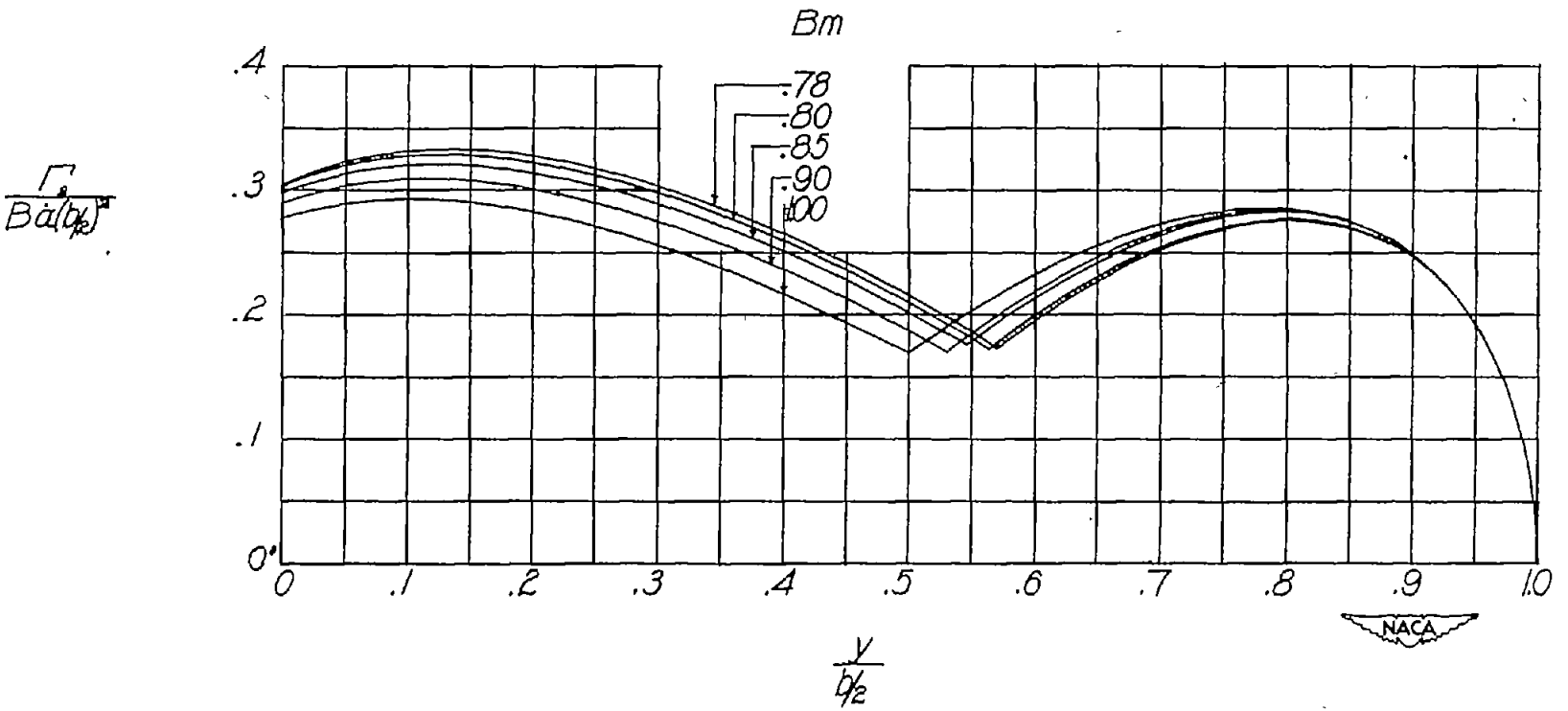

(a) AB = 2. Concluded.

Figure 26.- Continued.

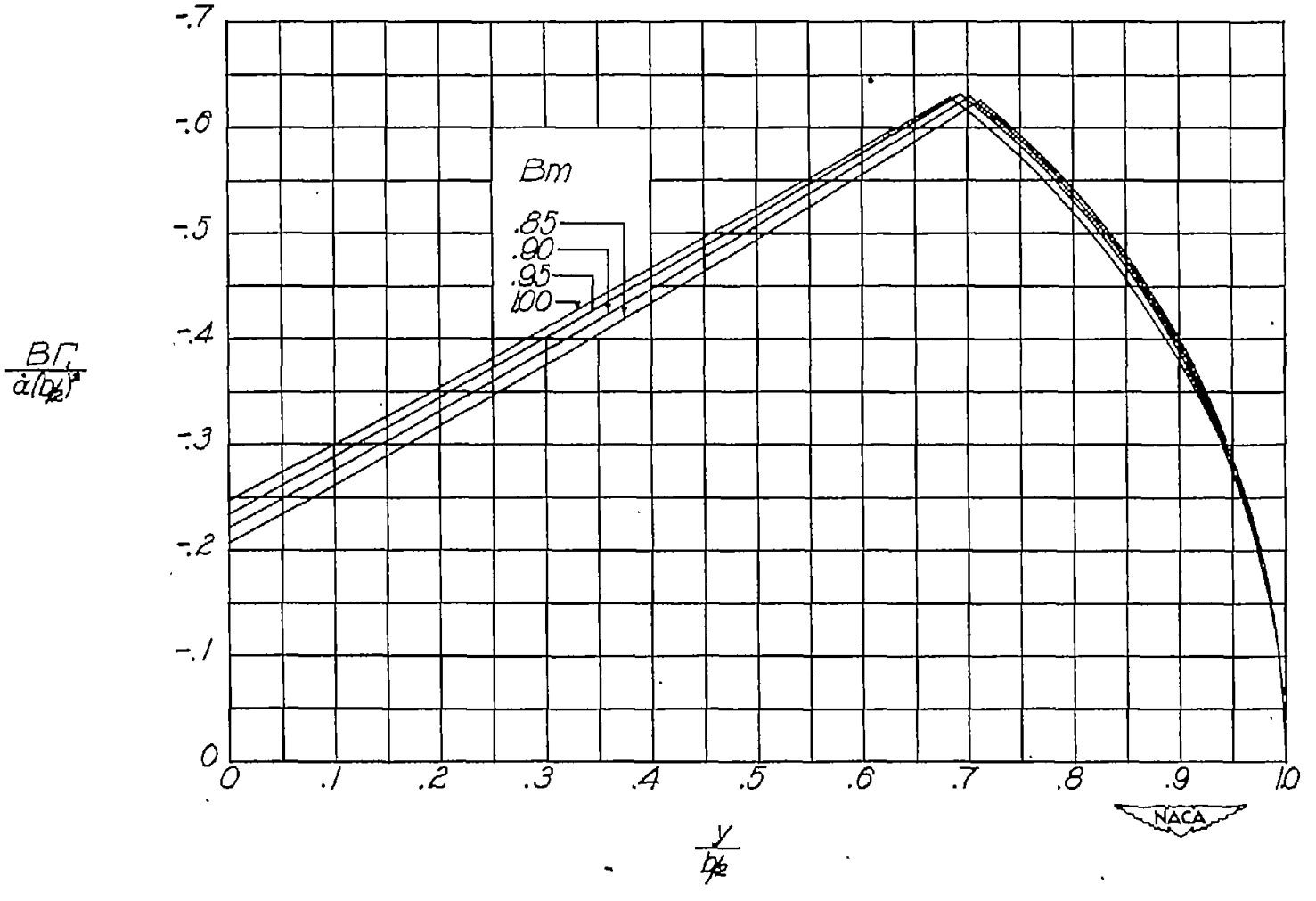

(b) AB = 3.

Figure 26.- Continued.

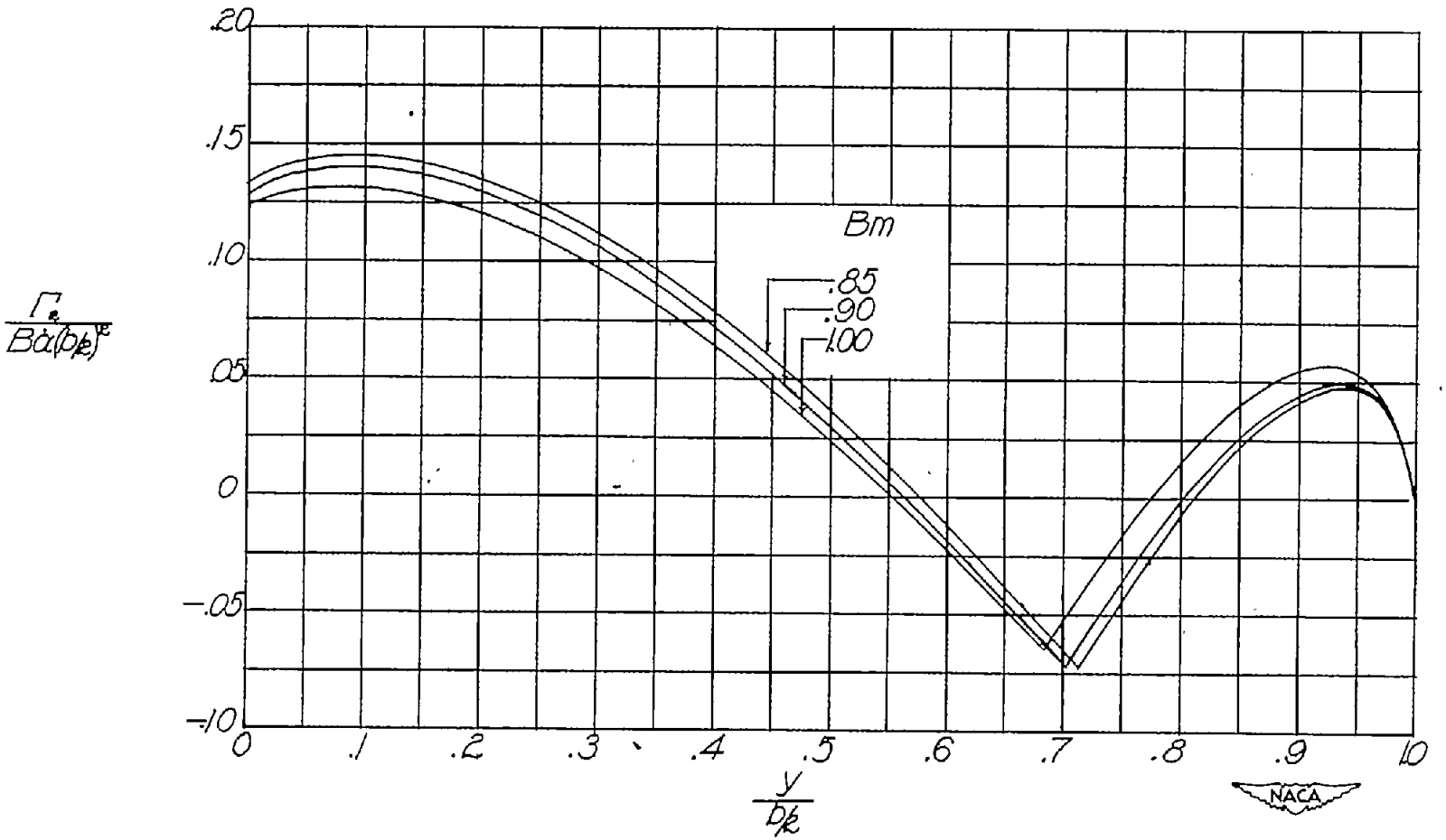

(b) AB = 3. Concluded.

Figure 26.- Continued.

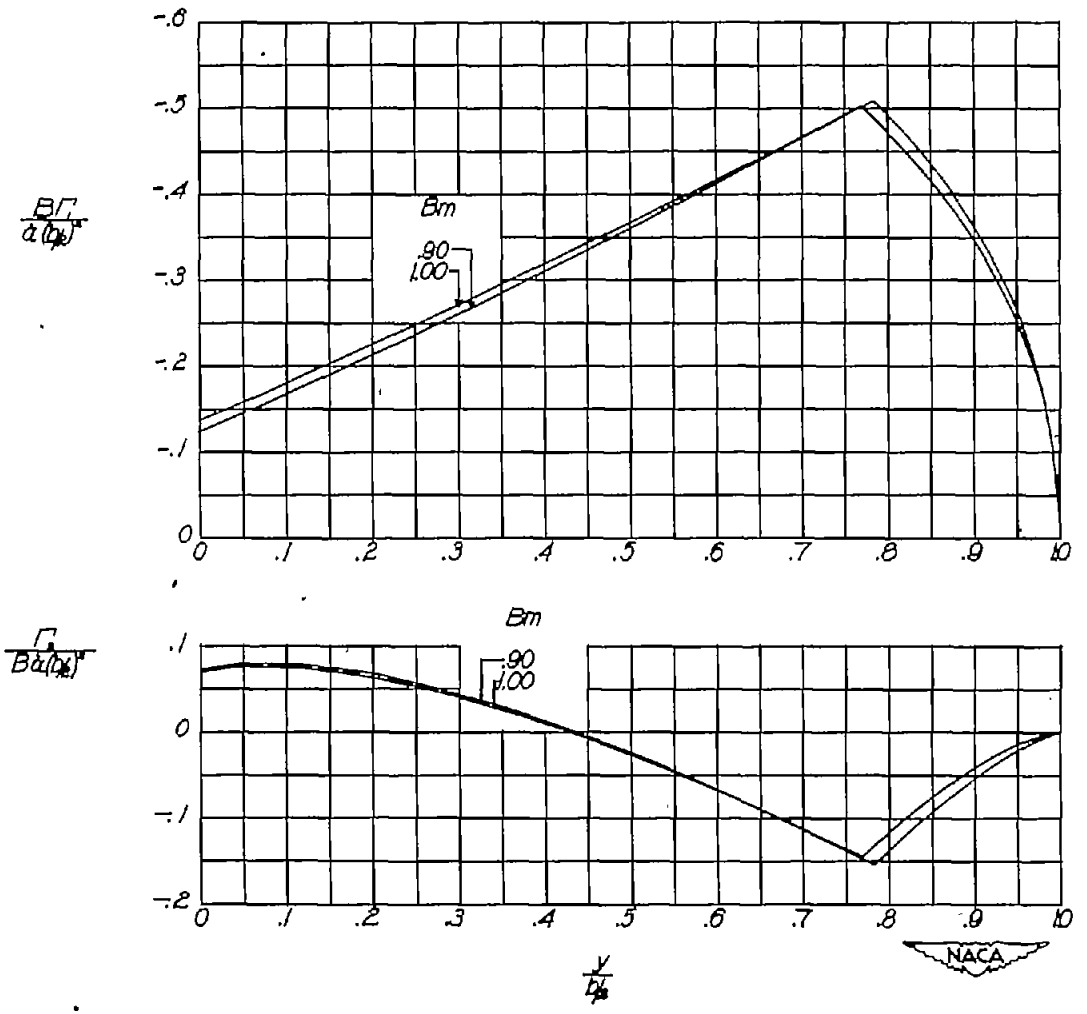

(c) AB = 4.

Figure 26.- Continued.

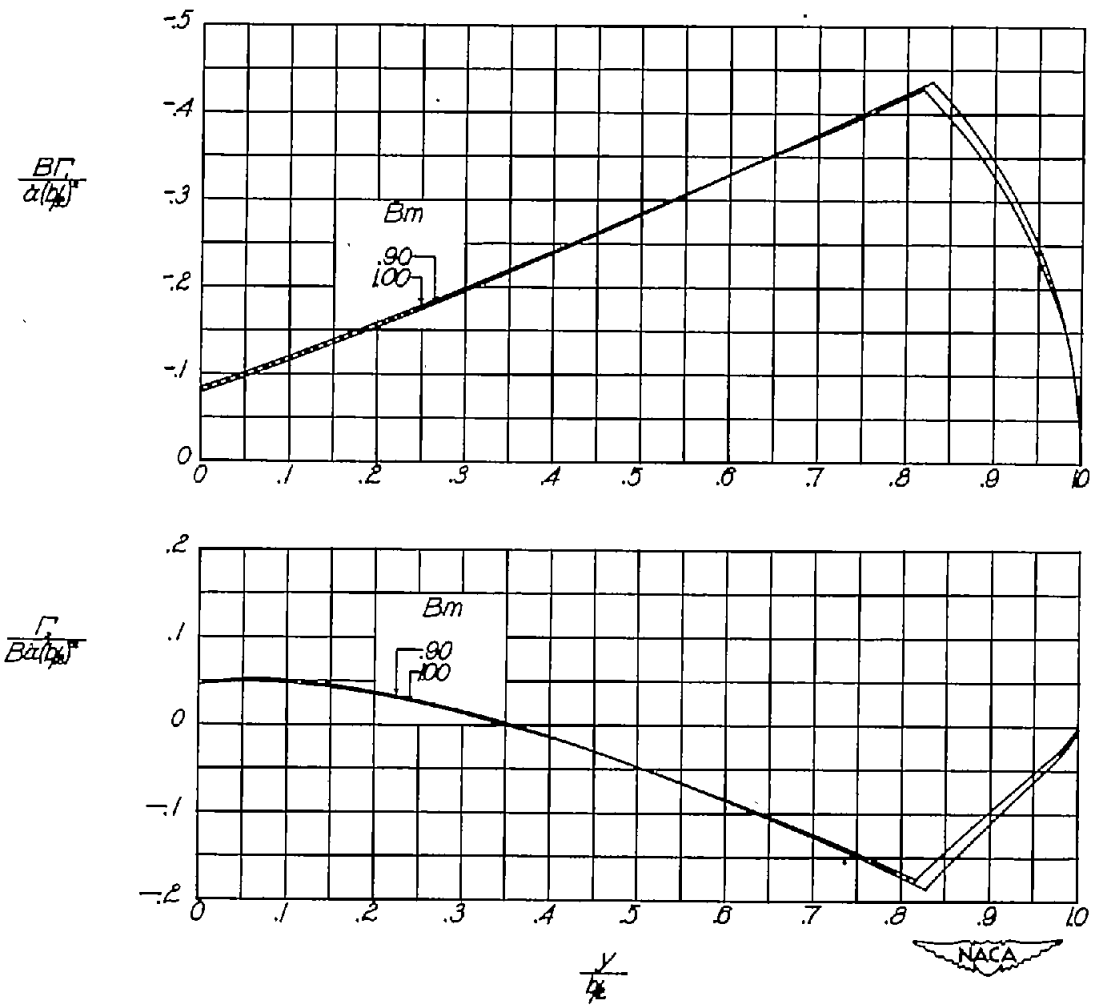

(d) AB = 5.

Figure 26.- Continued.

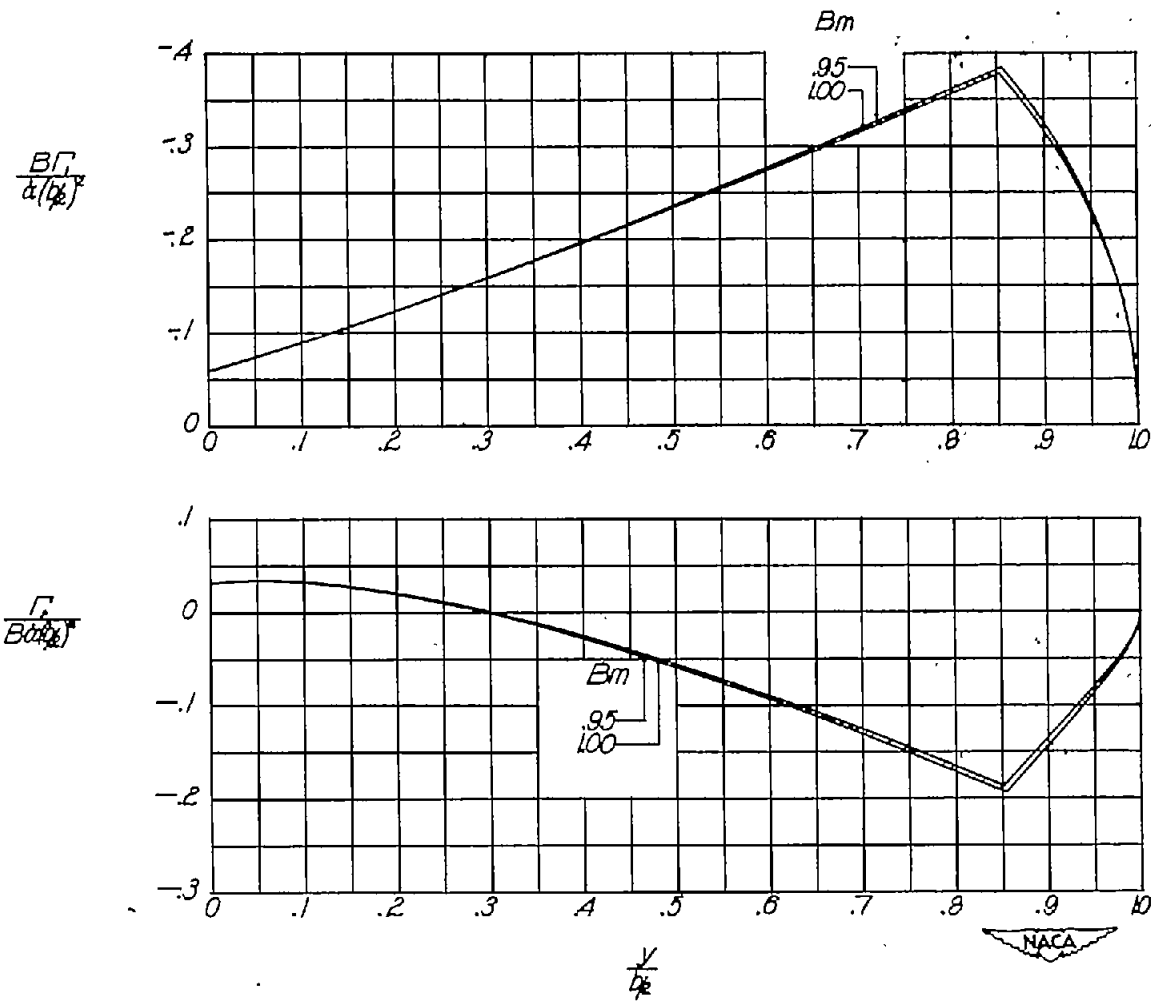

(e) AB = 6.

Figure 26.- Continued.

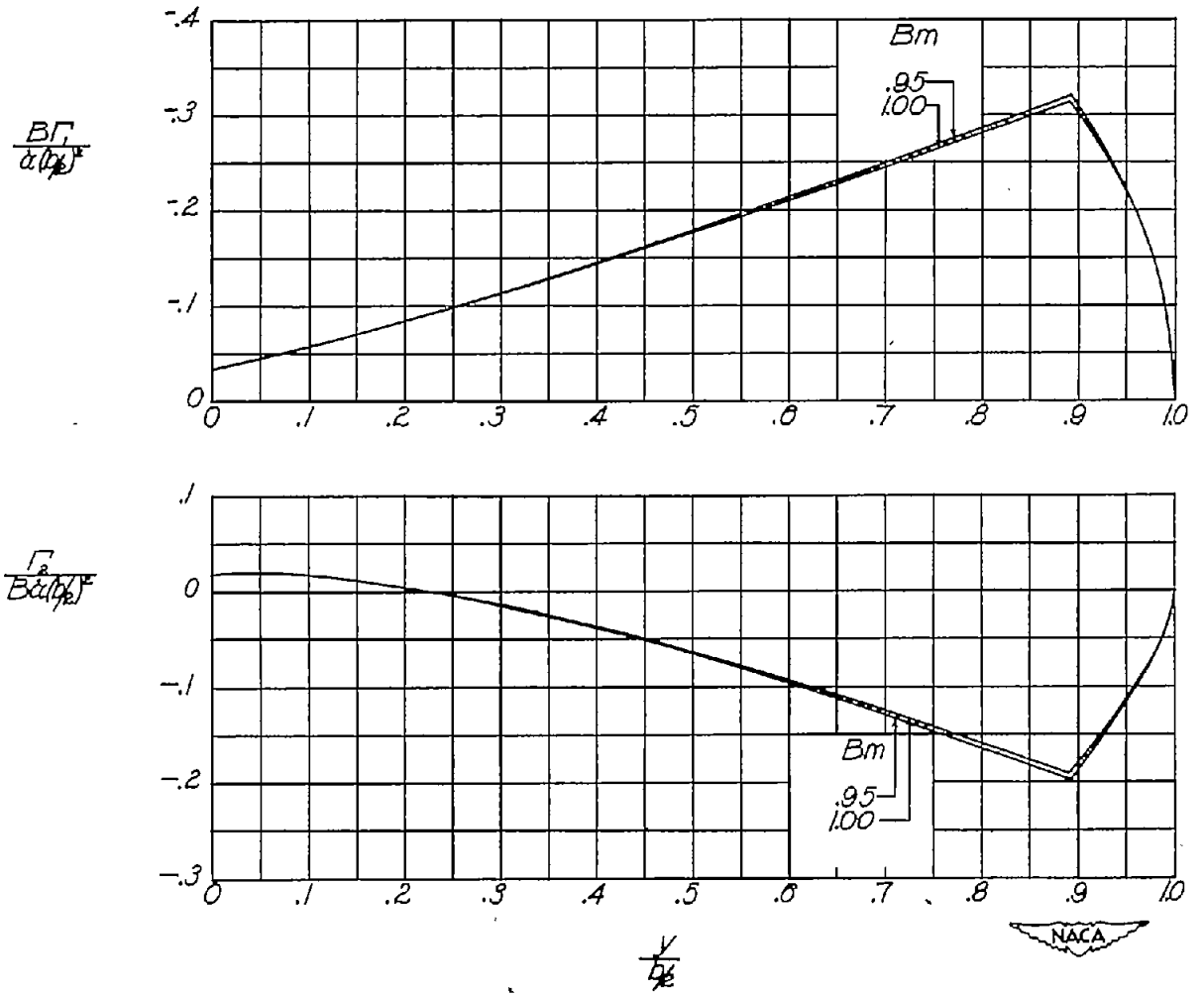

(f) AB = 8.

Figure 26.- Continued.

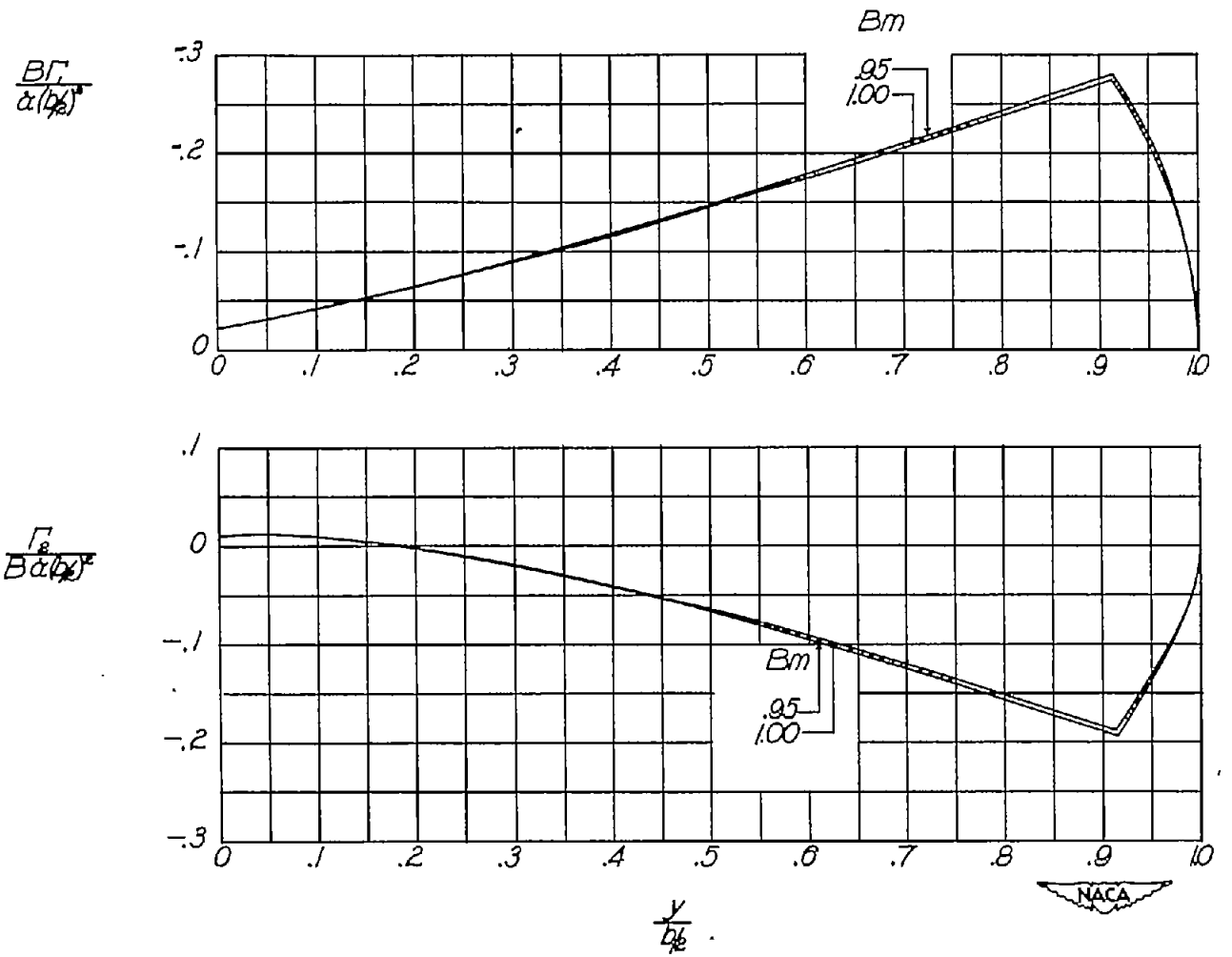

(g) AB = 10.

Figure 26.- Continued.

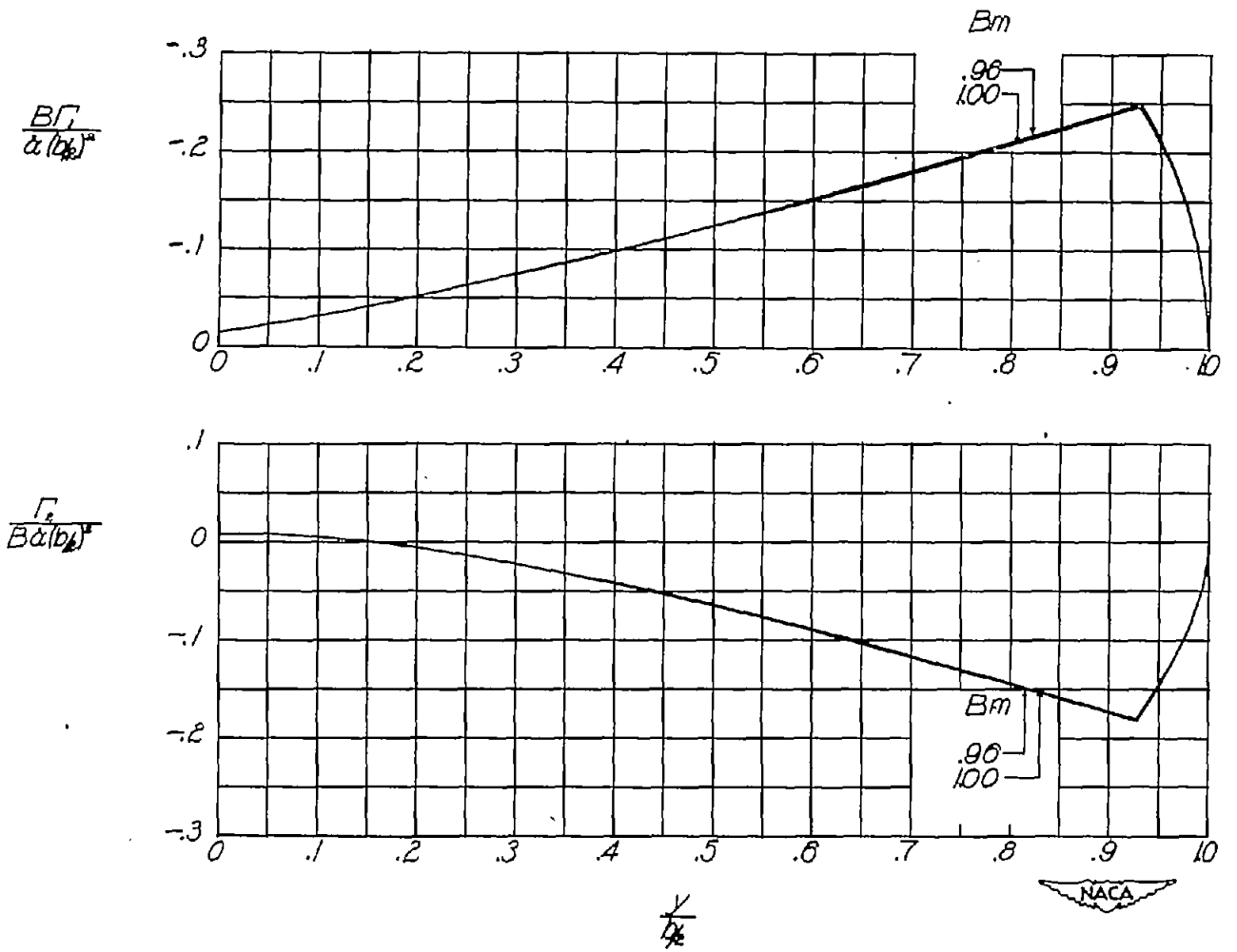

(h) AB = 12.

Figure 26.- Continued.

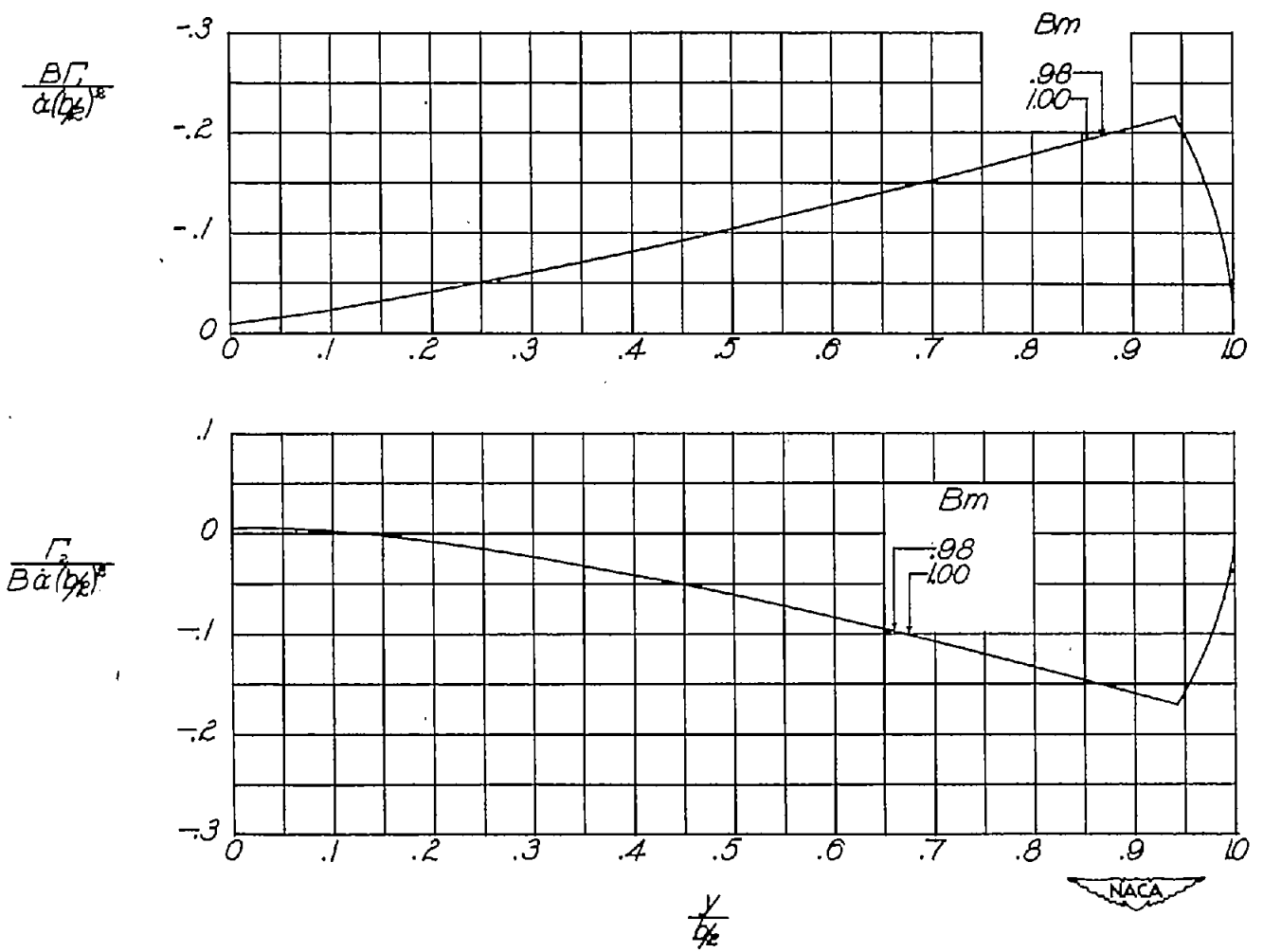

(i) AB = 15.

Figure 26.- Continued.

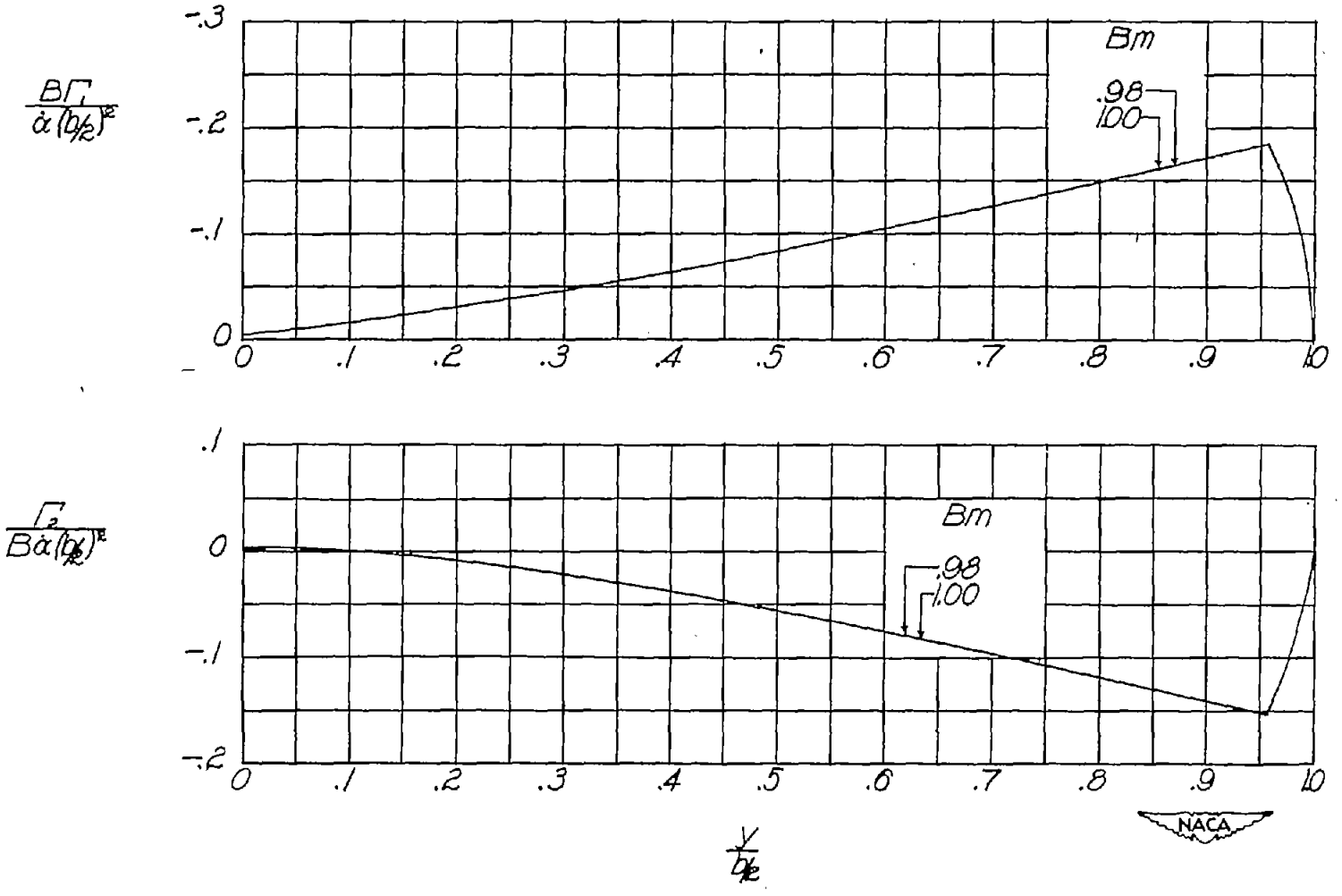

(j) AB = 20.

Figure 26.- Concluded.

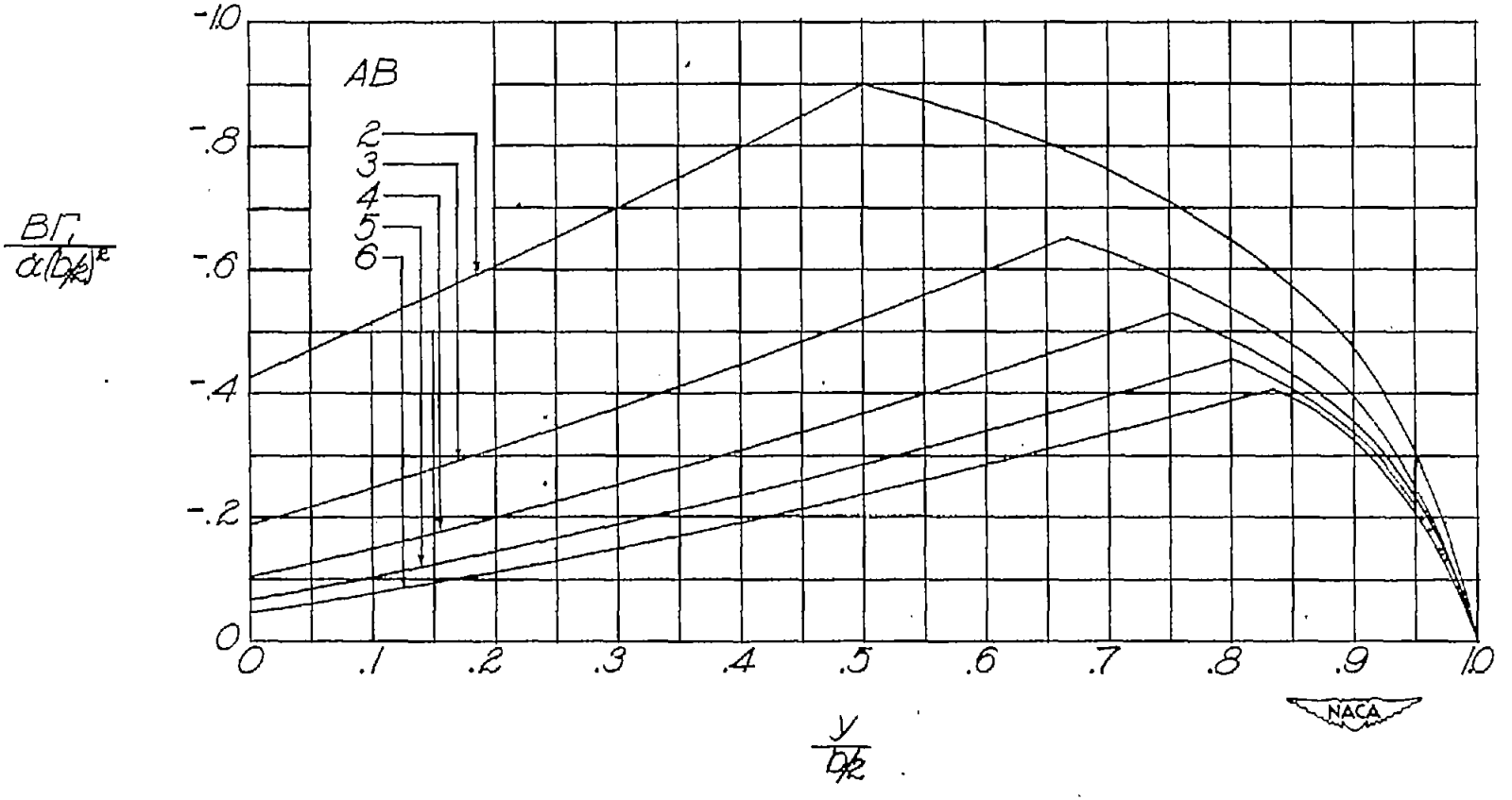

(a) AB = 2 to 6.

Figure 27.- Distribution of circulation along span for wings with constant vertical acceleration with λ = 1.00. Bm = 1.00.

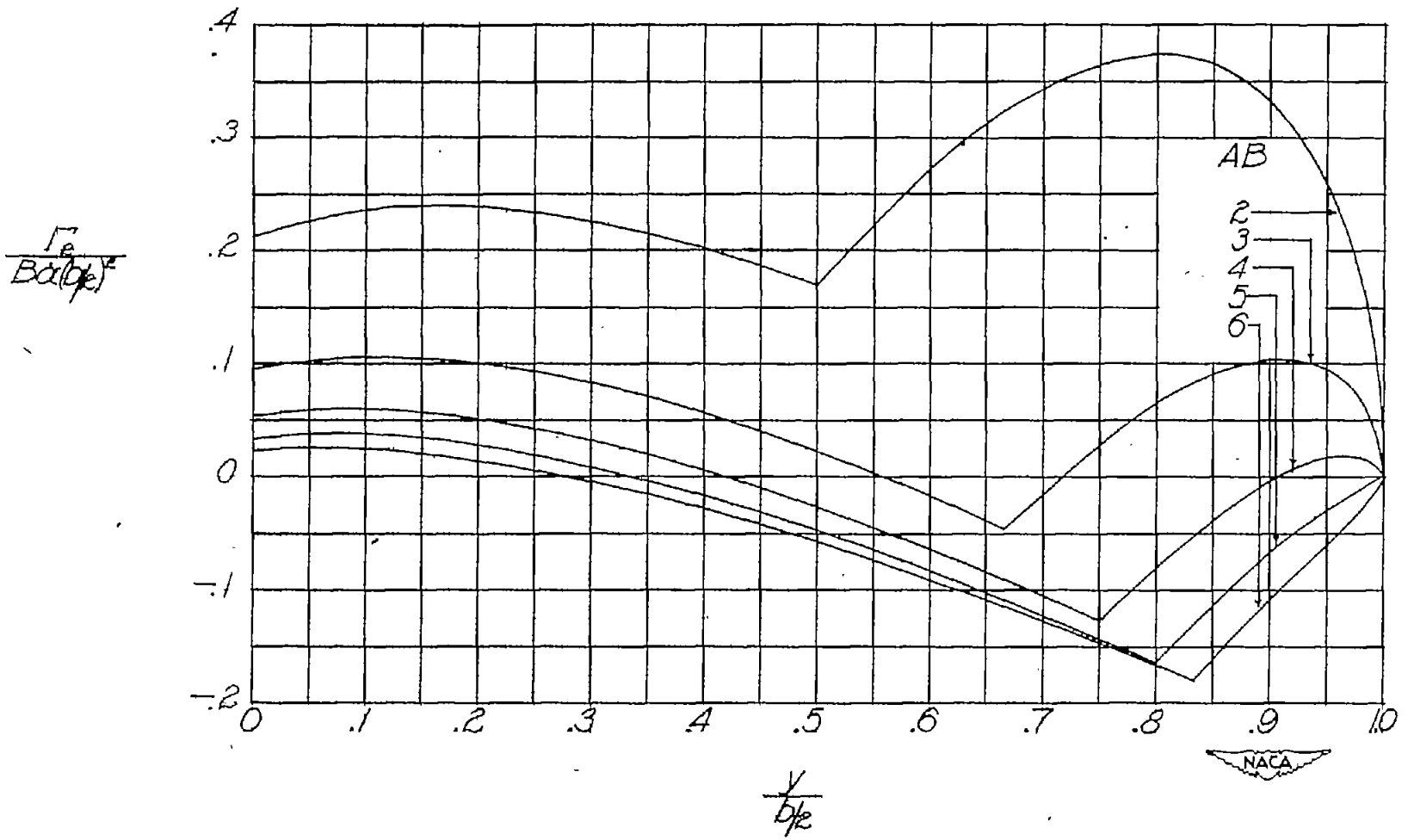

(a) AB = 2 to 6. Concluded.

Figure 27.- Continued.

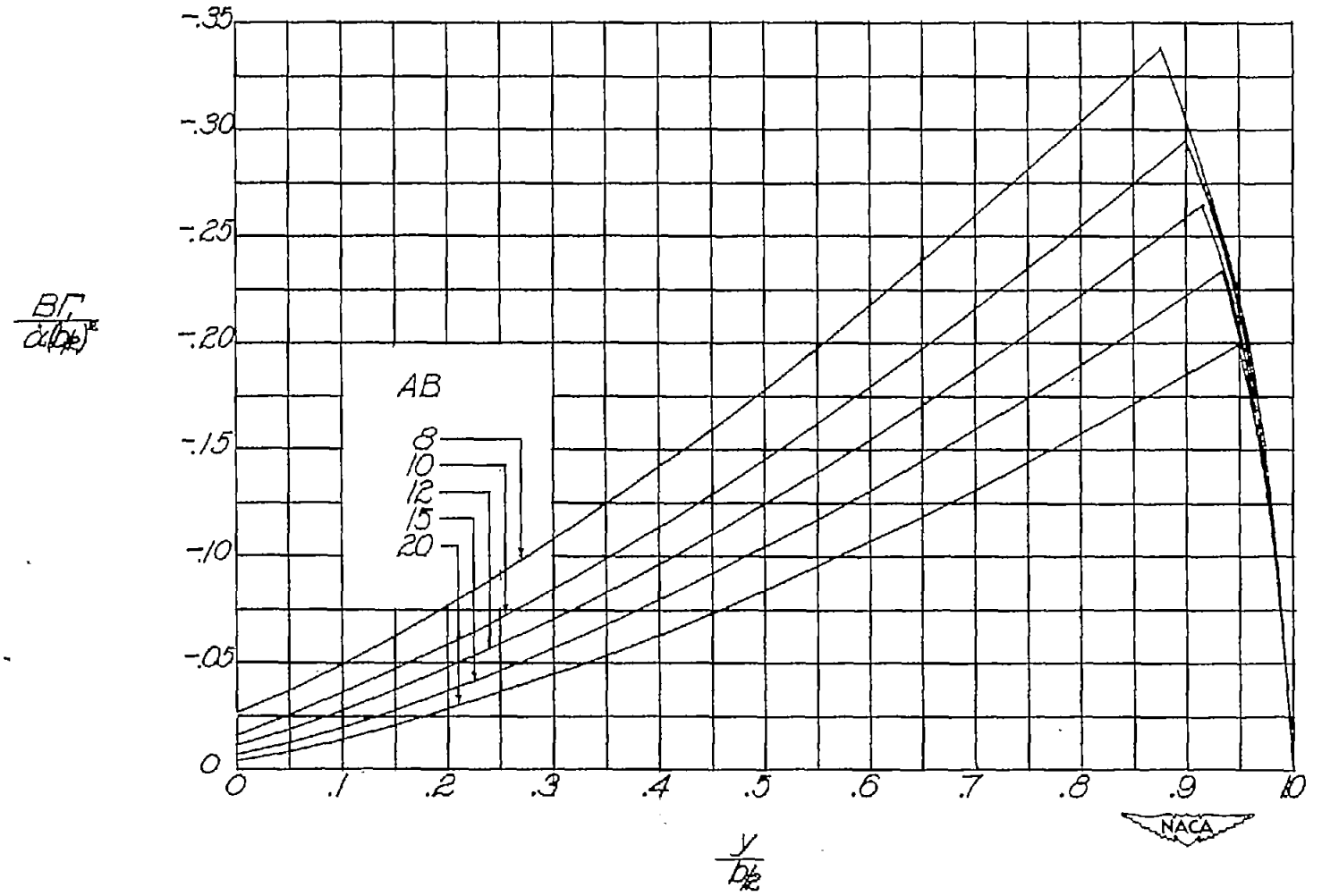

(b) AB = 8 to 20.

Figure 27.- Continued.

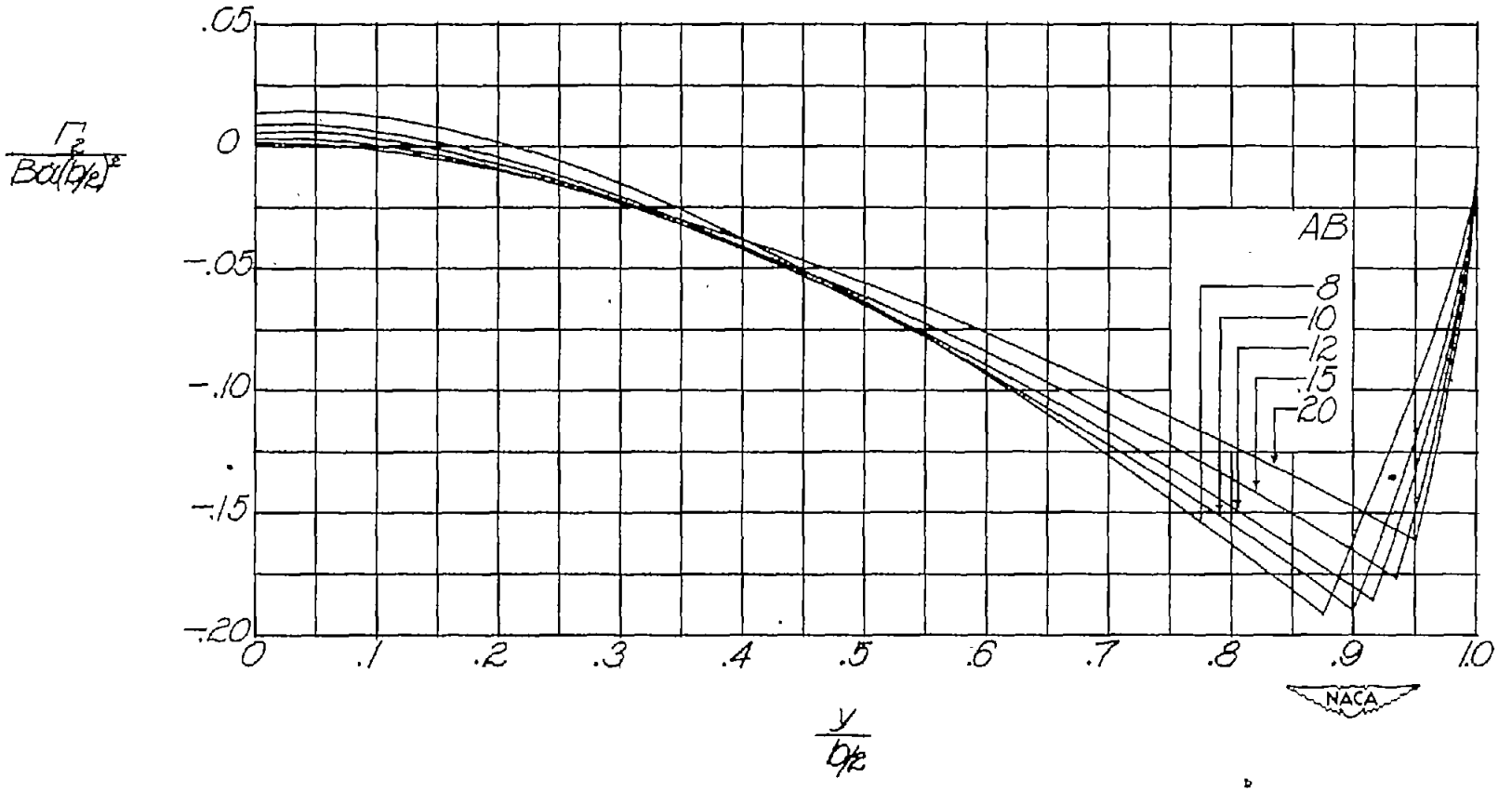

(b) AB = 8 to 20. Concluded.

Figure 27.- Concluded.

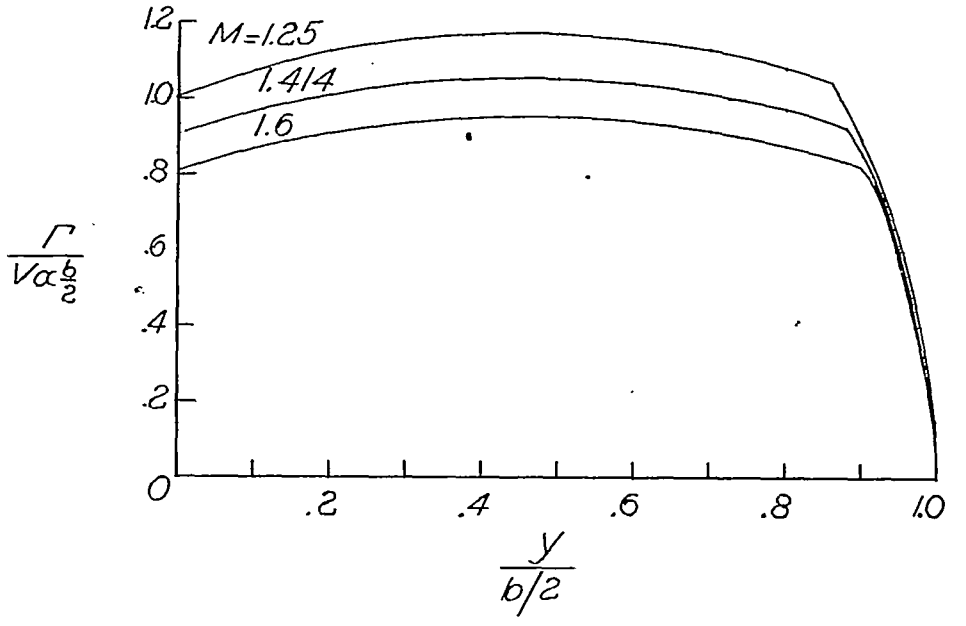

(a) Variation with Mach number. A = 4; Λ = 51.5°; λ = 0.25.

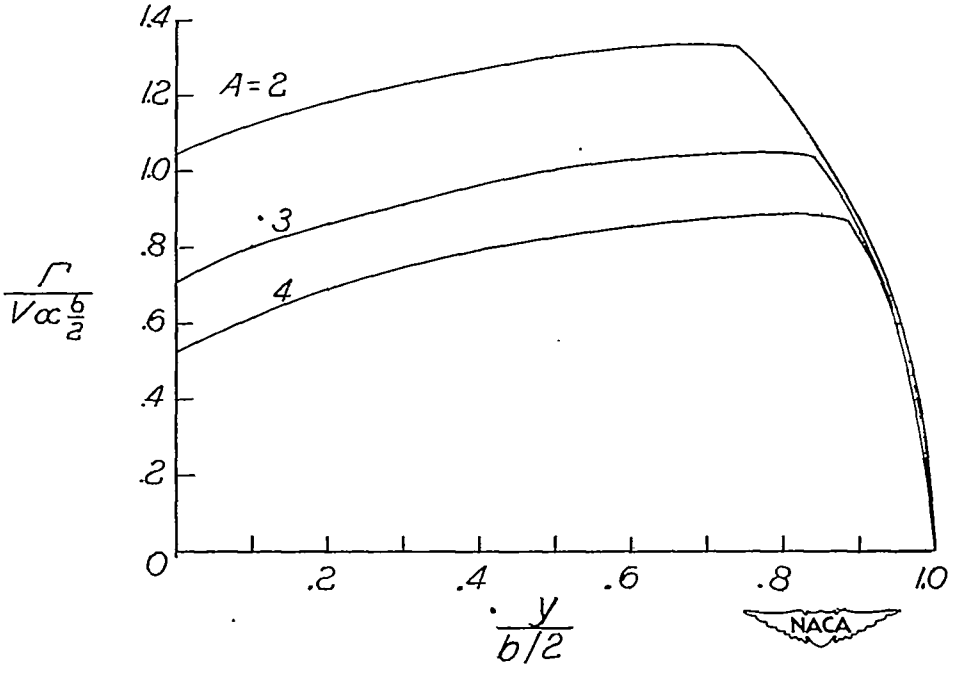

(b) Variation with aspect ratio. M = 1.8; Λ = 60°; λ = 0.50.

Figure 28.- Some illustrative variations of distribution of circulation along span with Mach number, aspect ratio, sweepback, and taper ratio for wings at a constant angle of attack.

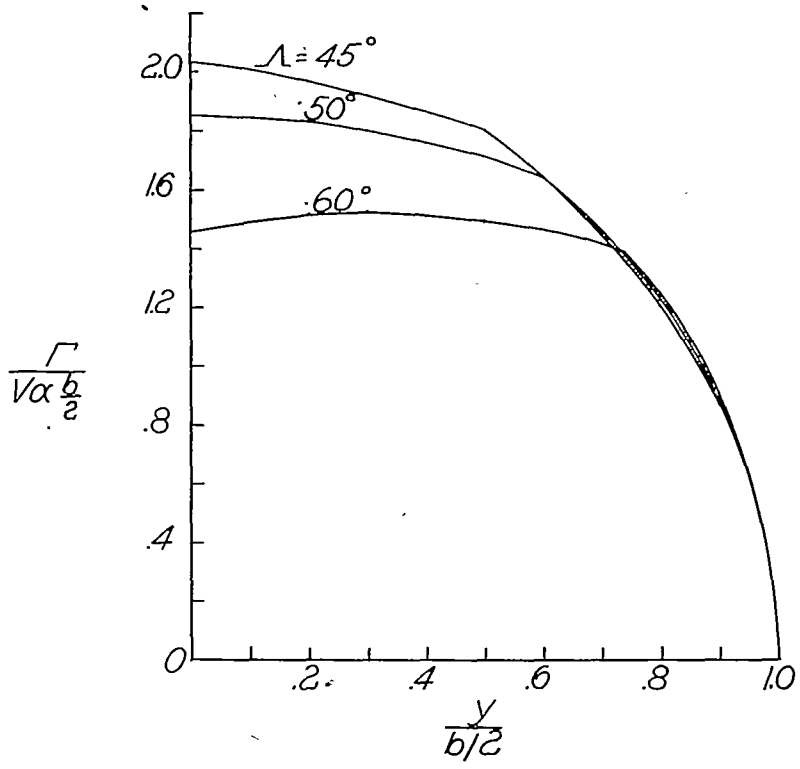

(c) Variation with sweepback. A = 2; M = 1.414; λ = 0.25.

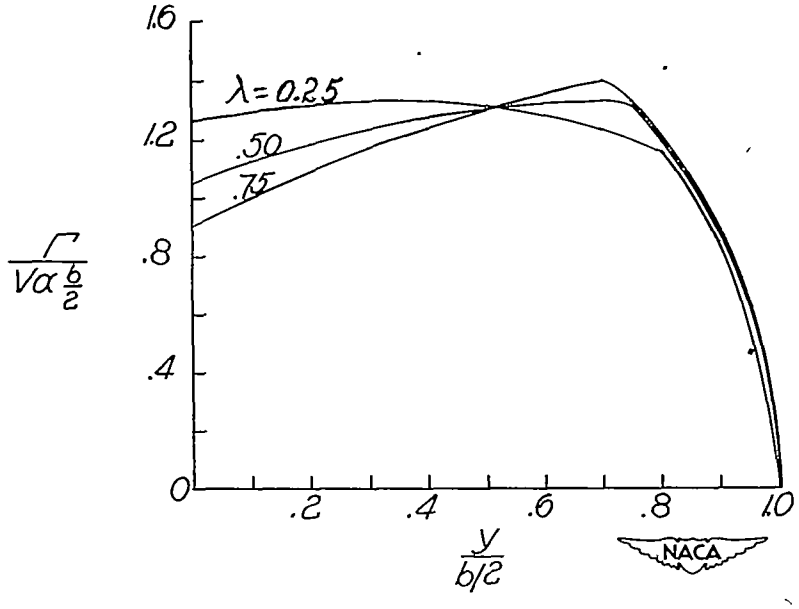

(d) Variation with taper ratio. A = 2; M = 1.8; Λ = 60°.

Figure 28.- Concluded.

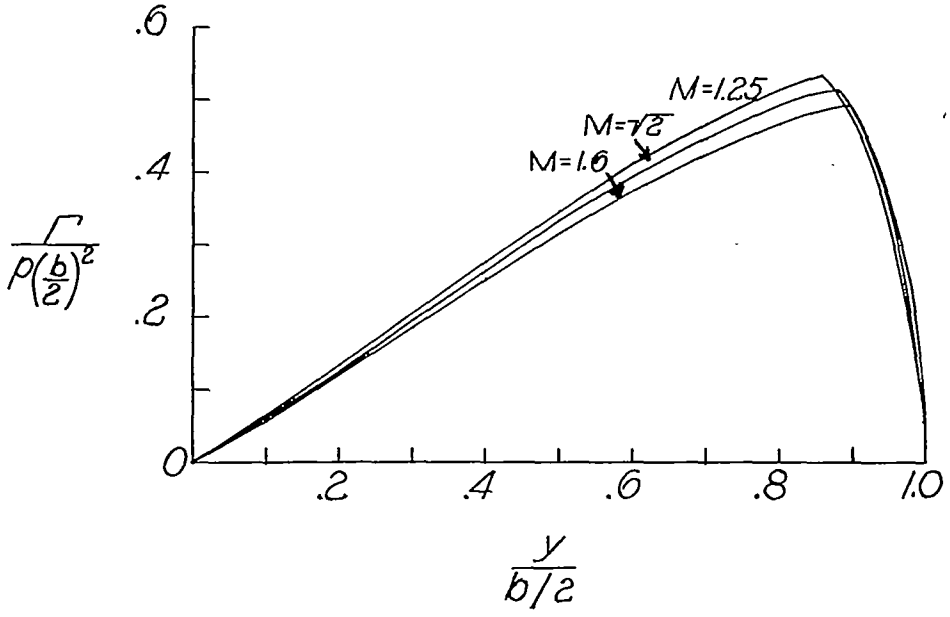

(a) Variation with Mach number. A = 4; Λ = 51.5°; λ = 0.25.

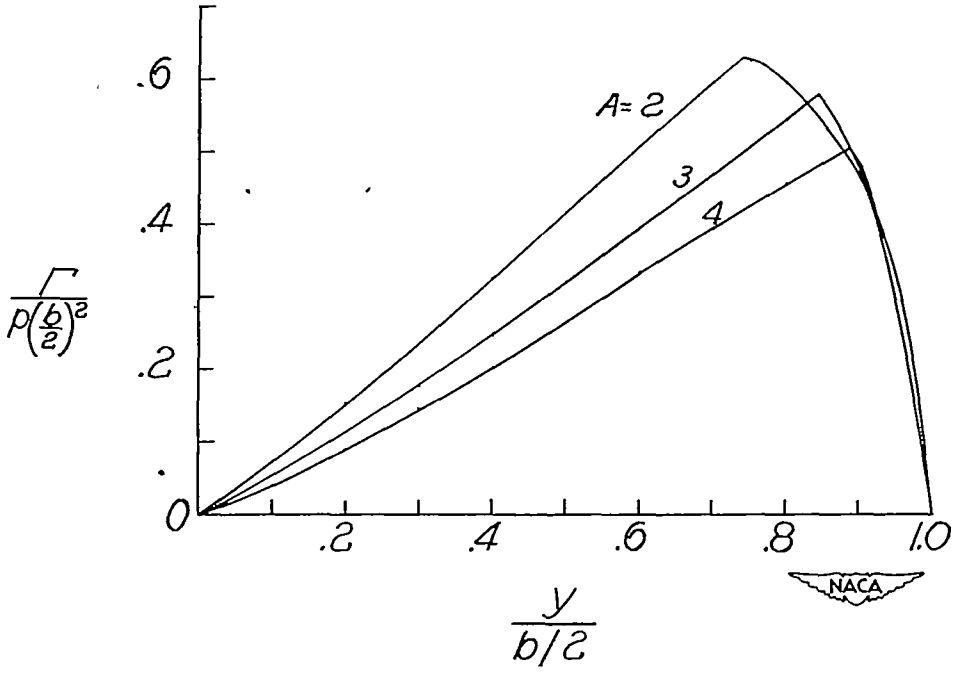

(b) Variation with aspect ratio. M = 1.8; Λ = 60°; λ = 0.50.

Figure 29.- Some illustrative variations of distribution of circulation along span with Mach number, aspect ratio, sweepback, and taper ratio for wings having steady rolling velocity.

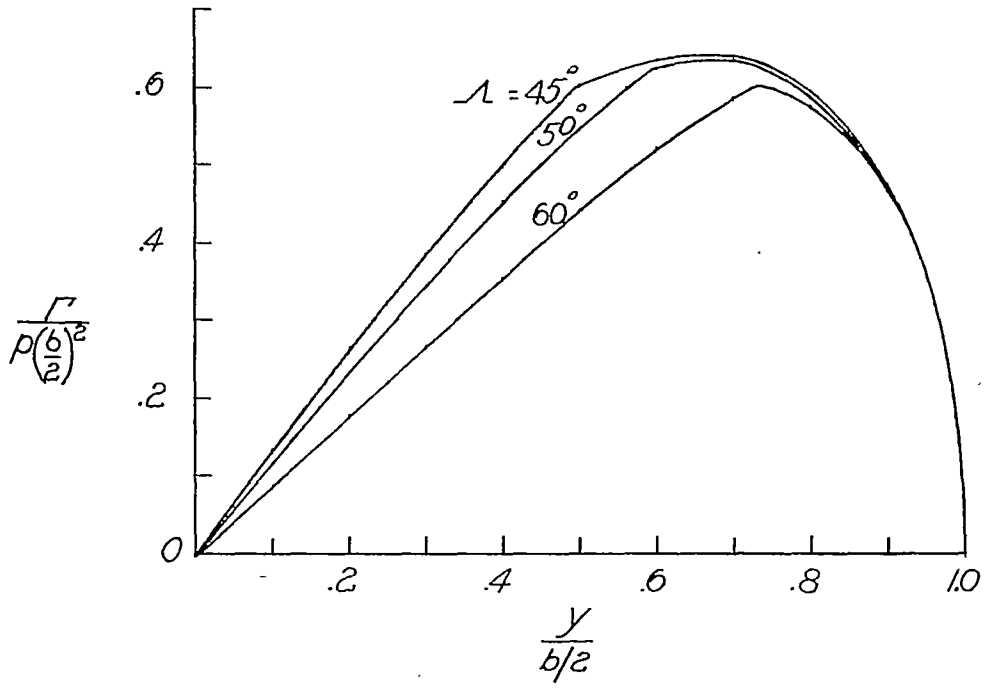

(c) Variation with sweepback. A = 2; M = 1.414; λ = 0.25.

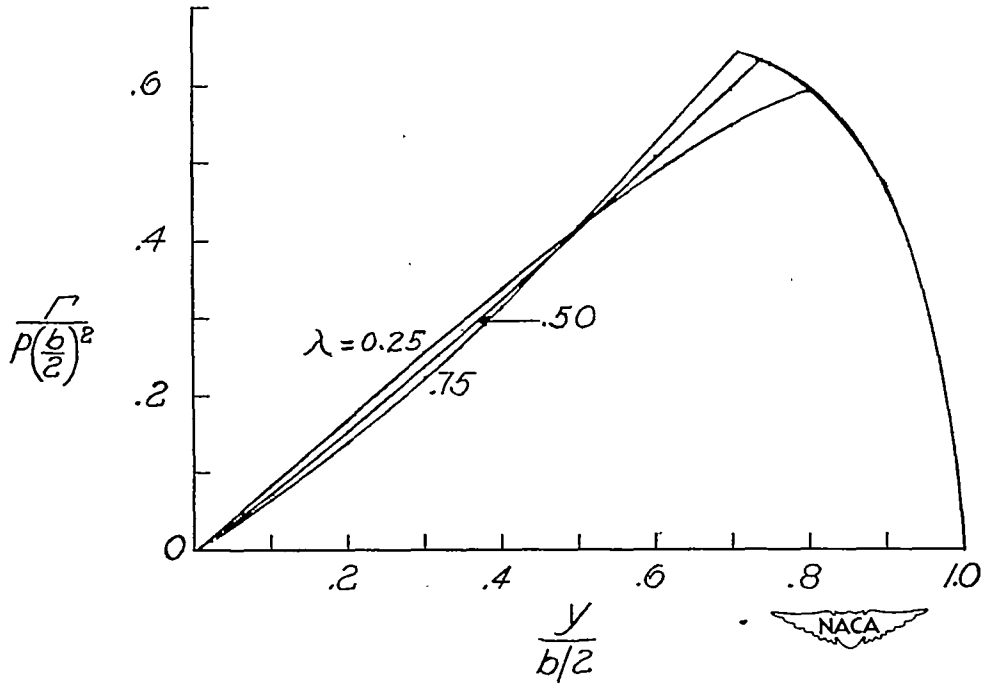

(d) Variation with taper ratio. A = 2; M = 1.8; $\Lambda = 60°$.

Figure 29.- Concluded.

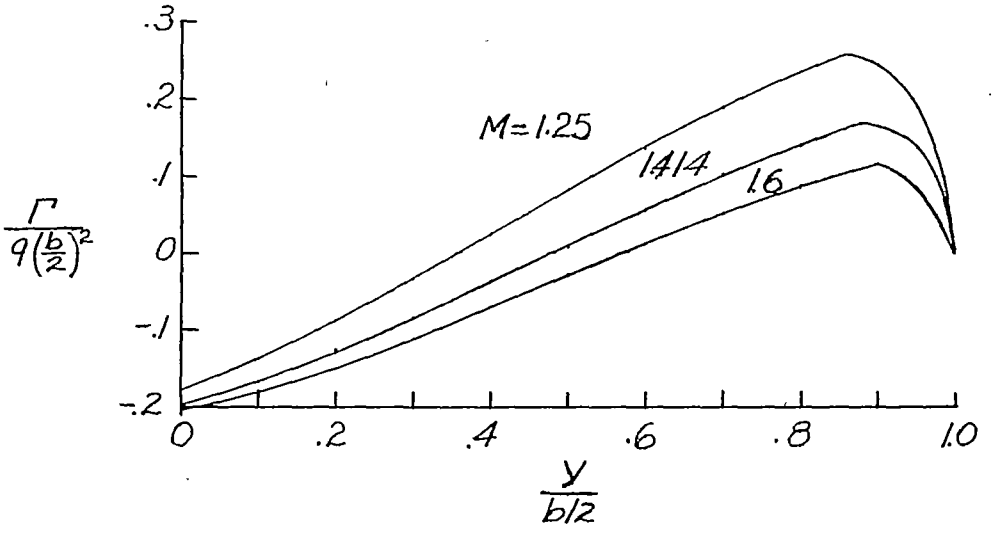

(a) Variation with Mach number. A = 4; Λ = 51.5°; λ = 0.25.

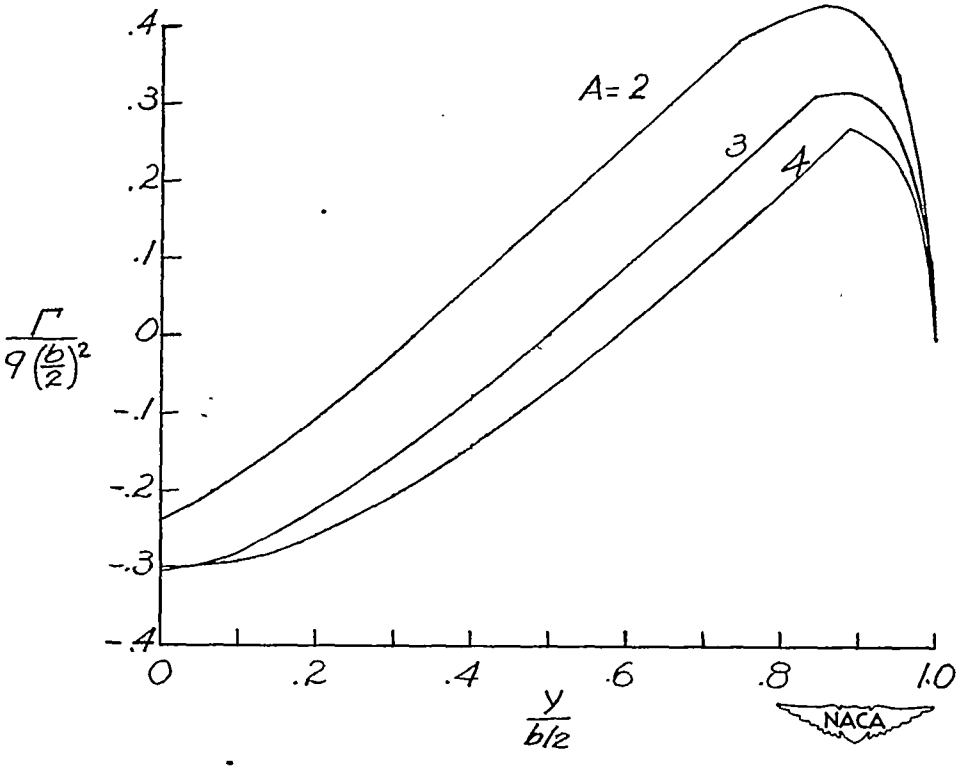

(b) Variation with aspect ratio. M = 1.8; Λ = 60°; λ = 0.50.

Figure 30.- Some illustrative variations of distribution of circulation along span with Mach number, aspect ratio, sweepback, and taper ratio for wings having steady pitching velocity. Static margin, 0.05$\bar{c}$.

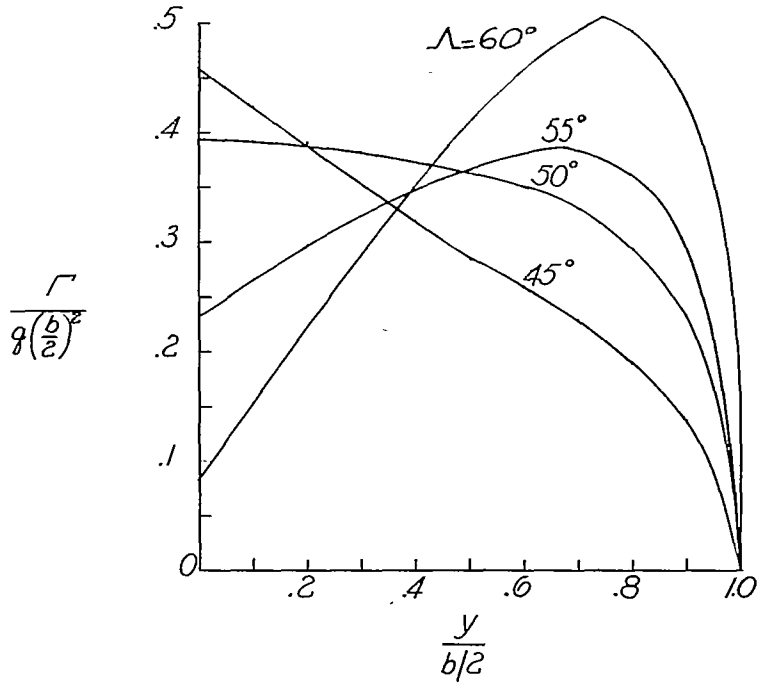

(c) Variation with sweepback. A = 2; M = 1.414; λ = 0.25.

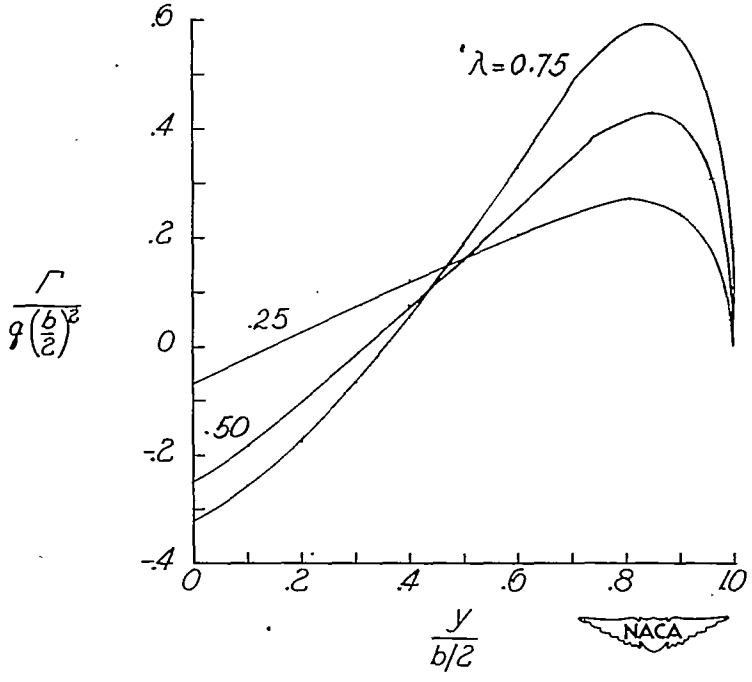

(d) Variation with taper ratio. A = 2; M = 1.8; Λ = 60°.

Figure 30.- Concluded.

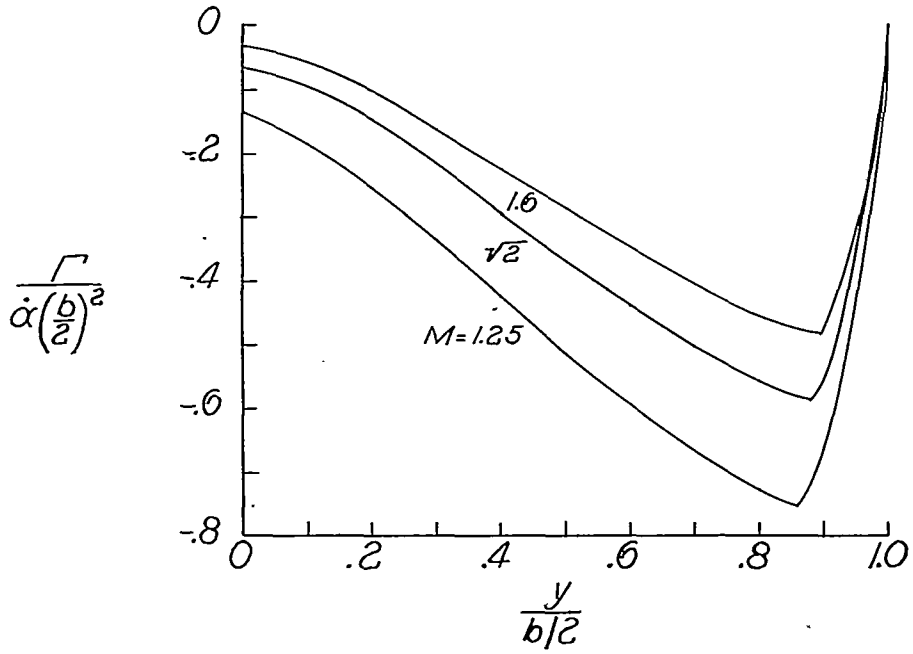

(a) Variation with Mach number. A = 4; Λ = 51.5°; λ = 0.25.

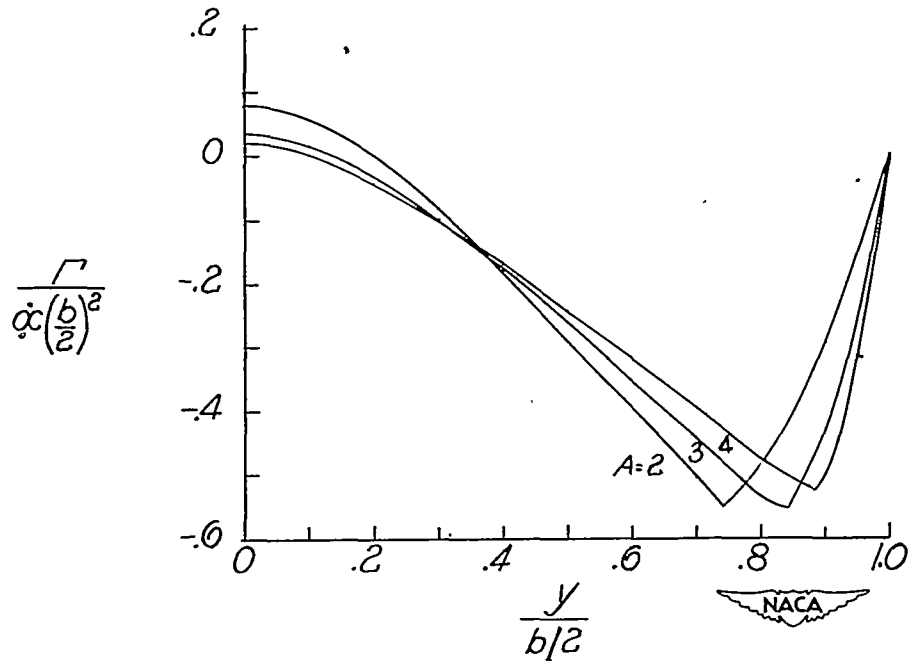

(b) Variation with aspect ratio. M = 1.8; Λ = 60°; λ = 0.50.

Figure 31.- Some illustrative variations of distribution of circulation along span with Mach number, aspect ratio, sweepback, and taper ratio for wings with constant vertical acceleration.

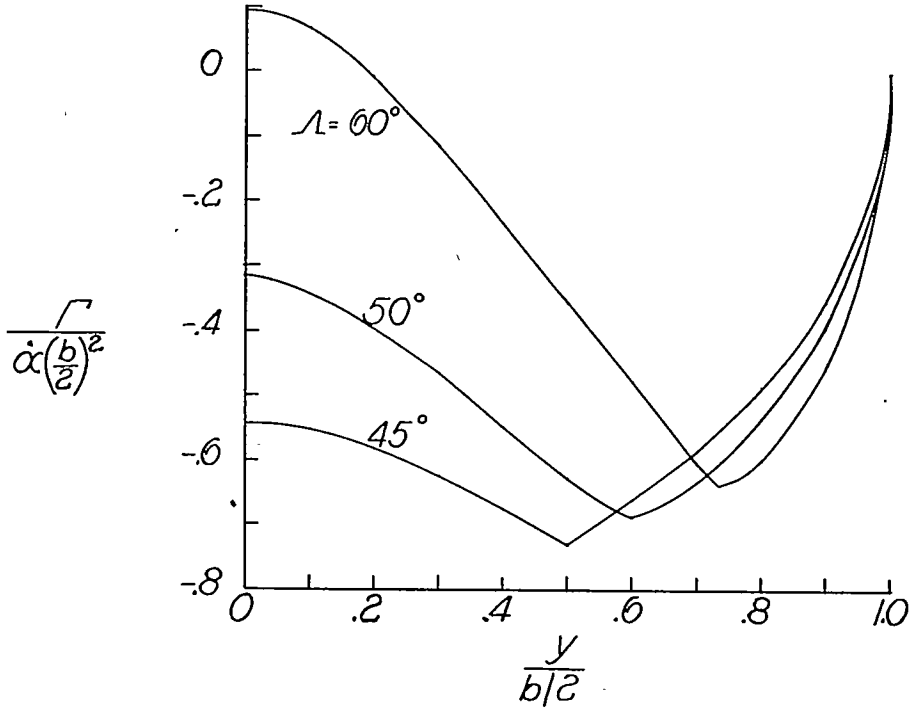

(c) Variation with sweepback. A = 2; M = 1.414; λ = 0.25.

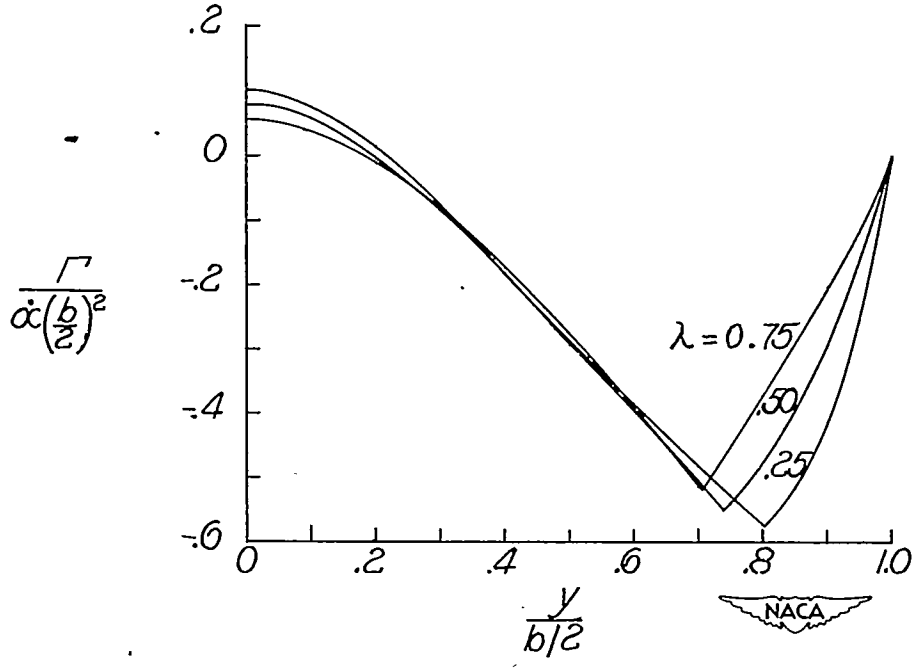

(d) Variation with taper ratio. A = 2; M = 1.8; Λ = 60°.

Figure 31.- Concluded.

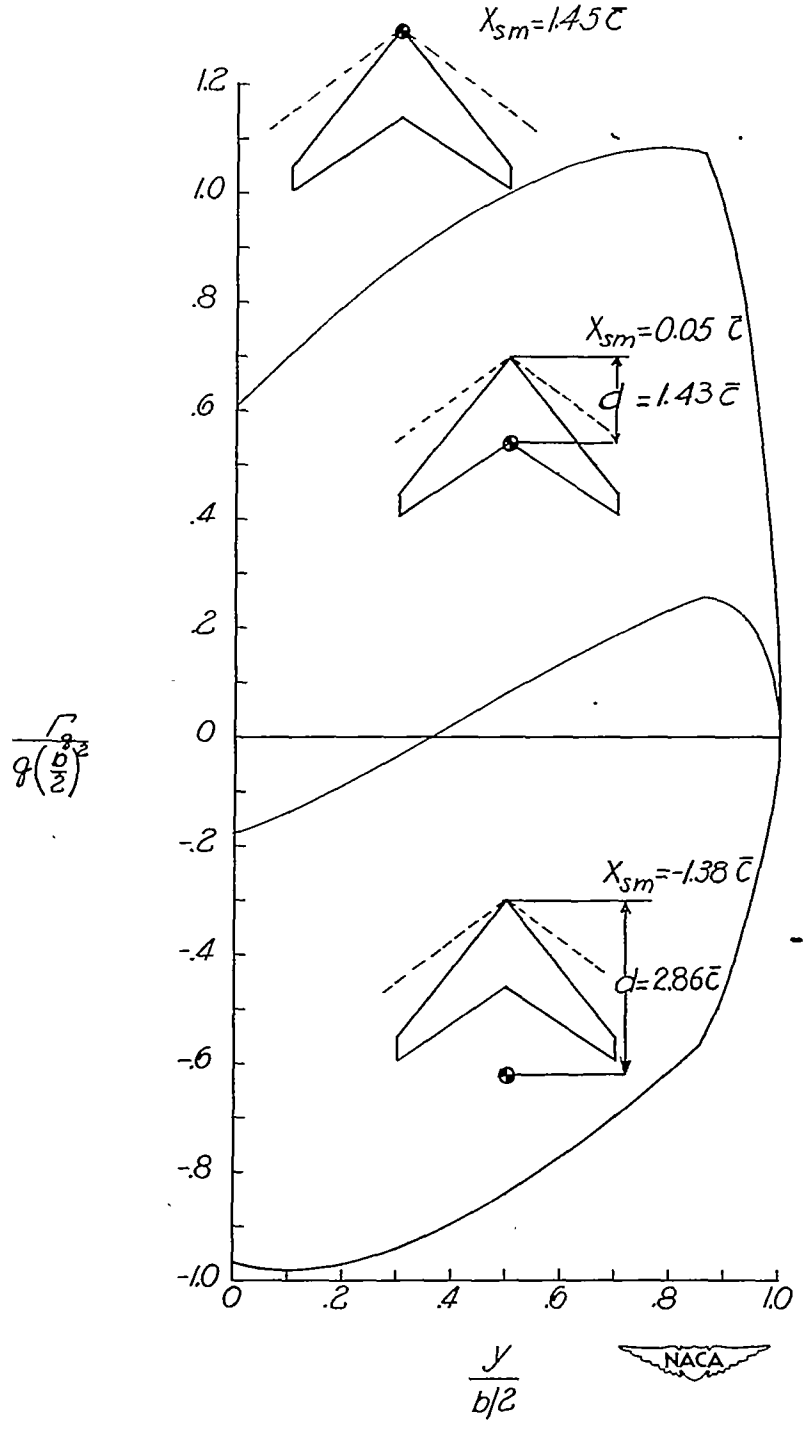

(a) M = 1.25; A = 4; $\Lambda = 51.5^{\circ}$; $\lambda = 0.25$.

Figure 32.- Some illustrative variations of distribution of circulation along span with axis-of-pitch location for wings with constant pitching velocity.

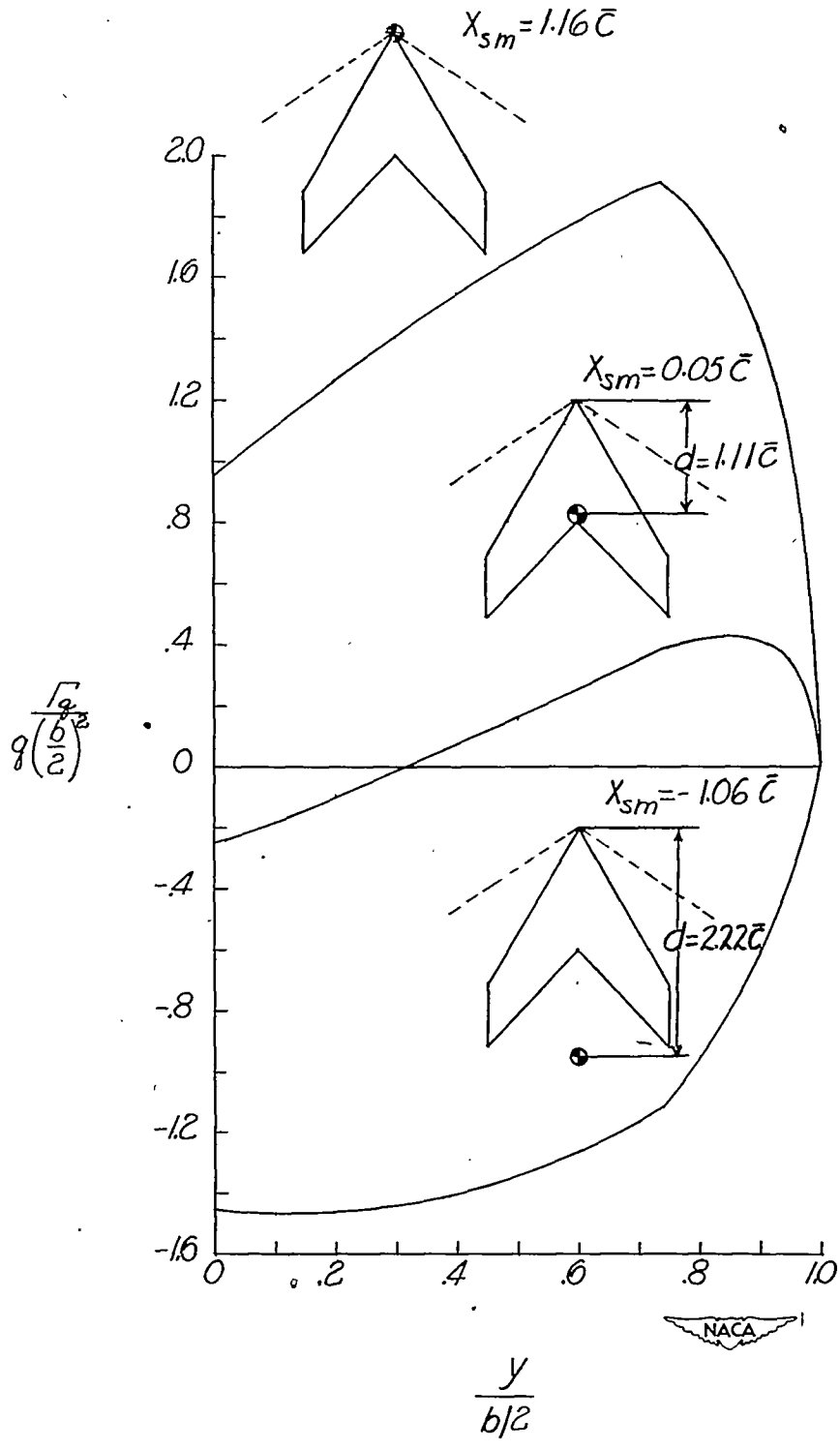

(b) M = 1.8; A = 2; $\Lambda = 60^{\circ}$; $\lambda = 0.50$.

Figure 32.- Concluded.

NACA-Langley - 12-2-52 - 1000